ELECTRON DETACHMENT DISSOCIATION OF SULFATED GLYCOSAMINOGLYCANS

by

JEREMY J. WOLFF

(Under the Direction of I. Jonathan Amster)

ABSTRACT

Glycosaminoglycans (GAGs) are a diverse group of linear, acidic, variably modified polysaccharides. Determining the sites of modification is of significant interest as these sites of modification are believed to influence the biological function of GAGs. However, the structural characterization of sulfated glycosaminoglycans has been a longstanding problem due to the lability of these oligosaccharides. In this work, the application of electron detachment dissociation (EDD) Fourier transform mass spectrometry (FTMS) to the analysis of sulfated GAGs is presented. EDD produces more abundant glycosidic and cross-ring cleavages for GAG oligosaccharides than does other more conventional ion activation methods, allowing sites of modification to be determined with a single tandem mass spectrometry experiment. EDD can also distinguish the epimers glucuronic acid (GlcA) and iduronic acid (IdoA) from each other in heparan sulfate oligosaccharides. The influence of the charge state on EDD, and characterization of products that arise from electron induced dissociation (EID) are also presented. Overall, EDD is shown to be a powerful tool for characterization of sulfated GAGs.

INDEX WORDS: Electron detachment dissociation, electron induced dissociation, tandem mass spectrometry, Fourier transform mass spectrometry, glycosaminoglycans, sulfated carbohydrates.

ELECTRON DETACHMENT DISSOCIATION OF SULFATED GLYCOSAMINOGLYCANS

by

JEREMY J. WOLFF

B.S., Pepperdine University, 1999

A Dissertation Submitted to the Graduate Faculty of the University of Georgia in Partial

Fulfillment of the Requirements for the Degree

DOCTOR OF PHILOSOPHY

ATHENS, GA

2008

ELECTRON DETACHMENT DISSOCIATION OF SULFATED GLYCOSAMINOGLYCANS

by

JEREMY J. WOLFF

Major Professor: I. Jonathan Amster

Committee: John L. Stickney
Ron Orlando

Electronic Version Approved:

Maureen Grasso
Dean of the Graduate School
The University of Georgia
May 2008

ACKNOWLEDGEMENTS

I would like to thank my family for the support they have given me during my tenure in graduate school. I would also like to thank my advisor, Jon Amster, for the advice and mentoring I received over the years.

TABLE OF CONTENTS

LIST OF TABLES

Page

LIST OF FIGURES

Page

CHAPTER 1

INTRODUCTION AND LITERATURE REVIEW

This dissertation presents the development of new mass spectrometry techniques for examining the structural features of glycosaminoglycan (GAG) carbohydrates. GAGs are a diverse group of linear, highly acidic polysaccharides. GAGs comprise the carbohydrate portion of proteoglycans, and can be found both intra- and extra-cellular in a wide variety of organisms, from bacteria to humans [1]. GAGs participate in a number of important reactions such as the binding of cofactors and chemokines [2, 3], influencing cellular adhesion [4], inhibiting proteolysis [5], and regulation inflammation reactions [6]. GAGs have also been implicated in a number of pathogenic infections [7-10] and have been shown to undergo alteration during in certain cancers [11].

GAGs are assigned into one of four groups based on the composition of their disaccharide subunits (see Figure 1 for structures): heparin/heparan sulfate (HS), chondroitin sulfate (CS)/dermatan sulfate (DS), keratin sulfate (KS), and hyaluronan [12]. With the exception of KS, GAGs consist of a repeating hexuronic acid-hexosamine disaccharide. KS consists of a repeating hexose-hexosamine disaccharide. At the molecular level, GAG disaccharides are variably modified with sulfation, acetylation, and C5 epimerization. For example, the sulfated GAG heparin contains a disaccharide repeat consisting of hexuronic acid and glucosamine. The hexuronic acid may be iduronic acid or glucuronic acid depending on the stereochemistry of C5, and may be sulfated at C2. The glucosamine may be sulfated C3 or C6, and may be sulfated, acetylated, or unmodified at the amino group. Complexity increases at the macromolecular level as GAGs of different composition and different length bind to variable protein cores, producing proteoglycans with molecular weights as large as 1 GDa. There has been significant interest in determining the sites of modification (sulfation, aceytlation, C5 stereochemistry) as the sites of modification are believed to influence GAG function. Unlike

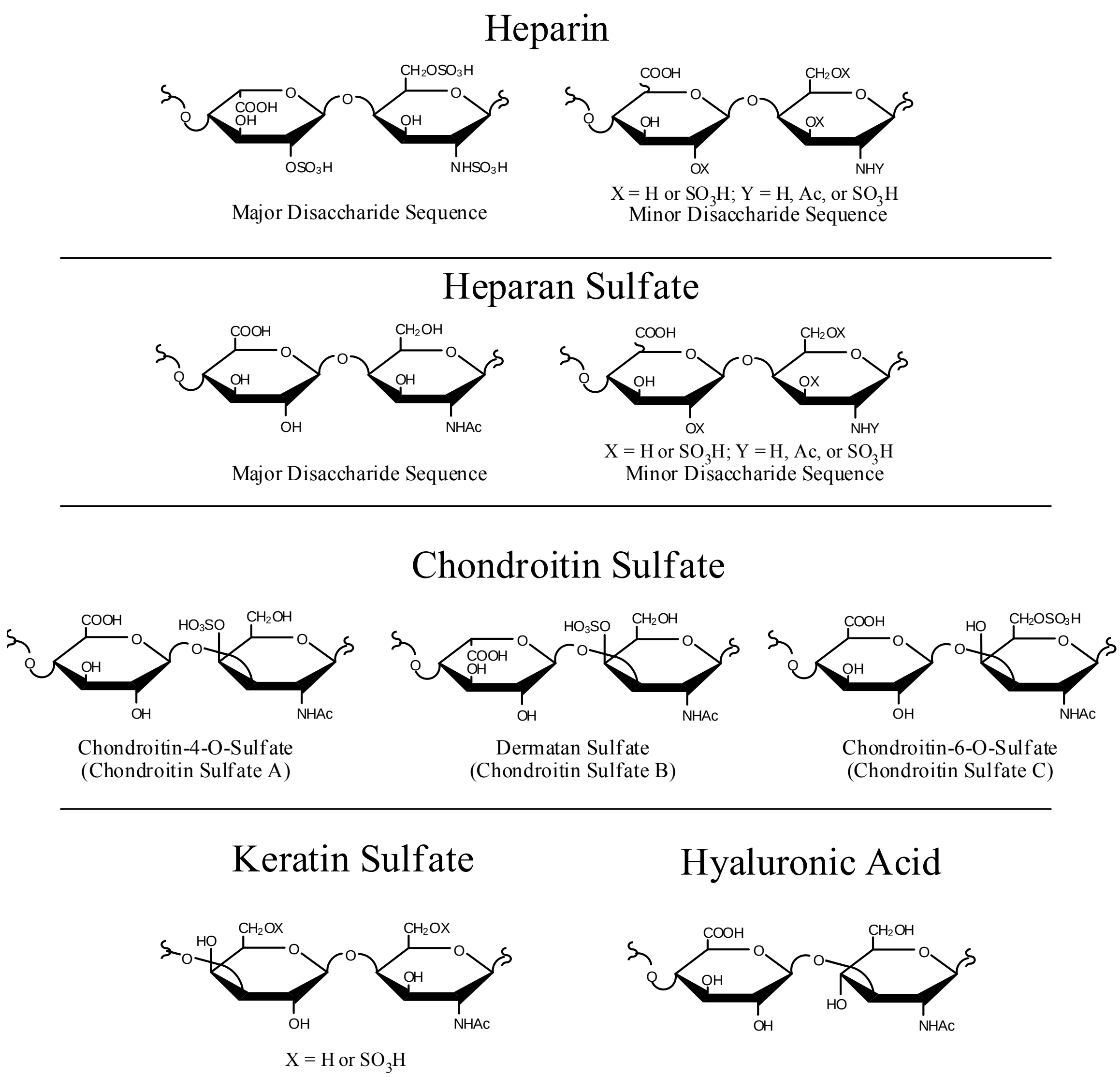

Figure 1.1. Major and minor disaccharide sequences for heparin/heparan sulfate, and disaccharide sequences for chondroitin sulfate, keratin sulfate, and hyaluronic acid.

proteins and nucleic acids, GAGs are not template-synthesized. Therefore, GAG samples must be isolated from natural sources that are often available in limited quantity and at low purity. One- and two-dimensional NMR can be used to determine the site and type of GAG modification, as well as C5 stereochemistry [13]. However, this method requires milligram quantities of high purity GAG, which may not be available. Mass spectrometry is a good alternative to analysis of sulfated GAGs as it requires small quantities of samples and can also analyze complex mixtures.

Mass Spectrometry of Sulfated GAGs

The production of gas phase sulfated GAG ions is challenging due to the acidic nature of these biomolecules, Na/H heterogeneity, and loss of the labile sulfate groups or fragmentation of the molecule during ionization. Sulfated GAGs have been ionized by fast atom bombardment (FAB) [14-16], matrix assisted laser desorption ionization (MALDI) [17-20], and electrospray ionization (ESI) [21]. With these ionization methods intact GAG molecular ions can be produced, allowing determination of GAG molecular weight. Currently, ESI is the favored ionization technique for producing gas-phase ions with little or no decomposition of the molecule, but the production of GAG ions by FAB and MALDI will be briefly described.

The first practical molecular weight determination of GAG oligosaccharides by mass spectrometry was performed using FAB-MS [14]. FAB-MS analysis of di- to octasaccharide of chondroitin sulfate was performed on sulfated GAGs in both positive and negative ion mode using glycerol and thioglycerol for matrices. Thioglycerol was preferred over glycerol, with a 4-6 fold increase in sensitivity was reported. Both positive and negative ion FAB-MS produced sodium cationized molecular ions that were accompanied by abundant Na/H heterogeneity. Also, both positive and negative ionization resulted in fragmentation of the oligosaccharides, typically at glycosidic bonds. The authors concluded that analysis of the oligosaccharides in negative ion mode was preferred due to enhanced sensitivity and a reduction in the formation of matrix-salt clusters. The authors later analyzed heparin oligosaccharides and came to similar conclusions [16]. However, unlike the chondroitin sulfate oligosaccharides, the heparin oligosaccharides did not fragment during ionization. While improvements were made in the analysis of sulfated GAGs by FAB-MS using techniques such as permethylation [15], the low signal-to-noise, presence of matrix peaks, loss of SO_3 from the molecular ion, and fragmentation of the sulfated GAGs decreased the analytical utility of this ionization technique.

Direct ionization of GAGs by MALDI can be quite difficult, often not producing any molecular ions. In order to aid ionization, GAG oligosaccharides can be mixed with basic peptides, producing a gas phase complex between the basic peptide and the anionic oligosaccharide [17, 18, 22]. In order to generate positive ions, the basic peptide must contain one or more sites of positive charge versus the number of anionic sites on the oligosaccharide. In order to achieve reasonable negative ion signal for direct analysis of sulfated GAGs, concentrations of 100 pmol/μL were necessary. With the addition of a basic peptide, sensitivity at 3 pmol/μL was achieved, with no fragmentation of the oligosaccharide or loss of SO_3 [17]. While this method is useful for determining the molecular weight of a sulfated GAG, tandem mass spectrometry of the GAG is not possible as charge is carried by the peptide. Recently, direct MALDI analysis of sulfated GAG oligosaccharides has been performed using ionic liquid matrices (ILM) [19, 20, 23]. Ionization of sulfated GAGs produces abundant sodiated molecular ions with no glycosidic or cross-ring fragmentation of the oligosaccharide, but abundant SO_3 loss was present [19]. Recent work on the development of newer matrices has shown great promise in reducing SO_3 loss [20]. However, Na/H heterogeneity is an issue, which can complicate the analysis of complex GAG mixtures. These newer ILMs have been used to determine the approximate molecular weight of a heterogeneous trypsin inhibitor proteoglycan [24].

ESI is the most commonly used technique for ionizing sulfated GAGs. Due to the highly acidic nature of this class of molecules, negative-ion ESI is typically used. The first successful demonstration of negative ion ESI was performed with hyaluronic acid and chondroitin sulfate oligosaccharides up to 14 sugar residues in length [21]. Complexing the anionic GAG with a basic peptide or protein, similar to the aforementioned MALDI work, has also been demonstrated using negative ion ESI [25], but offers no advantage over direct ionization of the sulfated GAGs. One common problem in the analysis of sulfated GAGs by ESI-MS is that they readily coordinate with cations. During separation and purification of sulfated GAGs, GAG sodium salts are created which will produce considerable Na/H heterogeneity by ESI-MS analysis. ESI-MS analysis of the sodium and ammonium salts of heparin oligosaccharides demonstrated a decrease in sensitivity and produced a more complex mass spectrum when GAG sodium salts were used [26]. Analysis of heparin octa- and decasaccharides ammonium salts by ESI-MS produced several unreported oligosaccharides, leading the authors to conclude that analysis of GAG ammonium salts was preferred for the analysis of complex GAG mixtures. Because of the improvement in GAG analysis by the use of ammonium salts, a systematic evaluation of the influence of counterions on the ESI mass spectra. The authors examined the model highly-sulfated disaccharide, sucrose octasulfate (SOS), using primary, secondary, tertiary, and quaternary ammonium counterions with the same number of carbon atoms. Second, quaternary ammonium salts with chains of increasing number of carbon atoms were examined. Finally, phosphonium and polyamine were also examined. Primary, secondary, and tertiary ammonium salts produced low signal-to-noise mass spectra with substantial fragmentation and SO_3 loss. Quaternary ammonium and phosphonium salts produced abundant molecular ions with very little SO_3 loss in both positive and negative ion mode. From this systematic study, tetraethylammonium was found to be the optimal counterion for positive and negative ion ESI-MS [27].

Tandem Mass Spectrometry of Sulfated GAGs

FAB, MALDI, and ESI can be used to produce molecular ions of GAGs while minimizing or eliminating fragmentation and SO_3 loss of these labile molecules. While this is useful for determining GAG molecular weight and analysis of GAG oligosaccharide mixtures, tandem mass spectrometry is needed to determine the locations and types of modifications. Tandem mass spectrometry is not necessary to determine the linkage type as this is constant for the length of the GAG oligosaccharide chain. In order to describe the products observed from tandem mass spectrometry of GAGs, fragments are annotated as shown in Figure 2 [28]. While glycosidic bonds (B, C, Y, and Z; Figure 1.2) can be used to determine the monosaccharide with the modification, cross-ring cleavages (A and X; Figure 1.2) are necessary to determine location of modification within the monosaccharide. In tandem mass spectrometry analysis of sulfated GAGs utilizing vibrational excitation (e.g. collisionally activated decomposition (CAD) or infrared multiphoton dissociation (IRMPD)), the S-O bond of the sulfate group is more labile than glycosidic bonds and will readily fragment resulting in SO_3 loss. The challenge for practical tandem mass spectrometry analysis of sulfated GAGs is to produce abundant glycosidic and cross-ring fragmentation while minimizing or eliminating SO_3 loss.

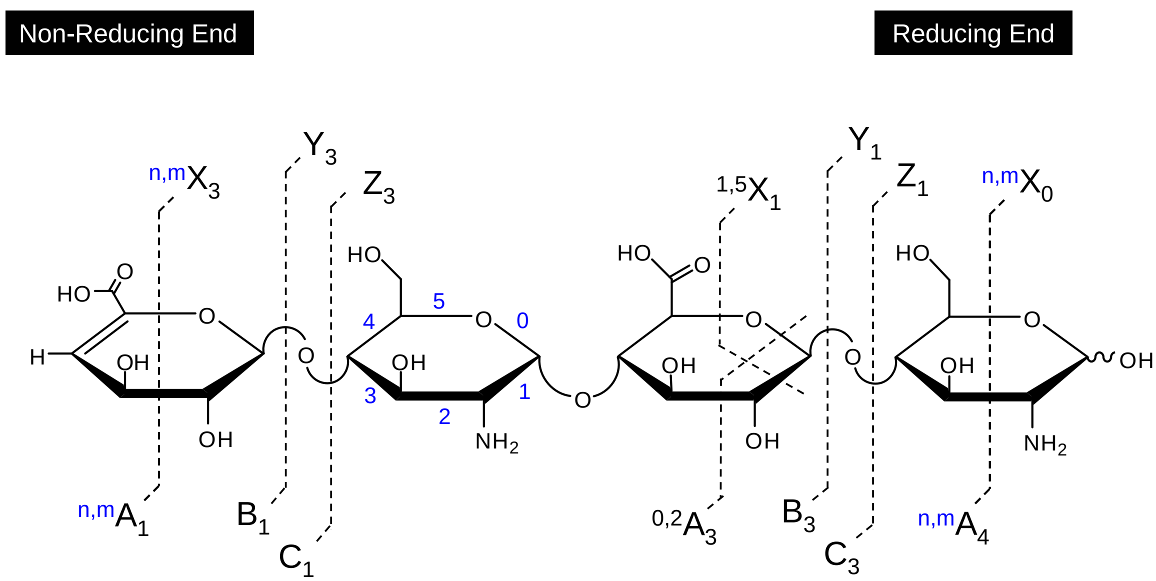

Figure 1.2. Fragment ion naming convention used for carbohydrates, adapted from Domon and Costello [28]. Superscripts in cross ring cleavage products refer to the bonds that are broken, which are numbered as shown for the second saccharide from the nonreducing end.

The initial study of sulfated GAGs by FAB-MS produced molecular ions accompanied by SO_3 loss, but also produced fragmentation of glycosidic bonds [14]. The authors conclude that this FAB-MS could be used for determining the sites of sulfation on sulfated GAGs. However, this method requires high sample purity, which may not be available as GAGs must be isolated from natural sources. Also, because only glycosidic bonds are cleaved the monosaccharide containing the modification can be determined, but the exact location of the modification cannot be determined. The first tandem mass spectrometry of GAGs using FAB-CAD-MS was reported on sulfated glucosamine monosaccharides in 1989 by Dallinga and coworkers [29]. FAB-CAD-MS of a series of isobaric monosulfated GAG disaccharides has been used to determine sulfate and linkage position [30]. The authors could not distinguish between isomers with the sulfate on the same saccharide unit (i.e. 4S vs. 6S), but could determine a 1→4 linkage was present based on the presence of the $^{0,2}A_2$ product ion. This work has also been demonstrated with negative ion ESI using either a quadrupole ion trap [31] or triple quadrupole mass spectrometer [32]. The challenge of tandem mass spectrometry analysis of sulfated GAGs larger than disaccharide was demonstrated by CAD-MS of trisulfated and tetrasulfated GAG tetrasaccharides [33]. CAD of singly-charged ions produced from FAB-MS resulted in some glycosidic and cross-ring cleavages that were inadequate for determining GAG structure. MS^3 produced more glycosidic cleavages, but did not increase the number of cross-ring cleavages that are necessary to determine the sites of sulfation. Using ESI, Zaia and coworkers later demonstrated that the GAG precursor ion charge state influences the number of type of observed product ions [34]. This work demonstrated that glycosidic cleavages could be maximized and SO_3 loss minimized if the charge state of the precursor ion is equal to or greater than the number of sulfate groups. The work also demonstrated that complexation with Ca^{2+} would minimize SO_3 loss, leading the authors to conclude that GAG sulfate groups are most stable when ionized. This research demonstrated that tandem mass spectrometry could be used to determine GAG modification. However, increasing the number of cross-ring cleavages would be necessary to determine the sites of modification of sulfated GAGs.

As previously mentioned, the low amount of information derived from tandem mass spectrometry using threshold dissociation makes structure determination of sulfated GAGs difficult. The few peaks observed were not enough to distinguish isobaric species (e.g. 4S vs. 6S sulfation) or determine C5 stereochemistry (e.g. GlcA vs. IdoA). A number of methods have been developed for determining GAG structure to overcome the problems from structure determination using only tandem mass spectrometry. The first application of oligosaccharide structure determination using mass spectrometry utilized MALDI-MS in combination with enzymatic digestion. The oligosaccharide is digested using enzymes that cleave at specific glycosidic bonds. The enzymatic products are analyzed with MALDI-MS by complexing the enzymatic products with a basic peptide. The combination of multiple lyases and mass spectrometry allow the sequence to be unambiguously determined, including distinguishing 4S from 6S sulfation and distinguishing GlcA form IdoA. This method has been used to sequence a hexasaccharide and two decasaccharides [22], an unusual 3-O-sulfate containing tetrasaccharide [35] and decasaccharide [36], and an octasaccharide that binds to the herpes simplex virus glycoprotein D [10]. A similar technique, referred to as the heparin oligosaccharide sequence tool (HOST) technique, combines enzymatic digestion with HPLC-ESI-MS and tandem mass spectrometry. The oligosaccharide of interest is enzymatically digested and the resulting disaccharides are separated by HPLC and interrogated by ESI-MS, including MS^2 and MS^3. Using the MS and tandem mass spectrometry data in combination with database searching, the disaccharide structure can be determined. The oligosaccharide structure is then determined by reassembling the data into the complete oligosaccharide [37]. Using HOST, isobaric disaccharides such as 4S and 6S sulfation can be distinguished using tandem mass spectrometry. However, enzymatic digestion produces a Δ-uronic acid (Δ-UA) at the non-reducing end (NRE), erasing the original C5 stereochemistry. As a result, C5 stereochemistry cannot be determined using the HOST technique.

The abundances of key product ions that result from tandem mass spectrometry have been used to determine sulfate position and distinguish GlcA from IdoA. For this work, a mixture of isobaric hexasaccharides differing only in sulfate position or C5 stereochemistry were analyzed by ESI-CAD-MS. The abundance of the B_5, B_3, and Y_1 product ions can be used to determine the sulfate position, while the abundance of the Y_5 and $^{0,2}X_5$ product ions distinguish GlcA from IdoA. Product ion abundances produced from tandem mass spectrometry of a series of known isobaric mixtures are used to create a "calibration curve." The unknown product ion abundances are compared to this calibration curve and used to determine sulfate position or C5 stereochemistry. Because this method requires comparison against known compounds, a new calibration curve must be created for each sample analyzed. Currently, this technique has only been reported for the analysis of chondroitin sulfate oligosaccharides [38].

Because of the limited amount of information produced from vibrational excitation of sulfated GAGs, improvements are needed to rapidly sequence these molecules. Recently, the application of electron-ion interactions has produced a number of dissociation techniques. Of these techniques, electron capture dissociation (ECD) has found widespread application for the characterization of biomolecules [39]. For ECD, low-energy electrons (≤1 eV) recombine with multiply-charged precursor ions and produce a radical species that fragments differently than by low-energy or threshold methods of dissociation. ECD has been used to determine the sites of labile post-translational modifications, such as glycosylation, sulfation, or phosphorylation on peptides and proteins [40-45]. Electron detachment dissociation (EDD) [46] is the negative ion complement of ECD [47], and is useful for the characterization of acidic molecules which do not easily form positive ions, such as oligodeoxynucleotides [48]. For EDD, multiply-charged precursor anions are irradiated with moderate energy (~19 eV) electrons, resulting in electron ejection from the precursor ion. Similar to ECD, a radical species is created which fragments differently than by low energy or threshold dissociation of the even-electron precursor ion. Because of the highly acidic nature of sulfated GAGs, EDD is ideally suited for the analysis of these molecules. For this work, the successful application and characterization of EDD to the characterization of sulfated GAGs is reported.

The experimental section in **Chapter 2** details carbohydrate sample preparation and operation of the ESI-FTMS instrument. The influence of solution conditions on charge state and degree of sodium cationization are also presented. A brief description of the parameters used to perform EDD experiments will be described, and tuning ideas for optimization of EDD is also described.

Chapter 3 presents the first application of EDD to the analysis of GAG tetrasaccharides. A series of heparan sulfate tetrasaccharides with varying modifications (e.g. 0 – 2 sulfates, acetylation) are analyzed by CAD, IRMPD and EDD. Compared to CAD and IRMPD, EDD produces cleavage of every glycosidic bond and abundant cross-ring fragmentation. Cross-ring fragmentation occurs primarily on hexuronic acid residues, in the form of both A- and X-ions. Fragmentation pathways are proposed based on the observed product ions, including proposed mechanisms based on radical ion rearrangement.

Mass spectrometry is typically a stereochemistry-insensitive technique. In **Chapter 4**, EDD of a pair of GAG epimers demonstrates that EDD can distinguish GlcA from IdoA in HS tetrasaccharides based on the presence of key product ions. These product ions, $^{0,2}A_3$, B_3', and B_3'-CO_2, which are not observed in IRMPD of the same ions, are present in EDD of GlcA but not in IdoA containing tetrasaccharides. Mechanisms are proposed to describe the preference for formation of these key product ions.

Chapters 3 and 4 demonstrate that EDD is a powerful tool for determining sites of modification and C5 stereochemistry of GAG tetrasaccharides. However, most GAG-protein interactions occur for GAGs longer than tetrasaccharide. Therefore, practical tandem mass spectrometry analysis of GAGs must be performed on GAGs larger than tetrasaccharide. EDD of DS oligosaccharides ranging in length from tetrasaccharide to decasaccharide is presented in **Chapter 5**. Cross-ring fragmentation occurs primarily in IdoA residues, and cleavage of all glycosidic bonds is observed. More glycosidic and cross-ring fragmentation is observed by EDD than by IRMPD of these molecules. A new annotation scheme is presented in Chapter 5 to present the large number of products produced from an EDD experiment that will be used for the remainder of this work.

EDD of DS oligosaccharides produces many products that are accompanied by the loss of SO_3. The ability to control SO_3 loss, while not influencing glycosidic or cross-ring fragmentation, is demonstrated in **Chapter 6**. Controlling the charge of the precursor ion eliminates SO_3 loss, producing a much simpler EDD mass spectrum. The charge on the precursor ion can be manipulated by selecting the proper charge state, or through the addition of sodium cations. Regardless of the charge on the precursor ion, cross-ring fragmentation occurs primarily on IdoA residues, and cleavage of most glycosidic bonds is observed.

The fragmentation of GAGs by EDD in Chapter 2 is proposed to occur through either electron detachment (EDD) or through electronic excitation of the precursor ion, referred to as electron induced dissociation (EID). In order to distinguish products that arise from direct fragmentation versus those that arise from electron detachment, a series of singly-charged GAG tetrasaccharides is analyzed by EID in **Chapter 7**. The observed product ions can only form as a result of direct dissociation by electronic excitation, allowing product formation via EID to be examined int eh absence of EDD. EID of GAG tetrasaccharides produces fragmentation similar to EDD of the same tetrasaccharides, with cross-ring fragmentation occurring primarily on hexuronic acid residues. These results indicate that many GAG products result from EID of the precursor ion.

This dissertation focuses on the characterization of structural features of sulfated GAGs using mass spectrometry and tandem mass spectrometry.

REFERENCES

1. Perrimon, N.; Bernfield, M., Cellular functions of proteoglycans--an overview. *Semin. Cell Dev. Biol.* **2001,** *12*, 65-67.
2. Fannon, M.; Forsten, K. E.; Nugent, M. A., Potentiation and Inhibition of bFGF Binding by Heparin: A Model for Regulation of Cellular Response. *Biochemistry* **2000,** *39*, 1434-1445.
3. Wu, Z. L.; Zhang, L.; Yabe, T.; Kuberan, B.; Beeler, D. L.; Love, A.; Rosenberg, R. D., The Involvement of Heparan Sulfate (HS) in FGF1/HS/FGFR1 Signaling Complex. *J. Biol. Chem.* **2003,** *278*, 17121-17129.
4. Smailbegovic, A.; Lever, R.; Page, C. P., The effects of heparin on the adhesion of human peripheral blood mononuclear cells to human stimulated umbilical vein endothelial cells. *Br. J. Pharmacol.* **2001,** *134*, 827-836.
5. Sadir, R.; Imberty, A.; Baleux, F.; Lortat-Jacob, H., Heparan Sulfate/Heparin Oligosaccharides Protect Stromal Cell-derived Factor-1 (SDF-1)/CXCL12 against Proteolysis Induced by CD26/Dipeptidyl Peptidase IV. *J. Biol. Chem.* **2004,** *279*, 43854-43860.
6. Gotte, M., Syndecans in Inflammation. *The FASEB Journal* **2003,** *17*, 575-591.
7. Batinic, D.; Robey, F. A., The V3 region of the envelope glycoprotein of human immunodeficiency virus type 1 binds sulfated polysaccharides and CD4-derived synthetic peptides. *J. Biol. Chem.* **1992,** *267*, 6664-6671.
8. Chen, Y.; Maguire, T.; Hileman, R. E.; Fromm, J. R.; Esko, J. D.; Linhardt, R. J.; Marks, R. M., Dengue virus infectivity depends on envelope protein binding to target cell heparan sulfate. *Nature Med.* **1997,** *3*, 866-871.

9. Williams, R. K.; Straus, S. E., Specificity and affinity of binding of herpes simplex virus type 2 glycoprotein B to glycosaminoglycans. *J. Virol.* **1997,** *71*, 1375-1380.

10. Liu, J.; Shriver, Z.; Pope, R. M.; Thorp, S. C.; Duncan, M. B.; Copeland, R. J.; Raska, C. S.; Yoshida, K.; Eisenberg, R. J.; Cohen, G.; Linhardt, R. J.; Sasisekharan, R., Characterization of a Heparan Sulfate Octasaccharide That Binds to Herpes Simplex Virus Type 1 Glycoprotein D. *J. Biol. Chem.* **2002,** *277*, 33456-33467.

11. Liu, D. F.; Shriver, Z.; Gi, Y. W.; Venkataraman, G.; Sasisekharan, R., Dynamic regulation of tumor growth and metastasis by heparan sulfate glycosaminoglycans. *Semin. Throm. Hemost.* **2002,** *28*, 67-78.

12. Chi, L. L.; Amster, J.; Linhardt, R. J., Mass spectrometry for the analysis of highly charged sulfated carbohydrates. *Curr. Anal. Chem.* **2005,** *1*, 223-240.

13. Horne, A.; Gettins, P., H-1-NMR Spectral Assignments for 2 Series of Heparin-Derived Oligosaccharides. *Carbohydr. Res.* **1992,** *225*, 43-57.

14. Carr, S. A.; Reinhold, V. N., Structural Characterization of Sulfated Glycosaminoglycans by Fast Atom Bombardment Mass-Spectrometry - Application to Chondroitin Sulfate. *J. Carb. Chem.* **1984,** *3*, 381-401.

15. Dell, A.; Rogers, M. E.; Thomas-Oates, J. E.; Huckerby, T. N.; Sanderson, P. N.; Nieduszynski, I. A., Fast-atom-bombardment mass-spectrometric strategies for sequencing sulphated oligosaccharides. *Carbohydr. Res.* **1988,** *179*, 7-19.

16. Reinhold, V. N.; Carr, S. A.; Green, B. N.; Petitou, M.; Choay, J.; Sinay, P., Structural Characterization of Sulfated Glycosaminoglycans by Fast-Atom-Bombardment Mass-Spectrometry - Application to Heparin Fragments Prepared by Chemical Synthesis. *Carbohydr. Res.* **1987,** *161*, 305-313.

17. Juhasz, P.; Biemann, K., Mass Spectrometric Molecular-Weight Determination of Highly Acidic Compounds of Biological Significance via Their Complexes with Basic Polypeptides. *Proc. Natl. Acad. Sci. U. S. A.* **1994,** *91*, 4333-4337.

18. Juhasz, P.; Biemann, K., Utility of non-covalent complexes in the matrix-assisted laser desorption ionization mass spectrometry of heparin-derived oligosaccharides. *Carbohydr. Res.* **1995,** *270*, 131-147.

19. Laremore, T. N.; Murugesan, S.; Park, T. J.; Avci, F. Y.; Zagorevski, D. V.; Linhardt, R. J., Matrix-Assisted Laser Desorption/Ionization Mass Spectrometric Analysis of Uncomplexed Highly Sulfated Oligosaccharides Using Ionic Liquid Matrices. *Anal. Chem.* **2006,** *78*, 1774-1779.

20. Laremore, T. N.; Zhang, F.; Linhardt, R. J., Ionic Liquid Matrix for Direct UV-MALDI-TOF-MS Analysis of Dermatan Sulfate and Chondroitin Sulfate Oligosaccharides. *Anal. Chem.* **2007,** *79*, 1604-1610.

21. Takagaki, K.; Kojima, K.; Majima, M.; Nakamura, T.; Kato, I.; Endo, M., Ion-Spray Mass-Spectrometric Analysis of Glycosaminoglycan Oligosaccharides. *Glycoconjugate J.* **1992,** *9*, 174-179.

22. Venkataraman, G.; Shriver, Z.; Raman, R.; Sasisekharan, R., Sequencing complex polysaccharides. *Science* **1999,** *286*, 537-542.

23. Laremore, T. N.; Linhardt, R. J., Improved matrix-assisted laser desorption/ionization mass spectrometric detection of glycosaminoglycan disaccharides as cesium salts. *Rapid Commun. Mass Spectrom.* **2007,** *21*, 1315-1320.

24. Chi, L.; Wolff, J. J.; Laremore, T. N.; Restaino, O. F.; Xie, J.; Schiraldi, C.; Toida, T.; Amster, I. J.; Linhardt, R. J., Structural Analysis of Bikunin Glycosaminoglycan. *J. Am. Chem. Soc.* **2008,** *130*, 2617-2625.

25. Siegel, M. M.; Tabei, K.; Kagan, M. Z.; Vlahov, I. R.; Hileman, R. E.; Linhardt, R. J., Polysulfated Carbohydrates Analyzed as Ion-paired Complexes with Basic Peptides and Proteins Using Electrospray Negative Ionization Mass Spectrometry. *J. Mass Spectrom.* **1997,** *32*, 760-772.

26. Chai, W.; Luo, J.; Lim, C. K.; Lawson, A. M., Characterization of Heparin Oligosaccharide Mixtures as Ammonium Salts Using Electrospray Mass Spectrometry. *Anal. Chem.* **1998,** *70*, 2060-2066.

27. Gunay, N. S.; Tadano-Aritomi, K.; Toida, T.; Ishizuka, I.; Linhardt, R. J., Evaluation of Counterions for Electrospray Ionization Mass Spectral Analysis of A Highly Sulfated Carbohydrate, Sucrose Octasulfate. *Anal. Chem.* **2003,** *75*, 3226-3231.

28. Domon, B.; Costello, C. E., A systematic nomenclature for carbohydrate fragmentations in FAB-MS/MS spectra of glycoconjugates. *Glycoconjugate J.* **1988,** *5*, 397-409.

29. Dallinga, J. W.; Rinkema, F. D.; Heerma, W., Fast atom bombardment mass spectrometry of some aminoglucoses and glucosamine phosphates and sulphates. *Biol. Mass Spectrom.* **1989,** *18*, 241-246.

30. Lamb, D. J.; Wang, H. M.; Mallis, L. M.; Linhardt, R. J., Negative ion fast-atom bombardment tandem mass spectrometry to determine sulfate and linkage position in glycosaminoglycan-derived disaccharides. *J. Am. Soc. Mass Spectrom.* **1992,** *3*, 797-803.

31. Desaire, H.; Leary, J. A., Detection and quantification of the sulfated disaccharides in chondroitin sulfate by electrospray tandem mass spectrometry. *J. Am. Soc. Mass Spectrom.* **2000,** *11*, 916-920.

32. Zaia, J.; Costello, C. E., Compositional Analysis of Glycosaminoglycans by Electrospray Mass Spectrometry. *Anal. Chem.* **2001,** *73*, 233-239.

33. Ii, T.; Kubota, M.; Hirano, T.; Ohashi, M.; Yoshida, K.; Suzuki, S., FAB CID-MS/MS Characterization of tetrasaccharide trisulfate and tetrasulfate derived from the antigenic determinant recognized by the anti-chondroiton sulfate monoclonal-antibody MO-225. *Glycoconjugate J.* **1995,** *12*, 282-289.

34. Zaia, J.; Costello, C. E., Tandem Mass Spectrometry of Sulfated Heparin-Like Glycosaminoglycan Oligosaccharides. *Anal. Chem.* **2003,** *75*, 2445-2455.

35. Liu, J.; Shriver, Z.; Blaiklock, P.; Yoshida, K.; Sasisekharan, R.; Rosenberg, R. D., Heparan Sulfate D-Glucosaminyl 3-O-Sulfotransferase-3A Sulfates N-Unsubstituted Glucosamine Residues. *J. Biol. Chem.* **1999,** *274*, 38155-38162.

36. Shriver, Z.; Raman, R.; Venkataraman, G.; Drummond, K.; Turnbull, J.; Toida, T.; Linhardt, R.; Biemann, K.; Sasisekharan, R., Sequencing of 3-O sulfate containing heparin decasaccharides with a partial antithrombin III binding site. *Proc. Natl. Acad. Sci.* **2000,** *97*, 10359-10364.

37. Saad, O. M.; Leary, J. A., Heparin Sequencing Using Enzymatic Digestion and ESI-MS with HOST: A Heparin/HS Oligosaccharide Sequencing Tool. *Anal. Chem.* **2005,** *77*, 5902-5911.

38. Zaia, J.; Li, X.-Q.; Chan, S.-Y.; Costello, C. E., Tandem mass spectrometric strategies for determination of sulfation positions and uronic acid epimerization in chondroitin sulfate oligosaccharides. *J. Am. Soc. Mass Spectrom.* **2003,** *14*, 1270-1281.

39. Zubarev, R. A.; Kelleher, N. L.; McLafferty, F. W., Electron Capture Dissociation of Multiply Charged Protein Cations. A Nonergodic Process. *J. Am. Chem. Soc.* **1998,** *120*, 3265-3266.

40. Hakansson, K.; Cooper, H. J.; Emmett, M. R.; Costello, C. E.; Marshall, A. G.; Nilsson, C. L., Electron Capture Dissociation and Infrared Multiphoton Dissociation MS/MS of an N-Glycosylated Tryptic Peptide To Yield Complementary Sequence Information. *Anal. Chem.* **2001,** *73*, 4530-4536.

41. Kelleher, N. L.; Zubarev, R. A.; Bush, K.; Furie, B.; Furie, B. C.; McLafferty, F. W.; Walsh, C. T., Localization of Labile Posttranslational Modifications by Electron Capture Dissociation: The Case of γ-Carboxyglutamic Acid. *Anal. Chem.* **1999,** *71*, 4250-4253.

42. Mirgorodskaya, E.; Roepstorff, P.; Zubarev, R. A., Localization of O-glycosylation sites in peptides by electron capture dissociation in a fourier transform mass spectrometer. *Anal. Chem.* **1999,** *71*, 4431-4436.

43. Niiranen, H.; Budnik, B. A.; Zubarev, R. A.; Auriola, S.; Lapinjoki, S., High-performance liquid chromatography-mass spectrometry and electron-capture dissociation tandem mass spectrometry of osteocalcin - Determination of gamma-carboxyglutamic acid residues. *Journal of Chromatography A* **2002,** *962*, 95-103.

44. Shi, S. D. H.; Hemling, M. E.; Carr, S. A.; Horn, D. M.; Lindh, I.; McLafferty, F. W., Phosphopeptide/phosphoprotein mapping by electron capture dissociation mass spectrometry. *Anal. Chem.* **2001,** *73*, 19-22.
45. Stensballe, A.; Jensen, O. N.; Olsen, J. V.; Haselmann, K. F.; Zubarev, R. A., Electron capture dissociation of singly and multiply phosphorylated peptides. *Rapid Commun. Mass Spectrom.* **2000,** *14*, 1793-1800.
46. Budnik, B. A.; Haselmann, K. F.; Zubarev, R. A., Electron detachment dissociation of peptide di-anions: an electron-hole recombination phenomenon. *Chem. Phys. Lett.* **2001,** *342*, 299-302.
47. Zubarev, R. A., Reactions of polypeptide ions with electrons in the gas phase. *Mass Spectrom. Rev.* **2003,** *22*, 57.
48. Yang, J.; Mo, J.; Adamson, J. T.; Hakansson, K., Characterization of Oligodeoxynucleotides by Electron Detachment Dissociation Fourier Transform Ion Cyclotron Resonance Mass Spectrometry. *Anal. Chem.* **2005,** *77*, 1876-1882.

CHAPTER 2

EXPERIMENTAL

Preparation of GAG Oligosaccharides

Heparan sulfate tetrasaccharides are prepared by partial enzymatic depolymerization of heparan sulfate sodium salt (Celsus Laboratories, Cincinnati, OH). A 20 mg/mL heparan sulfate solution in 50 mM Tris-HCl/60 mM sodium acetate buffer, pH 8 was incubated at 37°C with heparinase II (Sigma, St. Louis, MO). Dermatan sulfate (DS) oligosaccharides are prepared by partial enzymatic depolymerization of porcine intestinal mucosa dermatan sulfate (Celsus Laboratories, Cincinnati, OH). A 20 mg/mL dermatan sulfate solution in 50 mM Tris-HCl/60 mM sodium acetate buffer, pH 8 is incubated at 37°C with chondroitin ABC lyase from *Proteus vulgaris*, EC 4.2.2.4. (Seikagaku, Japan). For either sample, the absorbance at 232 nm is monitored to determine when the digestion was 50% complete. The digestion mixture is then heated at 100°C for 3 min. High-molecular-weight oligosaccharides and the glycosidic enzyme are removed by ultra-filtration using a 5000 MWCO membrane. The resulting oligosaccharide mixture is concentrated by rotary evaporation and fractionated by low pressure GPC on a Bio-Gel P10 (Bio-Rad, Richmond, CA) column. Fractions containing each oligosaccharide are desalted by GPC on a Bio-Gel P2 column and freeze-dried. Further purification of the oligosaccharides is carried out using strong anion exchange high-pressure liquid chromatography (SAX-HPLC) on a semi-preparative SAX S5 Spherisorb column (Waters Corp, Milford, MA). The SAX-HPLC fractions containing > 90% of each oligosaccharide are collected, desalted by GPC, and freeze-dried. The solid was reconstituted in water and purified a second time by SAX-HPLC. Only the top 30% of the chromatographic peak is collected, desalted, and freeze-dried. Concentration of each oligosaccharide solution is determined by measuring the absorbance at 232 nm ($\varepsilon = 3800\ M^{-1}cm^{-1}$). The resulting fraction containing individual oligosaccharides are characterized by PAGE, ESI-MS, and high-field nuclear magnetic resonance (NMR) spectroscopy.

Mass Spectrometry Analysis

Experiments are performed with a 9.4 T Bruker Apex QhFTMS (Billerica, MA) fitted with an Apollo II dual source, a 25 W CO_2 laser (Synrad model J48-2, Mukilteo, WA) for IRMPD, and an indirectly heated hollow cathode for generating electrons for ECD and EDD. Bruker Apex Control is used for data acquisition. The composition of the ESI solution has a tremendous influence on the charge state and degree of Na/H heterogeneity of the sulfated GAGs. Generally, decreasing the charge state of the oligosaccharides is accomplished by the addition of acid (e.g. formic acid) to the ESI solution, while increasing the oligosaccharide charge state is accomplished by addition of base to the ESI solution (e.g. NH_3). For example, ESI solutions for sulfated GAGs are typically made in 50:50 methanol:H_2O. A 5 μM solution of a DS octasaccharide in a solution of 50:50:0.1 methanol:H_2O:NH_3 will produce 5^-, 4^-, and 3^- ions. Typically, the 4^- ion is the most abundant ion, and Na/H heterogeneity is present for all charge states. A 5 μM solution of the DS octasaccharide in 50:50:0.1 methanol:H_2O:formic acid will eliminate Na/H heterogeneity and produce an abundant 4^- ion and some 3^- ion, but no 5^- ions. Because fewer charge states are present and Na/H heterogeneity has been minimized, the 4^- ion of the DS octasaccharide will be very abundant. For studies requiring sodium, the octasaccharide can be introduced at a concentration of 150 μM in 50:50 methanol:H_2O with 1 mM NaOH producing 5^-, 4^-, and 3^- ions with abundant Na/H heterogeneity, or by the addition of a volatile sodium salt, such as Na_2CO_3. An increase in DS octasaccharide concentration is necessary when sodium is present as the octasaccharide is distributed over many different charge states and degrees of Na/H heterogeneity. Sulfated GAGs can be ionized by either regular-flow ESI or nanospray. For regular-flow ESI, sample solutions are infused at a rate of 120 μL/hour. For nanospray, samples are infused at a rate of 10 μL/hour using a pulled fused silica tip (model# FS360-20-10-D-20, New Objective, Woburn, MA). The pulled fused silica tips with 20 μm capillary ID and 10 μm tip ID produce a more stable spray at a flow rate of 10 μL/hour than the fused silica tips with the 75 μm capillary ID and 15 μm tip ID.

Solution concentrations and ion accumulation time will vary and depends on the ability to produce enough ions for EDD. The precursor ion abundance prior to EDD must be $\geq 1 \times 10^7$, with the instrument amplifier gain is set to low (RGAIN = 0). For the EDD experiments, precursor ions are isolated in the external quadrupole and accumulated for 1–10 seconds before injection into the FTMS cell. The isolation/cell fill can be repeated up to 6 times. Typically, a maximum of 6 cell fills is used because no increase in ion intensity is observed when using more than 6 cell fills. The selection of the precursor ion is further refined by using in-cell isolation with a coherent harmonic excitation frequency (CHEF) event. The precursor ions are then irradiated with electrons for 1 second. For electron irradiation the cathode bias is set to -19 V, the ECD lens is set to approximately -19.5 V, and the cathode heater was set to 1.6 A. With the ECD lens set to a potential higher than the cathode potential, no electrons enter the analyzer cell. The ECD lens potential is increased in 0.1V steps until the precursor ion intensity decreases by 50%. Typically, this occurs within ±0.2V of the cathode potential. Ions are excited with an RF frequency chirp that covered the range of 100 – 2000 *m/z*. 24 acquisitions are signal averaged per mass spectrum. For each mass spectrum, 512K points were acquired at a 2.4 MHz digitization rate, padded with one zero fill, and apodized using a sinebell window. Background spectra are acquired by leaving all parameters the same but setting the cathode bias to 0 V to ensure that no electrons reached the analyzer cell. Background spectra are not subtracted from the EDD spectra, but are used to ensure that very few products were formed during ion accumulation and isolation. IRMPD spectra are acquired using the same experimental setup as EDD, but replacing the electron irradiation event with a laser pulse. For IRMPD, ions are irradiated for 0.01 – 0.2 seconds with beam attenuation set to pass from 40 – 60% of full power.

Typically, external calibration of IRMPD and EDD mass spectra produce mass accuracy of 5 ppm. Internal calibration is performed using confidently assigned glycosidic bond cleavage products as internal calibrants, providing mass accuracy of <1 ppm. Internal calibration is performed using Bruker Data Analysis. Due to the larger number of low intensity products formed by EDD, only peaks with S/N ≥ 10 are reported. Peaks are automatically picked using the "FTMS" peak picking feature in Data Analysis with the "S/N threshold" set to 10, the "Relative intensity threshold (base peak)" set to ≤0.001, and the "Absolute intensity threshold" set to 100. The "SNAP" peak picking feature in Data Analysis cannot be used because it is designed for peptide/protein analysis. Also, the large number of low intensity product ions and the presence of product ions differing by the mass of one or two hydrogen atoms cause considerable problems for the SNAP algorithm. After internal calibration of the EDD mass spectra, product ions can be assigned using accurate mass measurement.

^{18}O Labeling

^{18}O labeling of the anomeric carbon of the reducing end is performed by dissolving 2 nmol of the oligosaccharide into 10 μL of $H_2{}^{18}O$ (Cambridge Isotope Labs, Andover, MA). The microcentrifuge tube is sealed with Parafilm™ to ensure no ^{18}O-water escapes. The solution is heated overnight at 60°C. It may be necessary to heat the solution to 60°C for two days to increase ^{18}O-labeling efficiency. Prior to mass spectrometry analysis, the volume of ^{18}O-water is determined using a micropipette, and additional $H_2^{18}O$ is added to the solution to bring the total volume of $H_2^{18}O$ to 10 μL. 10 μL of methanol is then added to the $H_2^{18}O$ oligosaccharide solution before infusion into the mass spectrometer. If necessary, acid or base can be added to the methanol prior to addition to the $H_2^{18}O$ oligosaccharide solution.

CHAPTER 3

ELECTRON DETACHMENT DISSOCIATION OF GLYCOSAMINOGLYCAN TETRASACCHARIDES*

*Reproduced with permission from Wolff, J.J.; Lianli, C.; Linhardt, R.J.; Amster, I.J. Journal of the American Society for Mass Spectrometry, **2007**, *18*, 234-244.

ABSTRACT

The first application of electron detachment dissociation (EDD) to carbohydrates is presented. The structural characterization of glycosaminoglycan (GAG) oligosaccharides by mass spectrometry is a longstanding problem, because of the lability of these acidic, polysulfated carbohydrates. Doubly-charged negative ions of four GAG tetrasaccharides are examined by EDD, collisionally activated dissociation (CAD), and infrared multiphoton dissociation (IRMPD). EDD is found to produce information-rich mass spectra with both cross ring and glycosidic cleavage product ions. In contrast, most of the product ions produced by CAD and IRMPD result from glycosidic cleavage. EDD shows great potential as a tool for locating the sites of sulfation and other modifications in glycosaminoglycan oligosaccharides.

INTRODUCTION

Glycosaminoglycans (GAGs) are linear, polydisperse, sulfated polysaccharides found in a wide variety of organisms, from bacteria to humans [1]. GAGs play an important role in many biological processes such as cell-cell signaling [2], the regulation of biochemical pathways [3,4], and inflammation reactions [5]. GAGs form the carbohydrate portion of proteoglycans, which are high molecular weight (up to and >1 MDa) molecules of high complexity. GAGs are composed of a repeating disaccharide of an acidic sugar and an amino sugar, and exhibit complexity through the degree and sites of sulfation in each disaccharide unit, functionalization of the amino group in the glucosamine residues, and chirality of the C5 carbon on the hexuronic acid residues. Additional complexity arises at the proteoglycan level from the distribution of GAG chains that bind to the core proteins.

Heparin and heparan sulfate (HS) are the most structurally complex GAGs [6]. They consist of 1,4-linked repeating disaccharide of hexuronic acid and glucosamine. The hexuronic acid is either glucuronic (GlcA) or iduronic acid (IdoA), and may be sulfated at the hydroxyl group on carbon C2. The glucosamine (GlcN) may be sulfated at the hydroxyl group at carbon C3 or C6, and may be unmodified, acetylated, or sulfated at the amino group on carbon C2. Determining the pattern of modification (sulfation, N-acetylation, GlcA vs. IdoA) in heparin/HS polysaccharides is of significant interest as their biological activities are believed to be controlled by the pattern of modification [7-9].

Tandem mass spectrometry (MS/MS) is an excellent tool for characterizing the structure of biomolecules since it is rapid, versatile, and sensitive. However, the application of MS/MS to sulfated GAGs has been hindered by their large size, sulfation heterogeneity, and the lability of the sulfate groups, particularly during ion activation [10]. GAGs have been ionized by fast atom bombardment (FAB) [11,12], electrospray ionization (ESI) [13], and matrix assisted laser desorption/ionization (MALDI) [14-17]. Analysis of sulfated GAGs by FAB is relatively uninformative due to the abundant loss of $NaSO_3$ and SO_3 from the singly-charged precursor ions. Ion activation by collisionally activated dissociation (CAD) or infrared multiphoton dissociation (IRMPD) of singly-charged sulfated GAGs results in abundant loss of SO_3, frustrating efforts to determine sites of sulfation. ESI is the preferred ionization technique for retaining the labile sulfate groups. During MS/MS, SO_3 loss can be minimized and glycosidic cleavages maximized if the charge on the ion is equal to the number of sulfate groups [18]. However, the lack of significant cross ring cleavages makes it difficult to determine the site of modification within each saccharide ring.

In order to increase the structural information that can be derived by mass spectrometry, a number of techniques have been investigated. Sulfated oligosaccharides have been derivatized by permethylation [19]. Localization of the site of sulfation are then determined from MS/MS of the permethylated oligosaccharides. Small oligosaccharide sequences can be determined by a combination of enzymatic digestion, MS^n of the disaccharides, and database searching [20]. Capillary electrophoresis has been combined with MS/MS to sequence a complex mixture [21]. These methods do not provide sufficient cross-ring fragmentation to determine the pattern of sulfation, acetylation, and hexuronic acid stereochemistry on a GAG oligosaccharide. There is thus great interest in applying novel ion activation methods to advance the MS/MS analysis of sulfated carbohydrates.

Ion activation by electrons is finding widespread application to biomolecule structure analysis. First reported in 1998, electron capture dissociation (ECD) is an ion activation method in which an odd-electron ion is formed by the recombination of a multiply-charged positive ion with a low energy (<1 eV) electron [22]. Informative fragment ions result from the dissociation of the odd-electron ion. An intriguing aspect of ECD is that it is believed to be non-ergodic [23]. For example, it promotes extensive fragmentation of peptide backbones without loss of labile post-translational modifications such as glycosylation or phosphorylation [24,25]. Positively-charged oligosaccharides have been dissociated by ECD [26]. Due to the acidic nature of sulfated GAGs, the formation of multiply-charged positive ions is difficult. We have recently obtained results for the ECD analysis of sulfated GAGs (manuscript in preparation), but find that this approach is not widely applicable because of the difficulty in forming multiply-charged positive ions for these acidic molecules.

Given the propensity of GAGs to form negative ions, we have explored the application of electron detachment dissociation (EDD) for the fragmentation of multiply-charged negative ions of some model GAG tetrasaccharides. EDD is the negative ion complement of ECD [27]; although electron detachment can be achieved in high energy collisions with inert gases [28], it is more easily accomplished by irradiating a multiply charged negative ion with electrons of moderate kinetic energy (15 – 20 eV), causing electron detachment and leading to ion fragmentation [29-34]. This technique has been applied principally to peptides [29-32], but also to other compounds that can form negative ions, specifically nucleotides [34] and a ganglioside [33], but otherwise there are very few reports of EDD in the literature. Here we present the first examples of the application of EDD to the analysis of GAG tetrasaccharides.

EXPERIMENTAL

Preparation of Heparan Sulfate Tetrasaccharides

Heparan sulfate sodium salt was obtained from Celsus Laboratories (Cincinnati, OH).

The heparan sulfate was digested with heparinase II (Sigma, St. Louis, MO) and fractionated by gel-permeation chromatography using a P-10 column (Bio-Rad, Hercules, CA) to obtain uniform sized oligosaccharides. The fraction containing tetrasaccharides was desalted on a Bio-Rad P-2 column and concentrated by freeze-drying. Fractions containing individual tetrasaccharides were collected from semi-preparative SAX-HPLC (Shimadzu, Columbia, MD) using a Spherisorb column (Waters Corp, Milford, MA), desalted on a Bio-Rad P-2 column, and freeze-dried [35]. The structure of the three tetrasaccharides (structures ***1***, ***2***, and ***4***) were determined by 1D and 2D proton NMR. Tetrasaccharide ***3*** was prepared from tetrasaccharide ***1*** by *N*-sulfonation using the following protocol: 50 μg of tetrasaccharide ***1*** was dissolved in 12.5 μL of solution containing 10 mg/mL sodium bicarbonate and 10 mg/mL trimethylamine-sulfurtrioxide complex and incubated at 50 °C for 12 h. Equal portions of sodium bicarbonate and trimethylamine-sulfurtrioxide complex were added two more times at 12 h intervals. The solution was then desalted by a P-2 spin column (Bio-Rad, Hercules, CA) and the product was freeze-dried [36].

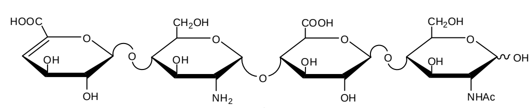

1

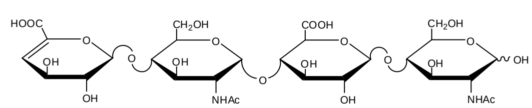

2

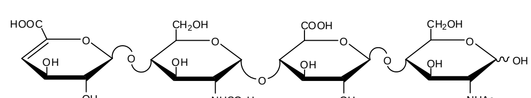

3

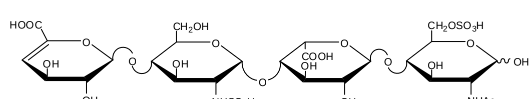

4

Mass Spectrometry Analysis

Experiments were performed with a 7 T Bruker Apex IV QeFTMS fitted with an Apollo II ESI source, a CO_2 laser for infrared multiphoton dissociation (IRMPD), and an indirectly heated hollow cathode for generating electrons for ECD and EDD. The hollow cathode implementation with the Infinity™ cell has been previously described [34]. Solutions of each tetrasaccharide were made at a concentration of 0.1 mg/mL in 50:50 methanol:H_2O (Sigma, St. Louis, MO) and ionized by nanospray using a pulled fused silica tip (model# FS360-75-15-D-5, New Objective, Woburn, MA). The sample solutions were infused at a rate of 10 µL/hour. All tetrasaccharides were examined in negative ion mode.

For the EDD experiments, precursor ions were isolated in the external quadrupole and accumulated for 1–2 seconds before injection into the FTMS cell. The isolation/cell fill was repeated up to 6 times. The selection of the precursor ion was further refined by using in-cell isolation with a coherent harmonic excitation frequency (CHEF) event. The precursor ions were then irradiated with electrons for 1 second. For electron irradiation the cathode bias was set to -19 V, the ECD lens was set to -17.5 V±0.5 V, and the cathode heater was set to 5–6 V. 24 acquisitions were signal averaged per mass spectrum. For each mass spectrum, 512k points were acquired, padded with one zero fill, and apodized using a sinebell window. Background spectra were acquired by leaving all parameters the same but setting the cathode bias to 0 V to ensure that no electrons reached the analyzer cell. External calibration produced mass accuracy of 5 ppm. Internal calibration was also performed using confidently assigned glycosidic bond cleavage products as calibrants, and produced mass accuracy of 1 ppm. All EDD products are reported using the Domon and Costello nomenclature, as shown in Figure 3.1 [37].

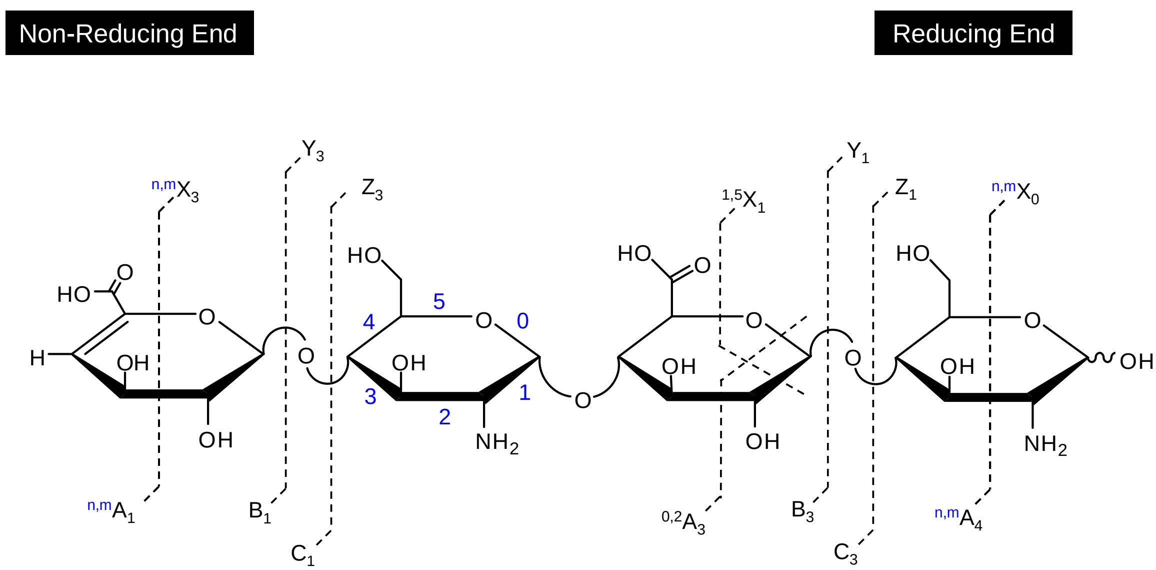

Figure 3.1. Fragment ion naming convention used in this paper, adapted from Domon and Costello [37]. Superscripts in cross ring cleavage products refer to the bonds that are broken, which are numbered as shown for the second saccharide from the nonreducing end.

RESULTS AND DISCUSSION

Irradiation of ΔUA-GlcN-GlcA-GlcNAc, ***1***, with 19 eV electrons produces the mass spectrum shown in Figure 3.2A. The mass spectrum contains mostly singly-charged product ions, including the charged reduced precursor, $[M\text{-}2H]^{-\bullet}$, as well as a small number of doubly-charged products. The efficiency of product ion conversion (the sum of product ion intensities divided by the precursor ion intensity measured prior to irradiation, as proposed by Gorshkov et al. [38]) is approximately 6%. The presence of both the doubly-charged product ions and the charge reduced precursor ion in the product ion spectrum indicates that products are formed via two fragmentation pathways, as shown in Scheme 3.1. Irradiation of the doubly-charged precursor ion with 19 eV electrons leads to an activated ion which can undergo direct decomposition to yield even-electron product ions that are doubly- or singly-charged. For example, direct decomposition of the doubly-charged precursor produces doubly-charged products such as C_3^{2-}, $^{2,4}A_4^{2-}$, $^{2,5}A_4^{2-}$, and $^{0,2}A_4^{2-}$. Alternatively, the activated precursor can lose an electron to form an odd-electron ion that undergoes further fragmentation to form singly-charged even- and odd-electron product ions. The charge-reduced molecular ion, $[M\text{-}2H]^{-\bullet}$, and other odd-electron species such as $[M\text{-}2H\text{-}CO_2]^{-\bullet}$ provide direct evidence of electron detachment.

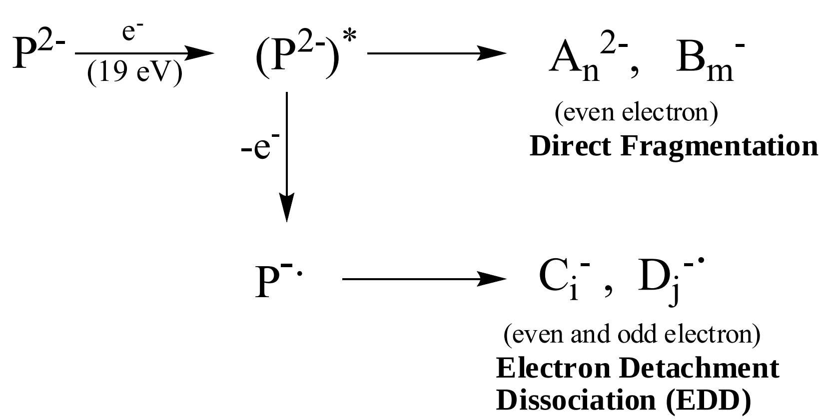

Scheme 3.1. Fragmentation observed when sulfated GAGs are irradiated with 19 eV electrons.

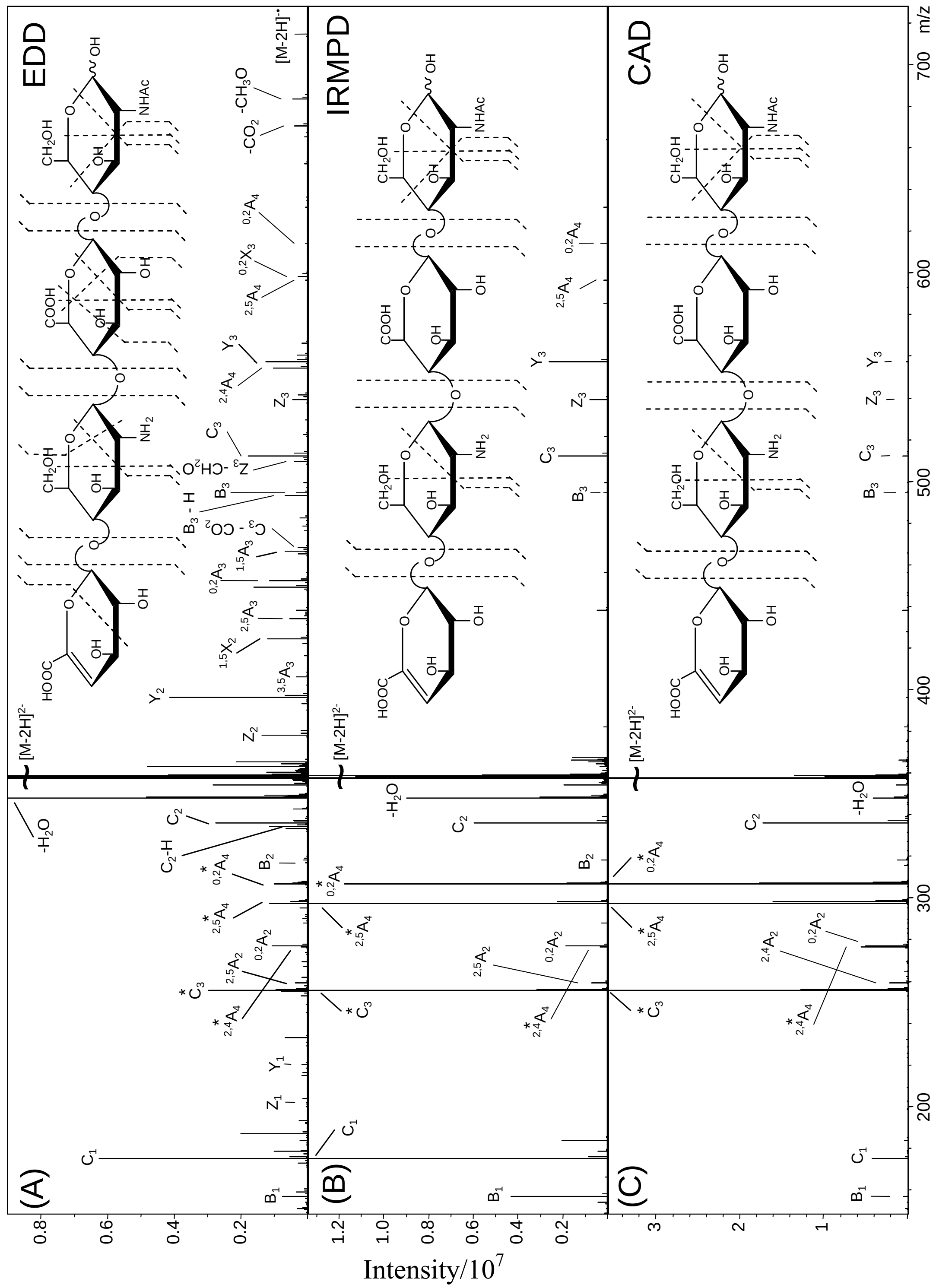

Figure 3.2. Tandem mass spectra of the $[M\text{-}2H]^{2-}$ precursor ion of tetrasaccharide ***1***, obtained by using (A) EDD, (B) IRMPD, and (C) CAD.

While doubly-charged product ions must arise via direct decomposition, and singly-charged odd-electron product ions must arise from electron detachment, singly-charged even-electron products can be formed by either dissociation pathway. In order to develop a correlation between molecular structure and fragmentation behavior, it is important to distinguish the dissociation pathways. The singly-charged even-electron products that arise from direct fragmentation of the doubly-charged negative ion can be identified by using IRMPD or CAD for ion activation, as their ions are produced by dissociation of an even-electron precursor. IRMPD of ***1*** produces the mass spectrum shown in Figure 3.2B, while CAD of ***1*** produces the mass spectrum shown in 1C. The major fragments in Figure 3.2B and 3.2C are principally from glycosidic bond cleavages (B, C, Y, and Z) and a small number of cross ring cleavages in the form of $^{0,2}A_4$ and $^{2,5}A_4$. Such cleavages have been observed in the CAD mass spectra of GAG of di- and tetrasaccharides [39,40]. All of the fragments observed in the CAD spectrum are found in the IRMPD spectrum, and all the IRMPD products are present in the EDD spectrum (Figure 3.2, insets). We have found this to be generally true for all of the GAG tetrasaccharides examined to date, i.e. EDD gives the most comprehensive set of fragment ions, while the IRMPD products are a subset of the ions in the EDD spectrum, and the CAD products are a subset of the ions in the IRMPD spectrum. The EDD products that also occur in the IRMPD and CAD spectrum probably arise from direct fragmentation of the doubly-charged precursor ion.

Electron activation of the precursor ion results in cleavage of every glycosidic bond and abundant cross-ring cleavages in the form of A ions, shown by dashed lines in the structure shown in the inset in Figure 3.2A. Product peak assignment was determined by comparison of the accurately measured masses with the theoretical product ions from glycosidic fragmentation of the tetrasaccharide. Other common cleavages such as the $^{0,2}A_n$, $^{2,5}A_n$, and loss of CO_2 were also identified in this manner. The N-acetyl group on the reducing end of the tetrasaccharide increases the mass defect of the product ions containing the reducing end relative to fragments from the non-reducing end, allowing one to distinguish A, B, and C products from X, Y, and Z products. The remainder of the product ions were identified from their exact mass differences from $[M-2H]^{-\bullet}$, which establishes the elemental composition of the neutral loss. For example, the peak at *m/z* 452.099 differs from the charge reduced species, $[M-2H]^{-\bullet}$, by 262.085 *u*. The calculated neutral loss for a $^{0,2}A_3$ cleavage is 262.093 *u*, while the calculated neutral loss for a $^{2,4}X_2$ cleavage is 262.069 *u*. The exact mass calculation of the observed neutral loss suggests that this product ion is $^{0,2}A_3$. This assignment was confirmed by comparison to the EDD spectrum of the closely related compound ***2*** (*vide infra*).

The EDD process can form a radical site by detachment of an electron from the doubly-charged precursor. Products from this singly-charged odd-electron ion can be either odd-electron or even-electron. The majority of the observed product ions are even- electron ions. Odd-electron products include ions from the loss of small, stable neutral molecules ($M^{-\bullet}$-2H-CO_2, $M^{-\bullet}$-2H-CH_2O), as well as some glycosidic (B_3-H, C_2-H) and cross-ring cleavages. Radical formation initially occurs at a site of negative charge. For ***1***, the two initial sites of negative charge are the carboxylic acid groups on the residues at the non-reducing end and the GlcA residue next to the reducing end. The large degree of fragmentation on the GlcA residue next to the reducing end indicates a preference for ion decomposition when the radical is located at this site. Radical site formation at the non-reducing end appears to form a stable species that is resistant to further fragmentation. Radical site formation at the GlcA carboxyl group can be followed by loss of CO_2 to form the odd-electron product ion at *m/z* 670.196. This species can undergo further radical-driven fragmentation of the glycosidic bond to produce the C_2-H ion, as shown in the proposed mechanism in Scheme 3.2. Alternatively, the radical ion $[M\text{-}2H\text{-}CO_2]^{-\bullet}$ can lose a hydrogen atom to form a more stable even electron ion, $[M\text{-}2H\text{-}CO_2H]^{-}$.

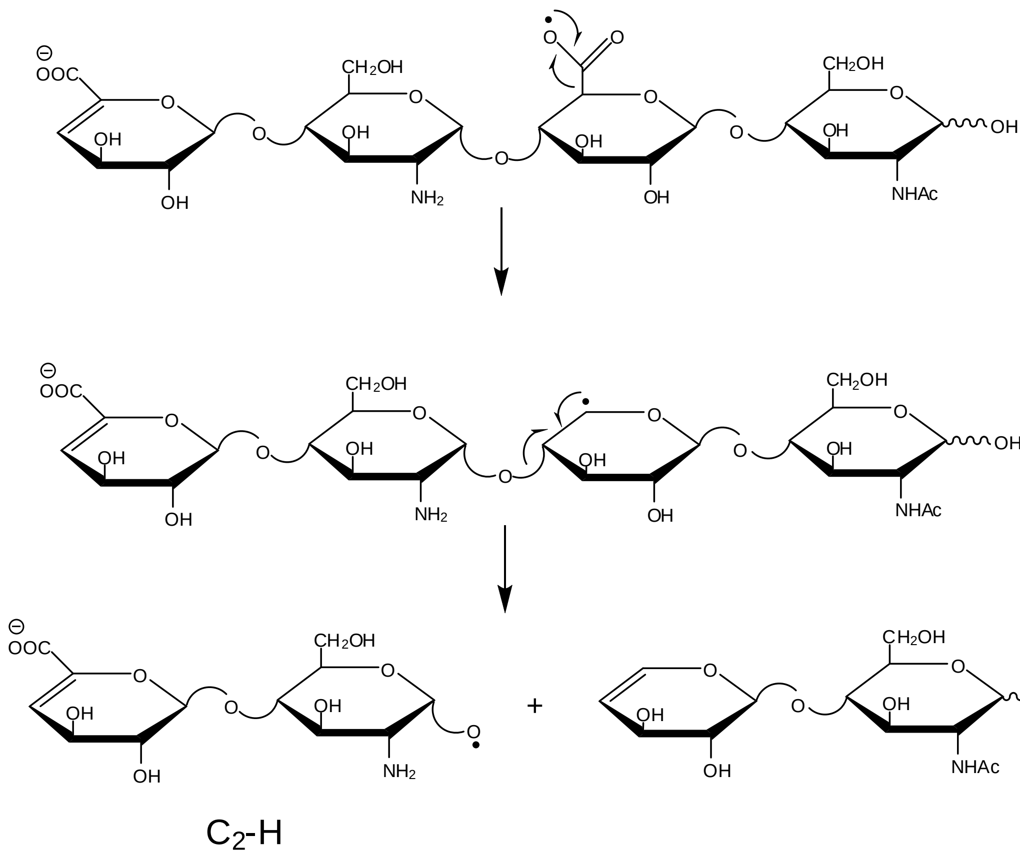

Scheme 3.2. Proposed fragmentation mechanism of ***1*** to form the C_2-H product ion.

There is also evidence of H atom transfer to the carboxyl radical from other positions in the glucuronic acid residue. One possibility is H-atom transfer from the hydroxyl group on carbon C3 to the carboxyl radical, moving the radical site to the C3 oxygen atom, as shown in Scheme 3.3a. This radical site can promote $^{3,5}A_3$ and $^{0,2}A_3$ fragmentation.

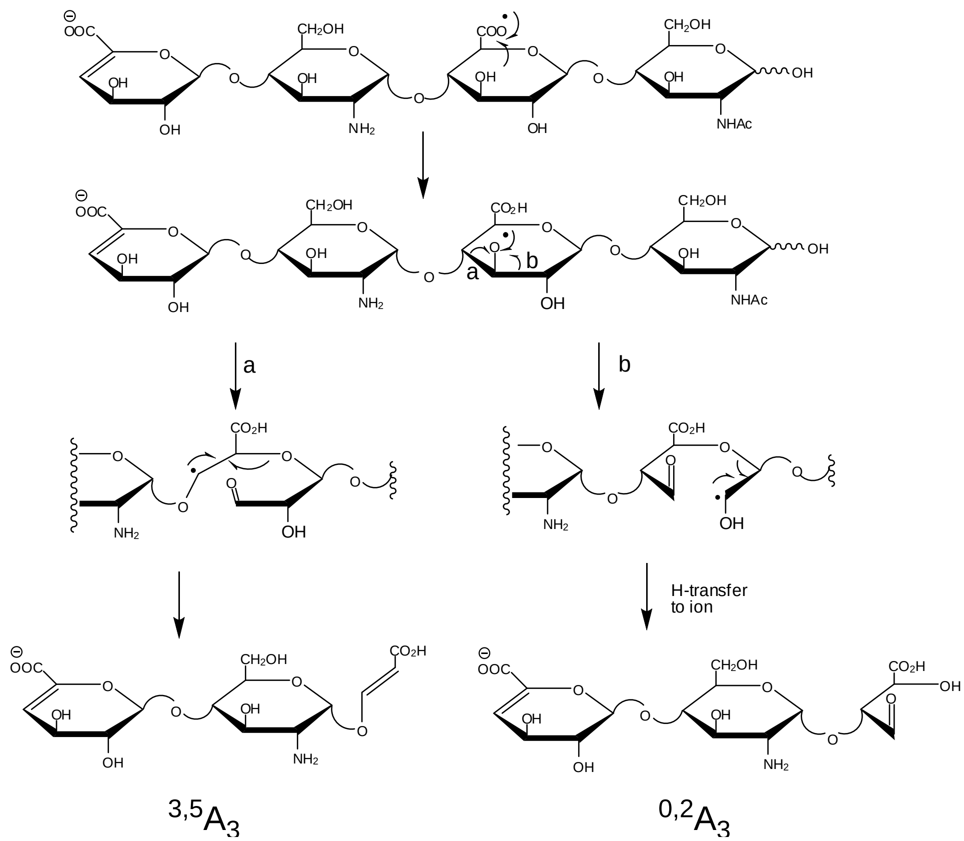

Scheme 3.3a. Proposed mechanism for H• transfer followed by fragmentation to form the $^{3,5}A_3$ and $^{0,2}A_3$ product ions.

Alternatively, H-atom transfer can come from C4 as shown in Scheme 3.3b. The resulting radical is stabilized by delocalization with the oxygen that forms the glycosidic bond to C4. H-atom transfer from carbon atoms in saccharide rings has been observed in collision induced electron detachment mass spectra of nucleotides [28], in reactions between phenyl radical cations and ribose [41], and in the ECD mass spectra of glycopeptides [42]. The radical site at C4 can promote $^{3,5}A_3$ and $^{0,2}A_3$ fragmentation as shown in Scheme 3.3b. The abundance of cross ring cleavage products from fragmentation in the second sugar residue from the reducing end in the EDD spectrum, and their absence in the CAD and IRMPD spectra, suggests radical-induced fragmentation of many of the bonds in this residue, which can be rationalized by mobility of the radical site via hydrogen rearrangement. The excess energy deposited into the ion during electron irradiation can supply the energy necessary to drive the hydrogen rearrangement.

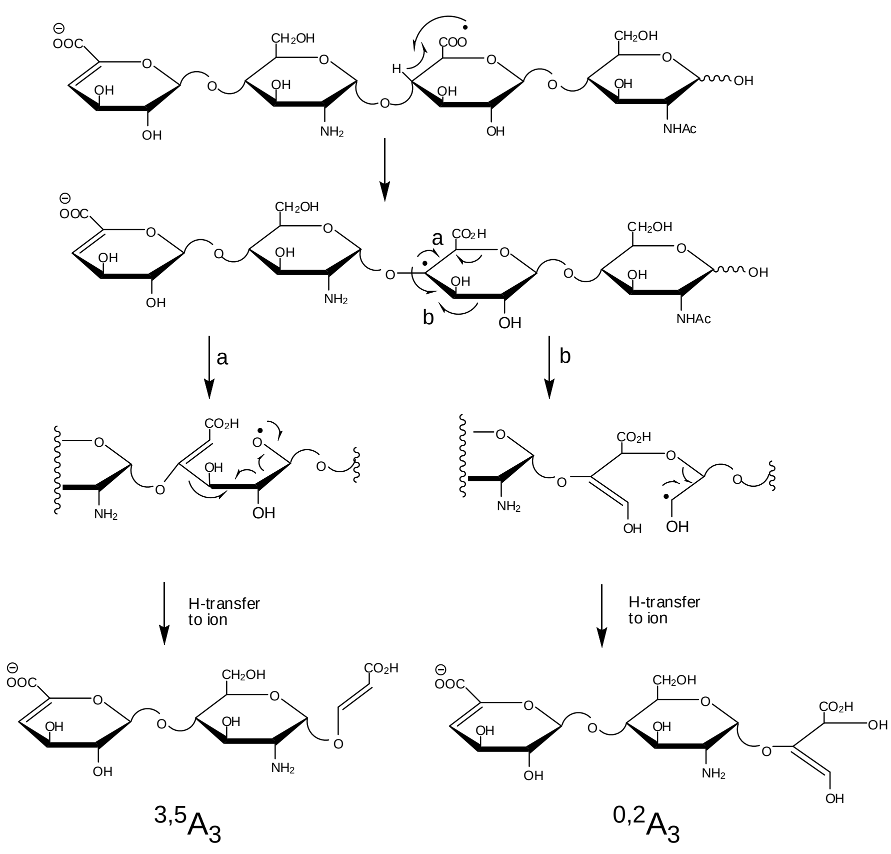

Scheme 3.3b. Alternative mechanism for H• transfer followed by fragmentation to form the $^{3,5}A_3$ and $^{0,2}A_3$ product ions.

Figure 3.3 shows the EDD mass spectrum of ΔUA-GlcNAc-GlcA-GlcNAc, ***2***, which differs from ***1*** by N-acetylation in the GlcNAc residue next to the non-reducing end. The product ions from EDD of ***2***, Figure 3.3, are similar in assignment and in abundance as observed products for EDD of ***1***. Some minor differences are evident. The C_2 and Z_2 ions are not assigned for EDD of ***2*** as they overlap with the precursor ion, and would be difficult to discern from the much more abundant remaining precursor. Some new cross-ring product ions are evident in the EDD mass spectrum of ***2***. The $^{2,4}A_3$ product ion present in the EDD spectrum of ***2*** is not assigned for ***1***, for if present, it would overlap with the Z_2 glycosidic cleavage for compound ***1***. The $^{1,4}X_2$ product ion is observed as it does not overlap with the $^{1,5}A_3$ cleavage, as it did for ***1***. Aside from these minor differences, a majority of the assigned products are the same for the two related tetrasaccharides ***1*** and ***2***. The similarity of the EDD spectra for these two related compounds shows that observed fragmentation is not highly sensitive to small modifications of the sugar residues, and suggests regularity in the types of fragments that are observed.

Figure 3.4 shows the EDD spectrum of the sulfated GAG tetrasaccharide ΔUA-GlcNSO$_3$-GlcA-GlcNAc, ***3***. Determining the sites of sulfation by MS/MS requires abundant glycosidic and cross-ring fragmentation without loss of SO_3 from the labile sulfate group. The sulfate group provides an additional site of ionization for the tetrasaccharide. As sulfuric acid is more ionized in solution then a carboxylic acid, doubly-charged negative ions formed by ESI are expected to be ionized at the sulfate group and one of the carboxylic acid groups. Electron detachment is expected to occur principally at carboxylate, since the electron affinity of sulfate is considerably higher than the electron affinity of the carboxylate (EA(HSO_4^-) ≈ 4.7 eV; EA(DCO_2^-) ≈ 3.5 eV) [43]. EDD of ***3***, Figure 3.4, results in no observed loss of SO_3. Similar to

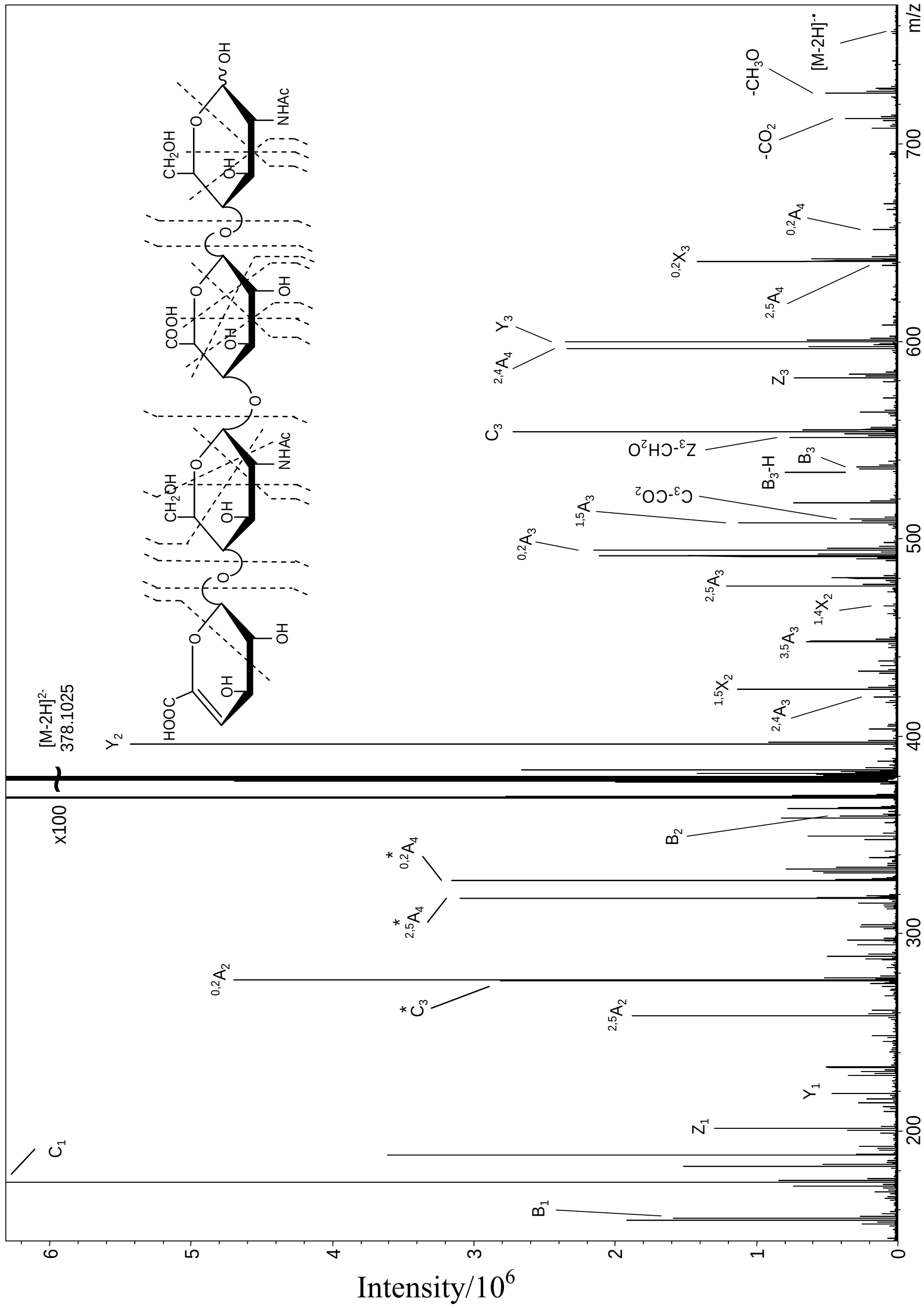

Figure 3.3. EDD mass spectrum of the $[M-2H]^{2-}$ precursor ion of tetrasaccharide ***2***. The $^{2,4}A_3$ product in ***1*** is not observed since it overlaps with the Z_2 product. The $^{1,4}X_2$ product in ***1*** is not observed since it overlaps with the $^{1,5}A_3$ product. C_2 and Z_2 are not observed since the products overlap with the precursor ion.

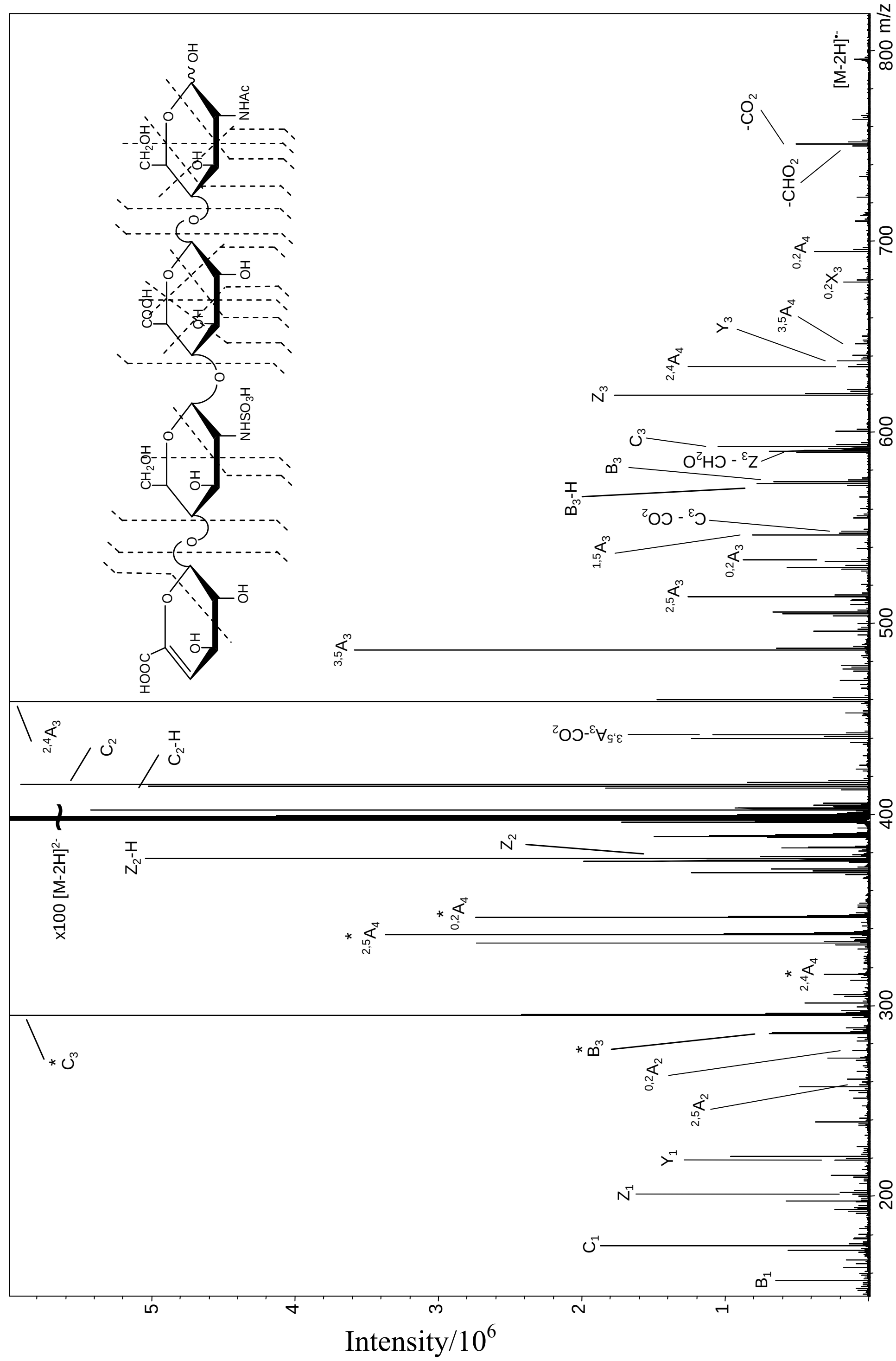

Figure 3.4. EDD mass spectrum of the $[M-2H]^{2-}$ precursor ion of tetrasaccharide ***3***. The B_2 and Y_2 product ions are not observed as they overlap with the precursor ion.

EDD of ***1*** and ***2***, the odd-electron product ion $[M\text{-}2H\text{-}CO_2]^{-\bullet}$ is observed, indicating a preference for electron detachment from the carboxylate group rather than the sulfate, as it is expected that the sulfate radical would exhibit SO_3 loss. The observed EDD product ions of ***3*** (Figure 3.4 inset) are similar to those ions observed for ***1*** and ***2***. The B_2 and Y_2 product ion are not assigned for ***3*** as they overlap with the precursor ion. In addition to the doubly-charged even-electron ions observed in the EDD of ***1*** and ***2***, the doubly-charged product ion B_3 is also observed in the EDD of ***3***. As with ***1*** and ***2***, there is substantial cross-ring cleavage in the residue next to the reducing end. $^{0,2}A_3$ and $^{3,5}A_3$ can be rationalized as resulting from hydrogen atom transfer from the hydroxyl group on C3 to the carboxyl radical at C5, followed by α-cleavage, similar to the mechanisms for ***1*** shown in Schemes 3a and 3b. EDD of ***3*** leads to fragmentation of every glycosidic bond. The glycosidic products establish that the site of sulfation lies within the glucosamine residue next to the reducing end. This glucosamine residue has three possible sites of sulfation. The $^{0,2}A_2$ and $^{2,5}A_2$ cross-ring fragments place the sulfation on the amine group, establishing this as a GlcNS residue.

Tetrasaccharide ***4***, ΔUA-GlcNSO$_3$-IdoA-GlcNAc-6-SO$_4$, contains two sulfate groups. In this case, the doubly-charged negative ion is expected to carry charge at the two sulfates, and EDD is expected to form a radical site at one of the sulfates. Dissociation of the $[M\text{-}2H]^{2-}$ precursor ion of ***4*** by IRMPD or CAD (Figure 3.5B or 5C, respectively) results in principally glycosidic cleavages. Some product ions are also found to lose SO_3, and some glycosidic cleavages are only found with the loss of SO_3. Although the residues that are sulfated can be determined from the glycosidic cleavage in the CAD and IRMPD spectra, identification of the sites of sulfation is difficult due to the limited amount of fragmentation that occurs by these methods of ion activation. In contrast, irradiation of the $[M\text{-}2H]^{2-}$ precursor ion of ***4*** with 19 eV electrons results in much more extensive fragmentation, as seen in the mass spectrum shown in Figure 3.5A. Predominantly singly-charged even-electron product ions are observed. Some doubly-charged product ions are observed such as $[M\text{-}2H\text{-}SO_3]^{2-}$ and $^{0,2}A_4^{2-}$, as well as the Y_3^{2-} and Z_3^{2-} glycosidic cleavages. Some product ions from the EDD fragmentation of ***4*** are observed both as product ions with two sulfates as well as with the loss of one molecule of SO_3. For example, the Z_3 and Y_3 product ions are also observed as $Z_3\text{-}SO_3$ and $Y_3\text{-}SO_3$. The odd-electron product ions $[M\text{-}2H\text{-}SO_3]^{-\bullet}$ and $[M\text{-}2H\text{-}CO_2]^{-\bullet}$ are observed along with the even-electron product ions $[M\text{-}2H\text{-}HSO_3]^-$ and $[M\text{-}2H\text{-}HCO_2]^-$. Doubly-charged negative ions of ***4*** formed by ESI are expected to be ionized at both sulfate groups. The presence of the $[M\text{-}2H\text{-}CO_2]^{-\bullet}$ odd-electron product ion implies that either a carboxylate anion was formed during ionization or that the carboxyl radical was formed as a result of H atom transfer. The presence of a carboxylate radical on the IdoA residue next to the reducing end results in fragmentation similar to EDD of ***1***, ***2***, and ***3***. Similar to CAD and IRMPD of ***1*** (Figure 3.2B and 3.2C), all of the product ions in the CAD spectrum are observed in the IRMPD spectrum, and all product ions in the IRMPD spectrum are observed in the EDD spectrum (Figure 3.5, insets). Compared to IRMPD and CAD of ***4***, the EDD mass spectrum of ***4*** exhibits peaks that result from cleavage of all glycosidic bonds as well as from abundant cross-ring cleavages. The cross-ring fragmentation of the reducing end sugar places the sulfate on C6 and identifies this sugar as GlcNAc-6-SO_4. Glycosidic fragmentation identifies the sugar next to the non-reducing end as a sulfated GlcN sugar. The cross-ring fragmentation places the sulfate on either the C2 amino group or C6. The observed fragmentation cannot isolate the site of sulfation on this sugar.

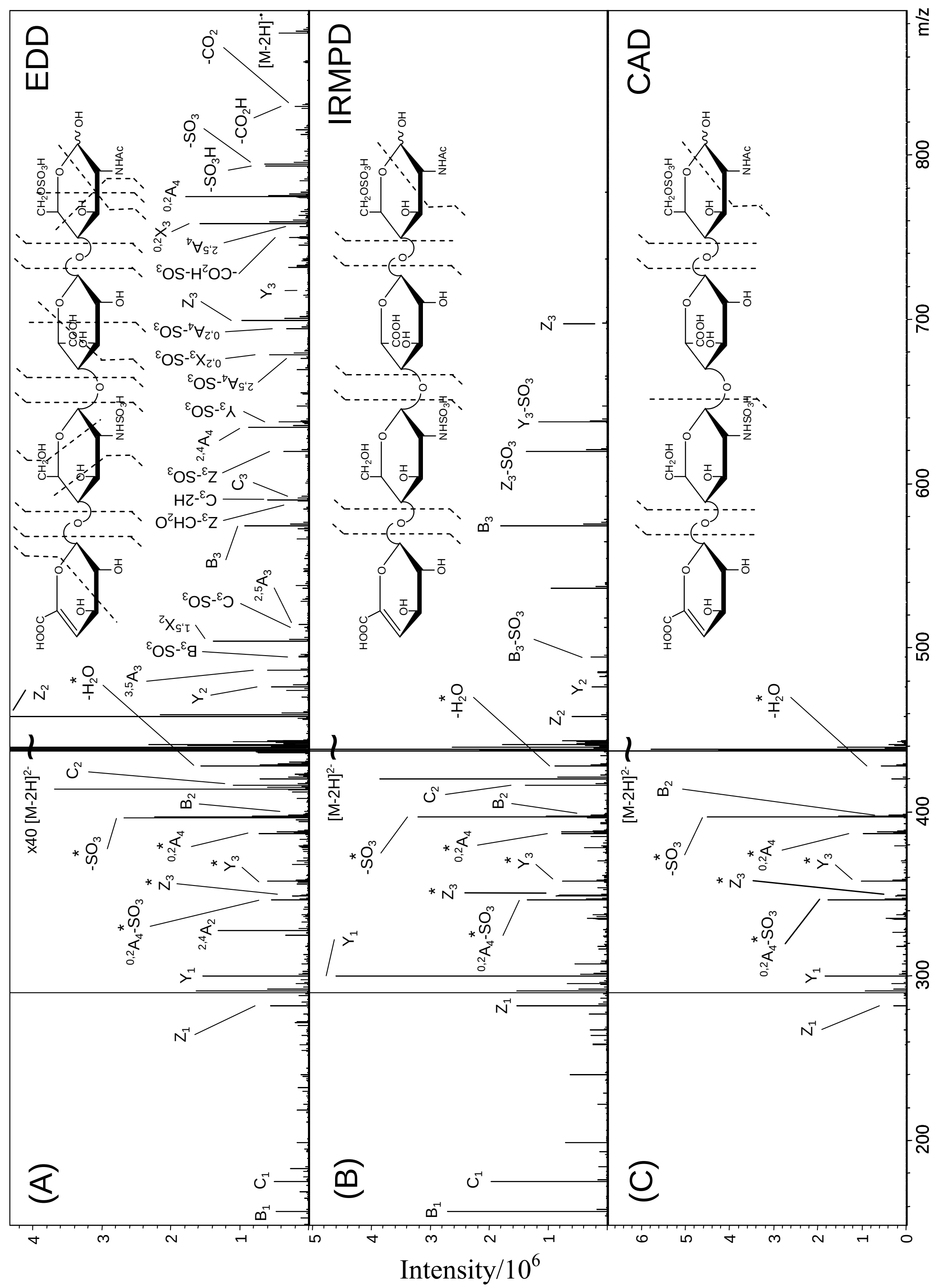

Figure 3.5. Tandem mass spectra of the [M-2H]$^{2-}$ precursor ion of tetrasaccharide ***4***, obtained by using (A) EDD, (B) IRMPD, and (C) CAD.

The EDD spectra of the GAG tetrasaccharides exhibit a substantial number of fragment ions, many with low relative abundances. We find that the majority of these peaks appear reproducibly from spectrum to spectrum. The reproducibility of EDD fragmentation has been ascertained by comparing the spectra from identical samples acquired at an interval of one month (data not shown). The peaks are found to be reproducible in both the mass-to-charge and abundance of the observed fragment ions. All previously identified product ions are present and no new product ions are observed. Even the unassigned, low abundance product ions are found to be remarkably reproducible. The close match between EDD spectra collected at different times is reminiscent of the reproducibility of electron ionization mass spectra, and suggests that the product ions do not result from random cleavage of the molecule, but rather that products result from well-defined fragmentation pathways. These data suggest that EDD should be useful for characterizing the sites of modification in other GAG tetrasaccharides.

CONCLUSIONS

Irradiation of GAG tetrasaccharides with 19 eV electrons results in predominantly even-electron product ions. EDD uses moderate energy electrons compared to the low energy electrons used in ECD. These moderate energy electrons promote ion dissociation by direct fragmentation as well as via electron detachment. The abundance of glycosidic and cross-ring cleavage products by EDD will aid in the identification of this important class of compounds.

H-atom transfer has been observed to occur between hydroxyl groups and carboxylate radicals. Since such atom transfers require proximity between the donor and acceptor sites, the particular hydroxyl group that participates in this rearrangement may be influenced by the stereochemistry of the C5 carbon. Future experiments on GAG epimers will determine whether the stereochemistry of the hexuronic acid C5 carbon influences EDD fragmentation in a manner that allows one to distinguish IdoA from GlcA. While we have confined these studies to tetrasaccharides, we believe that this approach should be extensible to longer GAG oligosaccharides.

ACKNOWLEDGMENTS

We gratefully acknowledge financial support from the National Institutes of Health grant #2R01-GM038060-16.

REFERENCES

1. Perrimon, N.; Bernfield, M. Cellular functions of proteoglycans--an overview. *Semin. Cell Dev. Biol.* **2001**, *12*, 65-67.
2. Linhardt, R. J.; Toida, T. Role of Glycosaminoglycans in Cellular Communication. *Acc. Chem. Res.* **2004**, *37*, 431-438.
3. Fannon, M.; Forsten, K. E.; Nugent, M. A. Potentiation and Inhibition of bFGF Binding by Heparin: A Model for Regulation of Cellular Response. *Biochemistry* **2000**, *39*, 1434-1445.
4. Wu, Z. L.; Zhang, L.; Yabe, T.; Kuberan, B.; Beeler, D. L.; Love, A.; Rosenberg, R. D. The Involvement of Heparan Sulfate (HS) in FGF1/HS/FGFR1 Signaling Complex. *J. Biol. Chem.* **2003**, *278*, 17121-17129.
5. Gotte, M. Syndecans in Inflammation. *FASEB J.* **2003**, *17*, 575-591.
6. Rabenstein, D. L. Heparin and Heparan Sulfate: Structure and Function. *Nat. Prod. Rep.* **2002**, *19*, 312-331.
7. Lindahl, U.; Kusche-Gullberg, M.; Kjellen, L. Regulated Diversity of Heparan Sulfate. *J. Biol. Chem.* **1998**, *273*, 24979-24982.
8. Turnbull, J.; Powell, A.; Guimond, S. Heparan sulfate: decoding a dynamic multifunctional cell regulator. *Trends Cell Biol.* **2001**, *11*, 75-82.
9. Salmivirta, M.; Lidholt, K.; Lindahl, U. Heparan sulfate: a piece of information. *FASEB J.* **1996**, *10*, 1270-1279.
10. Naggar, E. F.; Costello, C. E.; Zaia, J. Competing Fragmentation Processes in Tandem Mass Spectrometry of Heparin-Like Glycosaminoglycans. *J. Am. Soc. Mass Spectrom.* **2004**, *15*, 1534-1544.

11. Carr, S. A.; Reinhold, V. N. Structural Characterization of Sulfated Glycosaminoglycans by Fast Atom Bombardment Mass-Spectrometry - Application to Chondroitin Sulfate. *J. Carb. Chem.* **1984**, *3*, 381-401.

12. Reinhold, V. N.; Carr, S. A.; Green, B. N.; Petitou, M.; Choay, J.; Sinay, P. Structural Characterization of Sulfated Glycosaminoglycans by Fast-Atom-Bombardment Mass-Spectrometry - Application to Heparin Fragments Prepared by Chemical Synthesis. *Carbohydr. Res.* **1987**, *161*, 305-313.

13. Takagaki, K.; Kojima, K.; Majima, M.; Nakamura, T.; Kato, I.; Endo, M. Ion-Spray Mass-Spectrometric Analysis of Glycosaminoglycan Oligosaccharides. *Glycoconjugate J.* **1992**, *9*, 174-179.

14. Dai, Y.; Whittal, R. M.; Bridges, C. A.; Isogai, Y.; Hindsgaul, O.; Li, L. Matrix-assisted laser desorption ionization mass spectrometry for the analysis of monosulfated oligosaccharides. *Carbohydr. Res.* **1997**, *304*, 1-9.

15. Juhasz, P.; Biemann, K. Utility of non-covalent complexes in the matrix-assisted laser desorption ionization mass spectrometry of heparin-derived oligosaccharides. *Carbohydr. Res.* **1995**, *270*, 131-147.

16. Lo-Guidice, J.-M.; Herz, H.; Lamblin, G.; Plancke, Y.; Roussel, P.; Lhermitte, M. Structures of sulfated oligosaccharides isolated from the respiratory mucins of a non-secretor (O, Lea+b-) patient suffering from chronic bronchitis. *Glycoconjugate J.* **1997**, *14*, 113-125.

17. Schiller, J.; Arnhold, J.; Benard, S.; Reichl, S.; Arnold, K. Cartilage degradation by hyaluronate lyase and chondroitin ABC lyase: a MALDI-TOF mass spectrometric study. *Carbohydr. Res.* **1999**, *318*, 116-122.

18. Zaia, J.; Costello, C. E. Tandem Mass Spectrometry of Sulfated Heparin-Like Glycosaminoglycan Oligosaccharides. *Anal. Chem.* **2003**, *75*, 2445-2455.

19. Viseux, N.; de Hoffmann, E.; Domon, B. Structural Assignment of Permethylated Oligosaccharide Subunits Using Sequential Tandem Mass Spectrometry. *Anal. Chem.* **1998**, *70*, 4951-4959.

20. Saad, O. M.; Leary, J. A. Heparin Sequencing Using Enzymatic Digestion and ESI-MS with HOST: A Heparin/HS Oligosaccharide Sequencing Tool. *Anal. Chem.* **2005**, *77*, 5902-5911.

21. Zamfir, A.; Seidler, D. G.; Kresse, H.; Peter-Katalinic, J. Structural characterization of chondroitin/dermatan sulfate oligosaccharides from bovine aorta by capillary electrophoresis and electrospray ionization quadrupole time-of-flight tandem mass spectrometry. *Rapid Commun. Mass Spectrom.* **2002**, *16*, 2015-2024.

22. Zubarev, R. A.; Kelleher, N. L.; McLafferty, F. W. Electron Capture Dissociation of Multiply Charged Protein Cations. A Nonergodic Process. *J. Am. Chem. Soc.* **1998**, *120*, 3265-3266.

23. Zubarev, R. A.; Haselmann, K. F.; Budnik, B.; Kjeldsen, F.; Jensen, F. Towards an understanding of the mechanism of electron-capture dissociation: a historical perspective and modern ideas. *Eur. J. Mass Spectrom.* **2002**, *8*, 337-349.

24. Stensballe, A.; Jensen, O. N.; Olsen, J. V.; Haselmann, K. F.; Zubarev, R. A. Electron capture dissociation of singly and multiply phosphorylated peptides. *Rapid Commun. Mass Spectrom.* **2000**, *14*, 1793-1800.

25. Hakansson, K.; Cooper, H. J.; Emmett, M. R.; Costello, C. E.; Marshall, A. G.; Nilsson, C. L. Electron Capture Dissociation and Infrared Multiphoton Dissociation MS/MS of an

N-Glycosylated Tryptic Peptide To Yield Complementary Sequence Information. *Anal. Chem.* **2001**, *73*, 4530-4536.

26. Budnik, B. A.; Haselmann, K. F.; Elkin, Y. N.; Gorbach, V. I.; Zubarev, R. A. Applications of electron-ion dissociation reactions for analysis of polycationic chitooligosaccharides in Fourier transform mass spectrometry. *Anal. Chem.* **2003**, *75*, 5994.

27. Zubarev, R. A. Reactions of polypeptide ions with electrons in the gas phase. *Mass Spectrom. Rev.* **2003**, *22*, 57.

28. Liu, B.; Hvelplund, P.; Nielsen, S. B.; Tomita, S. Electron loss and dissociation in high energy collisions between multiply charged oligonucleotide anions and noble gases. *International Journal of Mass Spectrometry* **2003**, *230*, 19.

29. Anusiewicz, I.; Jasionowski, M.; Skurski, P.; Simons, J. Backbone and side-chain cleavages in electron detachment dissociation (EDD). *J. Phys. Chem. A* **2005**, *109*, 11332.

30. Budnik, B. A.; Haselmann, K. F.; Zubarev, R. A. Electron detachment dissociation of peptide di-anions: an electron-hole recombination phenomenon. *Chem. Phys. Lett.* **2001**, *342*, 299-302.

31. Cooper, H. J.; Hakansson, K.; Marshall, A. G. The role of electron capture dissociation in biomolecular analysis. *Mass Spectrom. Rev.* **2005**, *24*, 201-222.

32. Kjeldsen, F.; Silivra, O. A.; Ivonin, I. A.; Haselmann, K. F.; Gorshkov, M.; Zubarev, R. A. Cα-C Backbone Fragmentation Dominates in Electron Detachment Dissociation of Gas-Phase Polypeptide Polyanions. *Chem. Eur. J.* **2005**, *11*, 1803-1812.

33. McFarland, M. A.; Marshall, A. G.; Hendrickson, C. L.; Nilsson, C. L.; Fredman, P.; Mansson, J. E. Structural characterization of the GM1 ganglioside by infrared multiphoton dissociation/electron capture dissociation, and electron detachment dissociation electrospray ionization FT-ICR MS/MS. *J. Am. Soc. Mass Spectrom.* **2005**, *16*, 752.

34. Yang, J.; Mo, J.; Adamson, J. T.; Hakansson, K. Characterization of Oligodeoxynucleotides by Electron Detachment Dissociation Fourier Transform Ion Cyclotron Resonance Mass Spectrometry. *Anal. Chem.* **2005**, *77*, 1876-1882.

35. Pervin, A.; Gallo, C.; Jandik, K. A.; Han, X.-J.; Linhardt, R. J. Preparation and structural characterization of large heparin-derived oligosaccharides. *Glycobiology* **1995**, *5*, 83-95.

36. Munoz, E.; Xu, D.; Avci, F.; Kemp, M.; Liu, J.; Linhardt, R. J. Enzymatic synthesis of heparin related polysaccharides on sensor chips: Rapid screening of heparin-protein interactions. *Biochem. Biophys. Res. Commun.* **2006**, *339*, 597-602.

37. Domon, B.; Costello, C. E. A systematic nomenclature for carbohydrate fragmentations in FAB-MS/MS spectra of glycoconjugates. *Glycoconjugate J.* **1988**, *5*, 397-409.

38. Gorshkov, M. V.; Masselon, C. D.; Nikolaev, E. N.; Udseth, H. R.; Pasa-Tolic, L.; Smith, R. D. Considerations for electron capture dissociation efficiency in FTICR mass spectrometry. *International Journal of Mass Spectrometry* **2004**, *234*, 131.

39. Zaia, J.; McClellan, J. E.; Costello, C. E. Tandem Mass Spectrometric Determination of the 4S/6S Sulfation Sequence in Chondroitin Sulfate Oligosaccharides. *Anal. Chem.* **2001**, *73*, 6030-6039.

40. Saad, O. M.; Leary, J. A. Delineating mechanisms of dissociation for isomeric heparin disaccharides using isotope labeling and ion trap tandem mass spectrometry. *J. Am. Soc. Mass Spectrom.* **2004**, *15*, 1274-1286.

41. Ramirez-Arizmendi, L. E.; Heidbrink, J. L.; Guler, L. P.; Kenttamaa, H. I. Reactivity of substituted charged phenyl radicals toward components of nucleic acids. *J. Am. Chem. Soc.* **2003**, *125*, 2272.

42. Mormann, M.; Paulsen, H.; Peter-Katalinic, J. Electron capture dissociation of O-glycosylated peptides: radical site-induced fragmentation of glycosidic bonds. *Eur. J. Mass Spectrom.* **2005**, *11*, 497.

43. Bartmess, J. E. *Negative Ion Energetics Data*; Linstrom, P. J. and Mallard, W. G., Ed.; National Institute of Standards and Technology: Gaithersburg, MD 20899, 2005.

CHAPTER 4

DISTINGUISHING GLUCURONIC FROM IDURONIC ACID IN GLYCOSAMINOGLYCAN TETRASACCHARIDES BY USING ELECTRON DETACHMENT DISSOCIATION*

ABSTRACT

Distinguishing the epimers iduronic acid (IdoA) versus glucuronic acid (GlcA) has been a longstanding challenge for the mass spectrometry analysis of glycosaminoglycan oligogosaccharides. In this work, electron detachment dissociation (EDD) and Fourier transform ion cyclotron resonance mass spectrometry is shown to provide mass spectral features that can distinguish GlcA from IdoA in heparan sulfate (HS) tetrasaccharides. EDD of HS tetrasaccharide dianions produces a radical species that fragments to produce information-rich glycosidic and cross-ring product ions which can be used to determine the sites of acetylation/sulfation. More significantly, EDD of HS tetrasaccharide epimers produces diagnostic product ions that can be used to distinguish IdoA from GlcA. These diagnostic product ions are not observed in the tandem mass spectra obtained by collisionally activated dissociation (CAD) or infrared multiphoton dissociation (IRMPD) of the tetrasaccharides, suggesting a radical-initiated mechanism for their formation. Differences in the observed product ions obtained by EDD of the tetrasaccharide epimers can be rationalized by simple α-cleavage of an oxy-radical located at C2 or C3 or a radical at C3 or C4. These radicals are proposed to arise from a hydrogen rearrangement in which a hydrogen atom is transferred from the C2 or C3 hydroxyl group or C3 or C4 to a carboxy radical at C5. This hydrogen transfer depends on the proximity of the carboxy radical to the hydroxyl group on C2 or C3 or the hydrogen on C3 or C4, and is thus influenced by C5 stereochemistry. These epimer-sensitive fragmentations should allow this approach to be applied to the structural analysis of a wide variety of GAG oligosaccharides.

INTRODUCTION

Glycosaminoglycans (GAGs) are complex polysaccharides which comprise the carbohydrate portion of proteoglycans, and are found in a variety of organisms ranging from bacteria to humans [1]. GAGs participate in a number of significant biological processes, such as cell-cell signaling [2], the regulation of biochemical pathways [3, 4], and the mediation of inflammatory reactions [5]. GAGs have also been implicated in the initial step of some pathogenic infections [6-8] and have been observed to undergo alteration in some types of cancer [9]. There is great interest in correlating the molecular structure of GAGs with their biological function, but the complexity of this class of molecules has slowed progress on this front. Although GAGs are linear biopolymers consisting of alternating acidic sugar and basic sugar residues, they exhibit complexity in a variety of ways. At the proteoglycan level, GAG chains of different length and composition bind core proteins that also exhibit compositional heterogeneity. At the subunit level, GAGs display complexity through their differing degrees of sulfation and N-acetylation. Heparin and heparan sulfate (HS) are the most complex of the GAGs; they are composed of a repeating disaccharide of hexuronic acid and glucosamine. The acidic sugar can be either glucuronic acid (GlcA) or iduronic acid (IdoA) depending on the C5 stereochemistry, and may be sulfated at the C2 hydroxyl group. The glucosamine may be sulfated at the C3 or C6 hydroxyl group, and sulfated, acetylated, or unmodified at the C2 amino group. The structural characterization of GAGs oligosaccharides requires identification of the location of sulfation/acetylation modifications as well as establishing the epimeric nature of the hexuronic acid. Characterizing GAGs is of significant interest since it is believed that the pattern of modification (sulfation, acetylation, GlcA vs. IdoA) affects their biological activity [10-12].

Short lengths of heparin/HS oligosaccharides resulting from enzymatic digestion can be analyzed by 1D and 2D NMR [13]. These methods can determine the type and location of chain modification and can distinguish IdoA from GlcA. However, analysis by NMR requires milligram quantities of a high purity sample. Unlike proteins and nucleic acids, GAGs are not synthesized by a template-driven mechanism, and so samples must be obtained by isolation of naturally occurring materials that are often available only in low quantity and purity. The development of other techniques for characterizing small amounts of GAGs and GAG mixtures is necessary to advance the goal of identifying structure/function relationships of this class of molecules. Mass spectrometry (MS) meets these requirements, but its development into a general purpose tool for GAG analysis remains incomplete.

Electrospray ionization (ESI) mass spectrometry is useful for obtaining the molecular weight of intact GAG oligosaccharides [14-16]. For small oligosaccharides this can be used to determine the degree of sulfation. To establish the specific sites of modification, more advanced methods are required. Tandem mass spectrometry (MS^2 and MS^3) using collisionally activated dissociation (CAD) of Δ-unsaturated disaccharides resulting from digestion of heparin/HS with heparin lyases has been used to determine the pattern of sulfation/acetylation on short heparin/HS lengths [17]. However, such disaccharides have lost chirality at the nonreducing end hexuronic acid, erasing the original epimeric nature of the acid residue at C5 [18]. Therefore, tetramers or longer oligosaccharides are needed for establishing IdoA versus GlcA composition. Generally speaking, mass spectrometry is not sensitive to chirality in molecules. However, Zaia and coworkers have shown that for chondroiton sulfate (CS) tetrasasaccharides and hexasaccharides, CAD can distinguish between IdoA and GlcA based on the relative abundance of specific X and Y ions [19]. For this approach, the relative abundance of key fragment ions as a function of IdoA/GlcA composition was established for a series of tetrasaccharide and hexasaccharide standards, essentially producing a calibration curve for each mixture. This data was then used to determine the fractional abundance of IdoA vs. GlcA in tetrasaccharides and hexasaccharides from an enzymatic digestion of chondroiton/dermatan sulfate proteoglycans [20, 21]. The advantage of this approach is that it allows one to establish the epimer composition of an isobaric mixture of GAG oligosaccharides. The drawback is that the fragmentation versus chirality dependence must be established for each different type of GAG, e.g. the fragmentation behavior of CS oligosaccharides could not be applied to HS oligosaccharides. In these CAD experiments, one cannot predict the fragmentation behavior based on the structure of GAG oligosaccharides, and thus this approach is not useful as a general purpose tool for determining the epimeric state of hexuronic acids in other GAG oligosaccharides.

We have recently reported the application of electron detachment dissociation (EDD) [22-27] to the analysis of GAG tetrasaccharides [28]. EDD produces a radical anion from the closed shell, multiply-charged anionic precursor. The radical anion undergoes distinctly different types of fragmentation than its closed shell counterpart. EDD produces abundant fragmentation, and greatly improves the capability of mass spectrometry to determine the sites of sulfation/acetylation in GAG tetrasaccharides compared to CAD or infrared multiphoton dissociation (IRMPD) of the same precursors. We have proposed a mechanism for the cross-ring fragmentation of hexuronic residues in GAG tetrasaccharides in which electron detachment from the C6 carboxylate anion forms a carboxy radical, which can undergo hydrogen rearrangement from the hydrogens at C3 or C4, or from the hydroxyl groups at C2 or C3 [28]. The propensity for H atom transfer from C3 or C4 or the C2 versus C3 hydroxyl groups should depend on the proximity of these hydrogen atoms to the carboxy radical, which is a function of the C5 stereochemistry. Moreover, the product ions that result when fragmentation is initiated by an oxy-radical at C2 or a radical at C3 are expected to be different than from an oxy-radical at C3 or a radical at C4. Thus, the stereochemistry of the carbon that bears the carboxylic acid group should affect the subsequent fragmentation that is observed. Here we report evidence that GlcA can be distinguished from IdoA in HS tetrasaccharide epimers using EDD. Furthermore, differences in the EDD mass spectra of epimers can be rationalized by simple radical driven fragmentation mechanisms that should allow this approach to be extended to the structure analysis of a wide variety of GAG oligosaccharides.

EXPERIMENTAL

Preparation of Heparan Sulfate Tetrasaccharides

Heparan sulfate sodium salt was obtained from Celsus Laboratories (Cincinnati, OH), and digested with heparinase II (Sigma, St. Louis, MO) and fractionated by gel-permeation chromatography using a P-10 column (Bio-Rad, Hercules, CA) to obtain uniform sized oligosaccharides. The fraction containing tetrasaccharides was desalted on a Bio-Rad Micro Bio-Spin chromatography column packed with 1 mL of Bio-Rad P-2 resin. 50 μL of sample was loaded onto the resin and centrifuged at 1000 x *g*. After desalting, the fractions containing tetrasaccharides were pooled and concentrated by freeze-drying. Fractions containing individual tetrasaccharides were collected from semi-preparative SAX-HPLC (Shimadzu, Columbia, MD) using a Spherisorb column (Waters Corp, Milford, MA), desalted on a Bio-Rad P-2 column, and freeze-dried [29]. For the work reported here, four tetrasaccharides were examined, structures ***1*** – ***4***. The structure of tetrasaccharides ***2*** and ***3*** were determined by 1D and 2D proton NMR. Tetrasaccharide ***1*** was prepared from tetrasaccharide ***3*** by *N*-sulfonation using the following protocol: 50 μg of tetrasaccharide ***3*** was dissolved in 12.5 μL of solution containing 10 mg/mL sodium bicarbonate and 10 mg/mL trimethylamine-sulfurtrioxide complex and incubated at 50 °C for 12 h. Equal portion of sodium bicarbonate and trimethylamine-sulfurtrioxide complex was added two more times at 12 h intervals. The solution was then desalted by P-2 spin column and the product was freeze-dried [30]. Tetrasaccharide ***4*** was prepared from tetrasaccharide ***2*** using the following protocol: tetrasaccharide ***2*** sodium salt was converted to a pyridinium salt using a Dowex 50W cation exchange column (Sigma, St. Louis, MO). 200 μg of the pyridinium salt of ***2*** was dissolved in 10 μL of dimethyl sulfoxide (Acros, Geel, Belgium) containing 5% methanol and incubated for 1.5h at 50 °C [31]. The desulfated product, ***4***, was then purified on a Bio-Rad P-2 spin column and freeze-dried. The products of the sulfation and desulfation reactions differ in mass from the starting materials, and they can be easily isolated from each other for the EDD experiments. The sulfation and desulfation reactions do not affect the stereochemistry of the hexuronic residue, and so the chirality of the products has the same purity as that of the reactants, which have been established to be pure by NMR analysis.

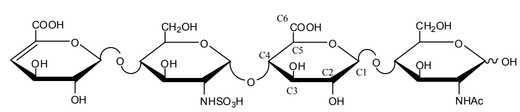

1

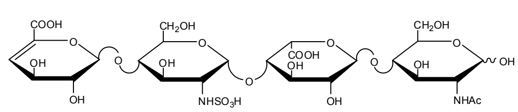

2

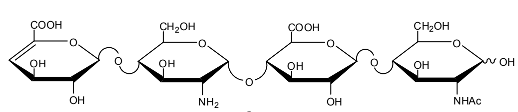

3

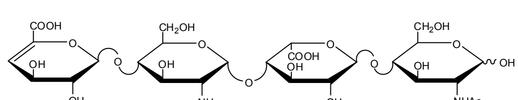

4

Mass Spectrometry Analysis

Experiments were performed with a 7 T Bruker Apex IV QeFTMS fitted with an Apollo II ESI source, a CO_2 laser for IRMPD, and an indirectly heated hollow cathode for generating electrons for ECD and EDD. The hollow cathode implementation with the Infinity™ cell has been previously described [27, 32]. Solutions of tetrasaccharides ***1***, ***2***, and ***3*** were made at a concentration of 0.1 mg/mL in 50:50 methanol:H_2O (Sigma, St. Louis, MO), tetrasaccharide ***4*** was made at a concentration of 1.0 mg/mL. All tetrasaccharides were ionized by nanospray using a pulled fused silica tip (model# FS360-75-15-D-5, New Objective, Woburn, MA). The sample solutions were infused at a rate of 10 μL/hour. All tetrasaccharides were examined in negative ion mode.

For the EDD experiments, precursor ions were isolated in the external quadrupole and accumulated for 1–2 seconds before injection into the FTMS cell. The isolation/cell fill was repeated up to 6 times. The selection of the precursor ion was further refined by using in-cell isolation with a coherent harmonic excitation frequency (CHEF) event. The precursor ions were then irradiated with electrons for 1 second. For electron irradiation the cathode bias was set to -19 V, the ECD lens was set to -17.5 V±0.5 V, and the cathode heater was set to 5–6 V. The electrons can potentially make multiple passes through the analyzer cell by reflection from the negative potential of the transfer ion optics and the hollow cathode, irradiating the sample at many different energies below the initial value of 19 eV. However, it appears that the efficiency of the EDD process is highly sensitive to the energy of the electrons, as irradiation of GAG tetrasaccharides with electrons at initial energies higher or lower than 19 eV by even a few tenths of an eV results in significantly less fragmentation. 24 acquisitions were averaged per mass spectrum. For each mass spectrum, 512k points were acquired, padded with one zero fill, and apodized using a sinebell window. Background spectra were acquired by leaving all parameters the same but setting the cathode bias to 0 V to ensure that no electrons reached the analyzer cell. All EDD products are reported using the Domon and Costello nomenclature [33].

RESULTS AND DISCUSSION

EDD of epimers ***1*** and ***2*** produces the mass spectra shown in Figures 4.1a and 4.1b, respectively. Glycosidic bond cleavage is the principal type of fragmentation that is observed, but cross-ring cleavage to produce A ions [33] is also significant. During EDD, a radical site is produced by detachment of a carboxylate electron in preference to a sulfate electron, as ~1.2 eV less energy is required [28]. This is evident from the presence of a $[M\text{-}2H\text{-}CO_2]^{-\bullet}$ product and the absence of a $[M\text{-}2H\text{-}SO_3]^{-\bullet}$ product. The abundance of fragmentation at the hexuronic acid near the reducing end of the tetrasaccharide suggests that the carboxyl group in this residue is a favored site for electron detachment. Many of the product ions observed in EDD of ***1*** are observed in the EDD of ***2*** (bond cleavage sites shown in insets, Figure 4.1), and can be used to establish the sites of modification [28]. On the other hand, there are a few peaks that are not common to the spectra of both epimers, for example, the $^{0,2}A_3$ product ion (*m/z* 532.059), which is observed only in the EDD of ***1***, albeit at a relatively low abundance. Closer examination of the EDD mass spectra above the precursor ion (*m/z* 397.047), Figures 4.2a and 4.2b, reveals a number of peaks specific to each epimer. An odd-electron ion at *m/z* 573.062 is present in EDD of ***1*** and not in EDD of ***2***. This product ion differs from the B_3 fragment by the exact mass of a hydrogen atom, and is more intense than the B_3 product ion in EDD of ***1***. We have assigned this product as $[B_3\text{-}H]^{-\bullet}$, which we denote as B_3'. The odd-electron ion at *m/z* 529.072 is present in EDD of ***1*** and not in EDD of ***2*** and differs from B_3' by the exact mass of CO_2. We have assigned

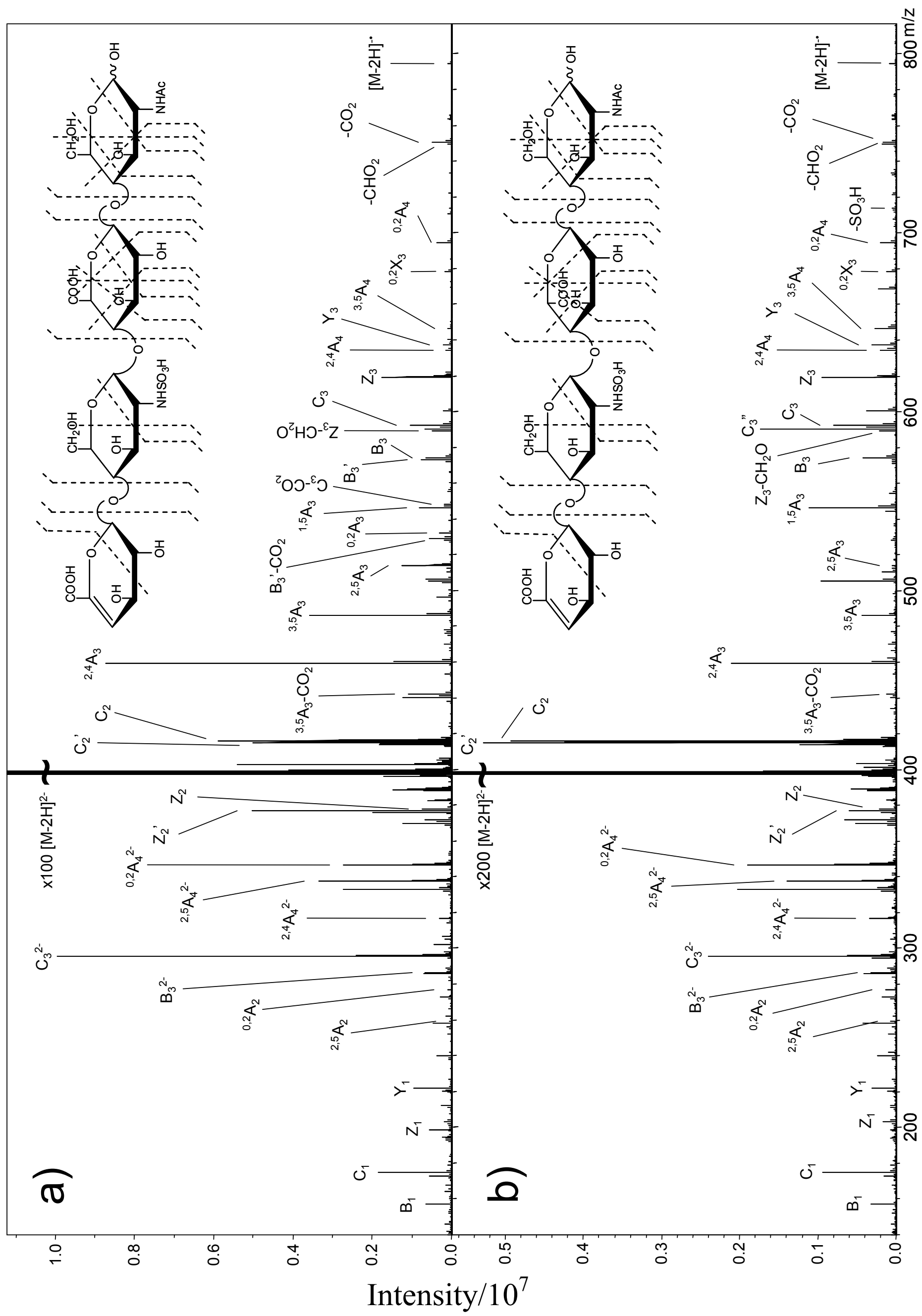

Figure 4.1. EDD mass spectra of the $[M\text{-}2H]^{2-}$ precursor ion of HS epimers: (a) GlcA-containing tetrasaccharide ***1***; (b) IdoA containing tetrasaccharide ***2***. EDD results in cleavage of every glycosidic bond and abundant cross-ring fragmentation without loss of the labile sulfate group, allowing structure determination of the tetrasaccharides. Insets: observed bond cleavages for the HS tetrasaccharides.

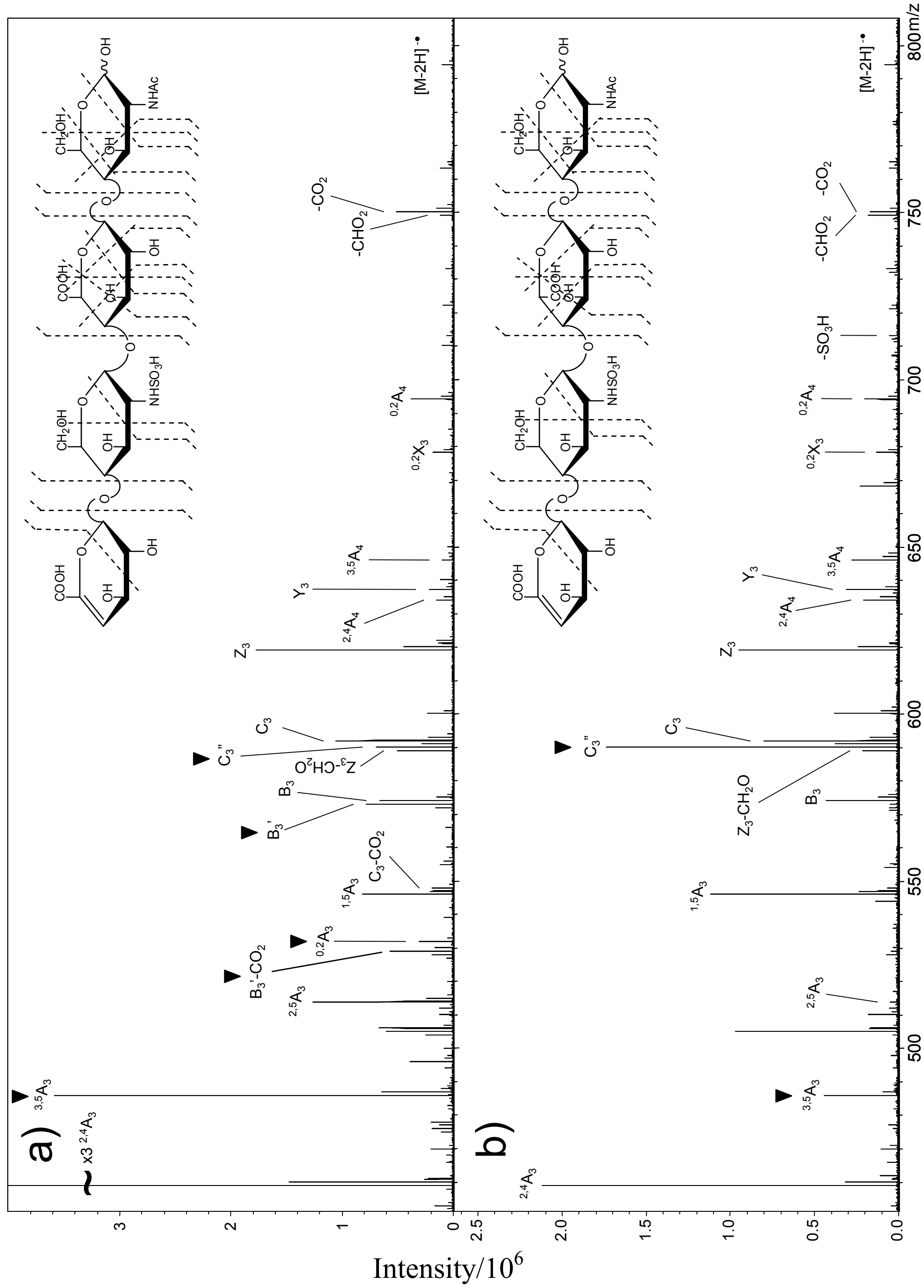

Figure 4.2. Expansion of the *m/z* 450 – 800 region of Figure 4.1. (a) EDD of ***1***, GlcA. (b) EDD of ***2***, IdoA. The ▼above the peak labels indicates product ions unique to each HS epimer.

this product as $[B_3\text{-H-}CO_2]^{-\bullet}$, which we denote as B_3'-CO_2. The ion at *m/z* 590.065 differs from C_3 by the exact mass of two hydrogens, and is assigned as $[C_3\text{-2H}]^-$, which we denote as C_3". This product ion is observed in both EDD spectra, but is significantly more intense than the C_3 product ion in the EDD spectrum of ***2***, while it is less abundant than the C_3 fragment in the EDD spectrum of ***1***. Likewise, the $^{3,5}A_3$ product ion is present in both EDD of ***1*** and ***2***, but is significantly more intense in the EDD of ***1***, where it is one of the most abundant product ions in the mass spectrum.

The differences in the observed product ions for the two epimers can be rationalized as arising from hydrogen rearrangement from C4 or the hydroxyl group on C3 of GlcA (tetrasaccharide ***1***) to the carboxy radical, versus rearrangement of a hydrogen atom from C3 or the C2 hydroxyl group to the carboxy radical for IdoA (tetrasaccharide ***2***), as proposed in Schemes 4.1 and 4.2 (see structure ***1*** for carbon atom nomenclature). Hydrogen rearrangement from C3 or the C2 hydroxyl group to the GlcA carboxy radical is not expected to occur for tetrasaccharide ***1***, as no conformation of the sugar ring brings the carboxy radical into the vicinity of C3 or the C2 hydroxyl group. Likewise, no conformation of tetrasaccharide ***2*** is expected to bring the IdoA carboxy radical close enough to the C3 hydroxyl group or C4 to permit H atom transfer. Subsequent radical-initiated cleavage of these radicals produces different fragmentations that can distinguish IdoA from GlcA.

The C3 oxy-radical or the C4 radical that results from the aforementioned hydrogen rearrangement for ***1*** can undergo α-cleavage to form the $^{0,2}A_3$ product ion, as proposed in Schemes 4.3a and 4.4a. The observed $^{0,2}A_3$ fragment ion is even-electron, formed by a mechanism that includes a rearrangement of a hydrogen atom from the departing neutral fragment to the product ion. H atom transfer to oxygen is often observed in the tandem mass spectra of carbohydrates when a carbon-oxygen bond is broken, for example in the cleavage of glycosidic bonds to form B, C, Y, and Z type ions [33]. The $^{0,2}A_3$ product ion is easily rationalized to result from α-cleavage of an oxy-radical located at C3 or a radical at C4, but not by α-cleavage from an oxy-radical located at C2 or a radical at C3. As H atom transfer is expected to occur between the IdoA carboxy radical and the C2 hydroxyl group or C3, but not with the C3 hydroxyl group or C4, formation of the $^{0,2}A_3$ product ion is not expected for epimer ***2***.

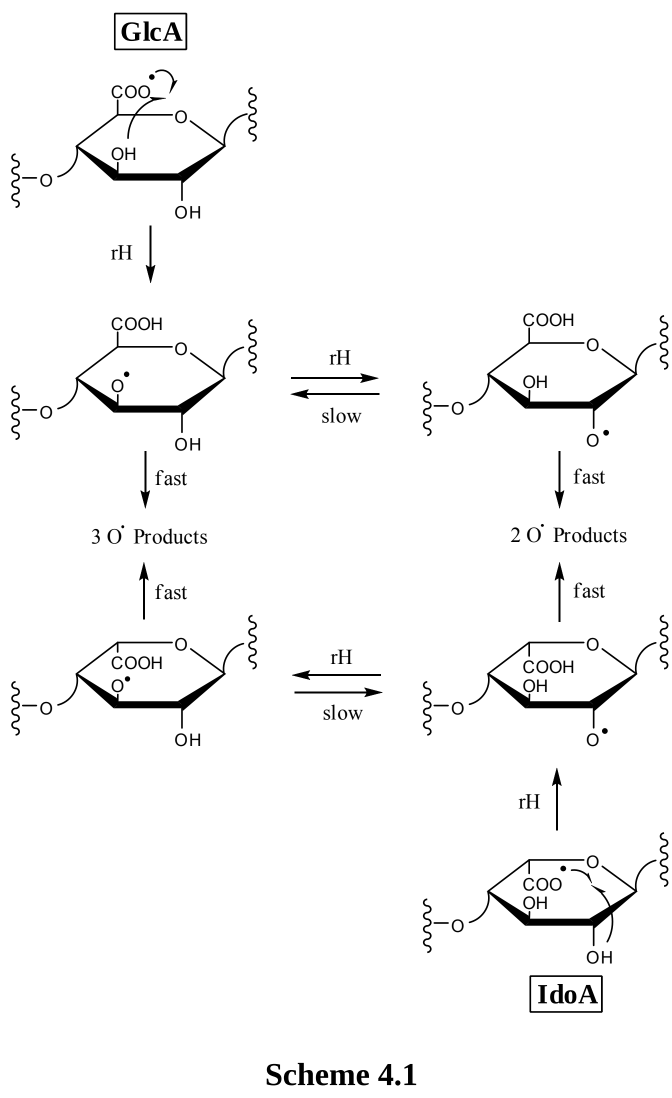

Scheme 4.1

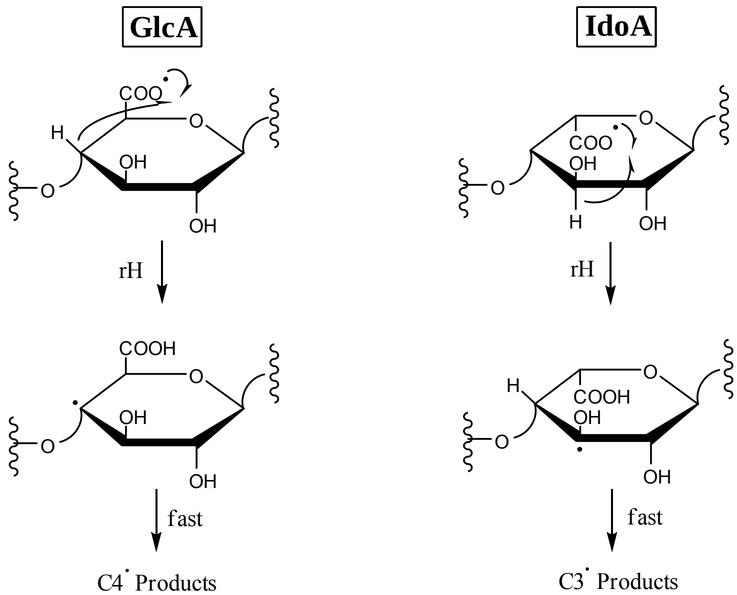

Scheme 4.2

Formation of an oxy-radical on C3 or a C4 radical may initiate a second fragmentation pathway (Schemes 4.3b and 4.4b), resulting in formation of the B_3' product ion. Fragmentation via this pathway occurs with the transfer of a hydrogen atom from the B_3' product ion to the oxygen atom of the neutral fragment. Similar to the formation of the $^{0,2}A_3$ product ion, formation of the B_3' should occur only when the oxy-radical is on C3, and not when the oxy-radical is located at C2, or when the radical is located at C4 and not C3. We find that B_3' is twice as abundant as B_3 in the EDD spectrum of ***1***, but in the EDD spectrum of ***2***, the B_3' product abundance is only 12% of the abundance of the B_3 product (see table of intensities in Appendix A.) Some of this peak is the isotopic contribution of the adjacent peaks, and very little, if any, is from B_3'. Also consistent with this proposed radical mechanism is the observation that B_3' occurs only as a singly-charged ion, while B_3 occurs as both a singly- and doubly-charged ion, i.e. only $[B_3\text{-H}]^{-\bullet}$ is observed, and not $[B_3\text{-H}]^{2-}$. Also observed in the EDD spectrum of ***1*** and not in the EDD spectrum of ***2*** is the B_3'-CO_2 ion, which may arise from the B_3' product ion as proposed in Schemes 4.3b and 4.4b. We do not believe that this product arises from the [M-2H-CO_2]$^{-\bullet}$ ion, as this species has lost its chirality at C5, and so were the B_3'-CO_2 to arise from [M-2H-CO_2]$^{-\bullet}$ it would be expected to appear in the EDD spectra for both epimers ***1*** and ***2***. Similar to B_3', the B_3'-CO_2 product ion is observed only as a singly-charged ion, consistent with our proposed radical mechanism.

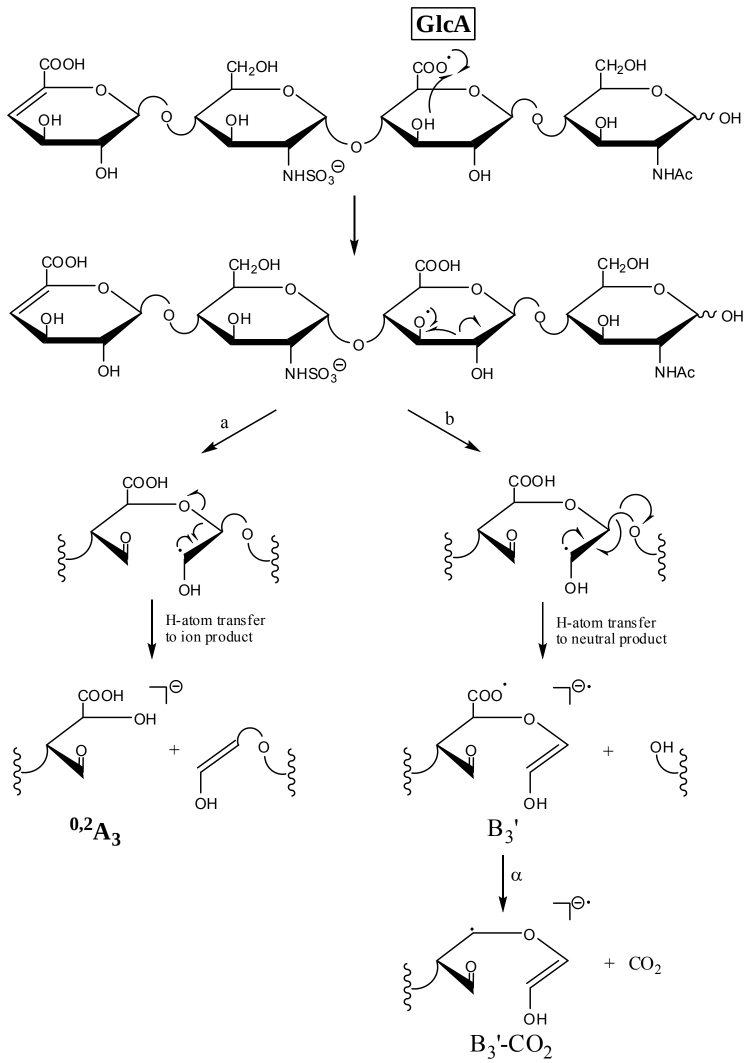

Scheme 4.3

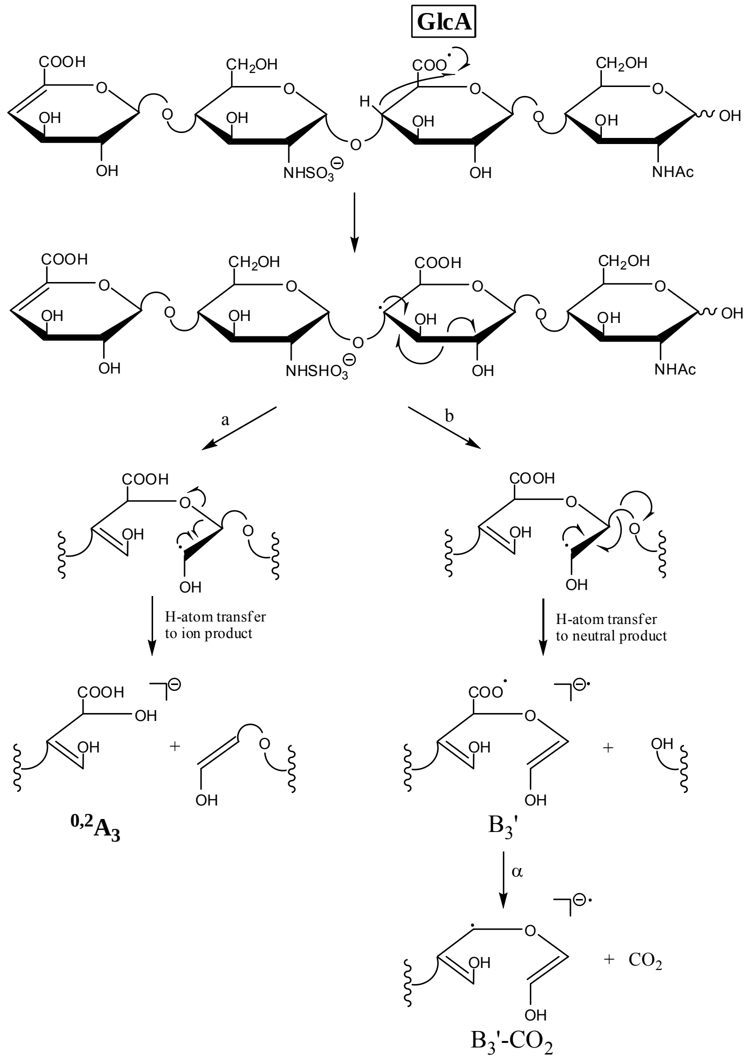

Scheme 4.4

For IdoA (tetrasaccharide ***2***), hydrogen transfer to form an oxy-radical at C2 or a radical at C3 can lead to the formation of the C_3" product ion by α-cleavage as proposed in Schemes 4.5 and 4.6, respectively. If the oxy-radical were located at C3 or the radical at C4, there would be no simple route to form the C_3" product. Since this product is observed in the EDD spectrum of ***1***, albeit at a much lower abundance than in the EDD spectrum of ***2***, it may also be produced by an additional, secondary fragmentation mechanism. An alternative possibility is that the small amount of C_3" product in the EDD of ***1*** results from hydrogen atom transfer between the oxygen atoms on C2 and C3, as proposed in Scheme 4.1. This H atom transfer is expected to be slow due to the unfavorable conformation of the sugar ring that would be necessary to align these groups sufficiently to allow this rearrangement to occur. The differences in the abundances of the diagnostic product ions for GlcA versus IdoA suggest that hydrogen transfer between the oxygens of C2 and C3, if it occurs at all, is slow compared to cross-ring and glycosidic fragmentations.

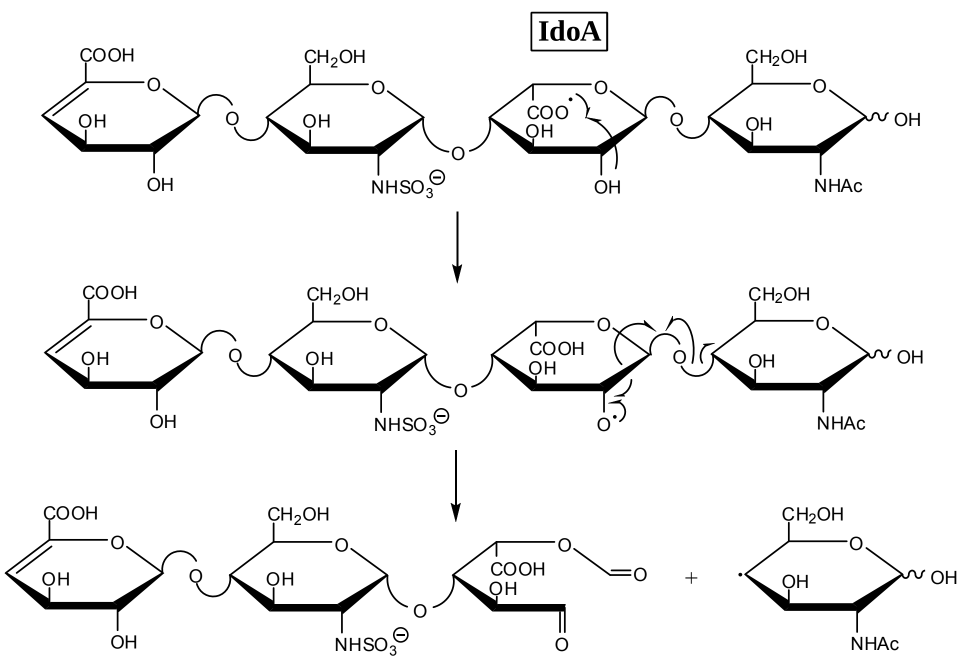

C_3''

Scheme 4.5

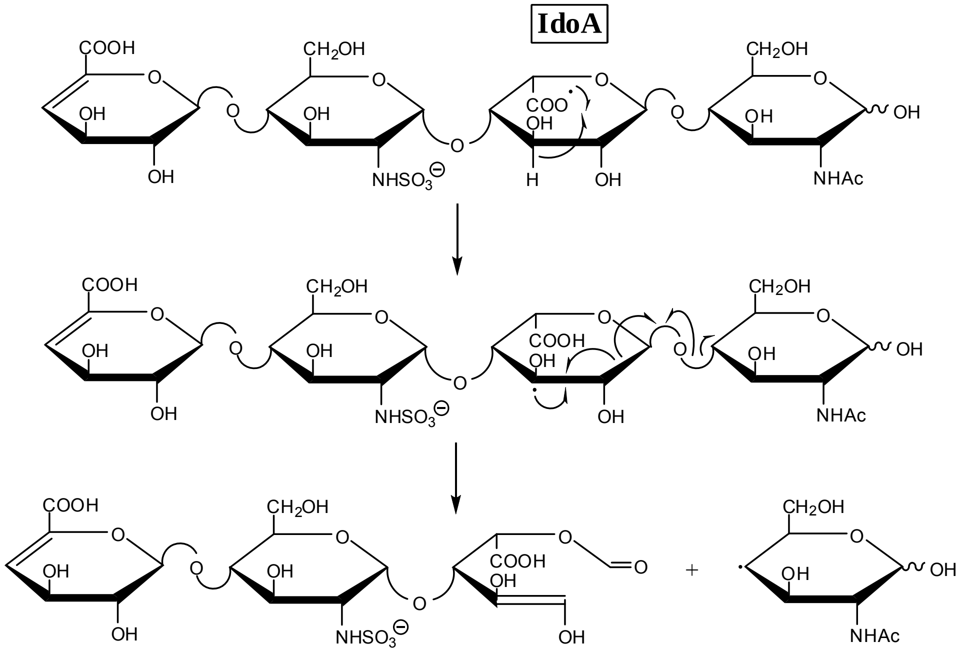

C_3"

Scheme 4.6

Similar to C_3", the $^{3,5}A_3$ product ion is observed in both the EDD of ***1*** and ***2***, but is significantly more intense in ***1***. This product ion may result from α-cleavage of an oxy-radical located at C3 as proposed in Scheme 4.7 or a radical at C4 as proposed in Scheme 4.8, but not by α-cleavage from an oxy-radical located at C2 or a radical at C3. The occurrence of the $^{3,5}A_3$ product at reduced ion intensity in the EDD of ***2*** can be rationalized as resulting from slow H atom transfer from the C3 hydroxyl group to the oxy-radical on C2 or production of this product via a second fragmentation mechanism.

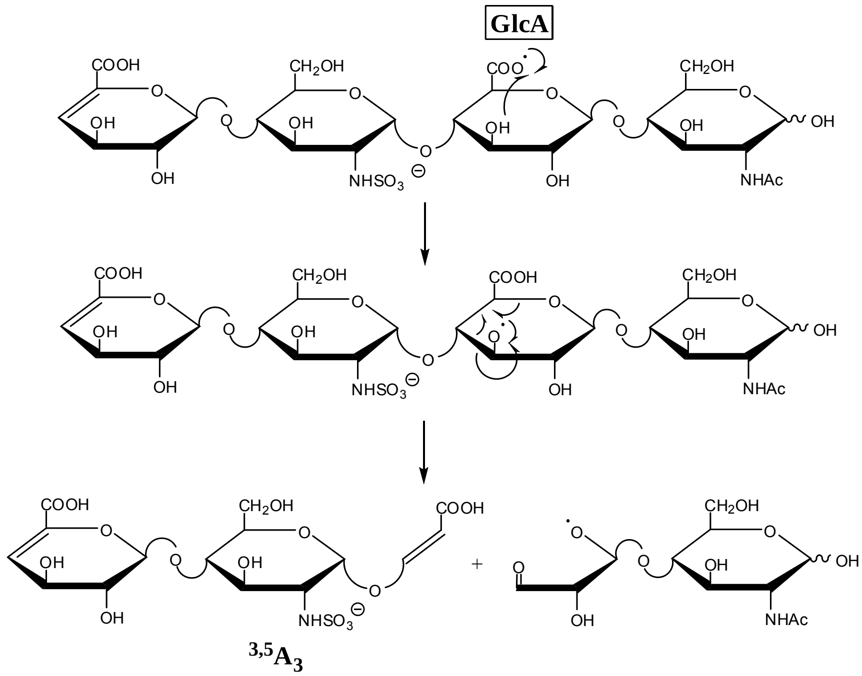

Scheme 4.7

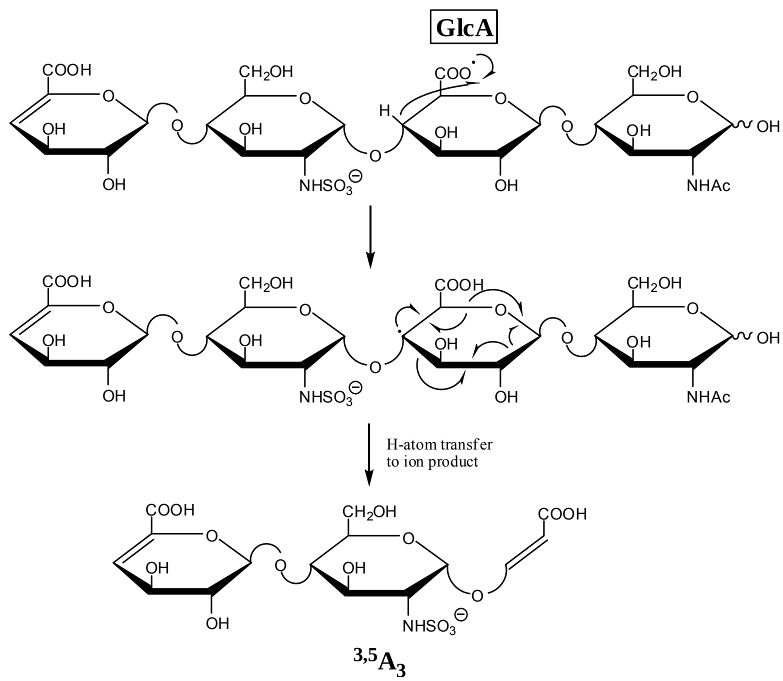

Scheme 4.8

A second set of epimers, ***3*** and ***4***, were analyzed by EDD (Figure 4.3a and 4.3b, respectively) to test these hypothesized fragmentation mechanisms. The epimers ***3*** and ***4*** differ from ***1*** and ***2*** by absence of N-sulfation on the glucosamine residue adjacent to the non-reducing end. Many of the same product ions observed for ***1*** and ***2*** are observed for ***3*** and ***4***. Consistent with the observations for ***1*** and ***2***, the $^{0,2}A_3$, B_3', and B_3'-CO_2 product ions are observed only in EDD of ***3***, the GlcA epimer, and not in EDD of the IdoA epimer, ***4***. Also, B_3' is more abundant than the B_3 product ion in ***3*** and the C_3" product ion is higher in abundance in the EDD spectrum of ***4*** versus ***3***. However, there are few differences between the EDD mass spectra of the two epimer pairs. For example, the C_3" product is less abundant than the C_3 product in the EDD spectrum of ***4***, the IdoA epimer, while it was more abundant than C_3 for the IdoA epimer, ***2***. C_3" was observed in the EDD spectra of both epimers ***1*** and ***2*** (and is more abundant for the IdoA epimer ***2*** than for the GlcA epimer ***1***), but for the other epimer pair this product is observed only in the EDD spectrum of the IdoA epimer ***4***. Since the C_3" product ion can distinguish IdoA from GlcA only by being more abundant in the former, it is useful only if one can directly compare EDD mass spectra of both epimers. Differences in the $^{3,5}A_3$ product ion abundance in ***1*** and ***2*** were attributed to the preference of GlcA forming a C3 oxy-radical or a C4 carbon radical. However, the abundance of the $^{3,5}A_3$ product ion is the same for epimers ***3*** and ***4***, indicating that $^{3,5}A_3$ is not diagnostic of IdoA versus GlcA for these nonsulfated tetrasaccharides. Nevertheless, the EDD spectra of tetrasaccharides ***3*** and ***4*** exhibit key diagnostic ions ($^{0,2}A_3$, B_3', and B_3'-CO_2) that allow GlcA to be distinguished from IdoA. These diagnostic product ions, and their observed relative intensities, are listed in Table 4.1 for each epimer pair.

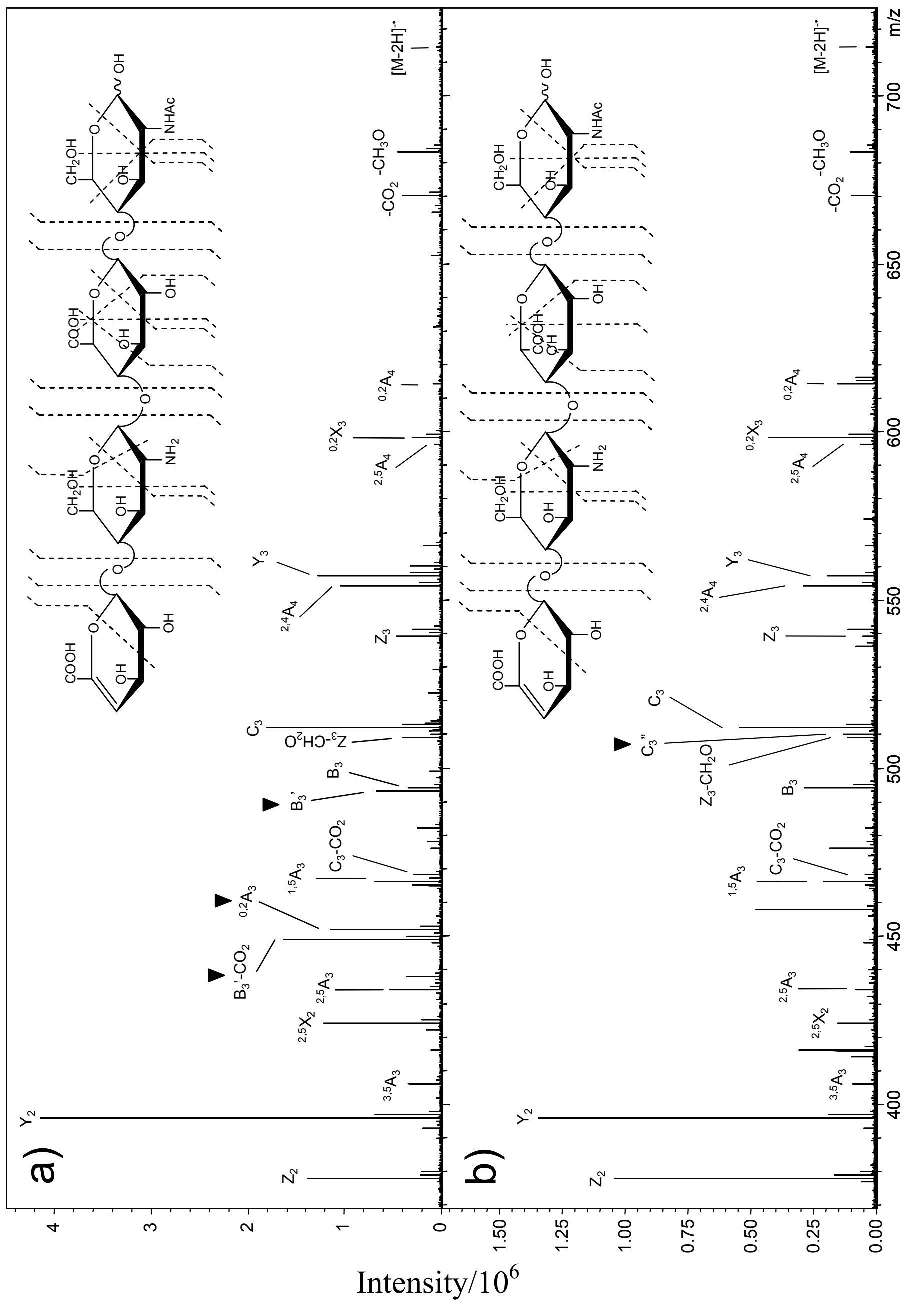

Figure 4.3. EDD mass spectra of the $[M\text{-}2H]^{2-}$ precursor ion of HS epimers expanded to show the region *m/z* 375 – 725: (a) GlcA containing tetrasaccharide ***3***; (b) IdoA containing tetrasaccharide ***4***. The ▼above the peak labels indicates product ions unique to each HS epimer. Insets: observed bond cleavages for the HS tetrasaccharides.

Table 4.1. Diagnostic product ions and their relative ion intensities. The relative ion intensities are reported with respect to the most intense product ion, C_2. NO = not observed.

	$^{0,2}A_3$	B_3'	B_3'-CO_2	C_3''	$^{3,5}A_3$
Tetrasaccharide ***1***	0.0516	0.1553	0.0991	0.1187	0.6050
Tetrasaccharide ***2***	NO	0.0117	0.0087	0.3570	0.0896
Tetrasaccharide ***3***	0.227	0.1767	0.3937	0.0274	0.0825
Tetrasaccharide ***4***	NO	0.0161	0.0232	0.1039	0.0742

CONCLUSIONS

EDD produces a radical anion which can undergo radical-driven fragmentation processes that are very different from the fragmentation of even electron anions that are formed by electrospray ionization. We have demonstrated the utility of EDD for distinguishing GlcA versus IdoA in GAG tetrasaccharides. The diagnostic ions for GlcA are the $^{0,2}A_3$, B_3', and B_3'-CO_2 product ions. IdoA can be distinguished by the absence of these ions in the EDD mass spectrum. To a lesser extent, the abundance of the C_3" product ion can be used to determine C5 stereochemistry. All of the diagnostic product ions can be rationalized as arising from a proposed radical species whose subsequent fragmentation is influenced by C5 stereochemistry. Consistent with the proposed radical mechanisms, these diagnostic ions are not observed by CAD or IRMPD of these GAG tetrasaccharides (data not shown). The EDD mass spectra are highly reproducible, even for acquisitions taken several months apart (see Appendix A), and so the ions that distinguish the epimers from each other have good diagnostic value. Of course, the proposed mechanisms are hypothetical at this point. Validation of these mechanisms will require considerable more effort, for example with isotope labeling experiments. Since it is possible for GAGs to contain a higher degree of sulfation than for the tetrasaccharides studied here, future work will examine the influence of the degree of sulfation on the capability to distinguish GlcA/IdoA epimers by EDD.

ACKNOWLEDGEMENTS

We gratefully acknowledge financial support from the National Institutes of Health grant #2R01-GM038060-16.

REFERENCES

1. Perrimon, N.; Bernfield, M., Cellular functions of proteoglycans--an overview. *Semin. Cell Dev. Biol.* **2001,** *12*, 65-67.
2. Linhardt, R. J.; Toida, T., Role of Glycosaminoglycans in Cellular Communication. *Acc. Chem. Res.* **2004,** *37*, 431-438.
3. Fannon, M.; Forsten, K. E.; Nugent, M. A., Potentiation and Inhibition of bFGF Binding by Heparin: A Model for Regulation of Cellular Response. *Biochemistry* **2000,** *39*, 1434-1445.
4. Wu, Z. L.; Zhang, L.; Yabe, T.; Kuberan, B.; Beeler, D. L.; Love, A.; Rosenberg, R. D., The Involvement of Heparan Sulfate (HS) in FGF1/HS/FGFR1 Signaling Complex. *J. Biol. Chem.* **2003,** *278*, 17121-17129.
5. Gotte, M., Syndecans in Inflammation. *The FASEB Journal* **2003,** *17*, 575-591.
6. Batinic, D.; Robey, F. A., The V3 region of the envelope glycoprotein of human immunodeficiency virus type 1 binds sulfated polysaccharides and CD4-derived synthetic peptides. *J. Biol. Chem.* **1992,** *267*, 6664-6671.
7. Chen, Y.; Maguire, T.; Hileman, R. E.; Fromm, J. R.; Esko, J. D.; Linhardt, R. J.; Marks, R. M., Dengue virus infectivity depends on envelope protein binding to target cell heparan sulfate. *Nature Med.* **1997,** *3*, 866-871.
8. Williams, R. K.; Straus, S. E., Specificity and affinity of binding of herpes simplex virus type 2 glycoprotein B to glycosaminoglycans. *J. Virol.* **1997,** *71*, 1375-1380.
9. Liu, D. F.; Shriver, Z.; Gi, Y. W.; Venkataraman, G.; Sasisekharan, R., Dynamic regulation of tumor growth and metastasis by heparan sulfate glycosaminoglycans. *Seminars in Thrombosis and Hemostasis* **2002,** *28*, 67-78.

10. Lindahl, U.; Kusche-Gullberg, M.; Kjellen, L., Regulated Diversity of Heparan Sulfate. *J. Biol. Chem.* **1998,** *273*, 24979-24982.

11. Salmivirta, M.; Lidholt, K.; Lindahl, U., Heparan sulfate: a piece of information. *The FASEB Journal* **1996,** *10*, 1270-1279.

12. Turnbull, J.; Powell, A.; Guimond, S., Heparan sulfate: decoding a dynamic multifunctional cell regulator. *Trends Cell Biol.* **2001,** *11*, 75-82.

13. Horne, A.; Gettins, P., H-1-Nmr Spectral Assignments for 2 Series of Heparin-Derived Oligosaccharides. *Carbohydr. Res.* **1992,** *225*, 43-57.

14. Naggar, E. F.; Costello, C. E.; Zaia, J., Competing Fragmentation Processes in Tandem Mass Spectrometry of Heparin-Like Glycosaminoglycans. *J. Am. Soc. Mass Spectrom.* **2004,** *15*, 1534-1544.

15. Takagaki, K.; Kojima, K.; Majima, M.; Nakamura, T.; Kato, I.; Endo, M., Ion-Spray Mass-Spectrometric Analysis of Glycosaminoglycan Oligosaccharides. *Glycoconjugate J.* **1992,** *9*, 174-179.

16. Zaia, J.; Costello, C. E., Tandem Mass Spectrometry of Sulfated Heparin-Like Glycosaminoglycan Oligosaccharides. *Anal. Chem.* **2003,** *75*, 2445-2455.

17. Saad, O. M.; Leary, J. A., Heparin Sequencing Using Enzymatic Digestion and ESI-MS with HOST: A Heparin/HS Oligosaccharide Sequencing Tool. *Anal. Chem.* **2005,** *77*, 5902-5911.

18. Sweeney, M. D.; Yu, Y.; Leary, J. A., Effects of Sulfate Position on Heparin Octasaccharide Binding to CCL2 Examined by Tandem Mass Spectrometry. *J. Am. Soc. Mass Spectrom.* **2006,** *17*, 1114-1119.

19. Zaia, J.; Li, X.-Q.; Chan, S.-Y.; Costello, C. E., Tandem mass spectrometric strategies for determination of sulfation positions and uronic acid epimerization in chondroitin sulfate oligosaccharides. *J. Am. Soc. Mass Spectrom.* **2003,** *14*, 1270-1281.

20. Hitchcock, A. M.; Costello, C. E.; Zaia, J., Glycoform quantification of chondroitin/dermatan sulfate using a liquid chromatography-tandem mass spectrometry platform. *Biochemistry* **2006,** *45*, 2350-2361.

21. Miller, M. J. C.; Costello, C. E.; Malmstrom, A.; Zaia, J., A tandem mass spectrometric approach to determination of chondroitin/dermatan sulfate oligosaccharide glycoforms. *Glycobiology* **2006,** *16*, 502-513.

22. Anusiewicz, I.; Jasionowski, M.; Skurski, P.; Simons, J., Backbone and side-chain cleavages in electron detachment dissociation (EDD). *J. Phys. Chem. A* **2005,** *109*, 11332.

23. Budnik, B. A.; Haselmann, K. F.; Zubarev, R. A., Electron detachment dissociation of peptide di-anions: an electron-hole recombination phenomenon. *Chem. Phys. Lett.* **2001,** *342*, 299-302.

24. Cooper, H. J.; Hakansson, K.; Marshall, A. G., The role of electron capture dissociation in biomolecular analysis. *Mass Spectrom. Rev.* **2005,** *24*, 201.

25. Kjeldsen, F.; Silivra, O. A.; Ivonin, I. A.; Haselmann, K. F.; Gorshkov, M.; Zubarev, R. A., Cα-C Backbone Fragmentation Dominates in Electron Detachment Dissociation of Gas-Phase Polypeptide Polyanions. *Chem. Eur. J.* **2005,** *11*, 1803-1812.

26. McFarland, M. A.; Marshall, A. G.; Hendrickson, C. L.; Nilsson, C. L.; Fredman, P.; Mansson, J. E., Structural characterization of the GM1 ganglioside by infrared multiphoton dissociation/electron capture dissociation, and electron detachment

dissociation electrospray ionization FT-ICR MS/MS. *J. Am. Soc. Mass Spectrom.* **2005,** *16*, 752.

27. Yang, J.; Mo, J.; Adamson, J. T.; Hakansson, K., Characterization of Oligodeoxynucleotides by Electron Detachment Dissociation Fourier Transform Ion Cyclotron Resonance Mass Spectrometry. *Anal. Chem.* **2005,** *77*, 1876-1882.
28. Wolff, J. J.; Chi, L.; Linhardt, R. J.; Amster, I. J., Electron Detachment Dissociation of Glycosaminoglycan Tetrasaccharides. *J. Am. Soc. Mass Spectrom.* **2007,** *18*, 234-244.
29. Pervin, A.; Gallo, C.; Jandik, K. A.; Han, X.-J.; Linhardt, R. J., Preparation and structural characterization of large heparin-derived oligosaccharides. *Glycobiology* **1995,** *5*, 83-95.
30. Munoz, E.; Xu, D.; Avci, F.; Kemp, M.; Liu, J.; Linhardt, R. J., Enzymatic synthesis of heparin related polysaccharides on sensor chips: Rapid screening of heparin-protein interactions. *Biochem. Biophys. Res. Commun.* **2006,** *339*, 597-602.
31. Inoue, Y.; Nagasawa, K., Selective N-desulfation of heparin with dimethyl sulfoxide containing water or methanol. *Carbohydr. Res.* **1976,** *46*, 87-95.
32. Tsybin, Y. O.; Witt, M.; Baykut, G.; Håkansson, P., Electron capture dissociation Fourier transform ion cyclotron resonance mass spectrometry in the electron energy range 0-50 eV. *Rapid Commun. Mass Spectrom.* **2004,** *18*, 1607-1613.
33. Domon, B.; Costello, C. E., A systematic nomenclature for carbohydrate fragmentations in FAB-MS/MS spectra of glycoconjugates. *Glycoconjugate J.* **1988,** *5*, 397-409.

CHAPTER 5

ELECTRON DETACHMENT DISSOCIATION OF DERMATAN SULFATE OLIGOSACCHARIDES*

*Reproduced with permission from Wolff, J.J.; Laremore, T.N.; Busch, A.M.; Linhardt, R.J.; Amster, I.J. Journal of the American Society for Mass Spectrometry, **2008**, *19*, 294-304.

ABSTRACT

The structural characterization of glycosaminoglycans (GAG) oligosaccharides has been a longstanding challenge in the field of mass spectrometry. In this work, we present the application of electron detachment dissociation (EDD) Fourier transform mass spectrometry to the analysis of dermatan sulfate (DS) oligosaccharides up to 10 residues in length. The EDD mass spectra of DS oligosaccharides were compared to their infrared multiphoton dissociation (IRMPD) mass spectra. EDD produces more abundant fragmentation than IRMPD with far less loss of SO_3 from labile sulfate modifications. EDD cleaves all glycosidic bonds, yielding both conventional glycosidic bond fragmentation as well as satellite peaks resulting from the additional loss of 1 or 2 hydrogen atoms. EDD also yields more cross-ring fragmentation than IRMPD. For EDD, abundant cross-ring fragmentation in the form of A- and X-ions is observed, with $^{1,5}X_n$ cleavages occurring for all IdoA residues and many of the GalNAc4S residues, except at the reducing and nonreducing ends. In contrast, IRMPD produces only A-type cross-ring fragmentation for long oligosaccharides (dp6 – dp10). As all the structurally informative fragment ions observed by IRMPD appear as a subset of the peaks found in the EDD mass spectrum, EDD shows great potential for the characterization of GAG oligosaccharides using a single tandem mass spectrometry experiment.

INTRODUCTION

Glycosaminoglycans (GAGs) are linear polysaccharides that comprise the carbohydrate portion of many proteoglycans and are found in a variety of organisms ranging from bacteria to humans [1]. GAGs participate in a number of important biological activities, such as binding growth factors and chemokines [2,3], inhibiting proteolysis [4], affecting angiogenesis [5], and acting as signaling molecules in response to cellular damage [6]. GAGs also play an important role in pathogenic infections [7-9], and have been shown to undergo alteration in certain types of cancer [10]. GAGs are assigned to one of four classes: heparin and heparan sulfate (HS), dermatan sulfate (DS) and chondroitin sulfate (CS), hylauronic acid, and keratan sulfate (KS) [11]. With the exception of KS, GAGs are composed of alternating uronic acid and hexosamine residues with variable degrees of sulfation and N-acetylation. KS is composed of a hexose-hexosamine disaccharide repeat. There is significant interest in determining the pattern of sulfation, N-acetylation of basic residues, and C5 epimerization of the acidic residues, as these modifications are believed to determine the biological activity of the GAG chain. 1D and 2D NMR have been used to determine the type and location of GAG modification [12], as well as the stereochemistry of C5 on hexuronic acid, but NMR analysis requires milligram quantities of a high purity sample. As GAGs must be isolated from natural sources, they are often available only in low quantity and purity, and there is considerable interest in the development of more sensitive methods for structural analysis of GAGs.

Mass spectrometry (MS) and tandem mass spectrometry (MS/MS) are viable alternatives for the structural analysis of GAGs as they require small quantities of sample and can be used to examine complex mixtures. Progress in the development of MS methods of GAG analysis has been slow compared to protein analysis due to the anionic nature of GAGs and the lability of sulfate as a carbohydrate modification. Electrospray ionization (ESI) [13] and matrix assisted laser desorption ionization (MALDI) [14-17] have been used to ionize sulfated GAGs in intact form. However, MS/MS of sulfated GAGs often leads to loss of SO_3, obscuring the position of modification. A number of tandem mass spectrometry approaches have been developed to overcome these problems. Zaia and Costello have shown that SO_3 loss can be minimized and glycosidic bond cleavages maximized by increasing the charge state of an ion so that the number of charges on the molecule is equal to the number of sulfates [18]. Their work also demonstrated that the addition of divalent calcium to sulfated GAGs decreased SO_3 loss during MS/MS. Saad and Leary [19] demonstrated that a mixture of heparin/HS disaccharides can be characterized using ESI with tandem mass spectrometry to distinguish isobaric disaccharides. Using this method, the authors were able to determine the disaccharide composition of biological samples using only mass spectrometry. Short lengths of GAGs can be analyzed by a combination of enzymatic digestion, tandem mass spectrometry (MS^2 and MS^3), and database searching [20]. While this approach can determine the pattern of modification (i.e. sulfation and acetylation), enzymatic digestion results in the formation of disaccharides containing C4 – C5 unsaturated uronic acid (ΔUA) at the non-reducing end (NRE), thereby converting glucuronic acid (GlcA) and iduronic acid (IdoA) into a single product (ΔUA) that eliminates chirality at C5 [21]. As the epimeric state of the hexuronic acid residues is thought to influence biological activity, it is important to be able to analyze GAG oligosaccharides which contain internal hexuronic acid residues that retain their chirality. Although tandem mass spectrometry is typically insensitive to stereochemistry, MS/MS of a series of isobaric CS samples has been shown to distinguish IdoA from GlcA as well as distinguish 4S- from 6S- sulfation based on the relative abundance of specific product ions [22].

We have recently reported the utility of electron detachment dissociation (EDD) [23-27] for the analysis of GAG HS tetrasaccharides [28,29]. EDD produces a radical anion, which undergoes more extensive fragmentation than that produced from activation of even electron ions by low energy or threshold dissociation methods. For HS tetrasaccharides, EDD produces both glycosidic bond and cross-ring fragmentation, revealing the sites of sulfation and acetylation, while minimizing SO_3 loss. More recently, we demonstrated that EDD can distinguish the epimers IdoA from GlcA in HS tetrasaccharides [29]. While application of EDD to the characterization of HS tetrasaccharides appears very promising, the extension of this fragmentation technique to longer oligosaccharides remains an important goal. Many protein binding sites on GAGs are 3-9 disaccharides in length, and GAG binding sites up to 15 disaccharides in length have been reported [30-35]. Here we demonstrate the applicability of EDD to the structural analysis of DS oligosaccharides up to 10 saccharides in length.

MATERIALS AND METHODS

Preparation of DS Oligosaccharides

Dermatan sulfate (DS) oligosaccharides were prepared by partial enzymatic depolymerization of porcine intestinal mucosa dermatan sulfate (Celsus Laboratories, Cincinnati, OH). A 20 mg/mL dermatan sulfate solution in 50 mM Tris-HCl/60 mM sodium acetate buffer, pH 8 was incubated at 37°C with chondroitin ABC lyase from *Proteus vulgaris*, EC 4.2.2.4. (Seikagaku, Japan). After the absorbance at 232 nm indicated the digestion was 50% completed, the digestion mixture was heated at 100°C for 3 min. High-molecular-weight oligosaccharides and the enzyme were removed by ultra-filtration using a 5000 MWCO membrane. The resulting oligosaccharide mixture was concentrated by rotary evaporation and fractionated by low pressure

GPC on a Bio-Gel P10 (Bio-Rad, Richmond, CA) column. Fractions containing tetra- to decasaccharides (dp4 – dp10, structures ***1*** **-** ***4***) were desalted by GPC on a Bio-Gel P2 column and freeze-dried [36]. Further purification of compounds ***1*** – ***4*** were carried out using strong anion exchange high-pressure liquid chromatography (SAX-HPLC) on a semi-preparative SAX S5 Spherisorb column (Waters Corp, Milford, MA). The SAX-HPLC fractions containing > 90% of ***1*** – ***4*** were collected, desalted by GPC, and freeze-dried. The solid was reconstituted in water and purified a second time by SAX-HPLC. Only the top 30% of the chromatographic peak was collected, desalted, and freeze-dried. Concentration of the oligosaccharide solutions was determined by measuring the absorbance at 232 nm ($\varepsilon = 3800\ M^{-1}cm^{-1}$). The resulting fractions containing individual DS oligosaccharides, structures ***1***, ***2***, ***3***, and ***4***, were characterized by PAGE, ESI-MS, and high-field nuclear magnetic resonance (NMR) spectroscopy.

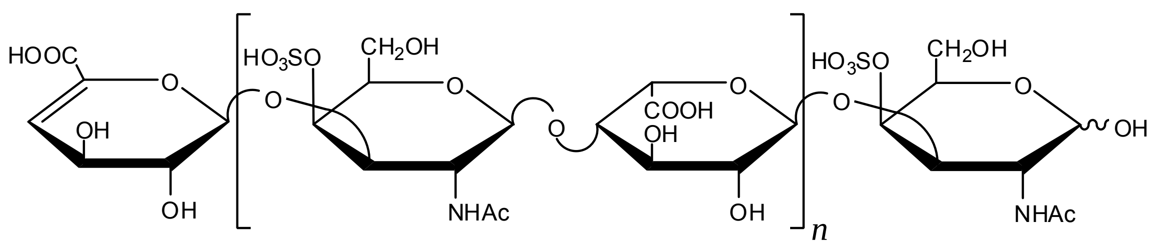

n	Structure
1	***1***
2	***2***
3	***3***
4	***4***

Mass Spectrometry Analysis

Experiments were performed with a 9.4 T Bruker Apex IV QeFTMS (Billerica, MA) fitted with an Apollo II dual source, a 25 W CO_2 laser (Synrad model J48-2, Mukilteo, WA) for infrared multiphoton dissociation (IRMPD), and an indirectly heated hollow cathode for generating electrons for ECD and EDD. Solutions of each oligosaccharide were introduced at a concentration of 0.1 – 0.2 mg/mL in 50:50:0.1 methanol:H_2O:NH_3 (Sigma, St. Louis, MO) and ionized by nanospray using a pulled fused silica tip (model# FS360-75-15-D-20, New Objective, Woburn, MA). The sample solutions were infused at a rate of 10 μL/hour. All DS oligosaccharides, ***1*** – ***4***, were examined in negative ion mode.

For the EDD experiments, precursor ions were isolated in the external quadrupole and accumulated for 1–2 seconds before injection into the FTMS cell. The isolation/cell fill was repeated up to 6 times. The selection of the precursor ion was further refined by using in-cell isolation with a coherent harmonic excitation frequency (CHEF) event [37]. The precursor ions were then irradiated with electrons for 1 second. For electron irradiation the cathode bias was set to -19 V, the extraction lens was set to -17.5 V±0.5 V, and the cathode heater was set to 1.6 A. 24 acquisitions were signal averaged per mass spectrum. For each mass spectrum, 512K points were acquired, padded with one zero fill, and apodized using a sinebell window. Background spectra were acquired by leaving all parameters the same but setting the cathode bias to 0 V to ensure that no electrons reached the analyzer cell. IRMPD spectra were acquired using the same experimental setup as EDD, but replacing the electron irradiation event with a laser pulse. For IRMPD, ions were irradiated for 0.01 – 0.2 seconds beam attenuation set to pass from 40 – 60% of full power. External calibration of IRMPD and EDD mass spectra produced mass accuracy of 5 ppm. Internal calibration was also performed using confidently assigned glycosidic bond cleavage products as internal calibrants, providing mass accuracy of <1 ppm. Due to the larger number of low intensity products formed by EDD, only peaks with S/N > 10 are reported (see Appendix B). Product ions were assigned using accurate mass measurement. All EDD products are reported using the Domon and Costello nomenclature [38].

^{18}O Labeling

^{18}O labeling of the anomeric carbon of the reducing end was performed by dissolving 2 nmol of the DS oligosaccharide into 10 μL of $H_2{}^{18}O$ (Cambridge Isotope Labs, Andover, MA). The solution was heated overnight at 60°C. Prior to mass spectrometry analysis, 10 μL of methanol was added to the $H_2{}^{18}O$ oligosaccharide solution before infusion into the mass spectrometer [39].

RESULTS AND DISCUSSION

EDD of DS Tetrasaccharide (dp4)

EDD of the $[M-2H]^{2-}$ of DS dp4, ***1***, by irradiation with 19 eV electrons produces the mass spectrum shown in Figure 5.1A, while IRMPD of the $[M-2H]^{2-}$ ion of ***1*** produces the mass spectrum shown in Figure 5.1B. EDD of ***1*** produces similar glycosidic bond cleavages to those observed in the IRMPD spectrum. However, more abundant cross-ring cleavages and less SO_3 loss are observed in EDD of ***1*** (insets, Figures 1A and 1B) compared to those produced by IRMPD. As observed with HS tetrasaccharides, the majority of cross-ring fragmentation resulting from EDD occurs in the residue bearing a carboxyl group, IdoA. As suggested previously, carboxylate readily undergoes electron detachment [28], and it seems reasonable that this group will become a radical site that will direct fragmentation to that residue.

The EDD mass spectrum of ***1*** contains predominantly singly-charged product ions and three doubly-charged product ions, $Y_3{}^{2-}$, $^{0,2}X_3{}^{2-}$, and $[M-2H-H_2O]^{2-}$. As described previously [28], the doubly-charged products show that some of the observed product ions result from activation of the precursor ion without electron detachment. These doubly-charged product ions result from fragmentation near the NRE of ***1*** and are also observed in the IRMPD mass spectrum

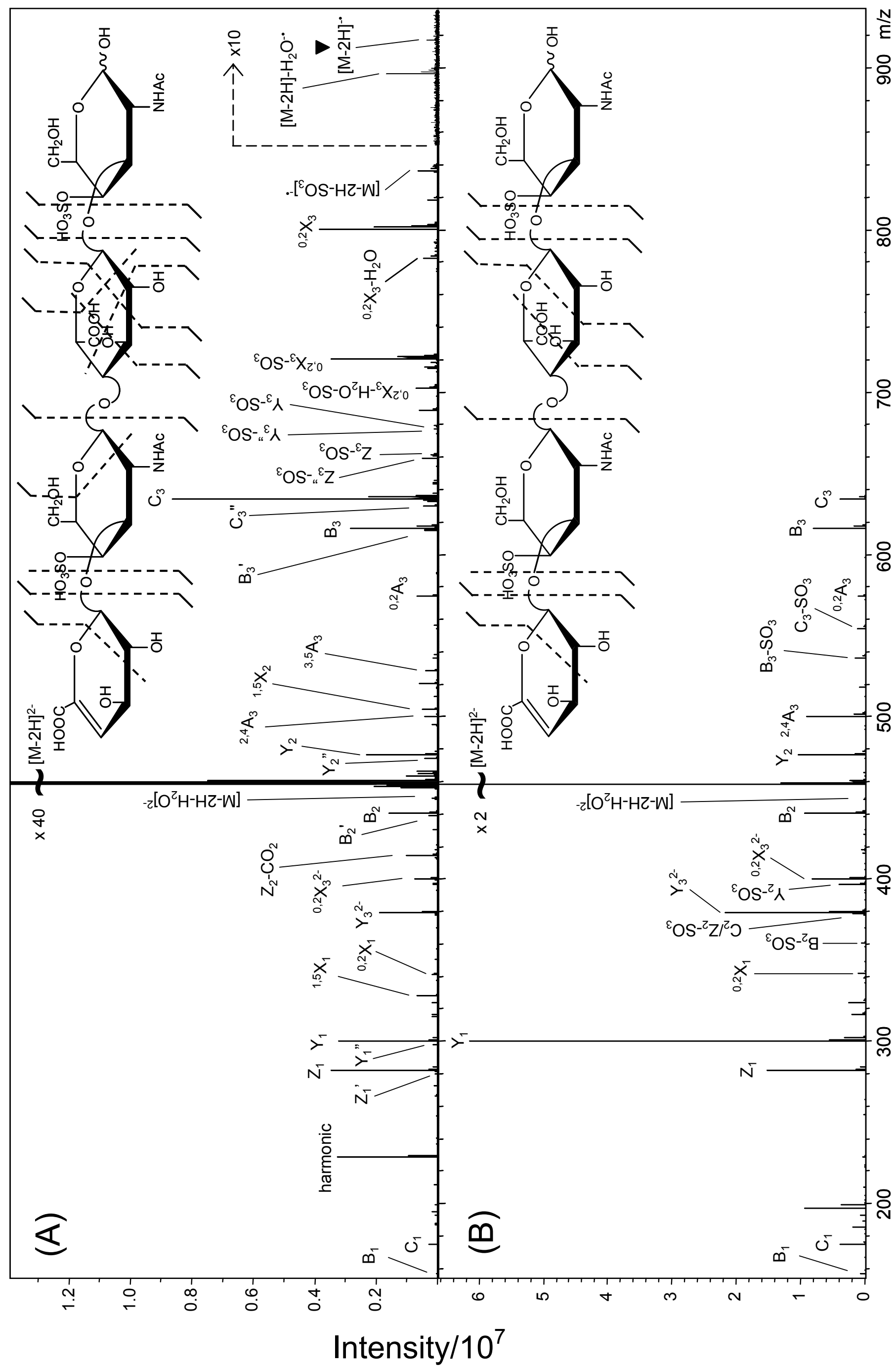

Figure 5.1. MS/MS of [M-2H]$^{2-}$ precursor ion DS dp4, ***1***, with (A) EDD and (B) IRMPD. Insets; product ions observed by the fragmentation methods. The charge reduced species in the EDD mass spectrum is indicated with a ▼over the peak label.

of ***1***, Figure 5.1B. For this tetrasaccharide, cleavage of all glycosidic bonds is observed both by IRMPD and by EDD, except for the Z_3 glycosidic bond cleavage, which is observed only with loss of SO_3, forming singly-charged, even-electron product ions Z_3-SO_3 and Z_3"-SO_3 in the EDD mass spectrum of ***1***. The C_2 and Z_2 glycosidic bond cleavages, if present, cannot be assigned as they overlap in mass-to-charge with the precursor ion. Cross-ring cleavages are observed both by EDD and IRMPD. However, IRMPD appears to produce fewer cross-ring fragments, and to favor the formation of A-type cross-ring fragments over X-type cross-ring fragments. The EDD mass spectrum shows considerably more cross-ring fragmentation, and X-ions are far more abundant than A-ions. It is important to note that all of the cross-ring fragments found by IRMPD also appear in the EDD spectrum.

Numerous odd-electron product ions are observed in the EDD mass spectrum of ***1***. The charge reduced species $[M\text{-}2H]^{-\bullet}$ is observed at *m/z* 916.125, albeit at low intensity, as well as the odd-electron product $[M\text{-}2H\text{-}SO_3]^{-\bullet}$. Since sulfuric acid is more ionized than a carboxylic acid in solution, and since ESI is thought to preserve the ionized state of species as they move from solution to the gas phase, the doubly-charged anion of ***1*** is expected to carry each of its charges at a sulfate group. As the radical site formation is proposed to initially occur at a site of charge, EDD is expected to form a sulfate radical, which can readily undergo loss of SO_3, consistent with the observation of the $[M\text{-}2H\text{-}SO_3]^{-\bullet}$ ion. However, the preponderance of cleavage on the ring with the carboxyl groups, IdoA, suggests the presence of a radical site on the uronic acid residue, even though it bears no sulfate. These data suggest radical site migration to the carboxyl group, most likely by hydrogen atom rearrangement. Alternatively, it is possible that the carboxyl group is a site of ionization in the doubly-charged precursor ion of ***1***, perhaps the result of proton migration. Detachment of an electron from a carboxylate anion is thermodynamically favorable, as it requires ~1 eV less energy than detachment of an electron from a sulfate anion, as noted previously [28]. Another explanation for the abundance of IdoA fragmentation is that EDD produces a hole in a molecular orbital, and that the hole migrates until it recombines with an electron in IdoA [24].

Another odd-electron ion of interest is the peak at *m/z* 898.116, which differs from the charge-reduced species, $[M\text{-}2H]^{-\bullet}$, by the exact mass of H_2O, and which is assigned as $[M\text{-}2H\text{-}H_2O]^{-\bullet}$. This product is unusual as H_2O loss from the charge-reduced species has not been observed previously in the EDD mass spectra of GAGs [28,29]. It is unlikely that this is a secondary product ion resulting from the detachment of an electron from the $[M\text{-}2H\text{-}H_2O]^{2-}$ product ion, given the low abundance of the $[M\text{-}2H\text{-}H_2O]^{2-}$ product ion and the low efficiency of EDD fragmentation.

The peak at *m/z* 800.111, assigned as the odd-electron product $^{0,2}X_3$, is unusual in that it is observed as both a singly-charged odd-electron product ion (*m/z* $800.111^{-\bullet}$) and a doubly-charged even-electron product ion (*m/z* 400.055^{2-}). The $^{0,2}X_3$ product ion is isobaric with the $^{2,5}A_4$ product ion, and to distinguish these we have performed ^{18}O-labeling of the hydroxyl group at the anomeric position of the reducing end (RE). EDD of the ^{18}O-labeled ***1*** (data not shown) caused both the singly- and doubly-charged ions to shift +2 amu, confirming that the products contain the reducing end of the GAG chain, consistent with the assignment of these as $^{0,2}X_3$ ions. The peak at *m/z* 720.153 differs from the odd-electron $^{0,2}X_3$ product by the exact mass of SO_3, and is assigned as the odd-electron product $^{0,2}X_3\text{-}SO_3^{-\bullet}$.

The ^{18}O-labeling of the reducing end of ***1*** allowed us to confirm the assignments of all the product ions. Those assigned as A, B, or C ions were found to undergo no mass shift upon labeling, while those assigned as X, Y, or Z all undergo a +2 amu shift. One exception is the peak at *m/z* 782.100 which differs from the $^{0,2}X_3$ fragment by the exact mass of H_2O. ^{18}O labeling was used to determine if this product was in fact the result of water loss from the $^{0,2}X_3$ cleavage. The peak at *m/z* 782.100 did not shift +2 amu, indicating that this product either does not contain the reducing end (i.e. may not be an X-type ion), or that the resulting H_2O loss removed the ^{18}O from the reducing end. Also, the product at *m/z* 702.143 differs from the peak at *m/z* 782.100 by the exact mass of SO_3, suggesting a composition of $[^{0,2}X_3\text{-}H_2O\text{-}SO_3]^{-\bullet}$. The peak at *m/z* 702.143 also did not shift +2 amu with ^{18}O-labeling, suggesting that either this product does not contain the reducing end, or that H_2O loss removed the ^{18}O from the reducing end, resulting in a $[^{0,2}X_3\text{-}H_2{}^{18}O\text{-}SO_3]^{-\bullet}$ product ion. We are unable to assign these two product ions to any NRE fragmentation (i.e. A-type cleavage) or any internal fragment ion.

In our prior work on HS tetrasaccharides, all products that result from IRMPD or CAD of sulfated GAGs are observed in the EDD mass spectrum. This is generally true for DS GAGs as well. The only product ions observed in IRMPD that are not observed in EDD are a small number that result from SO_3 loss accompanying other fragmentation. In fact, very little SO_3 loss is observed in the EDD mass spectrum of ***1***. Aside from the $[M\text{-}2H\text{-}SO_3]^{-\bullet}$ species, only one significant peak is observed to result from SO_3 loss, namely $^{0,2}X_3\text{-}SO_3$, which has the same abundance as the $^{0,2}X_3$ ion. A few low abundance product ions are found to result from SO_3 loss ($Z_3\text{-}SO_3$, $Y_3\text{-}SO_3$, and their -2H counterparts), and no products are observed with loss of two SO_3 molecules. The only product ion observed solely with SO_3 loss is the $[Z_3\text{-}SO_3]^-$ product. Compared to IRMPD of ***1***, far less SO_3 loss is observed by EDD fragmentation (Figure 5.1).

EDD of ***1*** results in numerous glycosidic bond cleavages that are accompanied by the loss of 1 or 2 H atoms (Figure 5.1). These satellite peaks are not observed in the IRMPD mass spectrum of ***1***, suggesting that they arise from a radical site induced hydrogen rearrangement.

Similar to EDD fragmentation previously observed in HS tetrasaccharides [28,29], the B_3 glycosidic bond cleavage is accompanied by a B_3-H product (labeled B_3'), and the C_3 glycosidic bond cleavage is accompanied by a C_3-2H product (labeled C_3").

Previous studies of the EDD of HS tetrasaccharides found the formation of the $^{0,2}A_3$ product occurred only for cross-ring cleavage of GlcA and not IdoA, and only by EDD, and not by IRMPD or CAD [29]. The preference for the formation of $^{0,2}A_3$ from GlcA versus IdoA was proposed to result from a radical mechanism involving an H atom rearrangement. Unlike HS tetrasaccharides, IRMPD of the DS tetrasaccharide ***1*** produces the $^{0,2}A_3$ product ion. The mechanism of its formation is clearly different from EDD of HS tetrasaccharides as the $^{0,2}A_3$ ion for ***1*** is produced from an even-electron ion. Furthermore, the ring undergoing fragmentation is IdoA, which does not produce $^{0,2}A_3$ in EDD or IRMPD of HS. Given its formation from an even-electron precursor, the $^{0,2}A_3$ fragment in the EDD spectrum is not expected to distinguish GlcA from IdoA in DS oligosaccharides.

In order to present a complete picture of the observed fragmentation, we propose an annotation scheme that can distinguish hydrogen transfer and SO_3 loss in addition to the standard A, B, C, X, Y, and Z fragmentations. The EDD and IRMPD products for ***1*** (insets, Figures 1A and 1B) are combined in this new fragmentation annotation scheme, shown in Figure 5.2. This scheme distinguishes products observed by IRMPD from those formed by EDD and can display additional hydrogen and SO_3 loss. This scheme is particularly useful for examining the large number of fragment ions that are found in the mass spectra of longer oligosaccharides, as shown below.

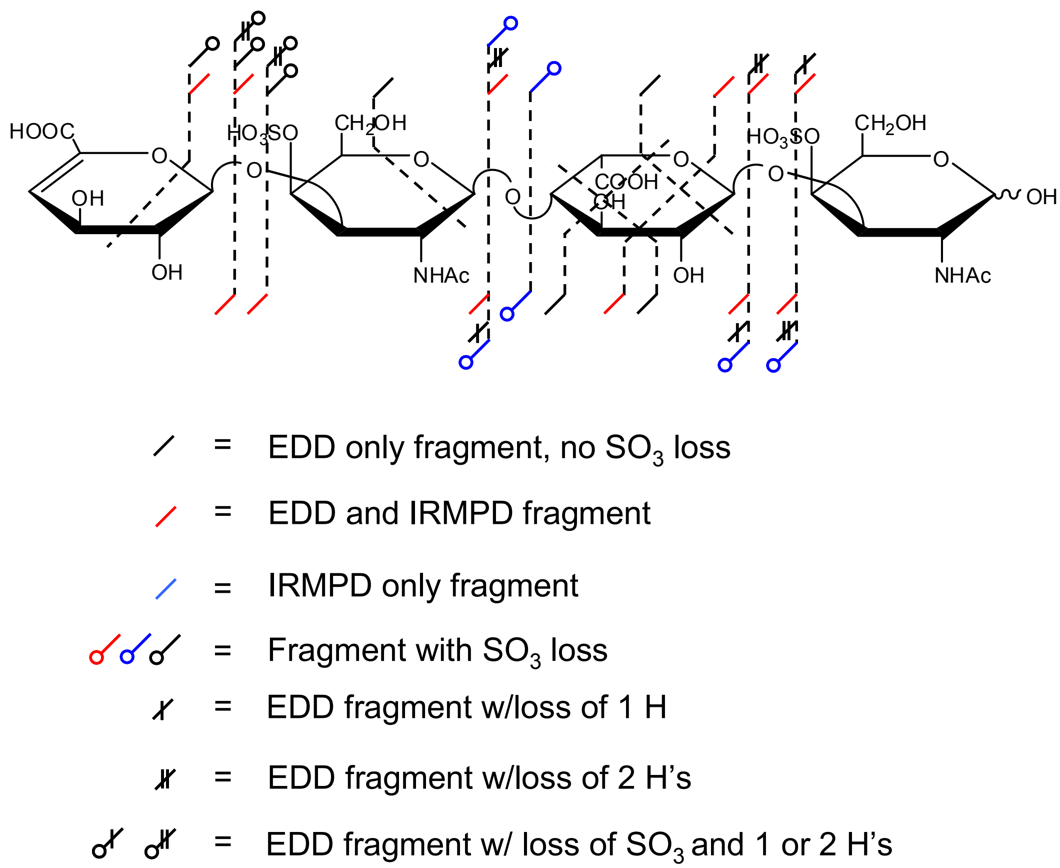

Figure 5.2. EDD and IRMPD fragmentation of the $[M\text{-}2H]^{2-}$ precursor ion of ***1*** combined and displayed using the new fragmentation notation.

EDD of DS dp6, dp8, and dp10

EDD of the $[M-3H]^{3-}$ of DS dp6, ***2***, produces the mass spectrum shown in Figure 5.3. The products observed in the IRMPD mass spectrum of the $[M-3H]^{3-}$ precursor ion of ***2*** (peak list and intensities in Appendix B) are compared to the observed EDD products in the annotated structure shown in Figure 5.2, inset. EDD of the $[M-4H]^{4-}$ precursor ion of DS dp8, ***3***, and the $[M-5H]^{5-}$ precursor ion of DS dp4, ***4***, produces the mass spectra shown in Figures 5.4 and 5.5, respectively. Due to the complexity of the EDD mass spectra of ***3*** and ***4***, the mass scale is divided into three different *m/z* ranges. Products observed in the IRMPD of $[M-4H]^{4-}$ precursor ion of ***3*** (peak list and intensities in Appendix B) are compared to the observed EDD products of ***3*** in the annotated structure shown in the inset of Figure 5.4C, inset, while the structure in the inset of Figure 5.6 compares products of IRMPD (peak list and intensities in Appendix B) and EDD for the $[M-5H]^{5-}$ precursor ion of ***4***.

Although the charge reduced species $[M-3H]^{2-\bullet}$ is not observed in the EDD spectrum of ***2***, the charge reduced species minus SO_3, $[M-3H-SO_3]^{2-\bullet}$ is observed. For EDD of ***3*** and ***4***, both the charge reduced species (labeled with a ▼ over the peak) and the charge reduced species minus SO_3 are observed. EDD produces more extensive fragmentation than IRMPD for ***2***, ***3***, and ***4***, as can be seen in the annotated structures shown as insets to Figures 3, 4, and 5, respectively. For ***2*** and ***3***, the small number of products that are observed only in the IRMPD mass spectra but are not observed by EDD are those that result from SO_3 loss. For ***4***, all products observed in the IRMPD spectrum are observed in the EDD spectrum.

EDD of ***2***, ***3***, and ***4*** produces abundant cleavage of glycosidic bonds. In contrast to IRMPD of these compounds, EDD cleaves all glycosidic bonds (Figures 3, 4, and 5, insets). Because of the symmetry of the oligosaccharides presented in this work, the even numbered C_n

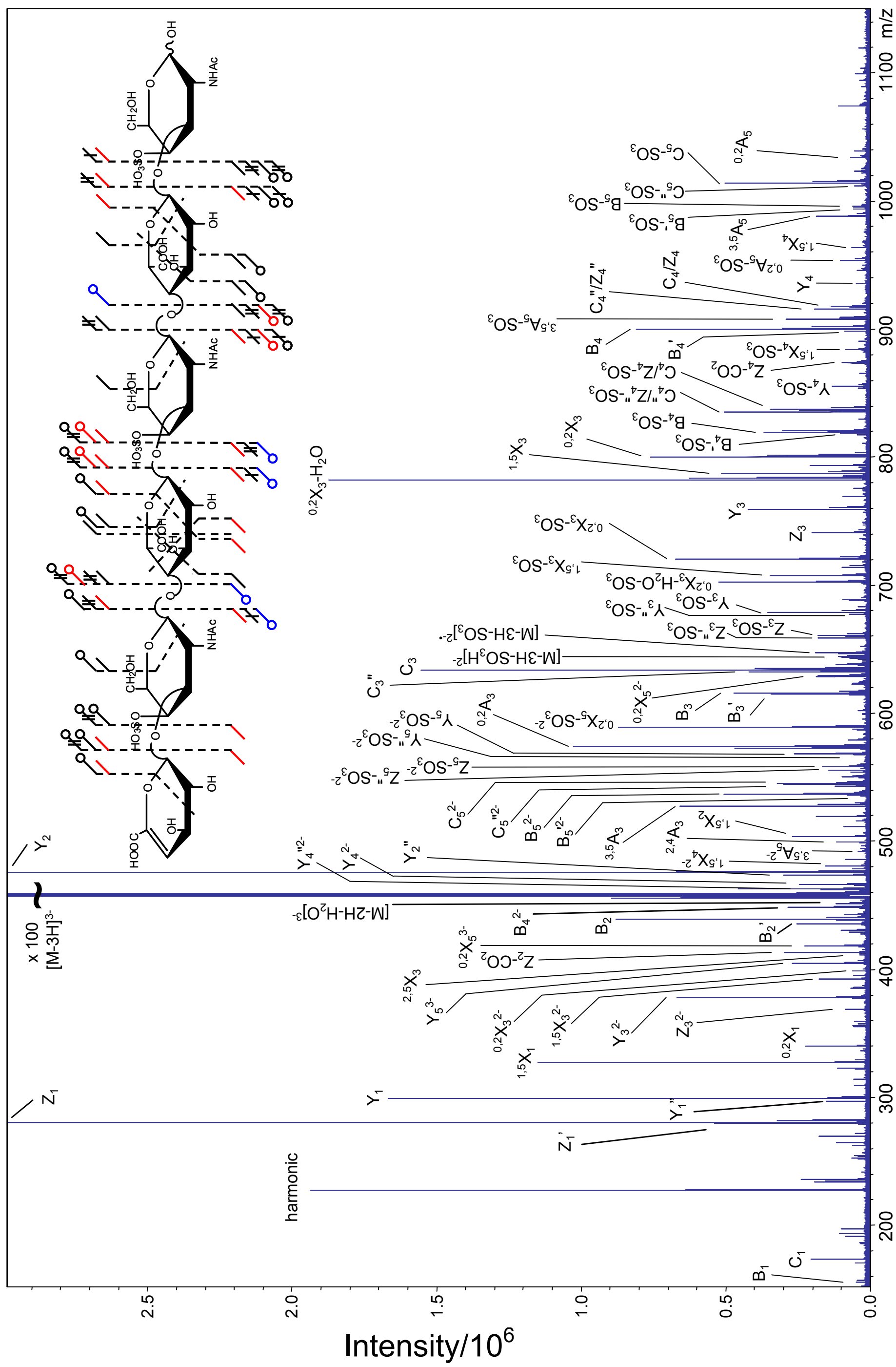

Figure 5.3. EDD mass spectrum of the $[M\text{-}3H]^{3-}$ precursor ion of ***2***. Inset: Observed product ions from the EDD and IRMPD MS/MS data of ***2*** combined and displayed using the modified fragmentation notation.

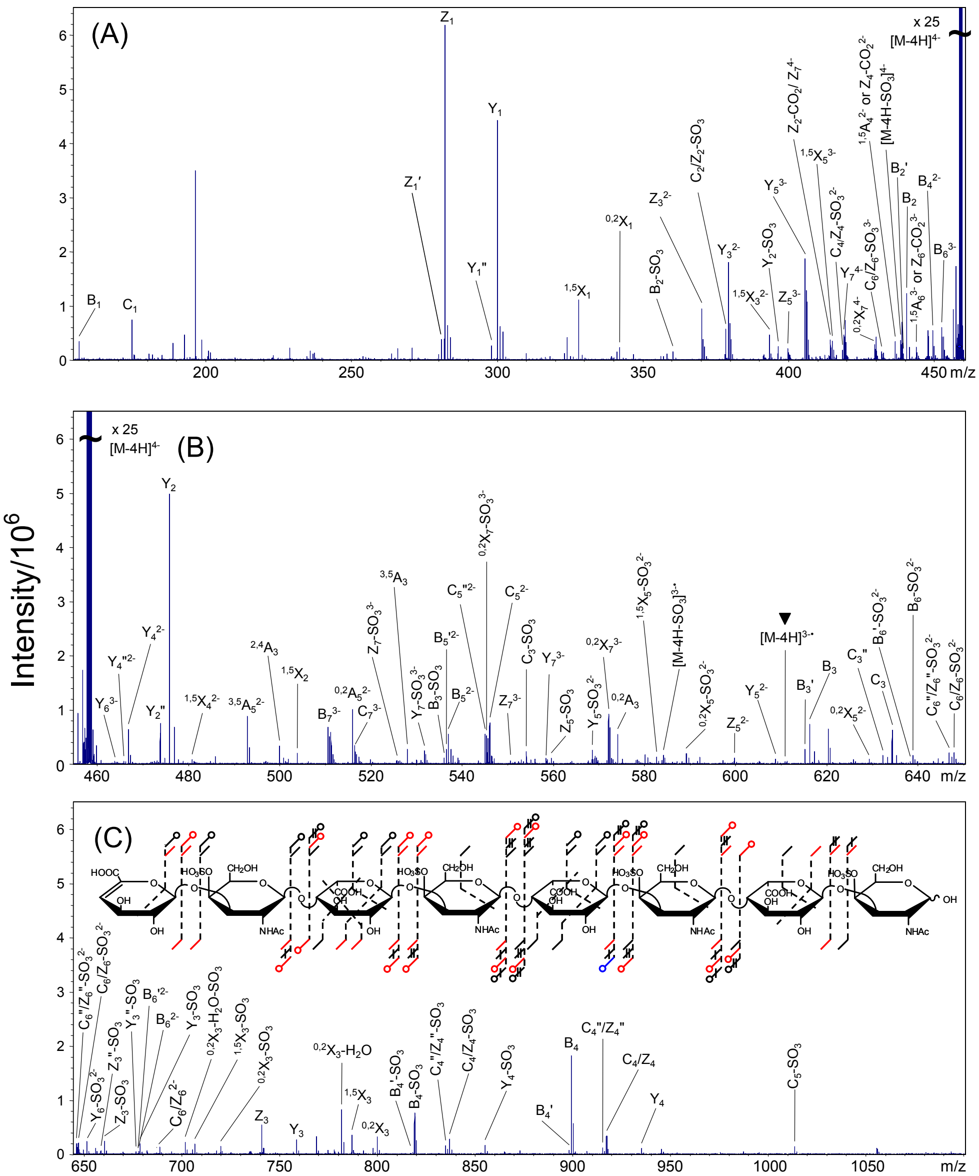

Figure 5.4. EDD mass spectrum of the $[M-4H]^{4-}$ precursor ion of ***3***. The EDD mass spectrum was divided into three different regions for publication. (A) *m/z* 155-460, (B) *m/z* 455-650, and (C*) m/z* 645-1100. Inset: observed product ions from the EDD and IRMPD MS/MS data of ***3*** combined and displayed using the modified fragmentation notation. The charge reduced species is indicated with a ▼over the peak label.

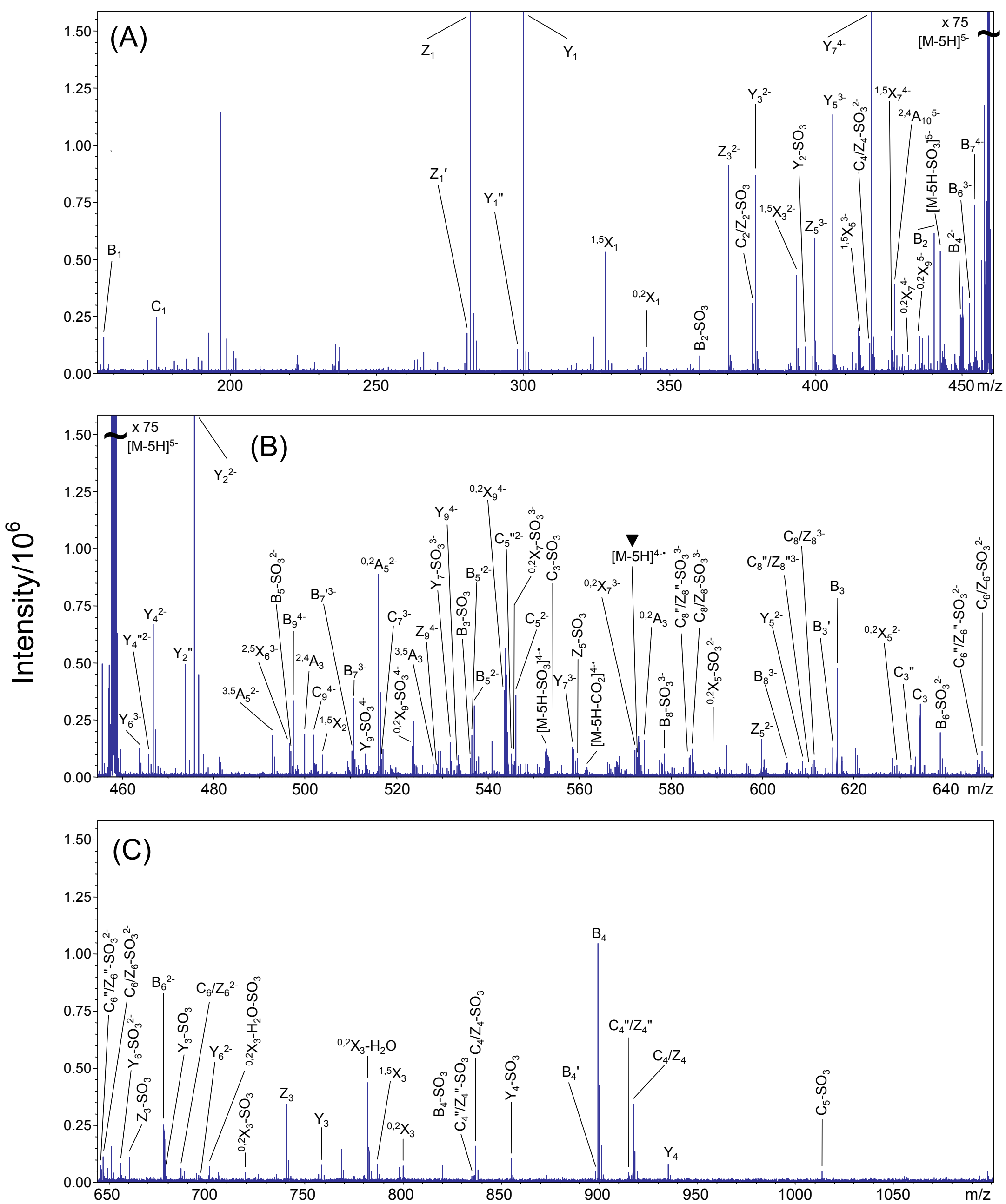

Figure 5.5. EDD mass spectrum of the $[M-5H]^{5-}$ precursor ion of ***4***. The EDD mass spectrum was divided into three different regions for publication. (A) *m/z* 155-460, (B) *m/z* 455-650, and (C*) m/z* 645-1100. The charge reduced species is indicated with a ▼over the peak label.

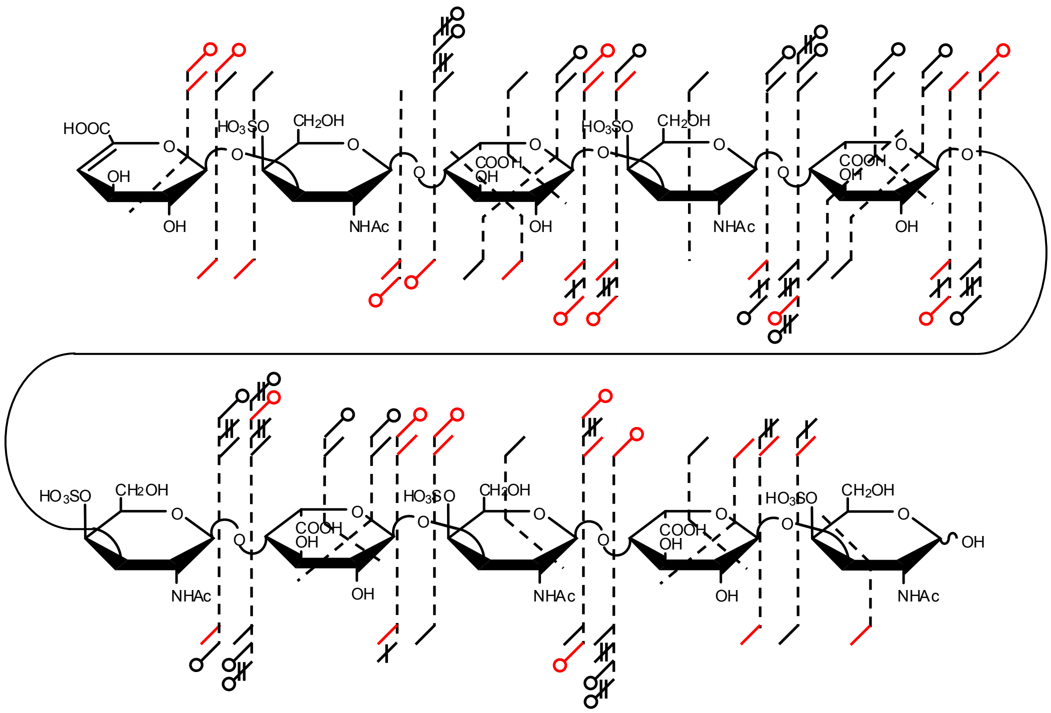

Figure 5.6. Observed product ions from the EDD and IRMPD MS/MS data of DS dp10, ***4***, combined and annotated using the scheme presented in Figure 5.2.

and Z_n glycosidic bond cleavages are isobaric (e.g. C_2/Z_2, C_4/Z_4, etc.), and cannot be distinguished. We are presently attempting to label the NRE or RE saccharide to allow the assignment of these ambiguous peaks. For all the DS oligosaccharides presented in this work, the isobaric C_2 and Z_2 singly-charged products are not assigned as they overlap with the precursor ion. However, for ***2***, the C_2/Z_2 glycosidic bond cleavages are observed as the even-electron product C_2/Z_2-SO_3 only in the IRMPD spectrum. The even-electron product C_2/Z_2-SO_3 is observed in both the EDD and IRMPD mass spectra for ***3*** and ***4***.

Some glycosidic bond cleavage products from IRMPD of ***2***, ***3***, and ***4*** are observed only with SO_3 loss. While SO_3 loss accompanying glycosidic bond cleavage is observed in EDD of ***2***, ***3***, and ***4***, these glycosidic bond cleavages are also observed without SO_3 loss, facilitating the easy assignment of these peaks. However, the Z_5 glycosidic bond cleavage is observed in the EDD mass spectrum of ***2*** only as the doubly-charged even-electron Z_5-SO_3 and Z_5''-SO_3 product ions, similar to the Z_3 fragmentation pattern for ***1***. For ***3*** and ***4***, Z_{m-1} (m = degree of polymerization) is observed in addition to Z_{m-1}-SO_3.

Hydrogen Rearrangement Accompanying Glycosidic Bond Cleavages

EDD of ***1***, ***2***, ***3***, and ***4*** (Figures 2-5, respectively) produces several glycosidic bond cleavages that are accompanied by the loss of 1 or 2 H atoms. The annotation for these cleavages are represented with one or two hatch marks bisecting the fragment label on the molecule (see Figure 5.2 for annotation scheme), and we refer to these products as B_n' and Z_n' indicating the loss of one additional hydrogen atom, and C_n'', Z_n'', and Y_n'' indicating the loss of an additional two hydrogen atoms. Brüll et al. have reported glycosidic bond cleavages with loss of 2 hydrogen atoms from CAD of native and permethylated oligosaccharides [40]. They found that only C-type glycosidic cleavages undergo the loss of two hydrogen atoms, and the normal glycosidic bond cleavage products were not observed in the CAD spectrum.

For the EDD work here, conventional glycosidic bond cleavage products are always present when any glycosidic bond cleavage is observed with additional hydrogen atom loss. Unlike products previously observed from EDD of HS tetrasaccharides [28,29], glycosidic bond cleavages with additional hydrogen loss are less intense than the accompanying glycosidic bond cleavage. These hydrogen atom loss satellite peaks are not observed in the IRMPD mass spectra of the DS oligosaccharides, suggesting that these products arise through a radical fragmentation mechanism. In the case of the loss of one additional hydrogen atom, the product ion is odd-electron (B_n' and Z_n'), strongly suggesting that the precursor ion was odd-electron. The other unusual glycosidic products are even-electron (C_n'', Z_n'', and Y_n'').

A number of the features of hydrogen atom loss are evident from the EDD mass spectra of all four compounds. The Z_1 and Y_1 are always accompanied by Z_1' and Y_1''. Aside from Z_1', the B_n cleavages are the only glycosidic cleavages observed with loss of a single hydrogen atom, B_n', that is, B-type glycosidic cleavages are not observed with loss of two hydrogen atoms. Also, Y_1, Y_2, and Y_4 are the only Y glycosidic cleavages observed with loss of 2 hydrogen atoms, Y_1'', Y_2'', and Y_4'', respectively.

Cross-Ring Cleavages

Cross-ring fragmentation from EDD of ***2-4*** occurs primarily within the IdoA residues rather than the GalNAc4S residues, similar to EDD of ***1***, and both A- and X-type cleavages are observed. Typically, only A-type cross-ring cleavages are observed in the CAD or IRMPD mass spectra of oligosaccharide even-electron ions. For example, predominately A-type cross-ring cleavages are observed in IRMPD of ***2-4*** (insets, Figures 3, 4, and 5). In contrast, EDD of ***2***, ***3***, and ***4*** produces abundant A- and X-type cross-ring cleavages.

$^{0,2}X_n$ and $^{1,5}X_n$ (n = odd #) cleavages of IdoA residues are found in the EDD mass spectra, but are not observed in IRMPD of ***2-4***, suggesting fragmentation through a radical mechanism. Only $^{0,2}X_1$ is observed in both the EDD and IRMPD mass spectra for ***1-4***, all other X-products are found only by EDD. Except for the IdoA saccharide next to the RE, these product ions are also observed with SO_3 loss. The preference for IdoA to undergo $^{1,5}X_n$ cleavage can be explained by the fragmentation mechanisms proposed in Schemes 5.1A and 5.1B. A radical site located at the carboxylic acid group on IdoA, formed from either the initial electron detachment or hydrogen rearrangement, may undergo a hydrogen atom rearrangement to create a C2 $O^{\bullet}$ radical (Scheme 5.1A) or a delocalization-stabilized $C3^{\bullet}$ radical (Scheme 5.1B). Either of these radical products can fragment to form $^{1,5}X_n$ from IdoA. These hydrogen rearrangement fragmentation mechanisms have been proposed to explain the products observed from fragmentation of the hexuronic acid residues in GAG tetrasaccharides [28]. $^{1,5}X_n$-type fragmentation is not predicted to occur for the ΔUA on the NRE through this proposed mechanism as the double bond restricts the conformational change necessary to bring the carboxyl radical into the proximity of the C2 OH or C3 hydrogen for hydrogen atom transfer.

Cross-ring cleavage of the NRE residue of ***2***, ***3***, and ***4*** is similar to that observed in EDD of ***1***. The $^{0,2}X_{m-1}$ (m = degree of polymerization) cleavage is observed as both an even-electron product with same charge as the precursor ion, and an odd-electron product ion with one less charge than the precursor ion. The odd-electron product is also accompanied by the loss of SO_3, forming the odd-electron $^{0,2}X_{m-1}$-SO_3 product ion.

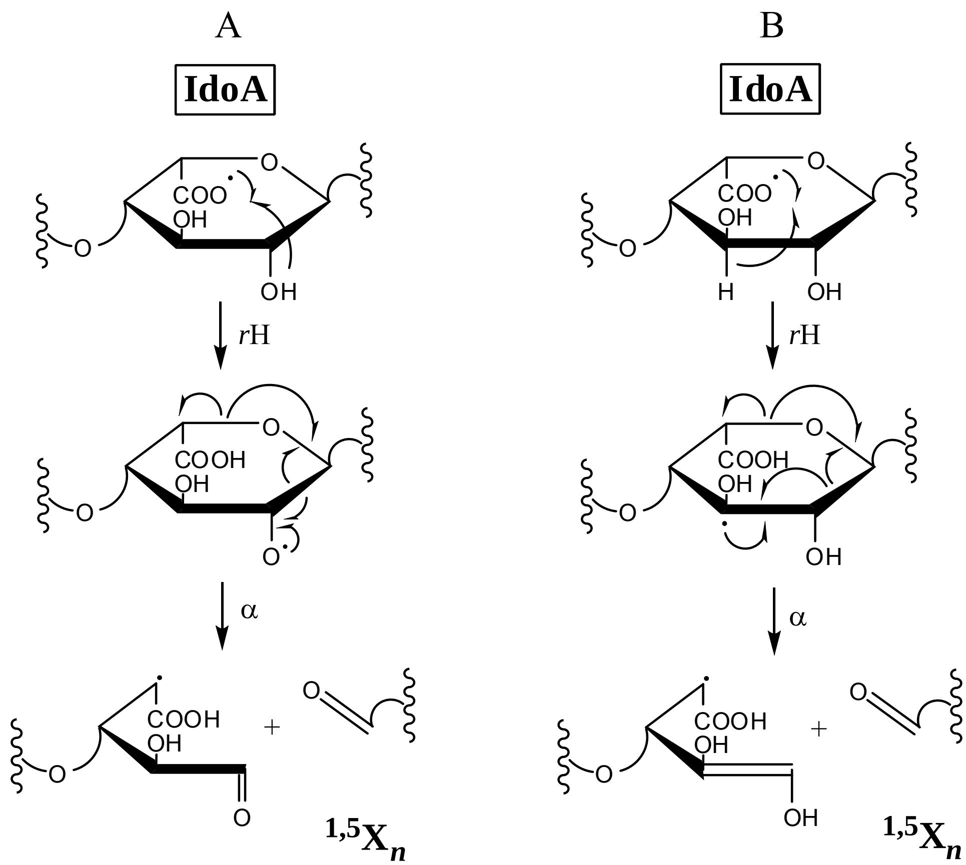

Scheme 5.1

$^{1,5}X_n$ (n = even #) cleavages are also observed for many of the GalNAc4S residues for ***1*-*4***, except for the RE GalNAc4S. While $^{1,5}X_0$ cleavage may occur on the RE, the resulting product ion is outside the *m/z* detection range. The preference for GalNAc4S to form the $^{1,5}X_n$ cleavage can be rationalized by the mechanisms proposed in Schemes 2A and 2B. A radical site located at the sulfate group on GalNAc4S undergoes hydrogen atom rearrangement to create a $C6^{\bullet}$ (Scheme 5.2A), or loses SO_3 and then undergoes hydrogen atom rearrangement to create a $C6^{\bullet}$ (Scheme 5.2B). The $C6^{\bullet}$ species can undergo facile decomposition to form the $^{1,5}X_n$ product.

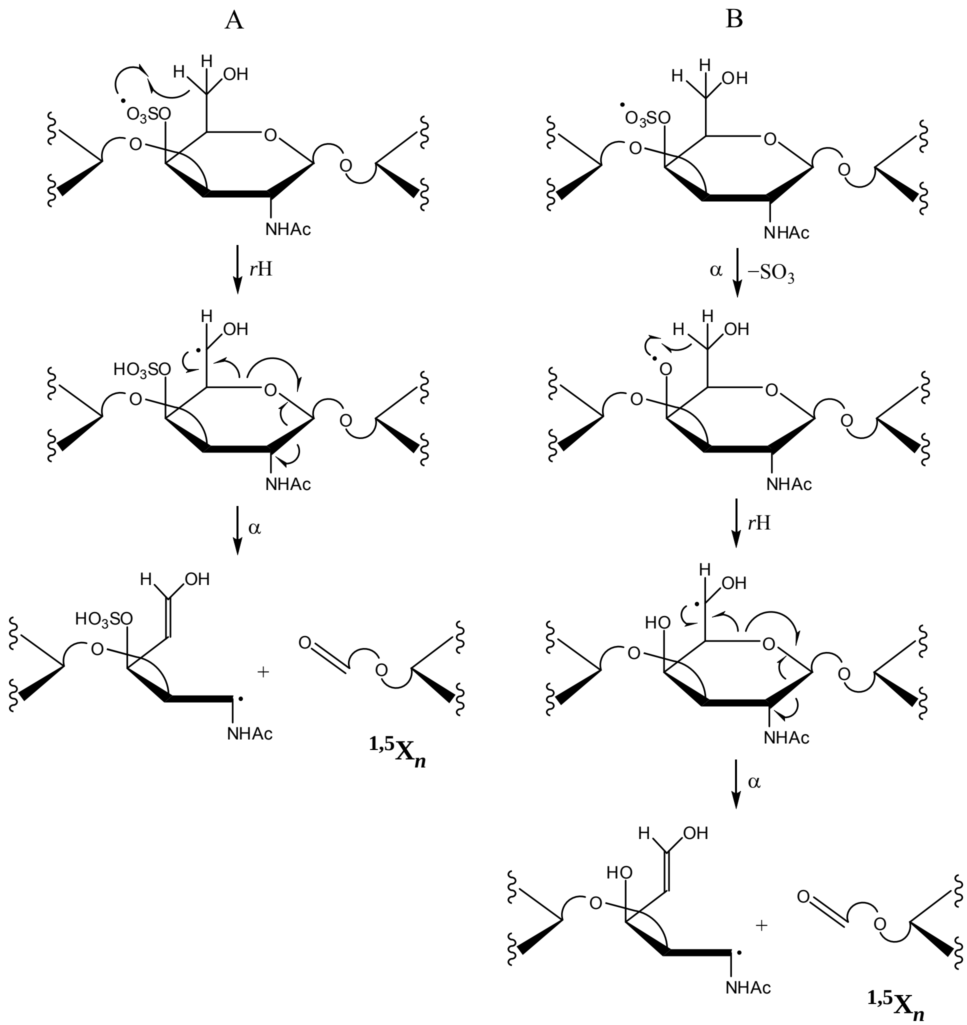

Scheme 5.2

EDD of ***1***, ***2***, and ***3*** does not produce cross-ring cleavage within the reducing end residue, GalNAc4S. This is in contrast to our previous results obtained with HS tetrasaccharides, for which cross-ring products were observed for the reducing end sugar [28]. For EDD of the HS tetrasaccharides, products from cleavage of the reducing end were typically observed in the IRMPD mass spectra, suggesting formation of these products through a non-radical pathway. As no products from the cleavage of the reducing end are observed in EDD or IRMPD spectra, these data suggest that the reducing end is more stable toward fragmentation for DS oligosaccharides than for HS oligosaccharides, perhaps as a result of the β1-3 linkage as opposed to β1-4 linkage of the amino sugar.

Product Ion SO_3 Loss

Sulfate is labile under most CAD or IRMPD conditions and readily undergoes the cleavage of the half-ester bond, resulting in the loss of SO_3. The extent of SO_3 loss is lower in EDD than in IRMPD of ***1*** - ***4***. Generally, EDD product ions that exhibit SO_3 loss are accompanied by the related fragments that have retained SO_3. Such product ion pairs are easy to identify as they differ by 79.957 *u*. For ***2*** and ***3***, the only products that are exclusive to the IRMPD mass spectra result from SO_3 loss (shown in blue in the annotation scheme). All products observed by IRMPD of ***4*** are observed for EDD of ***4***. For EDD of ***1*** and ***2***, SO_3 loss from the precursor ion is not observed. For EDD of ***3*** and ***4***, SO_3 loss from the precursor ion is observed as $[M\text{-}4H\text{-}SO_3]^{4-}$ and $[M\text{-}5H\text{-}SO_3]^{5-}$, respectively. The charge reduced species minus SO_3 (e.g. $[M\text{-}3H\text{-}SO_3]^{2-\bullet}$ for ***2***, $[M\text{-}4H\text{-}SO_3]^{3-\bullet}$ for ***3***) is observed in the EDD spectra of all four DS oligosaccharides studied here.

While several bond cleavages are observed to occur both with and without SO_3 loss, no products are observed with loss of two or more equivalents of SO_3. For EDD of ***2***, ***3***, and ***4*** (Figures 3, 4, and 5, respectively), the extent of SO_3 loss is related to the amount of charge relative to the number of sulfate modifications on the product ion. Our results indicate that if the charge of the product ion is equal to the number of sulfates, no SO_3 loss is observed. If the charge of the product ion is less than the number of sulfates, the product ion is typically observed with and without SO_3 loss. For example, in EDD of ***2*** (Figure 5.3), the singly-charged peak at *m/z* 899.117 has been assigned as a B_4 glycosidic cleavage, and contains two sulfate groups.

The singly-charged peak at *m/z* 819.160 differs from the B_4 product by the exact mass of SO_3, and has been assigned as B_4-SO_3. The doubly-charged peak at *m/z* 440.056 has also been assigned as a B_4 product. However, no product ion is present that differs from the doubly-charged B_4 product by the exact mass of SO_3. The relationship of charge state to SO_3 loss has been previously observed by Zaia and coworkers for heparin-like molecules [18]. During CAD, SO_3 loss can be minimized and glycosidic cleavages maximized if the number of charges on the GAG precursor is equal to the number of sulfate groups, suggesting that protonated form of sulfate is unstable toward SO_3 loss. The exception to this observation can be found in the EDD mass spectrum of ***2***, in which the $[Z_5\text{-}SO_3]^{2-}$ product has no corresponding Z_5 fragment. Also, for EDD of ***3*** and ***4***, the singly-charged B_3 and C_3 products, which contain one sulfate, and are accompanied by peaks corresponding to B_3-SO_3 and C_3-SO_3. These products with SO_3 loss are also observed in the IRMPD spectra of these compounds, and are therefore expected in the EDD spectra.

CONCLUSIONS

EDD of GAG oligosaccharides produces more glycosidic and cross-ring cleavages than are observed by IRMPD. EDD produces predominately even-electron product ions; although some odd-electron product ions are also observed. While the EDD products are low intensity relative to IRMPD products, the large number of glycosidic cleavages permits the determination of the degree of sulfation for each residue, while cross-ring fragmentation can locate the site of sulfation within each residue. Cross-ring cleavages occur predominately on IdoA saccharides. ${}^{1,5}X_n$ cleavages are observed for most residues except the NRE and RE, and are observed for all IdoA residues. The preference for cross-ring fragmentation of the IdoA residue suggests a radical site on the IdoA residue, either formed initially by EDD, or by hydrogen atom transfer. Also, the stability of the GalNAc4S, evidenced by the small number of observed cross-ring products of GalNAc4S residues may result from the linkage location at C3 instead of C4. EDD produces far fewer product ions observed only with SO_3 loss compared to IRMPD. For longer oligosaccharides, many EDD products are observed with SO_3 loss. Where SO_3 loss does occur, fragment pairs separated by the exact mass of SO_3 generally occur, facilitating the assignment of these peaks. Overall, the large degree of fragmentation from EDD permits the analysis of sulfated GAG oligosaccharides through a single MS/MS experiment.

ACKNOWLEDGMENTS

We gratefully acknowledge financial support from the National Institutes of Health grant #2R01-GM038060-16.

REFERENCES

1. Perrimon, N.; Bernfield, M. Cellular functions of proteoglycans--an overview. *Semin. Cell Dev. Biol.* **2001**, *12*, 65-67.
2. Fannon, M.; Forsten, K. E.; Nugent, M. A. Potentiation and Inhibition of bFGF Binding by Heparin: A Model for Regulation of Cellular Response. *Biochemistry* **2000**, *39*, 1434-1445.
3. Wu, Z. L.; Zhang, L.; Yabe, T.; Kuberan, B.; Beeler, D. L.; Love, A.; Rosenberg, R. D. The Involvement of Heparan Sulfate (HS) in FGF1/HS/FGFR1 Signaling Complex. *J. Biol. Chem.* **2003**, *278*, 17121-17129.
4. Sadir, R.; Imberty, A.; Baleux, F.; Lortat-Jacob, H. Heparan Sulfate/Heparin Oligosaccharides Protect Stromal Cell-derived Factor-1 (SDF-1)/CXCL12 against Proteolysis Induced by CD26/Dipeptidyl Peptidase IV. *J. Biol. Chem.* **2004**, *279*, 43854-43860.
5. Iozzo, R. V.; San Antonio, J. D. Heparan sulfate proteoglycans: heavy hitters in the angiogenesis arena. *J. Clin. Invest.* **2001**, *108*, 349-355.
6. Gotte, M. Syndecans in Inflammation. *The FASEB Journal* **2003**, *17*, 575-591.
7. Batinic, D.; Robey, F. A. The V3 region of the envelope glycoprotein of human immunodeficiency virus type 1 binds sulfated polysaccharides and CD4-derived synthetic peptides. *J. Biol. Chem.* **1992**, *267*, 6664-6671.
8. Chen, Y.; Maguire, T.; Hileman, R. E.; Fromm, J. R.; Esko, J. D.; Linhardt, R. J.; Marks, R. M. Dengue virus infectivity depends on envelope protein binding to target cell heparan sulfate. *Nature Med.* **1997**, *3*, 866-871.
9. Williams, R. K.; Straus, S. E. Specificity and affinity of binding of herpes simplex virus type 2 glycoprotein B to glycosaminoglycans. *J. Virol.* **1997**, *71*, 1375-1380.

10. Liu, D. F.; Shriver, Z.; Gi, Y. W.; Venkataraman, G.; Sasisekharan, R. Dynamic regulation of tumor growth and metastasis by heparan sulfate glycosaminoglycans. *Seminars in Thrombosis and Hemostasis* **2002**, *28*, 67-78.

11. Chi, L. L.; Amster, J.; Linhardt, R. J. Mass spectrometry for the analysis of highly charged sulfated carbohydrates. *Current Analytical Chemistry* **2005**, *1*, 223-240.

12. Horne, A.; Gettins, P. H-1-Nmr Spectral Assignments for 2 Series of Heparin-Derived Oligosaccharides. *Carbohydr. Res.* **1992**, *225*, 43-57.

13. Takagaki, K.; Kojima, K.; Majima, M.; Nakamura, T.; Kato, I.; Endo, M. Ion-Spray Mass-Spectrometric Analysis of Glycosaminoglycan Oligosaccharides. *Glycoconjugate J.* **1992**, *9*, 174-179.

14. Juhasz, P.; Biemann, K. Utility of non-covalent complexes in the matrix-assisted laser desorption ionization mass spectrometry of heparin-derived oligosaccharides. *Carbohydr. Res.* **1995**, *270*, 131-147.

15. Dai, Y.; Whittal, R. M.; Bridges, C. A.; Isogai, Y.; Hindsgaul, O.; Li, L. Matrix-assisted laser desorption ionization mass spectrometry for the analysis of monosulfated oligosaccharides. *Carbohydr. Res.* **1997**, *304*, 1-9.

16. Lo-Guidice, J.-M.; Herz, H.; Lamblin, G.; Plancke, Y.; Roussel, P.; Lhermitte, M. Structures of sulfated oligosaccharides isolated from the respiratory mucins of a non-secretor (O, Lea+b-) patient suffering from chronic bronchitis. *Glycoconjugate J.* **1997**, *14*, 113-125.

17. Schiller, J.; Arnhold, J.; Benard, S.; Reichl, S.; Arnold, K. Cartilage degradation by hyaluronate lyase and chondroitin ABC lyase: a MALDI-TOF mass spectrometric study. *Carbohydr. Res.* **1999**, *318*, 116-122.

18. Zaia, J.; Costello, C. E. Tandem Mass Spectrometry of Sulfated Heparin-Like Glycosaminoglycan Oligosaccharides. *Anal. Chem.* **2003**, *75*, 2445-2455.

19. Saad, O. M.; Leary, J. A. Compositional Analysis and Quantification of Heparin and Heparan Sulfate by Electrospray Ionization Ion Trap Mass Spectrometry. *Anal. Chem.* **2003**, *75*, 2985-2995.

20. Saad, O. M.; Leary, J. A. Heparin Sequencing Using Enzymatic Digestion and ESI-MS with HOST: A Heparin/HS Oligosaccharide Sequencing Tool. *Anal. Chem.* **2005**, *77*, 5902-5911.

21. Sweeney, M. D.; Yu, Y.; Leary, J. A. Effects of Sulfate Position on Heparin Octasaccharide Binding to CCL2 Examined by Tandem Mass Spectrometry. *J. Am. Soc. Mass Spectrom.* **2006**, *17*, 1114-1119.

22. Zaia, J.; Li, X.-Q.; Chan, S.-Y.; Costello, C. E. Tandem mass spectrometric strategies for determination of sulfation positions and uronic acid epimerization in chondroitin sulfate oligosaccharides. *J. Am. Soc. Mass Spectrom.* **2003**, *14*, 1270-1281.

23. Anusiewicz, I.; Jasionowski, M.; Skurski, P.; Simons, J. Backbone and side-chain cleavages in electron detachment dissociation (EDD). *J. Phys. Chem. A* **2005**, *109*, 11332.

24. Budnik, B. A.; Haselmann, K. F.; Zubarev, R. A. Electron detachment dissociation of peptide di-anions: an electron-hole recombination phenomenon. *Chem. Phys. Lett.* **2001**, *342*, 299-302.

25. Cooper, H. J.; Hakansson, K.; Marshall, A. G. The role of electron capture dissociation in biomolecular analysis. *Mass Spectrom. Rev.* **2005**, *24*, 201.

26. Kjeldsen, F.; Silivra, O. A.; Ivonin, I. A.; Haselmann, K. F.; Gorshkov, M.; Zubarev, R. A. Cα-C Backbone Fragmentation Dominates in Electron Detachment Dissociation of Gas-Phase Polypeptide Polyanions. *Chem. Eur. J.* **2005**, *11*, 1803-1812.

27. McFarland, M. A.; Marshall, A. G.; Hendrickson, C. L.; Nilsson, C. L.; Fredman, P.; Mansson, J. E. Structural characterization of the GM1 ganglioside by infrared multiphoton dissociation/electron capture dissociation, and electron detachment dissociation electrospray ionization FT-ICR MS/MS. *J. Am. Soc. Mass Spectrom.* **2005**, *16*, 752.

28. Wolff, J. J.; Chi, L.; Linhardt, R. J.; Amster, I. J. Electron Detachment Dissociation of Glycosaminoglycan Tetrasaccharides. *J. Am. Soc. Mass Spectrom.* **2006**, Submitted.

29. Wolff, J. J.; Chi, L. L.; Linhardt, R. J.; Amster, I. J. Distinguishing glucuronic from iduronic acid in glycosaminoglycan tetrasaccharides by using electron detachment dissociation. *Anal. Chem.* **2007**, *79*, 2015-2022.

30. Lortat-Jacob, H.; Turnbull, J. E.; Grimaud, J. A. Molecular-Organization of the Interferon Gamma-Binding Domain in Heparan-Sulfate. *Biochem. J.* **1995**, *310*, 497-505.

31. Spillmann, D.; Witt, D.; Lindahl, U. Defining the interleukin-8-binding domain of heparan sulfate. *J. Biol. Chem.* **1998**, *273*, 15487-15493.

32. Stringer, S. E.; Gallagher, J. T. Specific binding of the chemokine platelet factor 4 to heparan sulfate. *J. Biol. Chem.* **1997**, *272*, 20508-20514.

33. Tollefsen, D. M.; Sugimori, T.; Maimone, M. M. Effect of Low-Molecular-Weight Heparin Preparations on the Inhibition of Thrombin by Heparin Cofactor-Ii. *Seminars in Thrombosis and Hemostasis* **1990**, *16*, 66-70.

34. Maccarana, M.; Casu, B.; Lindahl, U. Minimal Sequence in Heparin Heparan-Sulfate Required for Binding of Basic Fibroblast Growth-Factor. *J. Biol. Chem.* **1993**, *268*, 23898-23905.

35. Barzu, T.; Lormeau, J. C.; Petitou, M.; Michelson, S.; Choay, J. Heparin-Derived Oligosaccharides - Affinity for Acidic Fibroblast Growth-Factor and Effect on Its Growth-Promoting Activity for Human-Endothelial Cells. *J. Cell. Physiol.* **1989**, *140*, 538-548.

36. Pervin, A.; Gallo, C.; Jandik, K. A.; Han, X.-J.; Linhardt, R. J. Preparation and structural characterization of large heparin-derived oligosaccharides. *Glycobiology* **1995**, *5*, 83-95.

37. Heck, A. J. R.; de Koning, L. J.; Pinkse, F. A.; Nibbering, N. M. M. Mass-specific selection of ions in Fourier-transform ion cyclotron resonance mass spectrometry. Unintentional off-resonance cyclotron excitation of selected ions. *Rapid Commun. Mass Spectrom.* **1991**, *5*, 406-414.

38. Domon, B.; Costello, C. E. A systematic nomenclature for carbohydrate fragmentations in FAB-MS/MS spectra of glycoconjugates. *Glycoconjugate J.* **1988**, *5*, 397-409.

39. Saad, O. M.; Leary, J. A. Delineating mechanisms of dissociation for isomeric heparin disaccharides using isotope labeling and ion trap tandem mass spectrometry. *J. Am. Soc. Mass Spectrom.* **2004**, *15*, 1274-1286.

40. Brüll, L. P.; Kovácik, V.; Thomas-Oates, J. E.; Heerma, W.; Haverkamp, J. Sodium-cationized oligosaccharides do not appear to undergo "internal residue loss" rearrangement processes on tandem mass spectrometry. *Rapid Commun. Mass Spectrom.* **1998**, *12*, 1520-1532.

CHAPTER 6

INFLUENCE OF CHARGE STATE AND SODIUM CATIONIZATION ON THE ELECTRON DETACHMENT DISSOCIATION AND INFRARED MULTIPHOTON DISSOCIATION OF GLYCOSAMINOGLYCAN OLIGOSACCHARIDES*

*Reproduced with permission from Wolff, J.J.; Laremore, T.N.; Busch, A.M.; Linhardt, R.J.; Amster, I.J. Journal of the American Society for Mass Spectrometry, **2008**, in press.

ABSTRACT

Electron detachment dissociation (EDD) Fourier transform mass spectrometry has recently been shown to be a useful method for tandem mass spectrometry analysis of sulfated glycosaminoglycans (GAGs). EDD produces abundant glycosidic and cross-ring fragmentation that is useful for localizing sites of sulfation in GAG oligosaccharides. While EDD fragmentation can be used to characterize GAGs in a single tandem mass spectrometry experiment, SO_3 accompanies many peaks, and complicates the resulting mass spectra. In this work we demonstrate the ability to significantly decrease SO_3 loss by selection of the proper ionized state of GAG precursor ions. When the degree of ionization is greater than the number of sulfate groups in an oligosaccharide, a significant reduction in SO_3 loss is observed in the EDD mass spectra. This data suggested that SO_3 loss is reduced when an electron is detached from carboxylate groups instead of sulfate. Electron detachment occurs preferentially from carboxylate versus sulfate for thermodynamic reasons, provided that carboxylate is in its ionized state. Ionization of the carboxylate group is achieved by selecting the appropriate precursor ion charge state, or by the replacement of protons with sodium cations. Increasing the ionization state by sodium cation addition decreases, but does not eliminate, SO_3 loss from infrared multiphoton dissociation (IRMPD) of the same GAG precursor ions.

INTRODUCTION

Glycosaminoglycans (GAGs) participate in numerous important biological processes such as cell-cell signaling [1, 2], the regulation of biochemical pathways [3, 4], inhibiting proteolysis [5], and effecting angiogenesis [6]. GAGs also play an important role in pathogenic infections [7-9], and may undergo alteration in certain types of cancer [10]. Both intra- and extracellular GAG proteoglycans can be found in a wide variety of organisms, from bacteria to humans [11]. At the molecular level, GAGs are sulfated, linear carbohydrates consisting of alternating acidic sugar and basic sugar residues. GAG complexity arises through variable sulfation, N-modification of the basic residues, and C5 stereochemistry of the hexuronic acid residues. There is significant interest in developing methods to determine the pattern of modification in GAG oligosaccharides, as these are believed to influence the biological function of the GAG molecule. While 1D and 2D NMR can be used to determine the pattern and type of GAG modification [12], GAGs must be isolated from natural sources and may not often be available in the quantity and purity that is required for NMR analysis. Mass spectrometry is much more sensitive than NMR, and can be used to examine mixtures, particularly when combined with online chromatography. A wide variety of mass spectrometry and tandem mass spectrometry techniques have been developed to analyze this challenging class of molecules [13-20].

Recent work from this laboratory has demonstrated the analytical utility of electron detachment dissociation (EDD) [21] for the structural analysis of negatively-charged GAG oligosaccharides varying in length from tetrasaccharides to decasaccharides [22-24]. EDD produces more abundant glycosidic and cross-ring fragmentation for GAG oligosaccharides than is observed by more conventional dissociation methods such as collisionally activated dissociation (CAD) or infrared multiphoton dissociation (IRMPD). Moreover, it reduces the loss of SO_3 from labile sites of sulfation compared to other methods of ion activation. This fragmentation behavior has been proposed to result from a radical anion that is formed from electron detachment, and which yields product ions that are distinctly different from the dissociation products of closed shell anions via low energy or threshold fragmentation methods such as CAD or IRMPD. As in electron ionization mass spectra, the location of the radical site is expected to influence the resulting fragmentation and observed products. Our prior results suggest that electron detachment occurs at a site of negative charge, namely carboxylate and sulfate groups. The charge of the precursor ion determines how many of these sites are ionized, and are available as candidates for electron detachment. Thus the charge state of the precursor ion may have a significant influence on fragmentation, and on the ions produced by EDD.

The charge state of the precursor ion has been shown to influence fragmentation of closed-shell ions. For CAD fragmentation of heparin-like GAGs, Zaia and coworkers demonstrated that glycosidic cleavages increased and SO_3 loss decreased as the charge state of the precursor ion increased [25]. The work by Zaia et al. also demonstrated that the addition of Ca^{2+} to the precursor ion minimized SO_3 loss during CAD of closed-shell ions. It is possible that replacing protons with monovalent cations such as sodium may also suppress SO_3 loss in the dissociation of sulfated GAG oligosaccharides by EDD. In the present work, we examine the influence of charge state and sodium cationization on the EDD fragmentation of a GAG octasaccharide, and compare these products with those obtained by IRMPD.

MATERIALS AND METHODS

Preparation of DS Oligosaccharides

Dermatan sulfate (DS) octasaccharides were prepared by partial enzymatic depolymerization of porcine intestinal mucosa dermatan sulfate (Celsus Laboratories, Cincinnati, OH). A 20 mg/mL dermatan sulfate solution in 50 mM Tris-HCl/60 mM sodium acetate buffer, pH 8 was incubated at 37°C with chondroitin ABC lyase from *Proteus vulgaris*, EC 4.2.2.4. (Seikagaku, Japan). The absorbance at 232 nm was monitored to determine when the digestion was 50% completed. The digestion mixture was then heated at 100°C for 3 min. High-molecular-weight oligosaccharides and the glycosidic enzyme were removed by ultra-filtration using a 5000 MWCO membrane. The resulting oligosaccharide mixture was concentrated by rotary evaporation and fractionated by low pressure GPC on a Bio-Gel P10 (Bio-Rad, Richmond, CA) column. The fraction containing DS octasaccharides (dp8) was desalted by GPC on a Bio-Gel P2 column and freeze-dried [26]. Further purification of DS dp8 were carried out using strong anion exchange high-pressure liquid chromatography (SAX-HPLC) on a semi-preparative SAX S5 Spherisorb column (Waters Corp, Milford, MA). The SAX-HPLC fractions containing > 90% of DS dp8 were collected, desalted by GPC, and freeze-dried. The solid was reconstituted in water and purified a second time by SAX-HPLC. Only the top 30% of the chromatographic peak was collected, desalted, and freeze-dried. Concentration of the octasaccharide solution was determined by measuring the absorbance at 232 nm ($\varepsilon = 3800\ M^{-1}cm^{-1}$). The resulting fraction containing DS dp8 was characterized by PAGE, ESI-MS, and high-field nuclear magnetic resonance (NMR) spectroscopy.

Mass Spectrometry Analysis

Experiments were performed with a 9.4 T Bruker Apex Ultra QhFTMS (Billerica, MA) fitted with an Apollo II dual source, a 25 W CO_2 laser (Synrad model J48-2, Mukilteo, WA) for IRMPD, and an indirectly heated hollow cathode for generating electrons for ECD and EDD. For studies requiring sodium, the octasaccharide was introduced at a concentration of 150 μM in 50:50 methanol:H_2O with 1 mM NaOH (Sigma, St. Louis, MO) by ESI in negative ion mode. To produce abundant $[M-3H]^{3-}$ ions, the octasaccharide was introduced at a concentration of 20 μM in 50:50:1 methanol:H_2O:formic acid. All sample solutions were infused at a rate of 120 μL/hour.

For the EDD experiments, precursor ions were isolated in the external quadrupole and accumulated for 1–4 seconds before injection into the FTMS cell. The isolation/cell fill was repeated up to 6 times. The selection of the precursor ion was further refined by using in-cell isolation with a coherent harmonic excitation frequency (CHEF) event [27]. The precursor ions were then irradiated with electrons for 1 second. For electron irradiation the cathode bias was set to -19 V, the extraction lens was set to -18.5 V±0.5 V, and the cathode heater was set to 1.6 A. Ions were excited with an RF frequency chirp that covered the range of 100 – 2000 *m/z*. 24 acquisitions were signal averaged per mass spectrum. For each mass spectrum, 512K points were acquired at a 2.4 MHz digitization rate, padded with one zero fill, and apodized using a sinebell window. Background spectra were acquired by leaving all parameters the same but setting the cathode bias to 0 V to ensure that no electrons reached the analyzer cell. Background spectra were not subtracted from the EDD spectra, but were used to ensure that very few products were formed during ion accumulation and isolation. IRMPD spectra were acquired using the same experimental setup as EDD, but replacing the electron irradiation event with a laser pulse. For IRMPD, ions were irradiated for 0.01 – 0.2 seconds with beam attenuation set to pass from 40 – 60% of full power. External calibration of IRMPD and EDD mass spectra produced mass accuracy of 5 ppm. Internal calibration was also performed using confidently assigned glycosidic bond cleavage products as internal calibrants, providing mass accuracy of <1 ppm. Due to the larger number of low intensity products formed by EDD, only peaks with S/N > 10 are reported. Product ions were assigned using accurate mass measurement. For the work presented here, fragmentation of the DS octasaccharide is presented using a modification of the Domon and Costello annotation [28] that presents GAG fragmentation with SO_3 loss and hydrogen rearrangement that is observed in EDD of GAGs [22].

RESULTS AND DISCUSSION

DS dp8 has eight ionizable acidic sites; four carboxylic acid groups and four sulfate groups. This acidic molecule readily forms negative ions, but the charge state and Na/H heterogeneity depend strongly on solution conditions. The influence of ESI solution conditions is shown in Figures 6.1A and 6.1B. The addition of 1% formic acid to the ESI solution results in the mass spectrum shown in Figure 6.1A, in which abundant $[M-4H]^{4-}$ and $[M-3H]^{3-}$ molecular ions are observed, with only a low level of sodium cationization. The addition of 100 μM NaOH in place of formic acid to the ESI solution produces the more highly charged 5^- ion as well as the 4^- and 3^- ions. The presence of sodium cations in solution also results in the exchange of up to 5 protons by sodium cations, as shown in Figure 6.1B. Using these two solution conditions the influence of precursor ion charge (3^-, 4^-, 5^-) and sodium cationization (0 – 4) on sulfated GAGs is examined.

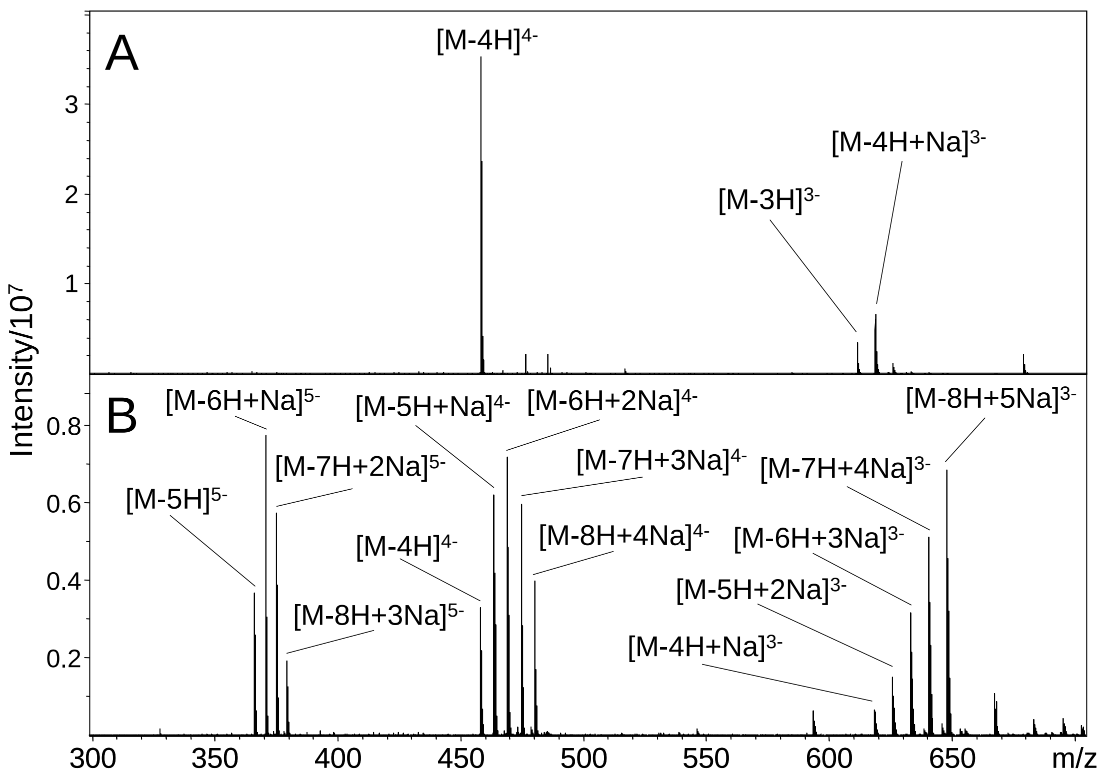

Figure 6.1. The influence of solution conditions on the observed ESI-FTMS spectra of DS dp8. (**A**) 15 μM DS dp8 dissolved in 50:50 methanol:H_2O with 1% formic acid results in no Na/H heterogeneity and the formation of a $[M\text{-}3H]^{3-}$ ion. (**B**) 150 μM DS dp8 dissolved in 50:50 methanol:H_2O with 100 μM NaOH results in abundant Na/H heterogeneity.

Influence of Charge State on EDD Fragmentation of DS dp8

EDD of the $[M-4H]^{4-}$ and $[M-3H]^{3-}$ precursor ions of DS dp8 produce many glycosidic and cross-ring cleavages that are also accompanied by the loss of SO_3. No product ions are observed with loss of two equivalents of SO_3 for any EDD mass spectrum, regardless of the charge state of the precursor ion. Product ions with SO_3 loss generally occur as satellite peaks to similar fragments without SO_3 loss, and are easily assigned as the pairs of peaks differ by the exact mass of SO_3, 79.957 u. While products ions accompanied by SO_3 loss are easily identified, they complicate the EDD mass spectrum by adding additional peaks and do not aid in deciphering the structure of the sulfated GAG. The additional complexity resulting from product ion SO_3 is apparent in Figure 6.2, where many of the product ions accompanied by the loss of SO_3 are present in the EDD mass spectrum of DS dp8. The Z_3 and Y_3 glycosidic cleavages are accompanied by Z_3-SO_3 and Y_3-SO_3 product ions, as well as many other products ions accompanied by the loss of SO_3 as shown in Figure 6.2A. However, a much simpler EDD mass spectrum is observed from EDD of the $[M-5H]^{5-}$ precursor ion (Figure 6.2B) due to the absence of satellite peaks from SO_3 loss. As shown in Figure 6.2B, the Z_3 and Y_3 glycosidic cleavages are not accompanied by SO_3-loss product ions. This behavior is observed throughout the EDD mass spectrum. The number of products accompanied by SO_3 loss is similar in EDD of $[M-3H]^{3-}$ and $[M-4H]^{4-}$, i.e. no decrease in SO_3 loss is observed when the precursor ion charge increases from 3^- to 4^-. In contrast, there is a dramatic decrease in the loss of SO_3 for precursor ion charge 5^- versus 4^- or 3^-, as shown in Figures 6.3A through 6.3C, respectively. Fragmentation accompanied by loss of SO_3 is denoted with an open circle. For EDD of $[M-3H]^{3-}$, 36 of the 88 observed cleavages are accompanied by SO_3 loss, and EDD of$[M-4H]^{4-}$ results in 34 of the 87 products are accompanied by SO_3 loss. In contrast to this, 3 of the 56 products from EDD of [M-

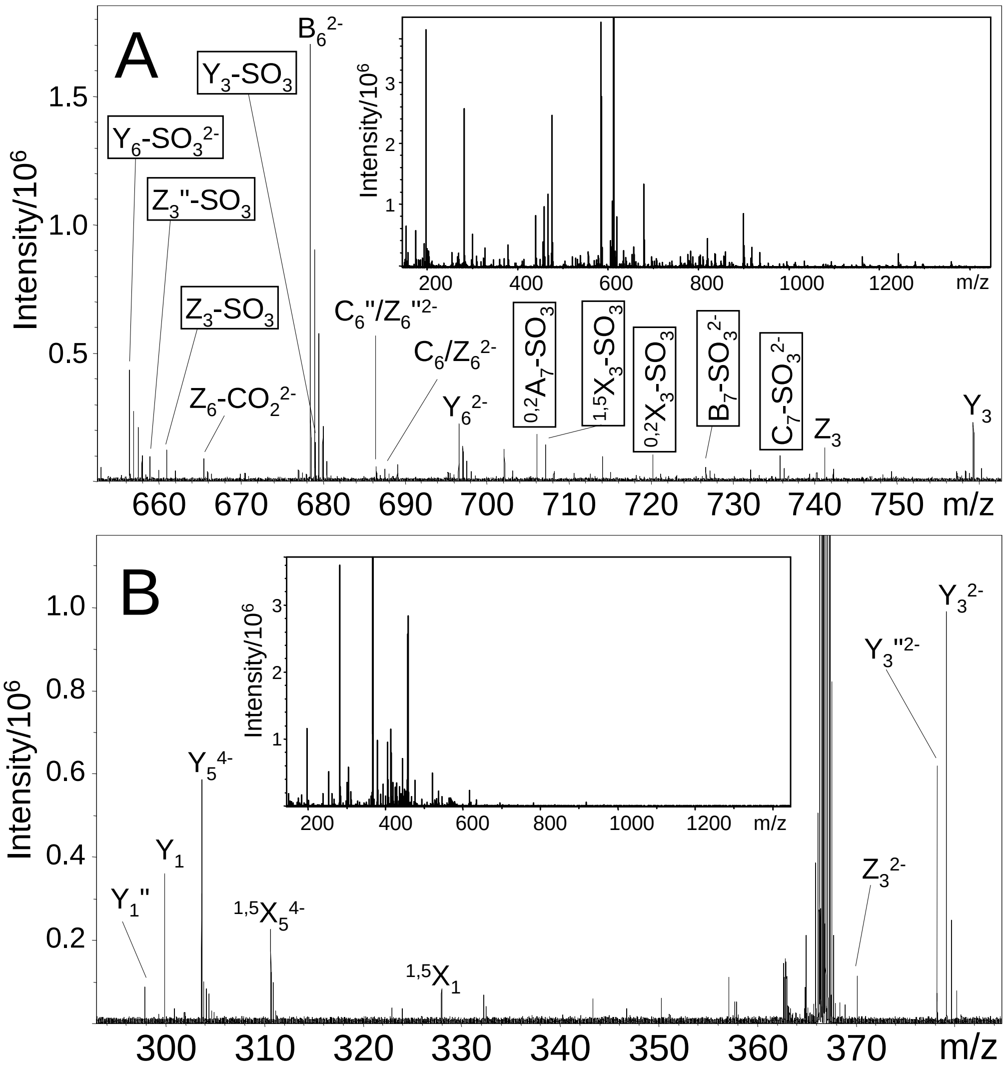

Figure 6.2. EDD mass spectrum complexity increases when product ions accompanied by SO_3 loss are present. (**A**) EDD of the $[M\text{-}3H]^{3-}$ of DS dp8 produces a more complex mass spectrum than (**B**) EDD of $[M\text{-}5H]^{5-}$. Insets, a reduction in mass spectrum complexity is observed when SO_3 loss is reduced.

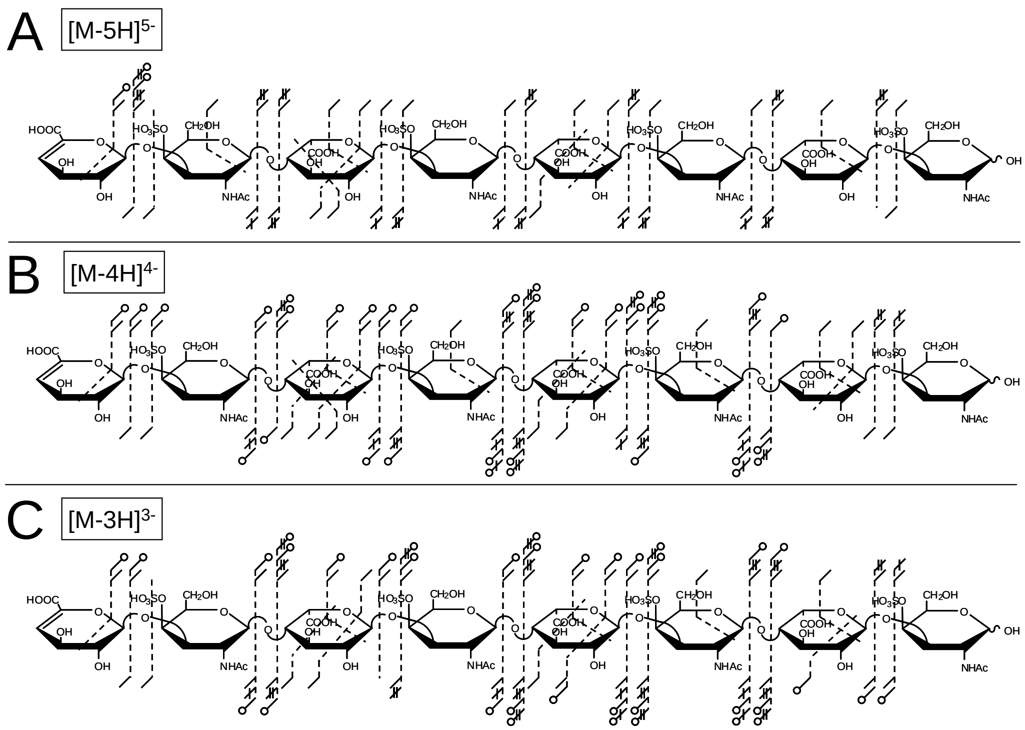

Figure 6.3. Influence of precursor ion charge on EDD of DS dp8. Product ions observed from EDD of (**A**) the $[M\text{-}5H]^{5-}$ precursor ion, (**B**) the $[M\text{-}4H]^{4-}$ precursor ion, and (**C**) the $[M\text{-}3H]^{3-}$ precursor ion of DS dp8.

5H]$^{5-}$ are accompanied by SO_3 loss. Most glycosidic cleavages of the 3^- or 4^- precursor occur with loss of SO_3, but are absent for the 5^- charge state. Abundant and similar glycosidic and cross-ring fragmentation is observed for EDD of all charge states. For EDD of [M-3H]$^{3-}$, [M-4H]$^{4-}$, and [M-5H]$^{5-}$, cleavage of most glycosidic bonds is observed. EDD of [M-5H]$^{5-}$ and [M-3H]$^{3-}$ produces 26 of the 28 possible products (Figures 6.3A and 6.3C, respectively) while EDD of [M-4H]$^{4-}$ precursor produces all 28 possible glycosidic products (Figure 6.3B). Differences in the number of observed glycosidic cleavages are due to the low abundance of the product ion, or overlap of the product ion with the precursor ion. Glycosidic bond cleavages accompanied by loss of one or two additional hydrogen atoms are observed for EDD of all charge states. Specifically, we observed B-H, C-2H, Y-2H, and Z-2H, which we refer to as B', C", Y", and Z", respectively. We have previously suggested radical mechanisms for the formation of these ions and found them useful for analyzing structural features, such as distinguishing IdoA form GlcA [24].

Previous results from CAD of sulfated GAGs suggest that the sulfate group readily loses SO_3 when it is protonated [25]. Because sulfate is more acidic than carboxylate in solution, sulfate groups will be ionized in preference to carboxyl groups in solution. Products observed from EDD of DS dp8 indicate that these sites of charge are preserved as the molecule moves from solution to the gas phase, and as a result sulfate groups will ionize in preference to carboxyl groups. Therefore it is expected that the [M-5H]$^{5-}$ precursor will have all four sulfate residues charged plus one carboxylate group charged. Electron detachment is expected to occur more readily from the carboxylate anion as it requires ~1.2 eV less energy than from a sulfate anion [23]. For the 3^- and 4^- precursor ions only sulfates will be ionized, and detachment will occur from the sulfate group. In support of this, EDD of [M-5H]$^{5-}$ produces the charge reduced species minus CO_2 ($[M\text{-}5H\text{-}CO_2]^{4-\bullet}$) and not the charge reduced species minus SO_3 ($[M\text{-}5H\text{-}SO_3]^{4-\bullet}$), indicating a preference for radical site formation at the carboxylate anion. Conversely, for EDD of $[M\text{-}3H]^{3-}$ and $[M\text{-}4H]^{4-}$, the charge-reduced species minus SO_3 ($[M\text{-}3H\text{-}SO_3]^{2-\bullet}$ and $[M\text{-}4H\text{-}SO_3]^{3-\bullet}$, respectively) is observed, but not the charge-reduced species minus CO_2. These data suggest that electron detachment from a sulfate anion produces a sulfate radical that readily loses SO_3 from EDD product ions, while electron detachment from a carboxylate anion does not promote the loss of SO_3. Therefore, if the charge on the precursor ion is greater than the number of sulfate groups, at least one ionized carboxyl group is present and available as a radical site after electron detachment, and SO_3 loss will greatly reduced in EDD fragmentation.

The pattern of SO_3 loss from the charge-reduced species suggests that the initial site of radical formation occurs on a sulfate group of the GalNAc4S residues for the 3^- and 4^- charge states of DS dp8, and on a carboxylate group of IdoA residues for the 5^- charge state of DS dp8. The majority of the cross-ring fragmentation products that are observed, however, originate across IdoA residues for all the charge states of the precursor. The preferential fragmentation of the acidic residues (IdoA) over fragmentation of basic residues (GalNAc4S), regardless of the initial site of electron detachment, can be rationalized by radical site migration from GalNAc4S to IdoA, for example by radical site initiated hydrogen rearrangement. Another explanation for these data is that many of the "EDD" products do not arise from radical site initiated fragmentation, but are a result of ion activation from the interaction of the precursor ions with the 19 eV electrons [29-31]. Clearly, the loss of CO_2 or SO_3 from the charge-reduced species are radical driven processes, as these products are strongly influenced by the initial site of radical formation. Other products appear to arise both from fragmentation of the odd-electron charge reduced species as well as from activation of the even-electron precursor ion. We have recently examined the electron induced dissociation (EID) of singly-charged GAG tetrasaccharides, for which all products must come from an even-electron precursor (manuscript in preparation). Many cross-ring fragmentation products of the hexuronic acid residues were found in the EID mass spectrum that were not found in the IRMPD mass spectrum of the same precursor ion. Previously, we had proposed the preponderance of cross-ring fragmentation of the hexuronic acid residues over amino sugars in heparan sulfate tetrasaccharides [23] and dermatan sulfate oligosaccharides [22] was related to radical-driven fragmentation processes originating from a carboxy-radical. However, the newer EID data suggests that hexuronic acid residues are more labile, and that fragmentation of the hexuronic acid residues occurs by electron activation of the even-electron precursor ion (EID) as well by as radical-driven fragmentation (EDD).

The gas phase ion conformation of proteins has been shown to influence the products observed by ECD. The combination of IRMPD with ECD, known as activated ion ECD (AI-ECD) [32], have been shown to increase the number of backbone cleavages by ECD, and this effect is also observed by increasing the precursor ion charge state [33]. This increase in fragmentation has been proposed to occur from a change in ion conformation that results from breaking intramolecular noncovalent bonds, producing a more extended structure. To examine the possibility that conformation affects fragmentation for GAG oligomers, activated ion EDD (AI-EDD) was performed on the $[M-4H]^{4-}$ precursor ion using CO_2 laser irradiation to warm the ions to the threshold of fragmentation, followed by irradiation with electrons. While the S/N of some product ions increased slightly, AI-EDD does not influence the type or relative abundance of the observed products, specifically products accompanied by SO_3 loss (data not shown). Therefore, the difference in SO_3 loss in the 3^- and 4^- versus 5^- charge states appears to be a result of electron detachment from a carboxylate anion and not due to a change in gas-phase conformation.

EDD of DS dp8 with Sodium Cations

The loss of SO_3 by MS/MS of sulfated GAG oligosaccharides complicates the mass spectrum and reduces its analytical utility. Thus, controlling SO_3 loss is important for the analysis of GAG oligosaccharides. The results of the charge state dependence studies show that SO_3 loss is reduced when at least one carboxyl group is ionized in the precursor ion. As an alternative to dissociation of higher charge states, which may not have substantial abundance by ESI, we have investigated the replacement of protons by sodium. In such ions, the charge state will be smaller than the number of ionized sites in the precursor. As Figure 6.1 shows, the $[M-5H]^{5-}$ ion is half as abundant as the $[M-5H+Na]^{4-}$. Both have five ionized sites and will therefore have an ionized carboxyl group available for electron detachment, providing a way to achieve a higher degree of ionization with precursor ions of a lower overall charge.

Products from EDD of the $[M-5H+Na]^{4-}$ precursor ion of DS dp8 are shown in Figure 6.4A (mass spectrum provided as Appendix C). When sodium is present in the precursor ion, product ions may occur as protonated or sodium cationized products. Product ions that are observed with sodium are indicated by a number above the fragment notation, with this number indicating the number of sodium cations in the product ion. For the work presented here, products containing sodium are described as the fragment plus the number of sodium cations, such as $^{0,2}X_7$+Na. EDD of the $[M-5H+Na]^{4-}$ precursor ion of DS dp8 produces abundant glycosidic and cross-ring fragmentation similar to EDD of the non-cationized (i.e. 3^-, 4^-, and 5^-) precursor ions of DS dp8. Glycosidic cleavages accompanied by the loss of 1 or 2 hydrogen

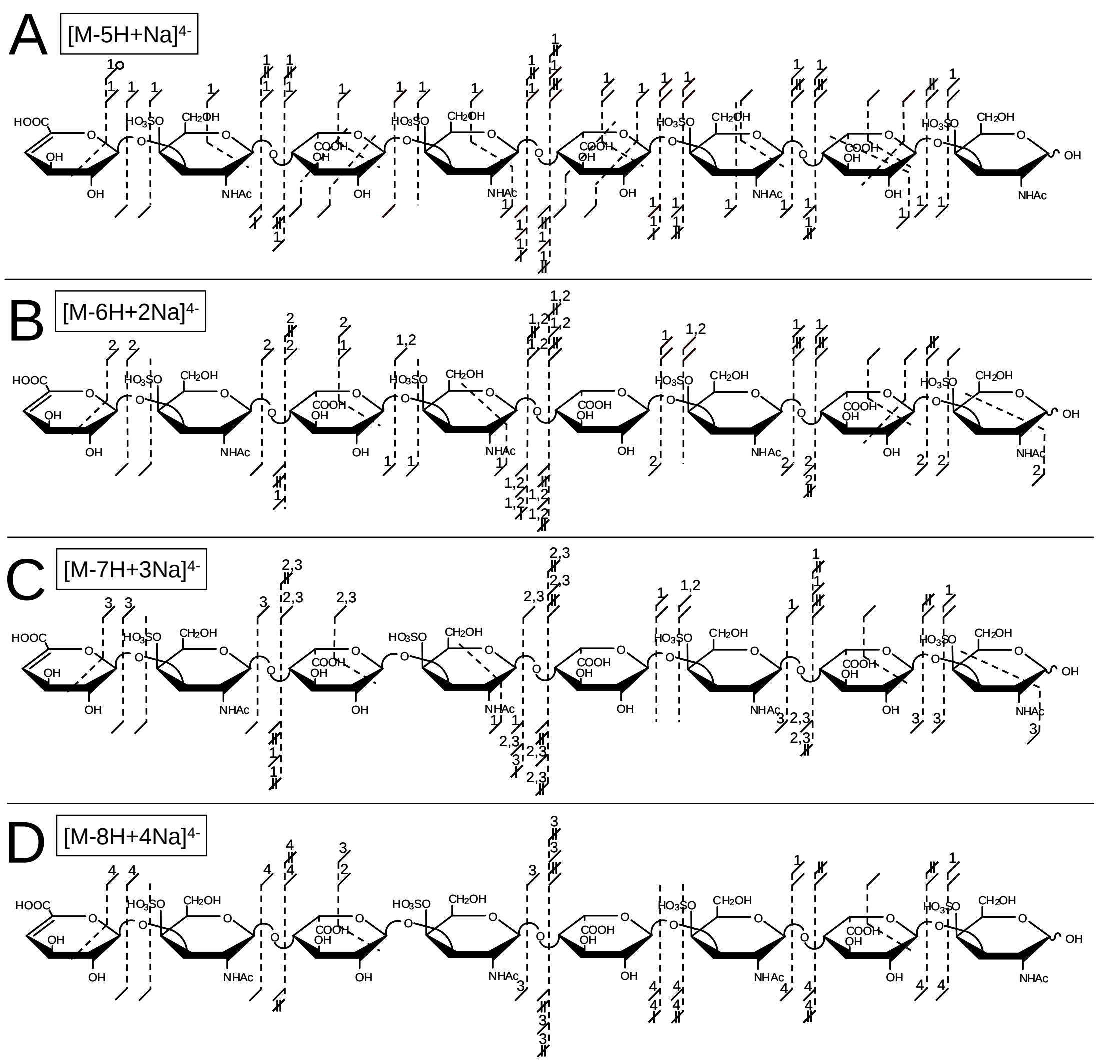

Figure 6.4. Product ions observed from EDD of the (**A**) $[M\text{-}5H\text{+}Na]^{4-}$, (**B**) $[M\text{-}6H\text{+}2Na]^{4-}$, (**C**) $[M\text{-}7H\text{+}3Na]^{4-}$, and (**D**) $[M\text{-}8H\text{+}4Na]^{4-}$ precursor ions of DS dp8.

atoms are also observed. Compared to EDD of $[M\text{-}4H]^{4-}$ (Figure 6.2B), EDD of $[M\text{-}5H\text{+}Na]^{4-}$ results in a significant decrease in product ions accompanied by SO_3 loss. When compared to the product ions observed from EDD of the 3-, 4-, and 5- precursor ions of DS dp8 (Figure 6.2), the products observed from EDD of the $[M\text{-}5H\text{+}Na]^{4-}$ precursor ion resemble more closely the products observed from EDD of the $[M\text{-}5H]^{5-}$ precursor ion. For example, cross-ring cleavages occur primarily on IdoA residues. Also, the charge-reduced species minus CO_2, $[M\text{-}5H\text{+}Na\text{-}CO_2]^{3-\bullet}$, and not SO_3 is observed. SO_3 loss accompanying other fragmentation is greatly reduced in EDD of both $[M\text{-}5H]^{5-}$ and $[M\text{-}5H\text{+}Na]^{4-}$, and the small number of products accompanied by SO_3 loss occur near the NRE of the octasaccharide for both precursors. For example, 34 or the 87 observed products from EDD of the $[M\text{-}4H]^{4-}$ precursor ion are accompanied by SO_3 loss, while 3 of the 56 and 1 of the 70 observed products from EDD of the $[M\text{-}5H]^{5-}$ and $[M\text{-}5H\text{+}Na]^{4-}$ precursor ions, respectively, are accompanied by SO_3 loss. Together, these data suggest a total of five ionized sites on DS dp8, with at least one ionized site on a carboxy group. These data are consistent with our proposal that electron detachment preferentially occurs from the carboxylate anion, with EDD of $[M\text{-}5H\text{+}Na]^{4-}$ exhibiting a significant decrease in SO_3 loss and fragmentation similar to EDD of $[M\text{-}5H]^{5-}$. These observations suggest SO_3 loss is suppressed when the total number of ionized sites on the GAG is one more than the number of sulfate groups. In further support of this observation, a significant decrease in SO_3 loss is observed for EDD of $[M\text{-}5H\text{+}2Na]^{3-}$ when compared to the EDD data of $[M\text{-}4H\text{+}Na]^{3-}$ (data not shown).

Additional replacement of protons by sodium cations can be used to increase the number of ionized sites. We have examined the EDD of DS dp8 with up to eight ionized acidic groups. Products from the EDD of the $[M\text{-}6H\text{+}2Na]^{4-}$, $[M\text{-}7H\text{+}3Na]^{4-}$, and $[M\text{-}8H\text{+}4Na]^{4-}$ precursor ions are shown in Figure 6.4B through 6.4C, respectively (see Appendix C for EDD mass spectra).

As shown in Figure 6.4, increasing the number of sodium cations, and thus the number of ionized sites on the DS dp8 precursor ion decreases the number of observed glycosidic and cross-ring fragmentations. For the 4^- ion of DS dp8 with 1 – 4 sodium cations, the charge reduced species minus CO_2 is observed for all ions, indicating preference for electron detachment at carboxylate on IdoA residues. While increasing the ionization state of the molecule such that one carboxylate is charged benefits fragmentation by decreasing SO_3 loss, further ionization of the GAG with sodium cations reduces EDD fragmentation. The decrease in fragmentation suggests that carboxyl hydrogens may play a role in the mechanism of cross-ring fragmentation, perhaps via hydrogen rearrangement reactions.

IRMPD of DS dp8 with Sodium Cations

SO_3 loss during electron activation methods such as EDD of EID differs from that observed during activation of even-electron ions by threshold or low-energy methods. Previous work by Zaia and coworkers suggests that sulfate groups are most labile and readily undergo loss of SO_3 during CAD when protonated [25]. While SO_3 loss can be minimized and glycosidic cleavages maximized by increasing the charge state so that all sulfate groups are charged, the abundance of precursor ions in which all sulfates are charged may be too small to be useful for MS/MS. The addition of sodium cations to the ESI solution allows IRMPD to be applied to more ionized sulfated GAGs. Products resulting from IRMPD of the $[M-4H]^{4-}$, $[M-5H+Na]^{4-}$, $[M-6H+2Na]^{4-}$, $[M-7H+3Na]^{4-}$, and $[M-8H+4Na]^{4-}$ precursor ions of DS dp8 are shown in Figures 6.5A – 6.5C, respectively. Compared to EDD of the same precursor ions (Figures 6.2A and 6.4A – 6.4C), IRMPD produces fewer glycosidic and cross-ring cleavages as well as more abundant SO_3 loss. Unlike EDD, IRMPD produces some product ions which are observed only

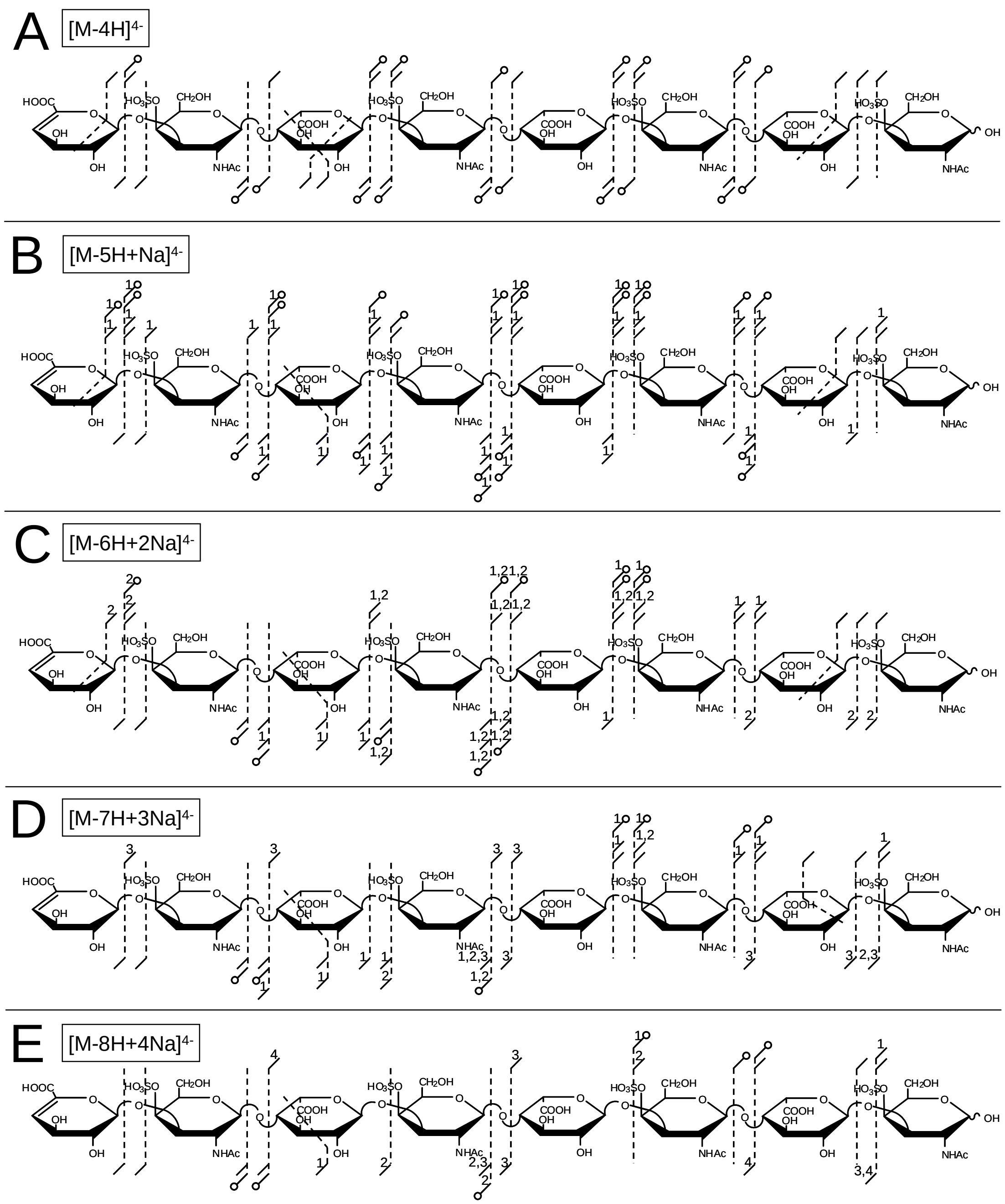

Figure 6.5. Product ions observed from IRMPD of the (**A**) [M-4H]$^{4-}$, (**B**) [M-5H+Na]$^{4-}$, (**C**) [M-6H+2Na]$^{4-}$, (**D**) [M-7H+3Na]$^{4-}$, and (**E**) [M-8H+4Na]$^{4-}$ precursor ions of DS dp8.

with SO_3 loss. However, product ion SO_3 loss decreases as the cationization of the precursor ion increases, for example IRMPD of the $[M-4H]^{4-}$ precursor ion produces 18 products accompanied by SO_3 loss, while IRMPD of the $[M-8H+4Na]^{4-}$ produces 6 products accompanied by SO_3 loss. These results are similar to the observations by Zaia et al. [25], suggesting that ionization of the sulfate groups prevents loss of SO_3 for ion activation via threshold dissociation. The number of glycosidic bond and cross-ring cleavages produced by IRMPD decreases when the ionization of the GAG is increased using sodium cations, similar to the observation for EDD. For example, IRMPD of the $[M-4H]^{4-}$ precursor ion produces a total of 41 glycosidic and cross-ring cleavages, while IRMPD of the $[M-8H+4Na]^{4-}$ produces 23 glycosidic and cross-ring ring cleavages.

CONCLUSIONS

The ionization state of a sulfated GAG affects the number of ionized sites available for electron detachment. Since electron detachment occurs at a site of negative charge, the pattern of SO_3 loss in EDD of sulfated GAGs is dependant on the number of ionized sites on the sulfated GAG. When electron detachment occurs at a sulfate anion, many product ions are accompanied by loss of SO_3. When electron detachment occurs at a carboxylate anion there is a significant decrease in the number of product ions that are accompanied by loss of SO_3. Increasing the degree of ionization can be achieved by either increasing the precursor ion charge state, or by the replacement of protons with sodium cations. Both methods can be used to ensure ionization of a carboxylate group. For EDD of sulfated GAGs, SO_3 loss is minimized if the ionization state of the sulfated GAG is equal to one more than the number of sulfate groups. Further increasing the ionization state of the molecule so that more carboxylate groups are charged eliminates SO_3 loss by EDD, but also decreases the number of glycosidic and cross-ring cleavages. For IRMPD of sulfated GAGs, increasing the ionization state of GAG precursor ions by replacement of protons with sodium cations decreases SO_3 loss, but also decreases glycosidic and cross-ring fragmentation.

ACKNOLWEDGMENTS

The authors wish to acknowledge the seminal contributions of Roman Zubarev to the field of electron-ion interactions, and offer congratulations on his selection as a Biemann awardee. We gratefully acknowledge financial support from the National Institutes of Health grant #2R01-GM038060-16.

REFERENCES

1. Linhardt, R. J.; Toida, T., Role of Glycosaminoglycans in Cellular Communication. *Acc. Chem. Res.* **2004,** *37*, 431-438.
2. Gotte, M., Syndecans in Inflammation. *FASEB J.* **2003,** *17*, 575-591.
3. Fannon, M.; Forsten, K. E.; Nugent, M. A., Potentiation and Inhibition of bFGF Binding by Heparin: A Model for Regulation of Cellular Response. *Biochemistry* **2000,** *39*, 1434-1445.
4. Wu, Z. L.; Zhang, L.; Yabe, T.; Kuberan, B.; Beeler, D. L.; Love, A.; Rosenberg, R. D., The Involvement of Heparan Sulfate (HS) in FGF1/HS/FGFR1 Signaling Complex. *J. Biol. Chem.* **2003,** *278*, 17121-17129.
5. Sadir, R.; Imberty, A.; Baleux, F.; Lortat-Jacob, H., Heparan Sulfate/Heparin Oligosaccharides Protect Stromal Cell-derived Factor-1 (SDF-1)/CXCL12 against Proteolysis Induced by CD26/Dipeptidyl Peptidase IV. *J. Biol. Chem.* **2004,** *279*, 43854-43860.
6. Iozzo, R. V.; San Antonio, J. D., Heparan sulfate proteoglycans: heavy hitters in the angiogenesis arena. *J. Clin. Invest.* **2001,** *108*, 349-355.
7. Batinic, D.; Robey, F. A., The V3 region of the envelope glycoprotein of human immunodeficiency virus type 1 binds sulfated polysaccharides and CD4-derived synthetic peptides. *J. Biol. Chem.* **1992,** *267*, 6664-6671.
8. Chen, Y.; Maguire, T.; Hileman, R. E.; Fromm, J. R.; Esko, J. D.; Linhardt, R. J.; Marks, R. M., Dengue virus infectivity depends on envelope protein binding to target cell heparan sulfate. *Nature Med.* **1997,** *3*, 866-871.

9. Williams, R. K.; Straus, S. E., Specificity and affinity of binding of herpes simplex virus type 2 glycoprotein B to glycosaminoglycans. *J. Virol.* **1997,** *71*, 1375-1380.

10. Liu, D. F.; Shriver, Z.; Gi, Y. W.; Venkataraman, G.; Sasisekharan, R., Dynamic regulation of tumor growth and metastasis by heparan sulfate glycosaminoglycans. *Semin. Thromb. Hemost.* **2002,** *28*, 67-78.

11. Perrimon, N.; Bernfield, M., Cellular functions of proteoglycans--an overview. *Semin. Cell Dev. Biol.* **2001,** *12*, 65-67.

12. Horne, A.; Gettins, P., H-1-Nmr Spectral Assignments for 2 Series of Heparin-Derived Oligosaccharides. *Carbohydr. Res.* **1992,** *225*, 43-57.

13. Chi, L. L.; Amster, J.; Linhardt, R. J., Mass spectrometry for the analysis of highly charged sulfated carbohydrates. *Current Analytical Chemistry* **2005,** *1*, 223-240.

14. Dai, Y.; Whittal, R. M.; Bridges, C. A.; Isogai, Y.; Hindsgaul, O.; Li, L., Matrix-assisted laser desorption ionization mass spectrometry for the analysis of monosulfated oligosaccharides. *Carbohydr. Res.* **1997,** *304*, 1-9.

15. Miller, M. J. C.; Costello, C. E.; Malmstrom, A.; Zaia, J., A tandem mass spectrometric approach to determination of chondroitin/dermatan sulfate oligosaccharide glycoforms. *Glycobiology* **2006,** *16*, 502-513.

16. Reinhold, V. N.; Carr, S. A.; Green, B. N.; Petitou, M.; Choay, J.; Sinay, P., Structural Characterization of Sulfated Glycosaminoglycans by Fast-Atom-Bombardment Mass-Spectrometry - Application to Heparin Fragments Prepared by Chemical Synthesis. *Carbohydr. Res.* **1987,** *161*, 305-313.

17. Saad, O. M.; Leary, J. A., Compositional Analysis and Quantification of Heparin and Heparan Sulfate by Electrospray Ionization Ion Trap Mass Spectrometry. *Anal. Chem.* **2003,** *75*, 2985-2995.

18. Saad, O. M.; Leary, J. A., Heparin Sequencing Using Enzymatic Digestion and ESI-MS with HOST: A Heparin/HS Oligosaccharide Sequencing Tool. *Anal. Chem.* **2005,** *77*, 5902-5911.

19. Zaia, J.; Li, X.-Q.; Chan, S.-Y.; Costello, C. E., Tandem mass spectrometric strategies for determination of sulfation positions and uronic acid epimerization in chondroitin sulfate oligosaccharides. *J. Am. Soc. Mass Spectrom.* **2003,** *14*, 1270-1281.

20. Zaia, J.; McClellan, J. E.; Costello, C. E., Tandem Mass Spectrometric Determination of the 4S/6S Sulfation Sequence in Chondroitin Sulfate Oligosaccharides. *Anal. Chem.* **2001,** *73*, 6030-6039.

21. Budnik, B. A.; Haselmann, K. F.; Zubarev, R. A., Electron detachment dissociation of peptide di-anions: an electron-hole recombination phenomenon. *Chem. Phys. Lett.* **2001,** *342*, 299-302.

22. Wolff, J. J.; Laremore, T. N.; Busch, A. M.; Linhardt, R. J.; Amster, I. J., Electron Detachment Dissociation of Dermatan Sulfate Oligosaccharides. *J. Am. Soc. Mass Spectrom.* **2008,** *In Press*.

23. Wolff, J. J.; Amster, I. J.; Chi, L.; Linhardt, R. J., Electron Detachment Dissociation of Glycosaminoglycan Tetrasaccharides. *J. Am. Soc. Mass Spectrom.* **2007,** *18*, 234-244.

24. Wolff, J. J.; Chi, L. L.; Linhardt, R. J.; Amster, I. J., Distinguishing glucuronic from iduronic acid in glycosaminoglycan tetrasaccharides by using electron detachment dissociation. *Anal. Chem.* **2007,** *79*, 2015-2022.

25. Zaia, J.; Costello, C. E., Tandem Mass Spectrometry of Sulfated Heparin-Like Glycosaminoglycan Oligosaccharides. *Anal. Chem.* **2003,** *75*, 2445-2455.

26. Pervin, A.; Gallo, C.; Jandik, K. A.; Han, X.-J.; Linhardt, R. J., Preparation and structural characterization of large heparin-derived oligosaccharides. *Glycobiology* **1995,** *5*, 83-95.

27. Heck, A. J. R.; de Koning, L. J.; Pinkse, F. A.; Nibbering, N. M. M., Mass-specific selection of ions in Fourier-transform ion cyclotron resonance mass spectrometry. Unintentional off-resonance cyclotron excitation of selected ions. *Rapid Commun. Mass Spectrom.* **1991,** *5*, 406-414.

28. Domon, B.; Costello, C. E., A systematic nomenclature for carbohydrate fragmentations in FAB-MS/MS spectra of glycoconjugates. *Glycoconjugate J.* **1988,** *5*, 397-409.

29. Budnik, B. A.; Haselmann, K. F.; Elkin, Y. N.; Gorbach, V. I.; Zubarev, R. A., Applications of Electron-Ion Dissociation Reactions for Analysis of Polycationic Chitooligosaccharides in Fourier Transform Mass Spectrometry. *Anal. Chem.* **2003,** *75*, 5994-6001.

30. Cody, R. B.; Freiser, B. S., Electron impact excitation of ions from organics: an alternative to collision induced dissociation. *Anal. Chem.* **1979,** *51*, 547-551.

31. Cody, R. B.; Freiser, B. S., Electron impact excitation of ions in Fourier transform mass spectrometry. *Anal. Chem.* **1987,** *59*, 1054-1056.

32. Horn, D. M.; Ge, Y.; McLafferty, F. W., Activated Ion Electron Capture Dissociation for Mass Spectral Sequencing of Larger (42 kDa) Proteins. *Anal. Chem.* **2000,** *72*, 4778-4784.

33. Sze, S. K.; Ge, Y.; Oh, H.; McLafferty, F. W., Top-down mass spectrometry of a 29-kDa protein for characterization of any posttranslational modification to within one residue. *Proc. Natl. Acad. Sci.* **2002**, 1774-1779.

CHAPTER 7

ELECTRON INDUCED DISSOCIATION OF GLYCOSAMINOGLYCAN TETRASACCHARIDES*

* Wolff, J.J.; Laremore, T.N.; Aslam, H.; Linhardt, R.J.; Amster, I.J. To be submitted to the *Journal of the American Society for Mass Spectrometry*.

ABSTRACT

Electron detachment dissociation (EDD) Fourier transform mass spectrometry has recently been shown be a powerful tool for examining the structural features of sulfated glycosaminoglycans (GAGs). The characteristics of GAG fragmentation by EDD include abundant cross-ring fragmentation primarily on hexuronic acid residues, cleavage of all glycosidic bonds, and the formation of even- and odd-electron product ions. GAG dissociation by EDD has been proposed to occur through the formation of an excited species which can undergo direct decomposition, or eject an electron which then undergoes dissociation. In this work, we perform electron induced dissociation (EID) on singly-charged GAGs to distinguish products that form via direct decomposition versus products that arise through electron detachment. EID of GAG tetrasaccharides produces cleavage of all glycosidic bonds and abundant cross-ring fragmentation primarily on hexuronic acid residues, producing fragmentation similar to EDD of the same molecules, but distinctly different from the products of infrared multiphoton dissociation or collisionally activated decomposition. These results suggest that observed abundant fragmentation of hexuronic acid residues occur because they are more labile when they undergo electronic excitation. EID fragmentation of GAG tetrasaccharides is found to produce both even- and odd-electron products. EID of heparan sulfate tetrasaccharide epimers produces identical fragmentation, contrary to EDD, in which the epimers can be distinguished from their fragment ions. These data suggest that electron detachment fragmentation pathways play a significant role in distinguishing glucuronic acid from iduronic acid.

INTRODUCTION

Glycosaminoglycans (GAGs) are complex, sulfated carbohydrates that comprise the carbohydrate portion of proteoglycans and participate in diverse biological processes such as the regulation of biochemical pathways [1, 2] or inhibiting proteolysis [3], and are involved in some pathogenic infections [4-6]. GAGs are found both intra- and extracellularly in a wide variety of organisms, from bacteria to humans [7]. At the molecular level, GAGs are linear carbohydrates that consist of a repeating disaccharide containing one acidic sugar and one amino sugar. GAG complexity arises from variation in the degree and location of sulfation on either sugar, N-modification of the amino sugar, and C5 stereochemistry of the acidic sugar. There is significant interest in developing methods to characterize the pattern of GAG modification, as these structural details are believed to influence the biological function of GAGs. A wide variety of analytical techniques have been developed to characterize sulfated GAGs, including 1D and 2D NMR [8] as well as mass spectrometry and tandem mass spectrometry [9-17].

The application of electron-ion interactions to tandem mass spectrometry has produced a number of useful ion dissociation techniques. The recombination of low-energy electrons (≤1 eV) with multiply-charged precursor ions, known as electron capture dissociation (ECD) [18], has found widespread use in the characterization of biomolecules. ECD produces a radical species that fragments differently compared to low-energy or threshold methods of dissociation, and can be used to determine the sites of labile post-translational modifications, such as the glycosylation, sulfation, or phosphorylation of peptides and proteins [19-24]. Electron detachment dissociation (EDD) [25] is the negative ion complement of ECD [26], and is useful for the characterization of acidic molecules which do not easily form positive ions. For EDD, multiply-charged precursor anions are irradiated with moderate energy (~19 eV) electrons, resulting in electron ejection from the precursor ion. Similar to ECD, a radical species is created which fragments differently than do even-electron ions by low energy or threshold dissociation.

We have recently demonstrated the analytical utility of EDD for determining the important structural features of sulfated GAGs [27]. EDD produces more abundant cross-ring and glycosidic cleavages with minimal SO_3 loss compared to collisionally activated decomposition (CAD) or infrared multiphoton dissociation (IRMPD) of the same precursor ions. EDD has been demonstrated to be useful for GAG oligosaccharides ranging in size from tetrasaccharides to decasaccharides [28], and can distinguish glucuronic acid (GlcA) from iduronic acid (IdoA) in heparan sulfate oligosaccharides by the presence of key product ions [29]. While the experimental parameters influencing the efficiency of EDD for sulfated GAGs have recently been examined [30], the mechanistic details of GAG dissociation by EDD have not been studied. The mechanism of the EDD-induced dissociation of GAGs and the preference for GlcA/IdoA fragmentation was proposed based on the observed products [27]. Irradiation of the precursor anion with 19 eV electrons is proposed to produce an excited intermediate which can undergo direct decomposition or electron detachment. Electron detachment from a site of negative charge produces a radical species. A preference for cross-ring fragmentation of GlcA/IdoA residues was proposed to result from radical formation at the carboxyl group, inducing fragmentation in these residues. However, recent studies on the effect of precursor ion charge on the EDD spectra shows preferential fragmentation of GlcA/IdoA residues regardless of the initial site of electron detachment, suggesting that GlcA/IdoA residues are more labile when activated via electronic excitation than by vibrational excitation [31]. Carbohydrate fragmentation by EDD has also been proposed to occur by an electron capture mechanism [32].

While this proposal explains the formation of even- and odd-electron products, it does not explain the preference for fragmentation of GlcA/IdoA residues over the amino sugar residues.

Some fraction of product ions in an EDD experiment are produced by activation of the precursor without detachment of an electron. The irradiation of singly-charged ions with electrons below their second ionization energy, but with sufficient energy to promote electronic excitation (typically 6 – 20 eV) was originally termed electron-impact excitation of ions from organics (EIEIO) [33, 34]. It is now referred to as electron induced dissociation (EID) [35], which also applies to the excitation of multiply-charged ions with an electron beam. EID was first applied to small molecules and peptides [36], producing fragmentation similar to CAD or IRMPD, even though EID is expected to activate ions by electronic excitation rather than by vibrational excitation. Recent work on carbohydrate cations [35], phosphorylated metabolite anions [37], and amino acids [38] has shown promise for characterization of these small molecules using EID.

In order to distinguish products that arise from EID versus those than arise from electron detachment, in this work we examine the dissociation of singly-charged GAG tetrasaccharides by 19 eV electrons. Because electron detachment from a singly-charged GAG anion would produce a neutral molecule, products observed from irradiation of singly-charged GAG precursor ions can only result from EID. The products observed from EID provide insight into the degree of fragmentation and the type of products produced by electron detachment versus EID in an EDD experiment.

MATERIALS AND METHODS

Preparation of Tetrasaccharides

Heparan sulfate tetrasaccharides ***1*** and ***2*** were prepared by partial enzymatic depolymerization of heparan sulfate sodium salt (Celsus Laboratories, Cincinnati, OH). Dermatan sulfate tetrasaccharide, ***3***, was prepared by partial enzymatic depolymerization of porcine intestinal mucosa dermatan sulfate (Celsus Laboratories, Cincinnati, OH). A 20 mg/mL heparan sulfate or dermatan sulfate solution in 50 mM Tris-HCl/60 mM sodium acetate buffer, pH 8 was incubated at 37°C with heparinase II (Sigma, St. Louis, MO) or chondroitin ABC lyase (Seikagaku, Japan), respectively. The absorbance at 232 nm was monitored to determine when the digestion was 50% completed. Each digestion mixture was then heated at 100°C for 3 min. High-molecular-weight oligosaccharides and the glycosidic enzyme were removed by ultra-filtration using a 5000 MWCO membrane. The resulting oligosaccharide mixtures were each concentrated by rotary evaporation and fractionated by low pressure GPC on a Bio-Gel P10 (Bio-Rad, Richmond, CA) column. Fractions containing tetrasaccharides ***1***, ***2***, ***3***, and ***4*** were desalted by GPC on a Bio-Gel P2 column and freeze-dried [39]. Further purification of the tetrasaccharides was carried out using strong anion exchange high-pressure liquid chromatography (SAX-HPLC) on a semi-preparative SAX S5 Spherisorb column (Waters Corp, Milford, MA). The SAX-HPLC fractions containing > 90% of the tetrasaccharides were collected, desalted by GPC, and freeze-dried. The solid was reconstituted in water and purified a second time by SAX-HPLC. Only the top 30% of the chromatographic peak was collected, desalted, and freeze-dried. Concentration of the tetrasaccharide solutions was determined by measuring the absorbance at 232 nm ($\varepsilon = 3800\ M^{-1}cm^{-1}$). The tetrasaccharides were characterized by PAGE, ESI-MS, and high-field nuclear magnetic resonance (NMR) spectroscopy. Tetrasaccharide ***5*** was prepared from tetrasaccharide ***2*** using the following protocol: tetrasaccharide ***2*** sodium salt was converted to a pyridinium salt using a Dowex 50W cation exchange column (Sigma, St. Louis, MO). 200 μg of the pyridinium salt of ***2*** was dissolved in 10 μL of dimethyl sulfoxide (Acros, Geel, Belgium) containing 5% methanol and incubated for 1.5h at 50 °C [40]. The desulfated product, ***5***, was then purified on a Bio-Rad P-2 spin column and freeze-dried. The product of the desulfation reaction differs in mass from the starting material, and can be easily isolated from each other for the EDD experiment. The desulfation reaction does not affect the stereochemistry of the hexuronic residue, and so the chirality of the product has the same purity as that of the reactants, which have been established to be pure by NMR analysis.

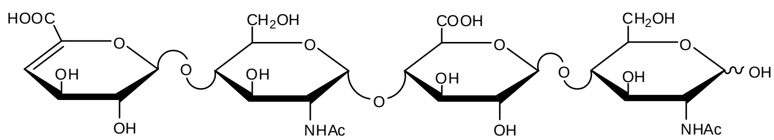

1

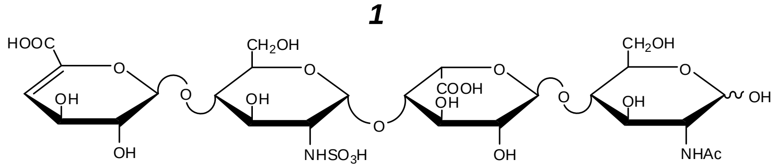

2

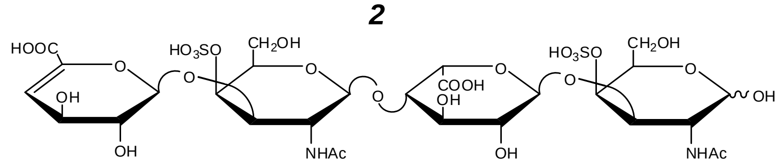

3

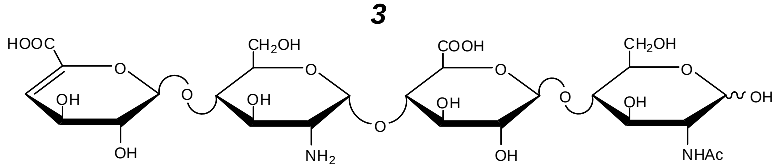

4

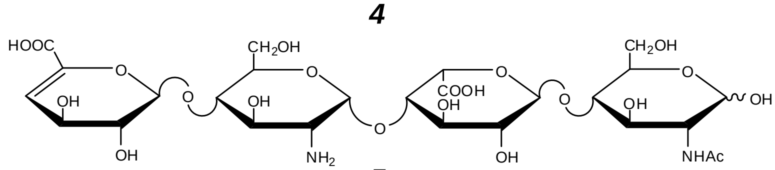

5

Mass Spectrometry Analysis

Experiments were performed with a 9.4 T Bruker Apex Ultra QhFTMS (Billerica, MA) fitted with an Apollo II dual source, a 25 W CO_2 laser (Synrad model J48-2, Mukilteo, WA) for

IRMPD, and an indirectly heated hollow cathode for generating electrons for EDD and EID. The tetrasaccharides were introduced at a concentration of 5 μM in 50:50:0.1 methanol:H_2O:formic acid (Sigma, St. Louis, MO) by ESI in negative ion mode. To produce abundant $[M-H]^-$ ions for ***3***, the tetrasaccharide was introduced at a concentration of 50 μM in 45:45:10 methanol:H_2O:formic acid. All sample solutions were infused at a rate of 120 μL/hour.

For the EID experiments, precursor ions were isolated in the external quadrupole and accumulated for 1 – 4 seconds before injection into the FTMS cell. The isolation/cell fill was repeated up to 6 times. The selection of the precursor ion was further refined by using in-cell isolation with a coherent harmonic excitation frequency (CHEF) event [41]. The precursor ions were then irradiated with electrons for 1 second. For electron irradiation the cathode bias was set to -19 V, the extraction lens was set to -18.5 V±0.5 V, and the cathode heater was set to 1.6 A. Precursor ions have been irradiated with electron energies varying from 12 – 25 eV, but no difference was observed other than changes in product ion intensity. Therefore, singly-charged GAG ions were irradiated with 19 eV electrons for comparison to previously published results. Ions were excited with an RF frequency chirp that covered the range of 100 – 2000 *m/z*. 24 acquisitions were signal averaged per mass spectrum. For each mass spectrum, 512K points were acquired at a 2.4 MHz digitization rate, padded with one zero fill, and apodized using a sinebell window. Background spectra were acquired by leaving all parameters the same but setting the cathode bias to 0 V to ensure that no electrons reached the analyzer cell. IRMPD spectra were acquired using the same experimental setup as EID, but replacing the electron irradiation event with a laser pulse. For IRMPD, ions were irradiated for 0.01 – 0.2 seconds with beam attenuation set to pass from 40 – 60% of full power. External calibration of IRMPD and EID mass spectra produced mass accuracy of 5 ppm. Internal calibration was also performed using confidently assigned glycosidic bond cleavage products as internal calibrants, providing mass accuracy of <1 ppm. Due to the larger number of low intensity products formed by EID, only peaks with S/N > 10 are reported. Product ions were assigned using accurate mass measurement. For the work presented here, fragmentation of the tetrasaccharides is presented using a modification of the Domon and Costello annotation [42] that presents GAG fragmentation with SO_3 loss and hydrogen rearrangement that is observed in EDD of GAGs [28].

RESULTS AND DISCUSSION

Irradiation of the $[M-H]^-$ precursor ion of ΔUA-GlcNAc-GlcA-GlcNAc, ***1***, with 19 eV electrons produces the EID mass spectrum shown in Figure 7.1A, while IRMPD of the same precursor ion produces the mass spectrum shown in Figure 7.1B. While the EID mass spectrum contains all the products found by IRMPD of ***1***, EID of ***1*** also results in many additional glycosidic and cross-ring cleavages, as shown in Figure 7.2A and 7.2B. The EDD mass spectrum of ***1*** has been published previously [27], and the products that result from irradiation of the $[M-2H]^{2-}$ precursor ion of ***1*** with 19 eV electrons (i.e. EDD of ***1***) are shown in Figure 7.2C. Interestingly, EID of the singly-charged precursor ion of ***1*** produces identical fragmentation products to those observed by EDD of the 2^- precursor, but differences in product ion intensity between EDD and EID are observed. Cleavage of all glycosidic bonds is observed, and cross-ring fragmentation occurs primarily on GlcA residues. However, a few more glycosidic cleavages (the isobaric C_2/Z_2 glycosidic cleavages) are observed in EID of ***1*** as they do not overlap in mass-to-charge with the precursor ion as they do for the doubly-charged precursor.

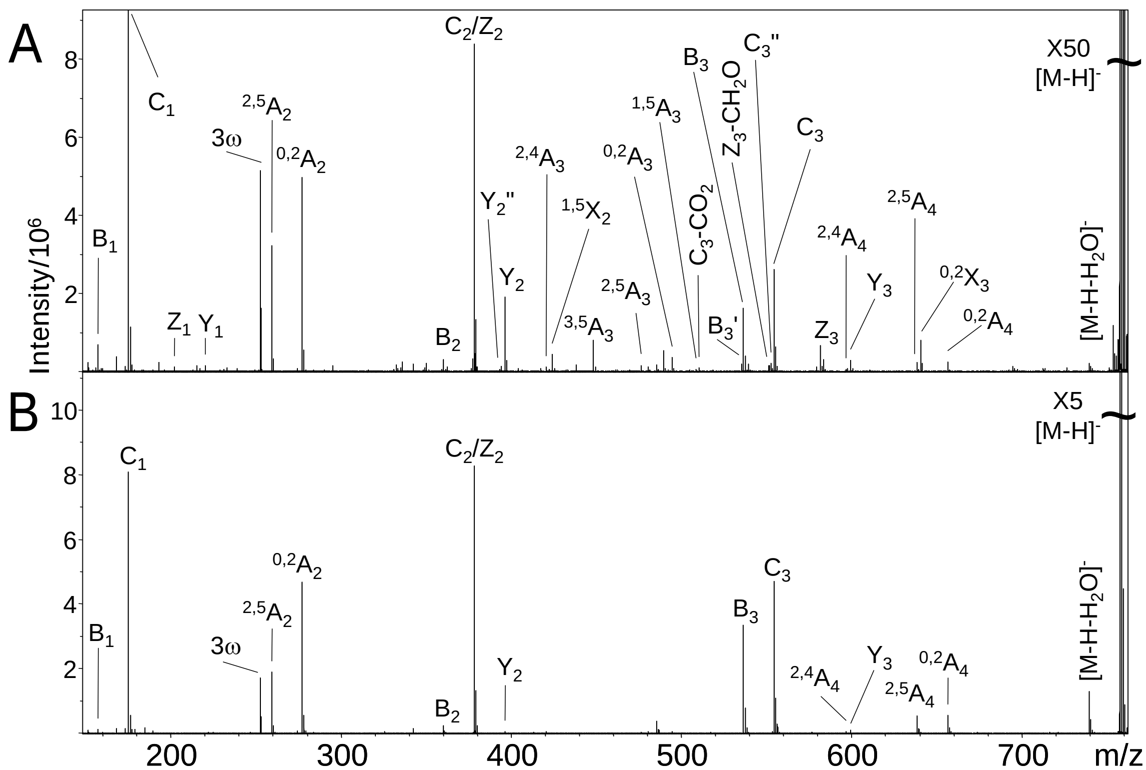

Figure 7.1. Tandem mass spectrum from the [M-H]$^-$ precursor ion of ***1*** obtained by (A) EID and (B) IRMPD.

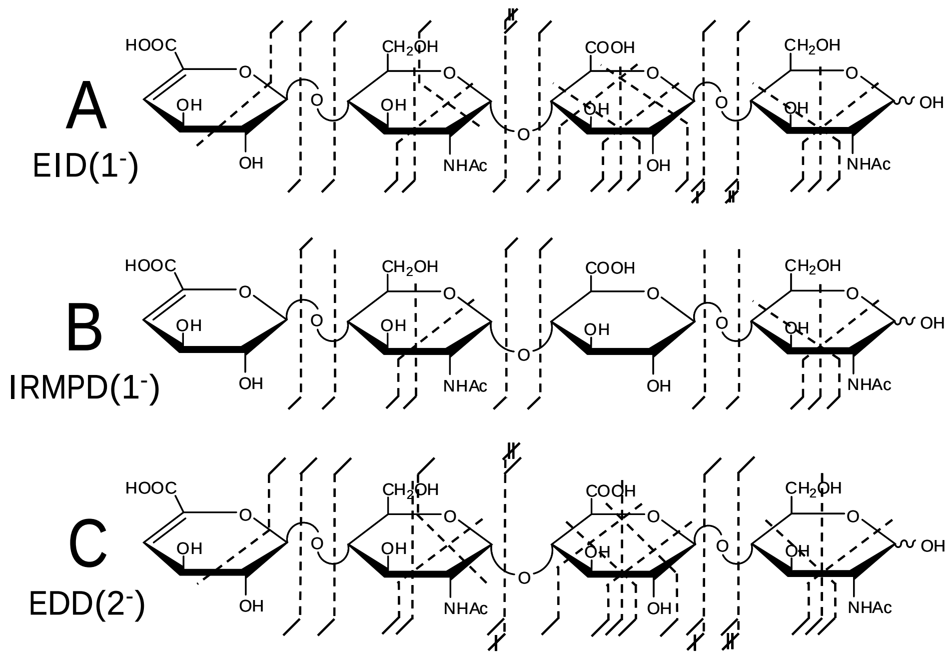

Figure 7.2. Products observed from (A) EID, (B) IRMPD, and (C) EDD of ***1***.

Cross-ring fragmentation in the amino sugar residues is found by IRMPD as well as by EID. In contrast, only EID leads to cross-ring fragmentation in the acidic residues. The preference for cross-ring fragmentation in GlcA/IdoA residues has been observed in EDD of GAG tetrasaccharides to decasaccharides [28]. It was proposed that the preference for fragmentation of the GlcA/IdoA residues results from radical formation via electron detachment from carboxylate functional groups on the GlcA/IdoA residues. However, recent studies of the effect of varying precursor ion charge state on the EDD mass spectrum showed preferential fragmentation of GlcA/IdoA residues regardless of the initial site of electron detachment, suggesting that the lability of GlcA/IdoA residues is due to electronic excitation rather than the presence of radical intermediate. In support of these observations, EID of ***1*** produces abundant cross-ring fragmentation of GlcA residues. Because these cross-ring cleavages are not observed by IRMPD (Figure 7.1B), it appears that cross-ring fragmentation of GlcA occurs only by electronic excitation of the even-electron precursor ion.

EID of ***1*** yields some product ions that have previously been observed only in EDD mass spectra. These product ions include both even- and odd-electron ions, such as those arising from glycosidic cleavages accompanied by the loss of 1 or 2 hydrogen atoms (e.g. B_3' and C_3''), and odd-electron cross-ring cleavages (e.g. $^{0,2}X_3$). Previously, we proposed that formation of these odd-electron products occurs through an odd-electron intermediate formed via electron detachment. This proposed fragmentation scheme was based on the assumption that odd-electron product ions can only form from an odd-electron precursor ion. However, the presence of singly-charged odd-electron products from EID, but not IRMPD, of ***1*** indicates that odd-electron products can also arise from electronic excitation of an even-electron precursor ion, albeit they are present at relatively low abundance. It is unusual for an even-electron precursor to yield an odd-electron product, and relatively few instances can be found in the literature [43, 44]. The EID of negatively-charged metabolite ions has recently been published, but odd-electron products were not reported [37].

EID of GAG Tetrasaccharides Containing Sulfate

Irradiation of the $[M-H]^-$ precursor ion of sulfate containing tetrasaccharide ΔUA-GlcNSO$_3$-IdoA-GlcNAc, ***2***, with 19 eV electrons produces the EID mass spectrum shown in Figure 7.3A, while IRMPD of the same precursor ion is shown in Figure 7.3B. The assignments of the product ions for both EID and IRMPD are shown in Figure 7.4A and 7.4B. The EDD mass spectra of ***2*** has been published previously [29], and products observed from EDD of the $[M-2H]^{2-}$ precursor ion of ***2*** are shown in Figure 7.4C. Irradiation of the $[M-H]^-$ precursor ion of the dermatan sulfate GAG, ΔUA-GalNAc-4-SO$_3$-IdoA-GalNAc-4-SO$_3$, ***3***, with 19 eV electrons produces the EID mass spectrum shown in Figure 7.5A, while IRMPD of the same precursor ion is shown in Figure 7.5B. Product ions for both EID and IRMPD are shown in Figure 7.6A and 7.6B. The EDD mass spectra of ***3*** has been published previously [28], and products observed from EDD of the $[M-2H]^{2-}$ precursor ion of ***3*** are shown in Figure 7.6C.

For ***2*** and ***3***, EID produces considerably more glycosidic and cross-ring fragmentation than IRMPD, as shown in Figures 7.4 and 7.6, respectively. Generally, EID produces similar fragmentation to EDD of the same molecules. However, a greater number of cross-ring cleavages are observed for EDD of these tetrasaccharides, and these are primarily found across hexuronic acid residues. The additional cross-ring fragmentation products that are not observed by either EID or IRMPD but are observed by EDD may arise as a result of electron detachment from the multiply-charged precursor ion. In support of the observations made on EID of ***1***,

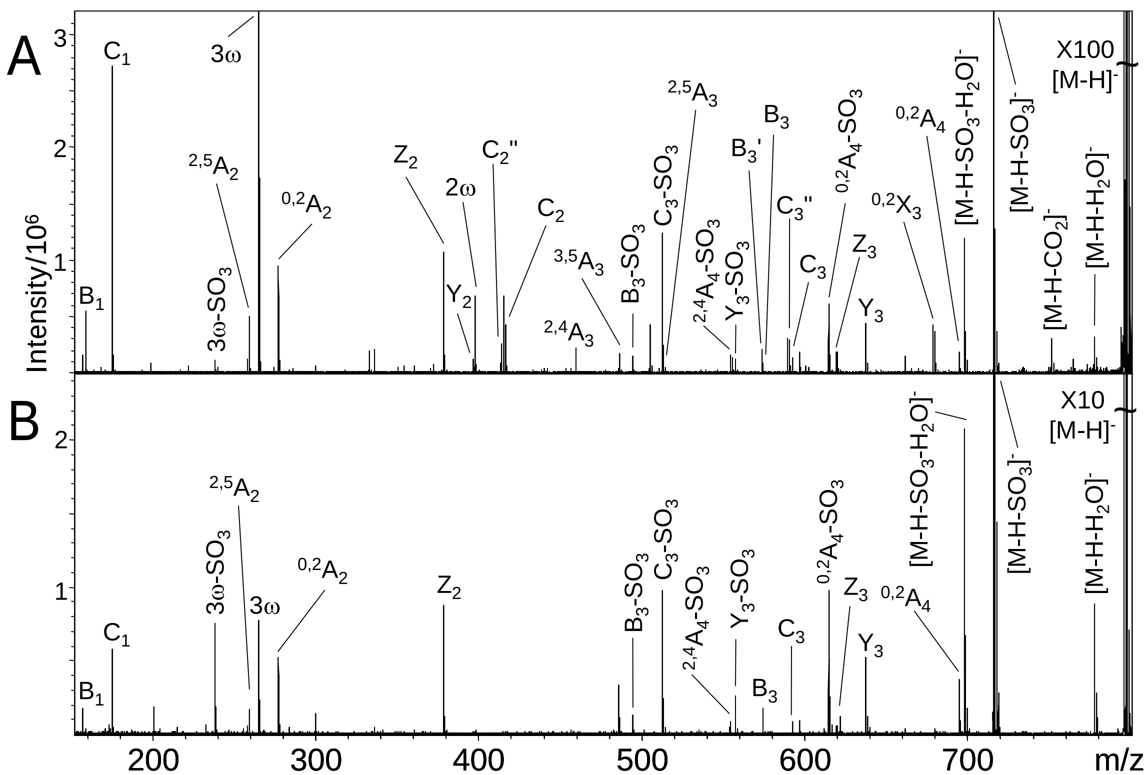

Figure 7.3. Tandem mass spectrum from the [M-H]$^-$ precursor ion of ***2*** obtained by (A) EID and (B) IRMPD

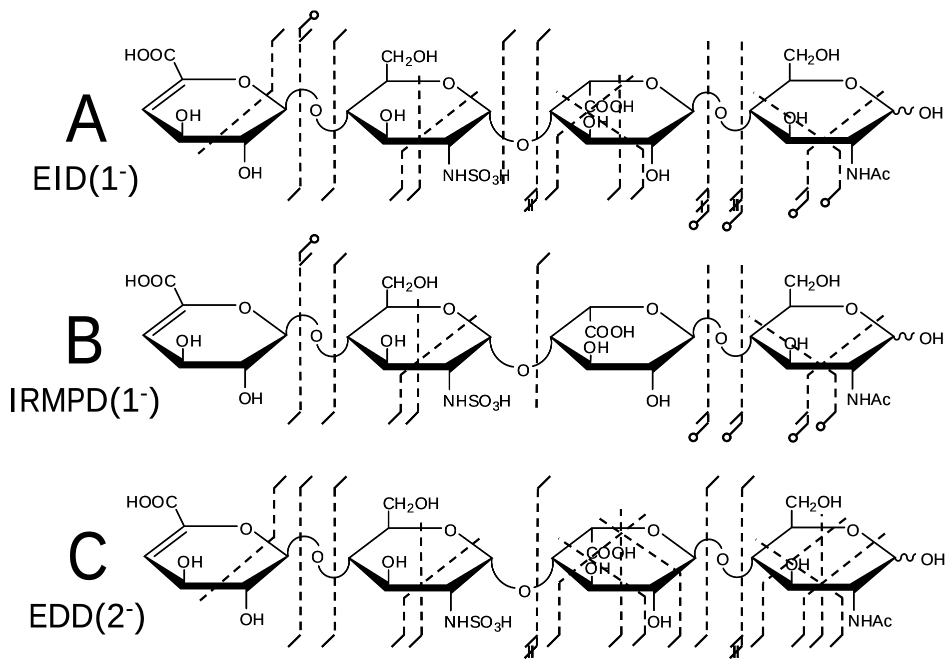

Figure 7.4. Products observed from (A) EID, (B) IRMPD, and (C) EDD of ***2***.

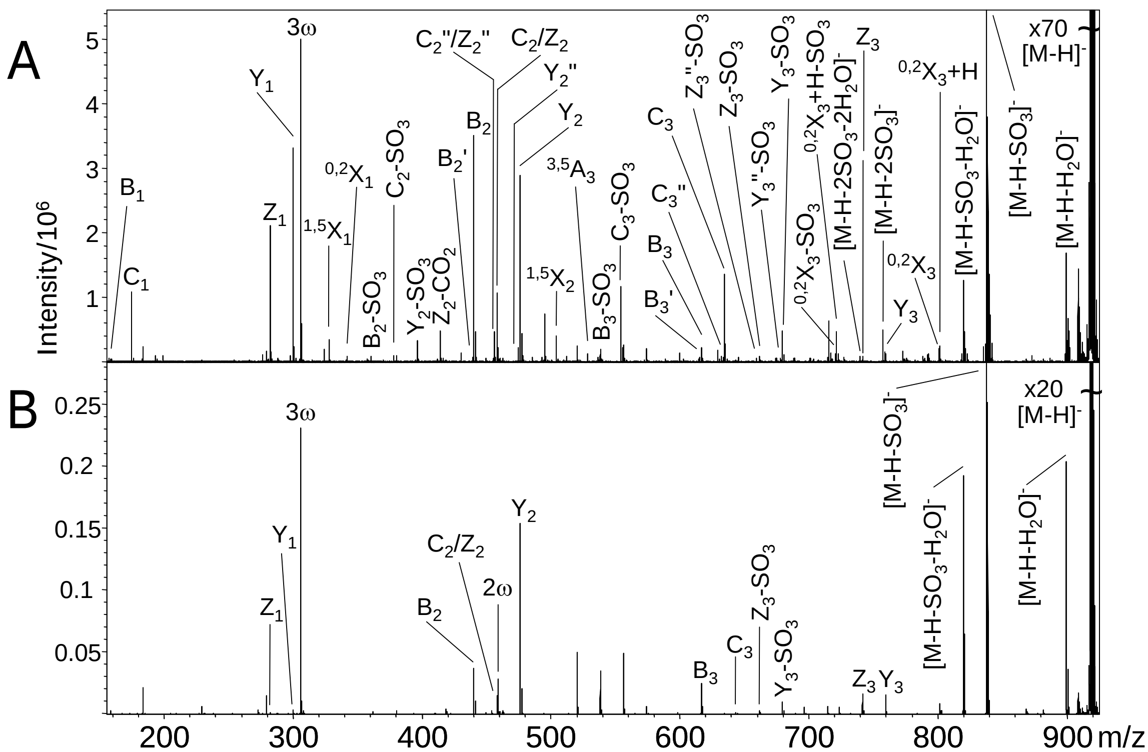

Figure 7.5. Tandem mass spectrum from the $[M-H]^-$ precursor ion of ***3*** obtained by (A) EID and (B) IRMPD.

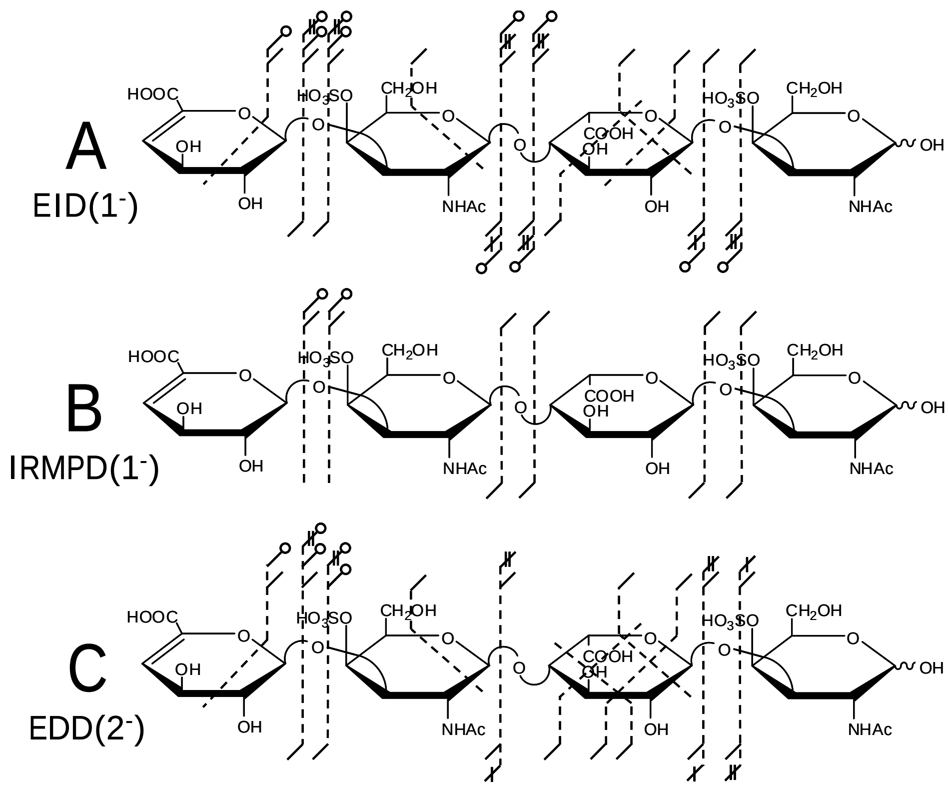

Figure 7.6. Products observed from (A) EID, (B) IRMPD, and (C) EDD of ***3***.

cross-ring cleavages occur primarily on hexuronic acid residues, indicating that these residues are most labile and readily undergo fragmentation as a result of electronic excitation. Similarly, the presence of odd-electron products, such as $^{0,2}X_3$, and glycosidic cleavages accompanied by the loss of 1 or 2 hydrogen atoms, such as B_3' and C_3'', are also observed in EID of ***2*** and ***3***. Cross-ring fragmentation of the reducing end residue is observed by EID of ***1*** and ***2***, but is not observed in EID of ***3***, suggesting that the 1→3 glycosidic inhibits this pathway of fragmentation. Similar results have been observed before for EDD of dermatan sulfate oligosaccharides [28], and for CAD of isobaric GAG oligosaccharides differing only in linkage position [45].

The presence of odd-electron product ions from EID suggests that different dissociation pathways are accessed by electronic activation of GAG precursor anions compared to slow-heating or low-energy ion activation. Generally speaking, odd-electron products are not produced from even-electron precursors. Their presence here raises questions about the mechanisms of dissociation. Perhaps electronic excitation produces a diradical that fragments to give a radical ion and a radical neutral. Another possibility is that electron capture produces an odd-electron doubly-charged ion which fragments to a singly-charged radical product ion. While electron capture by an anion seems energetically unfavorable, direct evidence of such a process has been recently reported [32]. In the measurements made for the current study, we find no direct evidence of electron capture, i.e. no doubly-charged ions were observed.

Because tetrasaccharides ***2*** and ***3*** contain sulfate groups, product ions may be accompanied by the loss of SO_3, which are annotated with an open circle at the end of the cleavage in Figures 7.4 and 7.6. Product ions accompanied by the loss of SO_3 are observed as pairs differing by the exact mass of SO_3, 79.957 *u*, aiding in their identification. We have previously observed a significant decrease in the number of products accompanied by SO_3 loss when the precursor ion charge is greater than the number of sulfate groups [31]. The reduction in SO_3 loss was proposed to result from electron detachment occurring at a carboxylate anion, versus electron detachment occurring as a sulfate anion which can then readily undergo radical driven loss of SO_3. For EID of ***2*** and ***3***, because products cannot result from electron detachment from the singly-charged precursor ions, SO_3 loss resulting from EID must occur via another route. There is significantly more SO_3 loss observed by EID than by EDD for compound ***3***, primarily accompanying glycosidic bond cleavage.

EID of GAG Epimers

We have previously reported the capability to distinguish GlcA from IdoA in GAG tetrasaccharides using EDD [29]. Product ions used to distinguish GlcA from IdoA ($^{0,2}A_3$, B_3', and B_3'-CO_2) were proposed to form via a radical intermediate, as a result of hydrogen atom transfer within the hexuronic acid to a carboxy radical. Because abundant cross-ring cleavages of the hexuronic acid residues are observed by EID, it is important to determine if product ions used to identify GlcA from IdoA resulted from EID versus the proposed radical mechanism. EID of ΔUA-GlcNAc-GlcA-GlcNAc, ***4***, was compared to EID of the epimer ΔUA-GlcNAc-IdoA-GlcNAc, ***5***, shown in Figure 7.7A and 7.7B, respectively. Products observed from EID of ***4*** and ***5*** are shown in the insets of Figure 7.7A and 7.7B, respectively. EDD mass spectra for ***4*** and ***5*** have been previously published [29]. Similar glycosidic and cross-ring fragmentation products are observed for EID of ***4*** and ***5***, as shown in the insets of Figures 7.7A and 7.7B. The product ions $^{0,2}A_3$ and B_3', used to distinguish GlcA from IdoA, are present in both EID mass spectra (Figures 7.7A and 7.7B) and thus do not distinguish GlcA from IdoA. Also, the B_3'-CO_2 peak is not observed in either EID mass spectrum (Figures 7.7A and 7.7B). These products are

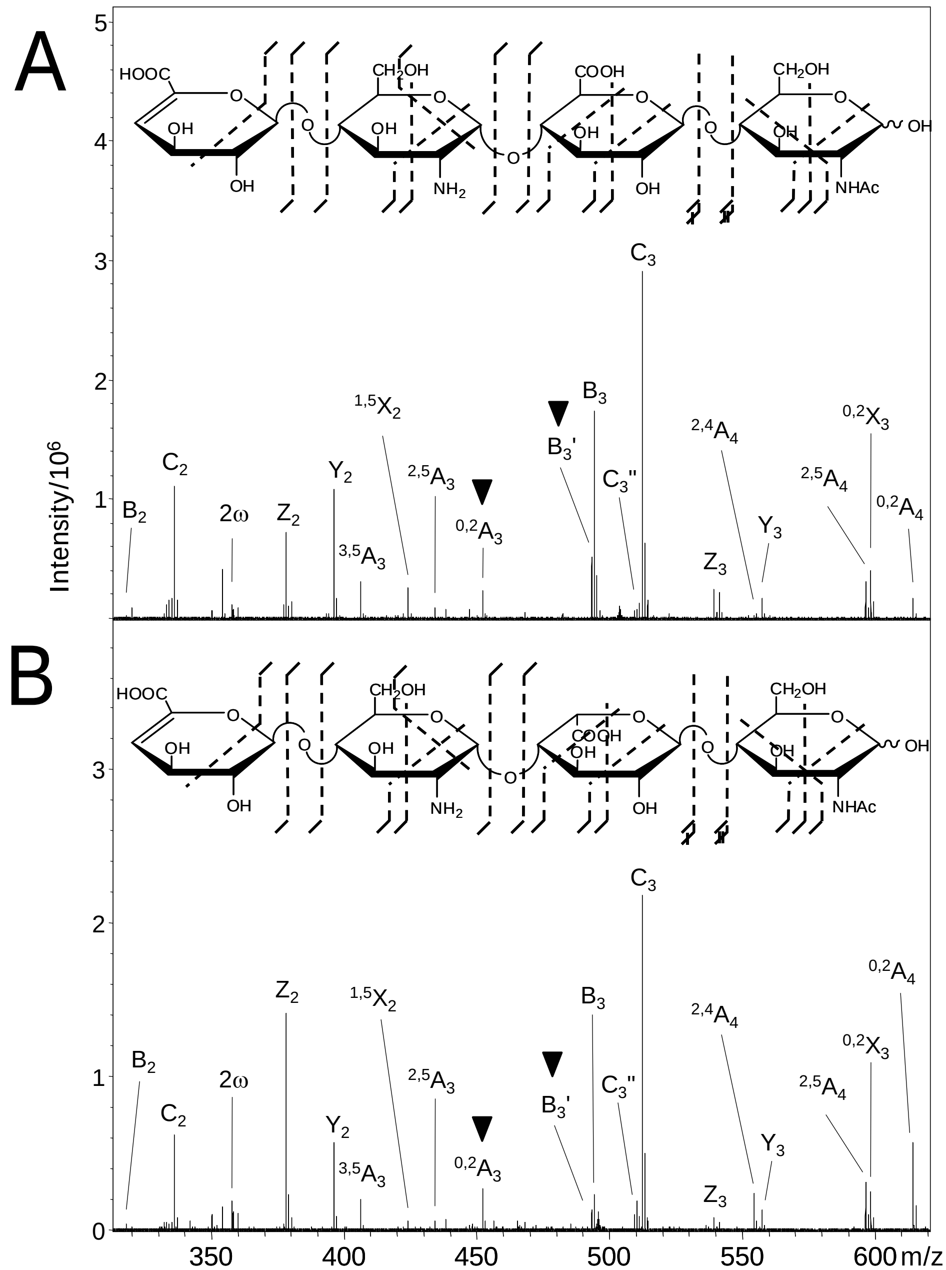

Figure 7.7. EID mass spectra of the epimer pair (A) ***4*** and (B) ***5***. The mass scale is expanded to show the region containing product ions that are used to distinguish GlcA from IdoA by EDD, indicated by the ▼ over the peak label. Insets: structures indicating product ions observed from EID of (A) ***4*** and (B) ***5***.

also not observed in IRMPD of ***4*** and ***5*** (data not shown). Clearly, the EID results are different than the results obtained by EDD of the 2^- precursor ion. This suggests that either the radical species proposed for EDD [29] plays a more significant role than EID in determining the products, or that the dissociation of doubly-charged ions differs from singly-charged precursors. However, no difference in glycosidic and cross-ring fragmentation is observed from IRMPD of the 1^- and 2^- precursor ion of ***4*** (data not shown), suggesting that charge state is not the primary influence in the differences between the observed product ions of EDD versus EID.

CONCLUSIONS

EID of singly-charged GAG tetrasaccharides has been used to identify products which arise from electronic excitation. These data provide insight into the origin of products in a EDD experiment. EID of singly-charged GAGs produces fragmentation products which have similarity to products observed by EDD of the same molecules. EID produces cross-ring fragmentation primarily on hexuronic acid residues, and both even- and odd-electron glycosidic and cross-ring products are observed. These features are not observed in IRMPD of the same precursor ions. These results suggest that fragmentation of the hexuronic acid residues by EDD and EID occurs because these residues are more labile under electronic excitation. Furthermore, these data show that for EDD, not all odd-electron products form via electronic detachment. However, EID mass spectra are similar for GlcA and IdoA residues in GAG epimers, in contrast to previously reported EDD results. These data suggest that a radical intermediate plays a significant role in the formation of the product ions that distinguish these epimers in EDD measurements.

REFERENCES

1. Fannon, M.; Forsten, K. E.; Nugent, M. A., Potentiation and Inhibition of bFGF Binding by Heparin: A Model for Regulation of Cellular Response. *Biochemistry* **2000,** *39*, 1434-1445.
2. Wu, Z. L.; Zhang, L.; Yabe, T.; Kuberan, B.; Beeler, D. L.; Love, A.; Rosenberg, R. D., The Involvement of Heparan Sulfate (HS) in FGF1/HS/FGFR1 Signaling Complex. *J. Biol. Chem.* **2003,** *278*, 17121-17129.
3. Sadir, R.; Imberty, A.; Baleux, F.; Lortat-Jacob, H., Heparan Sulfate/Heparin Oligosaccharides Protect Stromal Cell-derived Factor-1 (SDF-1)/CXCL12 against Proteolysis Induced by CD26/Dipeptidyl Peptidase IV. *J. Biol. Chem.* **2004,** *279*, 43854-43860.
4. Batinic, D.; Robey, F. A., The V3 region of the envelope glycoprotein of human immunodeficiency virus type 1 binds sulfated polysaccharides and CD4-derived synthetic peptides. *J. Biol. Chem.* **1992,** *267*, 6664-6671.
5. Chen, Y.; Maguire, T.; Hileman, R. E.; Fromm, J. R.; Esko, J. D.; Linhardt, R. J.; Marks, R. M., Dengue virus infectivity depends on envelope protein binding to target cell heparan sulfate. *Nature Med.* **1997,** *3*, 866-871.
6. Williams, R. K.; Straus, S. E., Specificity and affinity of binding of herpes simplex virus type 2 glycoprotein B to glycosaminoglycans. *J. Virol.* **1997,** *71*, 1375-1380.
7. Perrimon, N.; Bernfield, M., Cellular functions of proteoglycans--an overview. *Semin. Cell Dev. Biol.* **2001,** *12*, 65-67.
8. Horne, A.; Gettins, P., H-1-NMR Spectral Assignments for 2 Series of Heparin-Derived Oligosaccharides. *Carbohydr. Res.* **1992,** *225*, 43-57.

9. Adamson, J. T.; Hakansson, K., Electron Detachment Dissociation of Neutral and Sialylated Oligosaccharides. *J. Am. Soc. Mass Spectrom.* **2007,** *18*, 2162-2172.

10. Chi, L. L.; Amster, J.; Linhardt, R. J., Mass spectrometry for the analysis of highly charged sulfated carbohydrates. *Curr. Anal. Chem.* **2005,** *1*, 223-240.

11. Dai, Y.; Whittal, R. M.; Bridges, C. A.; Isogai, Y.; Hindsgaul, O.; Li, L., Matrix-assisted laser desorption ionization mass spectrometry for the analysis of monosulfated oligosaccharides. *Carbohydr. Res.* **1997,** *304*, 1-9.

12. Miller, M. J. C.; Costello, C. E.; Malmstrom, A.; Zaia, J., A tandem mass spectrometric approach to determination of chondroitin/dermatan sulfate oligosaccharide glycoforms. *Glycobiology* **2006,** *16*, 502-513.

13. Reinhold, V. N.; Carr, S. A.; Green, B. N.; Petitou, M.; Choay, J.; Sinay, P., Structural Characterization of Sulfated Glycosaminoglycans by Fast-Atom-Bombardment Mass-Spectrometry - Application to Heparin Fragments Prepared by Chemical Synthesis. *Carbohydr. Res.* **1987,** *161*, 305-313.

14. Saad, O. M.; Leary, J. A., Compositional Analysis and Quantification of Heparin and Heparan Sulfate by Electrospray Ionization Ion Trap Mass Spectrometry. *Anal. Chem.* **2003,** *75*, 2985-2995.

15. Saad, O. M.; Leary, J. A., Heparin Sequencing Using Enzymatic Digestion and ESI-MS with HOST: A Heparin/HS Oligosaccharide Sequencing Tool. *Anal. Chem.* **2005,** *77*, 5902-5911.

16. Zaia, J.; Li, X.-Q.; Chan, S.-Y.; Costello, C. E., Tandem mass spectrometric strategies for determination of sulfation positions and uronic acid epimerization in chondroitin sulfate oligosaccharides. *J. Am. Soc. Mass Spectrom.* **2003,** *14*, 1270-1281.

17. Zaia, J.; McClellan, J. E.; Costello, C. E., Tandem Mass Spectrometric Determination of the 4S/6S Sulfation Sequence in Chondroitin Sulfate Oligosaccharides. *Anal. Chem.* **2001,** *73*, 6030-6039.

18. Zubarev, R. A.; Kelleher, N. L.; McLafferty, F. W., Electron Capture Dissociation of Multiply Charged Protein Cations. A Nonergodic Process. *J. Am. Chem. Soc.* **1998,** *120*, 3265-3266.

19. Hakansson, K.; Cooper, H. J.; Emmett, M. R.; Costello, C. E.; Marshall, A. G.; Nilsson, C. L., Electron Capture Dissociation and Infrared Multiphoton Dissociation MS/MS of an N-Glycosylated Tryptic Peptide To Yield Complementary Sequence Information. *Anal. Chem.* **2001,** *73*, 4530-4536.

20. Kelleher, N. L.; Zubarev, R. A.; Bush, K.; Furie, B.; Furie, B. C.; McLafferty, F. W.; Walsh, C. T., Localization of Labile Posttranslational Modifications by Electron Capture Dissociation: The Case of γ-Carboxyglutamic Acid. *Anal. Chem.* **1999,** *71*, 4250-4253.

21. Mirgorodskaya, E.; Roepstorff, P.; Zubarev, R. A., Localization of O-glycosylation sites in peptides by electron capture dissociation in a fourier transform mass spectrometer. *Anal. Chem.* **1999,** *71*, 4431-4436.

22. Niiranen, H.; Budnik, B. A.; Zubarev, R. A.; Auriola, S.; Lapinjoki, S., High-performance liquid chromatography-mass spectrometry and electron-capture dissociation tandem mass spectrometry of osteocalcin - Determination of gamma-carboxyglutamic acid residues. *Journal of Chromatography A* **2002,** *962*, 95-103.

23. Shi, S. D. H.; Hemling, M. E.; Carr, S. A.; Horn, D. M.; Lindh, I.; McLafferty, F. W., Phosphopeptide/phosphoprotein mapping by electron capture dissociation mass spectrometry. *Anal. Chem.* **2001,** *73*, 19-22.

24. Stensballe, A.; Jensen, O. N.; Olsen, J. V.; Haselmann, K. F.; Zubarev, R. A., Electron capture dissociation of singly and multiply phosphorylated peptides. *Rapid Commun. Mass Spectrom.* **2000,** *14*, 1793-1800.

25. Budnik, B. A.; Haselmann, K. F.; Zubarev, R. A., Electron detachment dissociation of peptide di-anions: an electron-hole recombination phenomenon. *Chem. Phys. Lett.* **2001,** *342*, 299-302.

26. Zubarev, R. A., Reactions of polypeptide ions with electrons in the gas phase. *Mass Spectrom. Rev.* **2003,** *22*, 57.

27. Wolff, J. J.; Amster, I. J.; Chi, L.; Linhardt, R. J., Electron Detachment Dissociation of Glycosaminoglycan Tetrasaccharides. *J. Am. Soc. Mass Spectrom.* **2007,** *18*, 234-244.

28. Wolff, J. J.; Laremore, T. N.; Busch, A. M.; Linhardt, R. J.; Amster, I. J., Electron Detachment Dissociation of Dermatan Sulfate Oligosaccharides. *J. Am. Soc. Mass Spectrom.* **2008,** *19*, 294-304.

29. Wolff, J. J.; Chi, L. L.; Linhardt, R. J.; Amster, I. J., Distinguishing glucuronic from iduronic acid in glycosaminoglycan tetrasaccharides by using electron detachment dissociation. *Anal. Chem.* **2007,** *79*, 2015-2022.

30. Leach III, F. E.; Wolff, J. J.; Laremore, T. N.; Linhardt, R. J.; Amster, I. J., Evaluation of the Experimental Parameters Which Control Electron Detachment Dissociation, and Their Effect on the Fragmetnation Efficiency of Glycosaminoglycan Carbohydrates. *International Journal of Mass Spectrometry* **2008,** *Submitted*.

31. Wolff, J. J.; Laremore, T. N.; Linhardt, R. J.; Amster, I. J., Influence of Charge State and Sodium Occupation on the Electron Detachment Dissociation and Infrared Multiphoton Dissociation of Glycosaminoglycans Oligosaccharides. *J. Am. Soc. Mass Spectrom.* **2008,** *in press*.

32. Cheng, Z.; Xie, B.; Cournoyer, J. J.; Chan, S.-Y.; Zaia, J.; Costello, C. E.; O'Connor, P. B. Electron Capture Dissociation, Electron Detachment Dissociation and Collisionally Activated Dissociation Provide Complementary Structural Information Oligosaccharides, *55th ASMS Conference*, June 3 - 7, **2007**; Indianapolis, IN.

33. Cody, R. B.; Freiser, B. S., Electron impact excitation of ions from organics: an alternative to collision induced dissociation. *Anal. Chem.* **1979,** *51*, 547-551.

34. Cody, R. B.; Freiser, B. S., Electron impact excitation of ions in Fourier transform mass spectrometry. *Anal. Chem.* **1987,** *59*, 1054-1056.

35. Budnik, B. A.; Haselmann, K. F.; Elkin, Y. N.; Gorbach, V. I.; Zubarev, R. A., Applications of Electron-Ion Dissociation Reactions for Analysis of Polycationic Chitooligosaccharides in Fourier Transform Mass Spectrometry. *Anal. Chem.* **2003,** *75*, 5994-6001.

36. Wang, B.-H.; McLafferty, F. W., Electron impact excitation of ions from larger organic molecules. *Org. Mass Spectrom.* **1990,** *25*, 554-556.

37. Yoo, H. J.; Liu, H.; Hakansson, K., Infrared Multiphoton Dissociation and Electron-Induced Dissociation as Alternative MS/MS Strategies for Metabolite Identification. *Anal. Chem.* **2007,** *79*, 7858-7866.

38. Lioe, H.; O'Hair, R., Comparison of collision-induced dissociation and electron-induced dissociation of singly protonated aromatic amino acids, cystine and related simple

peptides using a hybrid linear ion trap–FT-ICR mass spectrometer. *Analytical and Bioanalytical Chemistry* **2007,** *389*, 1429-1437.

39. Pervin, A.; Gallo, C.; Jandik, K. A.; Han, X.-J.; Linhardt, R. J., Preparation and structural characterization of large heparin-derived oligosaccharides. *Glycobiology* **1995,** *5*, 83-95.

40. Inoue, Y.; Nagasawa, K., Selective N-desulfation of heparin with dimethyl sulfoxide containing water or methanol. *Carbohydr. Res.* **1976,** *46*, 87-95.

41. Heck, A. J. R.; de Koning, L. J.; Pinkse, F. A.; Nibbering, N. M. M., Mass-specific selection of ions in Fourier-transform ion cyclotron resonance mass spectrometry. Unintentional off-resonance cyclotron excitation of selected ions. *Rapid Commun. Mass Spectrom.* **1991,** *5*, 406-414.

42. Domon, B.; Costello, C. E., A systematic nomenclature for carbohydrate fragmentations in FAB-MS/MS spectra of glycoconjugates. *Glycoconjugate J.* **1988,** *5*, 397-409.

43. Attygalle, A. B.; Ruzicka, J.; Varughese, D.; Bialecki, J. B.; Jafri, S., Low-energy collision-induced fragmentation of negative ions derived from *ortho*-, *meta*-, and *para*-hydroxyphenyl carbaldehydes, ketones, and related compounds. *J. Mass Spectrom.* **2007,** *42*, 1207-1217.

44. Williams, J. P.; Nibbering, N. M. M.; Green, B. N.; Patel, V. J.; Scrivens, J. H., Collision-induced fragmentation pathways including odd-electron ion formation from desorption electrospray ionisation generated protonated and deprotonated drugs derived from tandem accurate mass spectrometry. *J. Mass Spectrom.* **2006,** *41*, 1277-1286.

45. Zhang, Z.; Xie, J.; Liu, J.; Linhardt, R. J., Tandem MS Can Distinguish Hyaluronic Acid from N-Acetylheparosan. *J. Am. Soc. Mass Spectrom.* **2008,** *19*, 82-90.

CONCLUSIONS

Irradiation of multiply-charged GAGs with 19 eV electrons produces more abundant fragmentation compared to ion activation methods that lead to vibrational excitation of the same precursor ions, namely infrared multiphoton dissociation (IRMPD) and low energy collisionally activated decomposition (CAD). Fragmentation by electron detachment dissociation (EDD) is proposed to occur through the formation of an excited species which can eject an electron to produce a radical species. Alternatively, the excited species can undergo direct decomposition. Products that form via electronic excitation (e.g. EID) and by electron detachment (e.g. EDD) are different than the products vibrational of excitation of GAGs, and can be used to determine the sites of GAG modification from a single tandem mass spectrometry experiment. EDD of sulfated GAGs produces a number of characteristic features. First, more abundant glycosidic and cross-ring fragmentation occurs compared to vibrational excitation of the same precursor ions. This fragmentation can also be used to distinguish GlcA from IdoA in GAG tetrasaccharides. Second, even-electron products both with the same charge and with less charge than the precursor ion are observed, as well as odd-electron products of lower charge than the precursor ion. Fourth, although some bond cleavages are observed with and without SO_3 loss, the cleavages are never are observed to occur only with SO_3 loss, and no more than one equivalent of SO_3 is lost. Thus, SO_3 loss produces pairs of peaks that differ in mass by 79.957 *u*. Finally, EID studies of singly-charged GAGs demonstrates that many of the product ions observed in the EDD mass spectra of sulfated GAGs, including odd-electron products, arise from direct fragmentation of the precursor ion.

EDD effectively dissociates sulfated GAGs ranging in size from tetrasaccharides to decasaccharides. This work also demonstrates that the cross-ring fragmentation products can be used to determine the stereochemistry of C5 in hexuronic acid residues in heparan sulfate tetrasaccharides based on the presence of key product ions. These product ions, $^{0,2}A_3$, B_3', and B_3'-CO_2, are present from EDD of GlcA but not IdoA. Because these key product ions are observed in EID of the tetrasaccharide epimers, the ability to distinguish GlcA from IdoA is proposed to occur from the formation of a radical species which fragments differently than electronically or vibrationally excited ions. One challenging aspect of EDD of GAGs is the presence of product ions accompanied by the loss of SO_3. However, the work presented here demonstrates that SO_3 loss can be minimized by selecting the correct charge state of the precursor ion. Multiply-charged GAG precursor ions may contain either carboxylate or sulfate anions. If no carboxylate anion is present, electron detachment will occur from a sulfate anion, creating a radical species which readily undergoes loss of SO_3. In contrast, if a carboxylate anion is present, electron detachment will produce a carboxy radical which does not undergo loss of SO_3. Ionization of the carboxylate group can be achieved through selection of a higher charge state or the precursor, or by the replacement of protons by sodium cations.

Because the initial site of electron detachment can be controlled through charge state selection, the residue containing the radical can be predicted in many cases. However, preferential cross-ring fragmentation of hexuronic acid residues occurs regardless of the initial site of electron detachment, suggesting that hexuronic acid residues are more labile under conditions of electronic excitation and readily undergo fragmentation. In support of this observation, EID of GAG tetrasaccharides results in preferential fragmentation of hexuronic acid residues which is not observed in IRMPD of the same molecules. EID of GAG tetrasaccharides also produces glycosidic and cross-ring odd-electron product ions that have previously only been observed in EDD mass spectra. This suggests that these product ions can be formed through electronic excitation as well as electron detachment. However, EID cannot distinguish GlcA from IdoA, suggesting that fragmentation via electron detachment plays a significant role in formation of product ions used to distinguish GlcA from IdoA. Historically, the structural analysis of sulfated GAGs by tandem mass spectrometry has been challenging. The work presented here demonstrates that EDD is a powerful tool for the structural characterization of sulfated GAGs.

APPENDICES

APPENDIX A

SUPPLEMENTAL DATA FOR CHAPTER 4

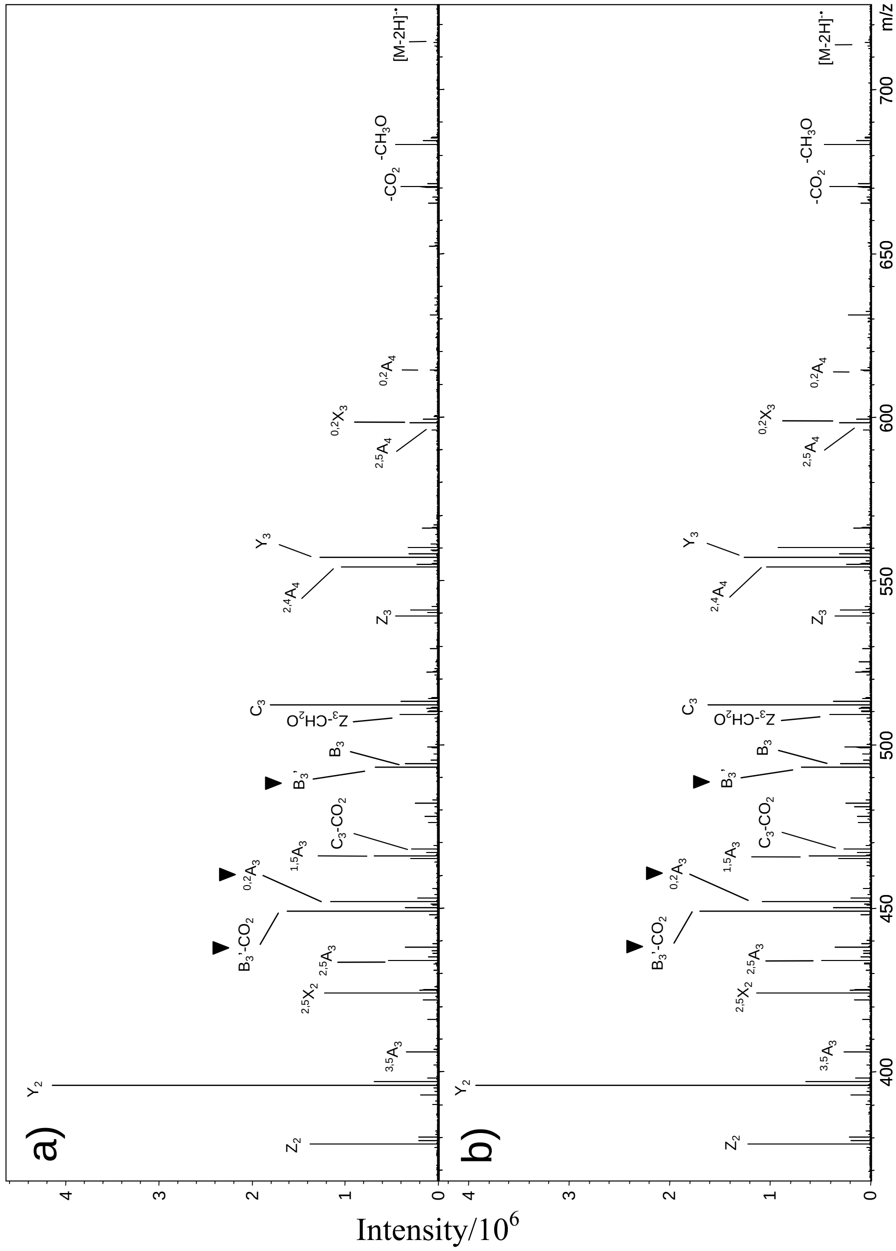

Figure. EDD mass spectra of the $[M-2H]^{2-}$ precursor ion of tetrasaccharide ***3*** at two different times to demonstrate reproducibility of EDD fragmentation. (a) EDD of tetrasaccharide ***3*** on 3.20.06. (b) EDD of tetrasaccharide ***3*** on 8.1.06. Fragmentation is identical and all diagnostic product ions are observed at similar intensities. The ▼above the peak labels indicates product ions unique the GlcA containing HS tetrasaccharide, ***3***.

Table. Peak list of product ions observed from EDD of ***1*** and ***2***, including relative intensity (RI) of peaks and ID of peaks.

Tetrasaccharide 1		Tetrasaccharide 2		
m/z	RI	m/z	RI	**ID**
157.0142	0.112716	157.0143	0.067786	B_1
173.009	0.097941	173.0091	0.035066	
175.0248	0.322369	175.0248	0.19351	C_1
202.0722	0.021727	202.072	0.011405	Z_1
202.9892	0.036285	202.9893	0.036676	
210.9916	0.020361	210.9917	0.016768	
211.9867	0.047084	211.9995	0.016947	
220.0825	0.042944	220.0825	0.02381	Y_1
222.0076	0.165805	222.0076	0.065311	
240.0181	0.064112	240.0183	0.049768	
258.0287	0.08546	258.0289	0.087397	
259.046	0.083033	259.0458	0.016507	${}^{2,5}A_2$
272.0533	0.017359	272.0536	0.016875	
273.0616	0.049677	273.0614	0.038031	
277.0563	0.020017	277.0563	0.029097	${}^{0,2}A_2$
286.0282	0.12203	286.0236	0.035332	
286.0362	0.114487	286.0362	0.087895	
286.5324	0.1132	286.5321	0.019578	B_3^{2-}
294.5297	0.021432	294.5298	0.06232	$C_3\text{-}2H^{2-}$
295.5375	1.682314	295.5375	0.489193	C_3^{2-}
296.5343	0.108313	296.5345	0.037169	
316.5428	0.052768	316.5427	0.069672	${}^{2,4}A_4^{2-}$
332.0618	0.04182	332.0623	0.04146	
333.0697	0.466127	333.0699	0.415616	
333.1062	0.110742	333.1062	0.146384	
337.548	0.571004	337.548	0.284969	${}^{2,5}A_4^{2-}$
346.5535	0.473739	346.5536	0.400564	${}^{0,2}A_4^{2-}$
369.037	0.03023	369.037	0.023211	
370.0454	0.218213	370.0455	0.108467	
372.0605	0.115679	372.0605	0.133251	
376.0882	0.347461	376.0884	0.042075	
377.0959	0.859294	377.0969	0.128271	$Z_2\text{-}H$
378.0994	0.132182	378.1044	0.046084	Z_2
382.5763	0.116335	382.5756	0.015266	
383.0789	0.074438	383.0795	0.027275	
388.0718	0.124535	388.0711	0.076885	
388.5768	0.259511	388.5771	0.078436	
389.0714	0.193642	389.0753	0.119948	$[M\text{-}2H\text{-}H_2O]^{2-}$

397.076	119.0124	397.0761	49.67004	precursor ion^{2-}
413.0265	0.035083	413.0267	0.035649	
414.0346	0.319661	414.0347	0.25647	
415.0423	0.866599	415.0424	1.10527	C_2-H
415.0785	0.671537	415.0788	0.857938	
416.0508	1	416.0507	1	C_2
440.0508	0.213258	440.0509	0.017395	
442.0659	0.168046	442.0662	0.027032	$^{3,5}A_3$-CO_2
459.0684	1.474862	459.0687	0.426186	$^{2,4}A_3$
470.0609	0.034169	470.0612	0.022625	
486.0558	0.605093	486.0562	0.089661	$^{3,5}A_3$
496.0403	0.065192			
504.0661	0.044209	504.0663	0.008438	
505.0737	0.105901	505.0744	0.195637	
506.0798	0.111196			
510.1097	0.022053	510.1089	0.036161	
512.1265	0.019443	512.1265	0.012311	
514.0505	0.212771	514.0494	0.011424	$^{2,4}A_3$
527.0596	0.01794			
528.0665	0.034526	528.0677	0.015911	
529.0743	0.099136			B_3'-CO_2
532.0609	0.051666			$^{0,2}A_3$
		544.0631	0.026706	
546.0775	0.140355	546.0767	0.224703	$^{1,5}A_3$
548.0926	0.0189	548.0958	0.014196	C_3-CO_2
		554.1358	0.01818	
555.0542	0.022023			
571.1051	0.004772	571.1086	0.011917	
572.0561	0.027979	572.057	0.013618	
573.065	0.1553	573.0643	0.011704	B_3'
574.0712	0.116286	574.0721	0.088508	B_3
589.1184	0.084124	589.1198	0.045367	Z_3-CH_2O
590.0673	0.118777	590.0671	0.357035	C_3''
592.0827	0.176393	592.0828	0.119569	C_3
600.1117	0.040436	600.1117	0.077216	
619.1298	0.298629	619.1297	0.191542	Z_3
634.0936	0.026323	634.0928	0.044409	$^{2,4}A_4$
637.1413	0.035836	637.1397	0.061999	Y_3
646.0941	0.017687	646.0941	0.057862	$^{3,5}A_4$
		668.1925	0.047264	
678.1436	0.032454	678.1446	0.02704	$^{0,2}X_3$
694.1144	0.063871	694.1135	0.040289	$^{0,2}A_4$
749.1584	0.020902	749.1572	0.038651	$[M-2H-CHO_2]^{-\bullet}$
750.1646	0.084904	750.1627	0.033485	$[M-2H-CO_2]^{-\bullet}$
794.153	0.01702	794.1541	0.015973	$[M-2H]^{-\bullet}$

Table. Peak list of product ions observed from EDD of ***3*** and ***4***, including relative intensity (RI) of peaks and ID of peaks.

Tetrasaccharide 3		Tetrasaccharide 4		
m/z	I	m/z	I	**ID**
157.0129	0.186454	157.013	0.196726	B_1
175.0233	1.530121	175.0233	1.084135	C_1
202.0703	0.016441	202.0704	0.030469	Z_1
220.0804	0.045258	220.0804	0.043652	Y_1
255.5566	0.741483	255.5565	0.192901	C_3^{2-}
259.0432	0.091871	259.043	0.13015	$^{2,5}A_2$
276.5615	0.05698	276.5614	0.271499	$^{2,4}A_4^{2-}$
277.0536	0.26103	277.0531	0.325279	$^{0,2}A_2$
297.5666	0.293569	297.5663	0.435	$^{2,4}A_4^{2-}$
306.5717	0.263051	306.5715	0.616931	$^{0,2}A_4^{2-}$
		307.5172	0.572409	
318.0803	0.037498	318.0785	0.032269	B_2
		327.576	0.108505	
		328.0296	0.166245	
333.1026	0.165318	333.1022	0.144204	
334.0748	0.050872			
334.1104	0.282425	334.11	0.259808	
336.0898	0.519693	336.0891	0.371991	C_2
342.5938	0.104351			
348.0897	4.206264			$[M\text{-}2H\text{-}H_2O]^{2-}$
		349.0348	0.891572	
357.0944	56.56165	357.0937	61.28651	precursor ion^{2-}
378.0996	0.339766	378.0988	0.777172	Z_2
380.1158	0.053156	380.1145	0.052732	
396.1097	1	396.1088	1	Y_2
406.0942	0.082536	406.0933	0.074242	$^{3,5}A_3$
		416.0441	0.228481	
422.125	0.038511			
424.1044	0.292544	424.1033	0.112623	$^{1,5}X_2$
434.0883	0.128579	434.0563	0.038016	$^{2,5}A_3$
434.1481	0.08973	434.147	0.064724	
438.12	0.084592			
449.1113	0.39374			$B_3'\text{-}CO_2$
452.0985	0.277125			$^{0,2}A_3$
		458.0527	0.34884	
465.1056	0.074956			
466.1142	0.164485	466.1123	0.152779	$^{1,5}A_3$
468.1296	0.072664	468.1284	0.036573	$C_3\text{-}CO_2$
476.1587	0.028059	476.0629	0.133457	
478.174	0.035609			
482.1448	0.059947			
493.1016	0.176727			B_3'
494.1078	0.087772	494.1068	0.217245	B_3

499.1225	0.028704			
509.155	0.098856	509.153	0.089634	Z_3-CH_2O
510.1028	0.027485	510.1003	0.103916	C_3''
512.1185	0.433624	512.1162	0.403658	C_3
522.1621	0.031508			
		536.0802	0.065892	
539.165	0.114891	539.1649	0.044245	Z_3
541.1807	0.075062	541.1777	0.089119	
554.1283	0.248965	554.1251	0.212519	$^{2,4}A_4$
557.1755	0.306407	557.1725	0.142909	Y3
560.1751	0.078029			
566.1294	0.042324			
596.137	0.019679	596.1358	0.051822	$^{2,5}A_4$
598.1778	0.078654	598.1743	0.314978	$^{0,2}X_3$
614.15	0.021088	614.1444	0.123784	$^{0,2}A_4$
652.1886	0.023747			
665.1599	0.025538			
670.1965	0.095483	670.1927	0.078937	$[M-2H-CO_2]^{-\bullet}$
683.1676	0.111147	683.1668	0.082506	$[M-2H-CH_3O]^{-\bullet}$
714.1835	0.014958	714.179	0.034296	$[M-2H]^{-\bullet}$

APPENDIX B

SUPPLEMENTAL DATA FOR CHAPTER 5

Table. List of observed product ions with corresponding S/N and assignment from IRMPD and EDD DS dp4 (***1***). N.O. = not observed, N.A. = not assigned.

IRMPD		EDD		
m/z	S/N	m/z	S/N	Assignment
157.0142	335	157.0142	19.2	B_1
175.0248	1504	175.0246	115.8	C_1
185.437	756.2	N.O.		N.A.
189.1933	187.6	N.O.		N.A.
193.0354	322.9	193.0352	39.7	N.A.
N.O.		194.9273	79.1	N.A.
N.O.		198.9917	39.7	N.A.
199.9952	88.7	N.O.		N.A.
202.0721	65.9	N.O.		N.A.
205.3711	68.1	N.O.		N.A.
210.3431	155.4	N.O.		N.A.
222.0078	55.3	N.O.		N.A.
N.O.		236.0232	14.7	N.A.
N.O.		237.0312	20.9	N.A.
N.O.		238.0394	13.5	N.A.
N.O.		240.0743	19.8	N.A.
N.O.		254.0338	28.9	N.A.
264.0184	52.8	N.O.		N.A.
N.O.		266.0339	33.2	N.A.
N.O.		266.7317	21	N.A.
N.O.		272.992	47.4	N.A.
N.O.		280.0131	37.5	N.A.
N.O.		281.0212	40.6	Z_1'
282.0288	5639.6	282.0288	1317	Z_1
N.O.		298.0238	63.6	Y_1''
300.0396	21983.1	300.0395	1208.3	Y_1
N.O.		315.0265	73.8	N.A.
316.543	726.8	316.5429	79.4	N.A.
324.0397	927	324.0396	75.4	N.A.
N.O.		328.0343	250.4	$^{1,5}X_1$
N.O.		337.3625	21.5	N.A.
339.0718	114.9	N.O.		N.A.
N.O.		341.0424	77.6	N.A.
342.0502	383.3	342.0505	54.7	$^{0,2}X_1$
N.O.		350.047	33.7	N.A.
360.0937	211.2	N.O.		B_2-SO_3
370.045	71.1	N.O.		N.A.
378.1043	615.6	N.O.		C_2/Z_2-SO_3
379.0505	6650.3	379.05	641.4	Y_3^{2-}
387.0823	34.2	N.O.		N.A.
391.0504	38.5	N.O.		N.A.

393.0479	37.7	N.O.		N.A.
N.O.		396.061	20.2	N.A.
396.1148	1233.4	N.O.		Y_2-SO_3
N.O.		397.032	44	N.A.
N.O.		399.5518	24	N.A.
400.0556	2428.2	400.0555	204.7	$^{0,2}X_3{}^{2-}$
409.0774	60	N.O.		N.A.
N.O.		412.0559	18.4	N.A.
N.O.		413.0635	28.6	N.A.
N.O.		414.0712	283.2	Z_2-CO_2
416.0505	159.2	N.O.		N.A.
418.0825	181.7	418.0825	24.9	N.A.
N.O.		420.9988	18.5	N.A.
427.0608	75.7	N.O.		N.A.
430.066	69.4	430.0659	36.9	N.A.
N.O.		439.0426	65.7	B_2'
440.0503	2913.9	440.0503	349.9	B_2
449.0551	84.3	449.0552	24.1	N.A.
N.O.		449.5591	48.2	N.A.
458.0606	32749.9	458.0586	91780.8	precursor ion
465.3044	127.2	N.O.		N.A.
474.1256	38.6	N.O.		N.A.
N.O.		474.0559	87.2	Y_2''
476.0716	3468.7	476.0718	467.6	Y_2
492.1362	52.9	N.O.		N.A.
494.1157	37.5	N.O.		N.A.
N.O.		495.0357	47	N.A.
500.0716	3115.2	500.0713	102.1	$^{2,4}A_3$
N.O.		504.0667	114.8	$^{1,5}X_2$
512.0719	44.7	512.0387	27.3	N.A.
518.0827	320.7	N.O.		N.A.
N.O.		520.0074	160.4	N.A.
N.O.		528.0666	102.4	$^{3,5}A_3$
536.1254	567.8	N.O.		B_3-SO_3
N.O.		538.0179	43.7	N.A.
554.1363	450.3	N.O.		C_3-SO_3
N.O.		556.0283	41.4	N.A.
N.O.		557.0676	10.9	N.A.
572.0929	49.1	N.O.		N.A.
574.0722	398.3	574.0719	207	$^{0,2}A_3$
N.O.		588.0887	22.4	N.A.
N.O.		614.1273	136.5	N.A.
N.O.		615.0747	142.1	B_3'
N.O.		615.9074	34.8	N.A.
616.0827	2872.1	616.0818	896.3	B_3
N.O.		629.1141	152.9	N.A.
N.O.		632.0775	113.2	C_3''
N.O.		633.0847	148.4	N.A.
634.0931	1417.8	634.0931	2697.9	C_3
N.O.		643.13	48.1	N.A.

N.O.		644.137	48.1	N.A.
N.O.		645.1457	46.9	N.A.
N.O.		659.1251	165.9	Z_3''-SO_3
N.O.		661.1417	69	Z_3-SO_3
N.O.		674.1248	22.2	N.A.
N.O.		677.1351	43.2	Y_3''-SO_3
679.1516	45.2	679.1517	45.8	Y_3-SO_3
N.O.		688.1035	197.1	N.A.
N.O.		702.1432	217.9	$^{0,2}X_3$-H_2O-SO_3
N.O.		712.0933	23.1	N.A.
N.O.		714.0497	103.5	N.A.
N.O.		715.0574	133	N.A.
N.O.		718.1131	69.2	N.A.
N.O.		720.1538	1057	$^{0,2}X_3$-SO_3
N.O.		782.1004	147	$^{0,2}X_3$-H_2O
N.O.		786.0715	24.4	N.A.
N.O.		788.144	31.3	N.A.
N.O.		790.1611	18.5	N.A.
N.O.		791.1671	30.2	N.A.
N.O.		792.1741	42.5	N.A.
N.O.		800.1108	1147.4	$^{0,2}X_3$
N.O.		818.1543	111.1	N.A.
N.O.		835.1581	44.2	N.A.
N.O.		836.1653	210.2	[M-2H-SO_3]-•
N.O.		898.1126	53.8	[M-2H-H_2O]-•
N.O.		916.1218	10.6	[M-2H]-•

Table. List of observed product ions with corresponding S/N and assignment from IRMPD and EDD DS dp6 (***2***). N.O. = not observed, N.A. = not assigned.

IRMPD		EDD		
m/z	S/N	m/z	S/N	Assignment
157.0142	376.3	157.0141	16.9	B_1
N.O.		172.0014	17.2	N.A.
175.0248	495.6	175.0248	74.8	C_1
180.9812	905.5	N.O.		N.A.
N.O.		193.0355	29.9	N.A.
N.O.		194.9275	38.5	N.A.
N.O.		198.9918	35.9	N.A.
N.O.		235.0158	70.5	N.A.
N.O.		236.0237	56.7	N.A.
N.O.		237.0314	86.7	N.A.
N.O.		254.0342	22.2	N.A.
N.O.		255.9896	19	N.A.
N.O.		264.0186	20.2	N.A.
N.O.		266.0341	41.4	N.A.
N.O.		270.9769	63.6	N.A.
N.O.		280.0129	14.2	N.A.
N.O.		281.0213	197	Z_1'
282.0288	3277.5	282.0292	1370.3	Z_1
290.088	188.7	N.O.		N.A.
N.O.		298.0239	54.2	Y_1''
300.0394	5448.6	300.0397	610.9	Y_1
N.O.		310.0238	18.8	N.A.
N.O.		315.0264	19.3	N.A.
318.083	243.8	N.O.		N.A.
324.0394	814.6	324.0397	39	N.A.
N.O.		328.0345	420.3	$^{1,5}X_1$
339.0717	68.2	N.O.		N.A.
N.O.		341.0423	79.2	N.A.
342.05	715.9	342.0516	15.2	$^{0,2}X_1$
349.0396	35.2	N.O.		N.A.
N.O.		356.0299	19.3	N.A.
N.O.		357.0364	20.2	N.A.
360.0936	151.1	N.O.		B_2-SO_3
370.0449	307.2	370.0454	27.7	Z_3^{2-}
378.1041	1071	N.O.		C_2/Z_2-SO_3
379.0501	817.1	379.0505	226.3	Y_3^{2-}
N.O.		386.0526	19.7	N.A.
391.0502	69.8	N.O.		N.A.
N.O.		393.0486	54.5	$^{1,5}X_3^{2-}$
396.1146	320.3	N.O.		N.A.
400.0556	60.7	400.0541	16.1	$^{0,2}X_3^{2}$-
405.3872	134.8	405.3881	77.5	Y_5^{3-}
N.O.		407.5503	11.2	$^{2,5}X_3^{2-}$

N.O.		414.0722	85.5	Z_2-CO_2
416.0504	93.9	N.O.		N.A.
418.0826	113.7	N.O.		N.A.
418.5838	56	N.O.		N.A.
419.3909	110.8	419.3913	60.2	$^{0,2}X_5^{3-}$
427.0875	30.3	N.O.		N.A.
430.066	150.5	430.0682	18.7	N.A.
N.O.		431.4103	25.8	N.A.
431.7426	75.9	N.O.		N.A.
N.O.		436.0669	62.1	Z_4-CO_2^{2-} or $^{1,5}A_4^{2-}$
N.O.		439.0434	27.3	B_2'
440.0503	504.5	440.0514	218.5	B_2
N.O.		443.7214	20.4	N.A.
449.0555	91.7	449.0566	70.4	B_4^{2-}
N.O.		452.0575	26.1	$[M\text{-}3H\text{-}H_2O]^{3-}$
458.0608	9902.9	458.06	46911.7	precursor ion
N.O.		466.0576	11.4	$Y_4''^{2-}$
467.0664	19.5	467.0671	55.1	Y_4^{2-}
N.O.		474.0563	68	Y_2''
476.0716	377.8	476.0722	841.9	Y_2
479.0661	52.4	N.O.		N.A.
N.O.		481.0637	34.3	$^{1,5}X_4^{2-}$
N.O.		486.0559	19.6	N.A.
500.0715	761.4	500.0708	27.4	$^{2,4}A_3$
N.O.		504.0667	65.4	$^{1,5}X_2$
N.O.		512.0714	21.3	N.A.
518.1154	37.5	N.O.		N.A.
N.O.		520.0069	48.7	N.A.
N.O.		521.01	10.6	N.A.
N.O.		528.0669	173.6	$^{3,5}A_3$
N.O.		530.5995	12.7	N.A.
N.O.		536.0936	19.7	$B_5'^{2-}$
536.1255	110.9			B_3-SO_3
537.0719	229.7	537.0723	134	B_5^{2-}
N.O.		543.5876	30.9	N.A.
N.O.		545.0695	78	$C_5''^{2-}$
N.O.		546.0775	84.6	C_5^{2-}
N.O.		550.5955	27	N.A.
554.1362	663.6	N.O.		C_3-SO_3
N.O.		556.0283	40.9	N.A.
N.O.		558.5926	47.3	Z_5''-SO_3^{2-}
N.O.		559.5999	19.1	Z_5-SO_3^{2-}
N.O.		567.598	15.9	Y_5''-SO_3^{2-}
568.6072	10.4	568.6058	75.8	Y_5-SO_3^{2-}
N.O.		573.0821	135.7	N.A.
574.0718	33.7	574.0717	299.8	$^{0,2}A_3$
N.O.		579.582	22.2	N.A.
581.1833	25.8	N.O.		N.A.
N.O.		587.0808	12.7	N.A.
N.O.		588.0853	17.3	N.A.

589.611	36.9	N.O.		N.A.
N.O.		589.1073	267	$^{0,2}X_5\text{-}SO_3^{2-}$
598.0729	7.3	N.O.		N.A.
599.1933	24.1	N.O.		N.A.
N.O.		614.1275	21	N.A.
N.O.		615.0746	107.6	B_3'
616.0825	492.5	616.0818	146.7	B_3
N.O.		623.1018	18.3	N.A.
N.O.		629.0835	57.2	$^{0,2}X_5^{2-}$
N.O.		629.1158	54.9	N.A.
N.O.		632.0779	130.7	C_3''
634.0931	357.4	634.0933	487.6	C_3
N.O.		638.1074	35.4	N.A.
N.O.		642.1183	11.4	N.A.
N.O.		643.1304	21	N.A.
N.O.		644.137	32.8	N.A.
N.O.		646.6086	33.6	$[M\text{-}3H\text{-}SO_3H]2\text{-}\bullet$
N.O.		647.1121	57.8	$[M\text{-}3H\text{-}SO_3]2\text{-}\bullet$
N.O.		659.125	56.9	$Z_3''\text{-}SO_3$
661.1399	40.4	661.1404	56.1	$Z_3\text{-}SO_3$
N.O.		677.1358	22.3	$Y_3''\text{-}SO_3$
679.1511	29.9	679.1516	112.6	$Y_3\text{-}SO_3$
N.O.		683.0921	11.6	N.A.
N.O.		688.1041	21.3	N.A.
N.O.		689.1377	27.8	N.A.
N.O.		702.1437	160.2	$^{0,2}X_3\text{-}H_2O\text{-}SO_3$
703.1506	34.4	N.O.		N.A.
N.O.		707.1464	104.8	$^{1,5}X_3\text{-}SO_3$
N.O.		714.0498	28.6	N.A.
N.O.		720.154	207	$^{0,2}X_3\text{-}SO_3$
N.O.		741.0971	60.4	Z_3
749.157	21.8	N.O.		N.A.
757.2145	21.3	N.O.		N.A.
N.O.		759.1077	122.5	Y_3
N.O.		769.0909	26.5	N.A.
N.O.		775.1714	15.5	N.A.
N.O.		782.1004	551.5	$^{0,2}X_3\text{-}H_2O$
N.O.		787.1024	149.2	$^{1,5}X_3$
N.O.		792.1709	10.1	N.A.
N.O.		800.1107	222.5	$^{0,2}X_3$
N.O.		818.1525	28.7	$B_4'\text{-}SO_3$
819.1613	40.5	819.1605	105.8	$B_4\text{-}SO_3$
N.O.		820.2789	86.8	N.A.
N.O.		835.1568	146.5	$C_4''/Z_4''\text{-}SO_3$
837.1716	24.7	837.1725	99.3	$C_4/Z_4\text{-}SO_3$
N.O.		855.1854	36.7	$Y_4\text{-}SO_3$
N.O.		873.1388	27	$Z_4\text{-}CO_2$
N.O.		883.1757	23.6	$^{1,5}X_4\text{-}SO_3$
N.O.		898.1133	24.2	B_4'
N.O.		899.1176	235	B_4

N.O.	907.1765	83.3	$^{3,5}A_5$-SO_3
N.O.	915.1119	54.7	C_4''/Z_4''
N.O.	917.1266	37.9	C_4/Z_4
N.O.	935.1356	12.4	Y_4
N.O.	945.1243	11.5	N.A.
N.O.	953.181	28.8	$^{0,2}A_5$-SO_3
N.O.	963.129	17.9	$^{1,5}X_4$
N.O.	987.1329	54.8	$^{3,}{}_{5A5}$
N.O.	993.2397	16.3	N.A.
N.O.	994.1772	15.8	B_5'-SO_3
N.O.	995.1882	17.1	B_5-SO_3
N.O.	1011.1828	14.8	C_5''-SO_3
N.O.	1013.2033	151	C_5-SO_3
N.O.	1022.2412	15.1	N.A.
N.O.	1033.1433	18.6	$^{0,2}A_5$
N.O.	1038.2342	15.7	N.A.
N.O.	1073.1961	33.2	N.A.
N.O.	1098.2605	14.2	N.A.

Table. List of observed product ions with corresponding S/N and assignment from IRMPD and EDD DS dp8 (***3***). N.O. = not observed, N.A. = not assigned.

IRMPD		EDD		
m/z	**S/N**	**m/z**	**S/N**	**Assignment**
157.0141	625.6	157.0142	131.4	B_1
175.0247	812.1	175.0248	285.7	C_1
193.0353	671	N.O.		N.A.
196.0615	28.4	N.O.		N.A.
N.O.		196.9438	1349.3	N.A.
198.9918	977.9	198.9918	142.6	N.A.
N.O.		201.237	65.2	N.A.
202.0721	218.8	N.O.		N.A.
N.O.		229.0309	84.8	N.A.
N.O.		236.0235	64.3	N.A.
N.O.		266.0341	79.6	N.A.
N.O.		270.9767	84.7	N.A.
N.O.		281.0212	146.7	Z_1'
282.0292	5351.5	282.029	2390.2	Z_1
N.O.		298.0239	99.5	Y_1''
300.0399	8346.8	300.0396	1612.5	Y_1
318.0838	250.6	N.O.		N.A.
324.0402	1035.3	324.0397	140.1	N.A.
N.O.		328.0345	362.2	$^{1,5}X_1$
330.0673	215.2	N.O.		$Z_3\text{-}SO_3^{2-}$
339.0726	122.4	N.O.		$Y_3\text{-}SO_3^{2-}$
342.0509	485.4	342.0503	73.1	$^{0,2}X_1$
360.0946	262.6	360.0937	22.8	$B_2\text{-}SO_3$
370.0459	2225.4	370.0451	278.1	Z_3^{2-}
378.1053	1544.6	378.1044	161	$C_2/Z_2\text{-}SO_3$
379.0513	1768.8	379.0504	511	Y_3^{2-}
391.0514	152.6	N.O.		N.A.
N.O.		393.0479	124.3	$^{1,5}X_3^{2-}$
396.116	465.5	396.1151	66.3	$Y_2\text{-}SO_3$
N.O.		399.3838	56	Z_5^{3-}
405.3884	1646.4	405.3873	504.2	Y_5^{3-}
409.0788	104.6	N.O.		N.A.
413.3886	182	N.O.		N.A.
N.O.		414.0714	99.2	Z_7
N.O.		414.719	95.8	$^{1,5}X_5^{3-}$
416.052	72.2	N.O.		N.A.
418.0841	459.4	418.0829	50.8	$C_4/Z_4\text{-}SO_3^{2-}$
418.5569	378.6	418.5557	129	Y_7^{4-}
N.O.		419.0561	201.5	N.A.
425.4065	41.5	N.O.		N.A.
427.0896	47.6	N.O.		N.A.
429.0597	197.5	429.0583	79.9	$^{0,2}X_7^{4-}$
N.O.		429.5589	119.1	N.A.

431.4103	125.9	N.O.		N.A.
N.O.		436.0664	94.5	$^{1,}{}_{5}A_4^{2-}$ or Z_4-CO_2^{2-}
437.4137	63.2	N.O.		N.A.
438.0733	178	438.0718	102.8	$[M\text{-}4H\text{-}SO_3]^{4-}$
N.O.		438.5726	196.2	N.A.
N.O.		439.0428	32.3	B_2'
440.0522	538	440.0507	357.1	B_2
N.O.		443.3979	67.3	$^{1,5}A_6^{3-}$ or Z_6-CO_2^{3-}
N.O.		447.3063	156.6	N.A.
449.0575	167.4	449.0558	156.4	B_4^{2-}
452.0593	427.6	452.0575	171.6	B_6^{3-}
N.O.		452.725	123.1	N.A.
458.0625	15910.5	458.0603	47619.5	precursor ion
N.O.		464.0647	14.2	Y_6^{3-}
N.O.		466.0584	15.2	$Y_4''^{2-}$
N.O.		467.0668	188	Y_4^{2-}
472.0665	205.4	N.O.		N.A.
N.O.		474.056	227.8	Y_2''
476.0738	1364.8	476.0719	1518.4	Y_2
479.0683	106.1	N.O.		N.A.
N.O.		481.0642	25.8	$^{1,5}X_4^{2-}$
484.0847	72.2	N.O.		N.A.
N.O.		493.064	274.6	$^{3,5}A_5^{2-}$
497.0958	114	N.O.		B_5-SO_3
500.0741	1154.8	500.0719	104.6	$^{2,4}A_3$
N.O.		504.067	61.5	$^{1,5}X_2$
506.1013	46.5	N.O.		C_5-SO_3^{2-}
510.7373	1021.3	510.7351	217.8	B_7^{3-}
N.O.		511.4025	187.3	N.A.
N.O.		516.0667	321.6	$^{0,2}A_5^{2-}$
N.O.		516.7384	70.8	C_7^{3-}
518.118	73.3	N.O.		N.A.
N.O.		525.7545	18.6	Z_7-SO_3^{3-}
N.O.		528.067	86.2	$^{3,5}A_3$
531.7605	40.7	531.7576	77	Y_7-SO_3^{3-}
536.1287	275.6	536.1265	35.7	B_3-SO_3
N.O.		536.5681	86.2	$B_5'^{2-}$
537.0749	399.8	537.0718	176.5	B_5^{2-}
N.O.		545.0695	177.4	$C_5''^{2-}$
N.O.		545.4253	170.2	$^{0,2}X_7$-SO_3^{3-}
545.7638	159.1	N.O.		N.A.
N.O.		546.0774	246.7	C_5^{2-}
N.O.		552.4065	12.4	Z_7^{3-}
N.O.		553.0777	24	N.A.
554.1396	892.5	554.1369	74.6	C_3-SO_3
N.O.		558.4104	33.8	Y_7^{3-}
559.6038	48.4	559.601	33.9	Z_5-SO_3
568.6092	31.6	568.6064	84	Y_5-SO_3^{2-}
572.0962	35.3	572.0773	301.2	$^{0,2}X_7^{3-}$
574.0753	14	574.0723	180.3	$^{0,2}A_3$

N.O.		580.1027	54.6	N.A.
581.1871	71.8	N.O.		N.A.
N.O.		582.6033	42.3	$^{1,5}X_5\text{-}SO_3^{2-}$
N.O.		584.0946	53.6	$[M\text{-}4H\text{-}SO_3]^{3-\bullet}$
584.4358	17.9	N.O.		N.A.
N.O.		589.1081	63.1	$^{0,2}X_5\text{-}SO_3^{2-}$
N.O.		592.083	41.3	N.A.
599.1982	52.3	599.5794	35.5	Z_5^{2-}
N.O.		608.5841	29.2	Y_5^{2-}
N.O.		610.7486	13.6	$[M\text{-}4H]^{3-\bullet}$
N.O.		615.0749	89.7	B_3'
616.0869	682.7	616.0831	243.2	B_3
N.O.		620.0807	216.4	N.A.
N.O.		625.6221	26.5	N.A.
N.O.		629.0854	20.6	$^{0,2}X_5^{2-}$
N.O.		629.1166	29.8	N.A.
N.O.		632.078	52.7	C_3''
634.0977	473.1	634.0936	208.1	C_3
N.O.		638.1076	14.7	$B_6'\text{-}SO_3^{2-}$
638.6156	49.7	638.6111	52.2	$B_6\text{-}SO_3$
N.O.		644.138	32.4	N.A.
N.O.		646.6091	67.6	$C_6''/Z_6''\text{-}SO_3^{2-}$
647.6219	23.7	647.6164	69.9	$C_6/Z_6\text{-}SO_3^{2-}$
N.O.		652.1043	78.5	N.A.
N.O.		656.6215	39.5	$Y_6\text{-}SO_3$
N.O.		659.1248	20.3	$Z_3''\text{-}SO_3$
661.1451	116.7	661.1409	81.3	$Z_3\text{-}SO_3$
668.6258	22.4	N.O.		N.A.
N.O.		677.1371	16.9	$Y_3''\text{-}SO_3$
N.O.		678.084	8.3	$B_6'^{2-}$
N.O.		678.5895	17.8	B_6^{2-}
679.1565	53.3	679.1514	65.9	$Y_3\text{-}SO_3$
N.O.		687.5959	9.5	C_6/Z_6^{2-}
N.O.		689.1363	45.7	N.A.
695.3684	12.8	N.O.		N.A.
N.O.		702.1435	76.2	$^{0,2}X_3\text{-}H_2O\text{-}SO_3$
703.1566	49.8	N.O.		N.A.
N.O.		707.1462	62.6	$^{1,5}X_3\text{-}SO_3$
N.O.		720.1537	51.5	$^{0,2}X_3\text{-}SO_3$
N.O.		741.0978	183.7	Z_3
757.2225	89.7	N.O.		N.A.
N.O.		759.1083	89.8	Y_3
N.O.		769.0925	109.3	N.A.
N.O.		778.1596	27.9	N.A.
N.O.		782.1005	273.4	$^{0,2}X_3\text{-}H_2O$
N.O.		787.1033	117.4	$^{1,5}X_3$
N.O.		793.1851	22.2	N.A.
N.O.		798.0952	37.9	N.A.
N.O.		800.1111	105.7	$^{0,2}X_3$
N.O.		818.1555	12.3	$B_4'\text{-}SO_3$

819.1705	47.5	819.1627	253.8	B_4-SO_3
N.O.		835.1574	53.5	C_4"/Z_4"-SO_3
837.1805	66.5	837.1729	94.5	C_4/Z_4-SO_3
N.O.		855.1292	57	Y_4-SO_3
879.1935	40.7	N.O.		N.A.
N.O.		898.1131	24.2	B_4'
N.O.		899.1193	616.1	B_4
N.O.		915.1143	41.7	C_4"/Z_4"
N.O.		917.1301	114.2	C_4/Z_4
N.O.		935.1416	35.6	Y_4
N.O.		945.1244	32.4	N.A.
N.O.		1013.2051	47.7	C_5-SO_3
N.O.		1055.1851	37.8	N.A.

Table. List of observed product ions with corresponding S/N and assignment from IRMPD and EDD DS dp10 (***4***). N.O. = not observed, N.A. = not assigned.

IRMPD		EDD		
m/z	S/N	m/z	S/N	Assignment
157.0137	267	157.0142	59.2	B1
175.0242	246.1	175.0248	93.5	C1
180.9807	436.9	N.O.		N.A.
182.0657	133.6	N.O.		N.A.
184.061	65.7	N.O.		N.A.
185.3514	307.7	N.O.		N.A.
189.193	140.8	N.O.		N.A.
193.0348	310	193.0353	66.8	N.A.
196.9435	3185.1	196.944	438.9	N.A.
198.9912	861.2	198.9918	57.3	N.A.
N.O.		201.2372	34.7	N.A.
202.0715	166.5	202.0721	23.3	N.A.
N.O.		236.0234	48.2	N.A.
N.O.		237.532	42.7	N.A.
N.O.		266.034	33.9	N.A.
N.O.		280.0133	16.2	N.A.
N.O.		281.0211	66.1	Z1'
282.0284	1747.8	282.0289	1324.9	Z1
N.O.		298.0237	38.2	Y1"
300.039	1425.9	300.0395	596.9	Y1
N.O.		310.024	25.7	N.A.
318.0826	80.3	N.O.		N.A.
324.039	236.9	324.0395	53.5	N.A.
N.O.		328.0344	180.3	1,5X1
330.0662	39.8	N.O.		N.A.
N.O.		341.0417	22.8	N.A.
342.0496	210.7	342.0502	27.9	0,2X1
360.0932	64.3	360.0937	22.8	B2-SO3
370.0446	594.2	370.045	286	Z32-
378.1039	448	378.1042	92.4	C2/Z2-SO3
379.0499	298.2	379.0502	264.5	Y32-
N.O.		393.0478	124.2	1,5X32-
396.1144	122.9	396.1151	32.1	Y2-SO3
N.O.		398.5663	21.3	N.A.
399.3832	346.7	399.3835	170	Z53-
405.3868	497.9	405.3872	330.6	Y53-
N.O.		412.0555	25.7	N.A.
414.0526	82.9	414.0527	56.2	Z74- or Z2-CO2
N.O.		414.7185	46.5	1,5X53-
N.O.		418.0826	38	C4/Z4-SO32-
418.5552	753.5	418.5554	478	Y74-
N.O.		424.555	15.6	N.A.
N.O.		425.5541	47.5	1,5X74-

426.4561	157.3	426.4565	113.5	2,4A105-
426.6574	27	N.O.		N.A.
N.O.		429.058	23.5	0,2X74-
430.0659	50.4	N.O.		N.A.
N.O.		431.4084	22.1	N.A.
434.8582	59	434.8582	47.8	0,2X95-
N.O.		436.0661	44.4	1,5A42- or Z4-CO22-
438.0713	53.4	438.0718	48.1	N.A.
440.0503	110.9	440.0505	187.4	B2
442.0691	148.3	442.0693	162.7	[M-5H-SO3]5-
N.O.		443.3974	37.5	1,5A63- or Z6-CO23-
N.O.		447.0641	23.9	N.A.
N.O.		448.5516	20.9	B4'2-
449.0553	37	449.055	77.1	B42-
N.O.		449.4565	73.7	N.A.
N.O.		449.6578	114.3	N.A.
452.0574	103.2	452.0575	92.3	B63-
453.558	380.8	453.5581	222.8	B74-
458.0605	27101.9	458.0602	34299.1	precursor ion
N.O.		464.0643	37.7	Y63-
N.O.		466.0587	29	Y4"2-
N.O.		467.0665	205.1	Y42-
N.O.		472.0649	10	N.A.
N.O.		474.056	153.7	Y2"
476.0717	261	476.0717	893.8	Y2
N.O.		481.3957	26	N.A.
N.O.		486.0554	17.5	N.A.
N.O.		493.0639	56.2	3,5A52-
N.O.		496.7314	45.7	2,5X63-
N.O.		497.0655	34.6	B5-SO32-
497.5662	175.5	497.5659	106.2	B94-
500.0718	168.7	500.0718	58.1	2,4A3
N.O.		502.0685	57.2	C94-
N.O.		504.0664	29.2	1,5X2
N.O.		509.3342	19.8	N.A.
N.O.		510.3986	35.5	B7'3-
510.735	161.4	510.7344	109.6	B73-
N.O.		513.3333	31.1	Y9-SO34-
N.O.		516.0665	285.8	0,2A52-
N.O.		516.7382	23.4	C73-
N.O.		518.8209	14.8	N.A.
N.O.		523.5841	42.6	0,2X9-SO34-
523.8359	102.5	523.8354	77.7	N.A.
N.O.		525.7537	15	Z7-SO33-
N.O.		528.0665	17	3,5A3
N.O.		529.0707	16.4	Z94-
N.O.		531.7567	47.9	Y7-SO3
N.O.		533.3214	14.7	Y94-
536.1263	57.5	536.1255	25.7	B3-SO3
N.O.		536.5679	58.5	B5'2-

537.0723	110.1	537.071	100.1	B52-
N.O.		540.8333	49.5	N.A.
N.O.		543.5728	123.9	0,2X94-
N.O.		543.8238	186.4	N.A.
N.O.		545.0691	31.9	C5"2-
N.O.		545.4247	16.8	0,2X7-SO33-
N.O.		546.0772	117.5	C52-
N.O.		548.3374	17.7	N.A.
N.O.		550.7563	16	N.A.
N.O.		552.5861	37.7	[M-5H-SO3]4-•
554.1368	227.9	554.1368	51.1	C3-SO3
N.O.		558.4097	41.9	Y73-
N.O.		559.6008	25.7	Z5-SO3
N.O.		561.5759	11.5	[M-5H-CO2]4-•
N.O.		566.0735	19.6	N.A.
N.O.		568.6055	28.2	N.A.
N.O.		572.077	37.4	0,2X73-
N.O.		572.576	27.2	[M-5H]4-•
N.O.		572.8264	58.1	N.A.
N.O.		574.0721	52.7	0,2A3
N.O.		577.4091	23.2	N.A.
578.4286	35	578.4276	32.4	B8-SO33-
N.O.		580.1035	11.7	N.A.
N.O.		582.6026	11.5	N.A.
N.O.		583.7594	26.6	C8"/Z8"-SO33-
N.O.		584.0934	29.9	N.A.
N.O.		584.4307	39.3	C8/Z8-SO33-
N.O.		589.1088	18.9	0,2X5-SO32-
N.O.		590.4341	12.1	N.A.
N.O.		592.0827	45	N.A.
N.O.		596.4213	17.8	N.A.
N.O.		599.5792	54	Z52-
N.O.		605.0944	18.9	B83-
N.O.		608.5829	20.9	Y52-
N.O.		610.4118	12.4	C8"/Z8"3-
N.O.		611.0812	23.7	C8/Z83-
N.O.		615.0751	42.8	B3'
616.0836	315	616.0826	160	B3
N.O.		620.0799	41.3	N.A.
N.O.		628.0773	26.6	N.A.
N.O.		629.0857	12.9	0,2X52-
N.O.		629.1144	15.9	N.A.
N.O.		632.0766	15.7	C3"
634.0944	139.3	634.0933	107.8	C3
N.O.		638.6112	64.6	B6-SO32-
N.O.		646.6086	23.6	C6"/Z6"-SO3
N.O.		646.7918	13.4	N.A.
N.O.		647.6163	37.1	C6/Z6-SO3
N.O.		650.0884	19.4	N.A.
N.O.		652.1039	51.8	N.A.

N.O.		656.6202	26.7	Y6-SO3
661.1425	35.1	661.1409	36.6	Z3-SO3
N.O.		678.5897	86.3	B62-
N.O.		679.1514	17.4	Y3-SO3
N.O.		687.5941	19.3	C6/Z62-
N.O.		689.1388	14.8	N.A.
N.O.		695.2686	11.4	N.A.
N.O.		696.5999	10	Y6
N.O.		702.1431	22.1	0,2X3-H2O-SO3
N.O.		706.1162	13.3	N.A.
N.O.		720.1553	13.4	0,2X3-SO3
N.O.		741.0977	116.5	Z3
757.218	40.1	757.2226	10.5	N.A.
N.O.		759.1083	24.6	Y3
N.O.		769.0929	48.3	N.A.
N.O.		782.0998	149	0,2X3-H2O
N.O.		787.1022	25	1,5X3
N.O.		798.0935	20.2	N.A.
N.O.		800.1131	23.2	0,2X3
N.O.		819.1617	90.9	B4-SO3
837.1762	32.8	837.1728	53	C4/Z4-SO3
N.O.		855.1302	33.8	Y4-SO3
N.O.		898.1143	14	B4'
N.O.		899.119	358.6	B4
N.O.		915.1163	12.8	C4"/Z4"
N.O.		917.1296	115.4	C4/Z4
N.O.		935.1386	24.6	Y4
N.O.		1013.2001	14.9	C5-SO3
N.O.		1097.4193	12.7	N.A.

APPENDIX C

SUPPLEMENTAL DATA FOR CHAPTER 6

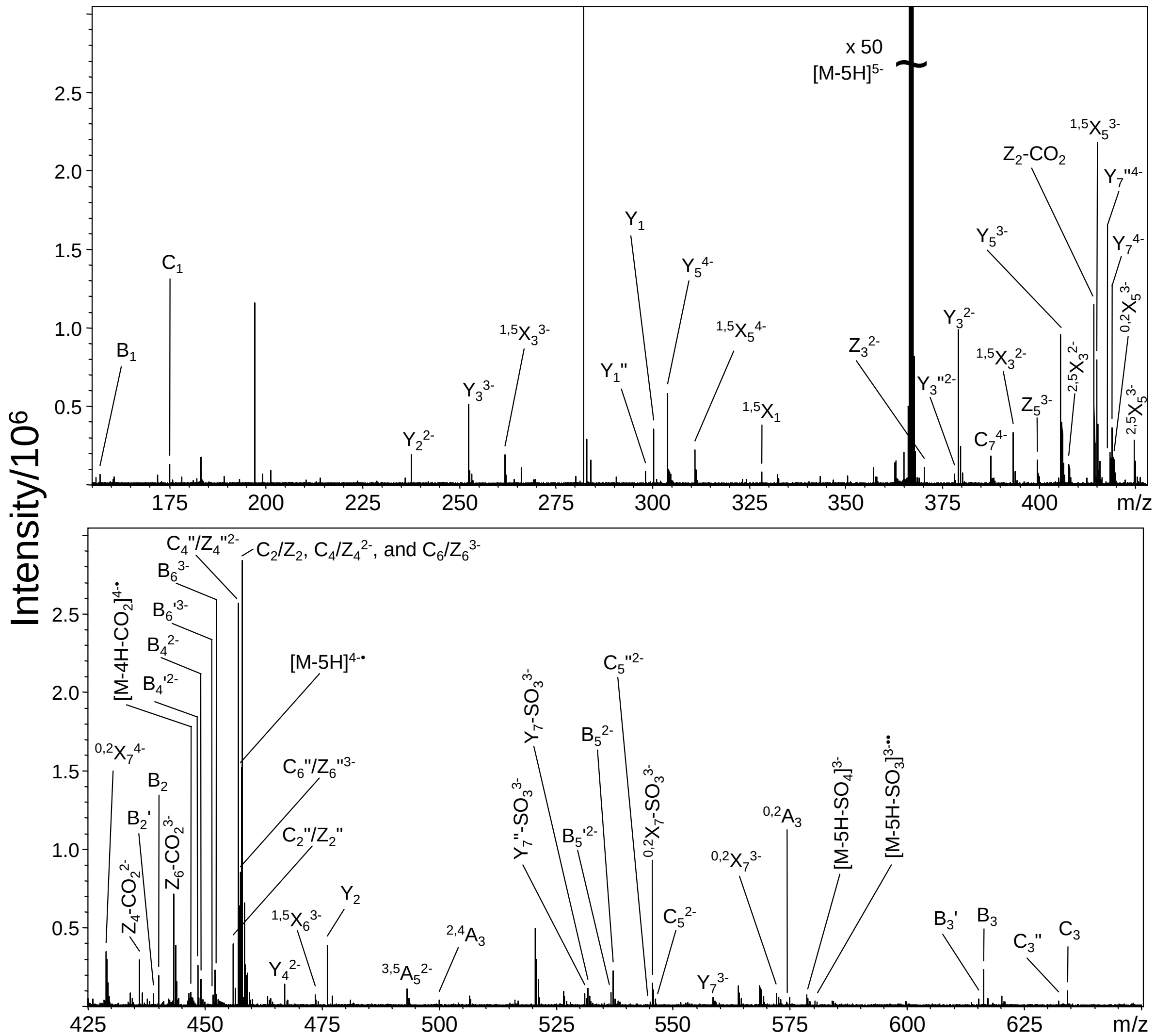

Figure. EDD mass spectrum of the $[M-5H]^{5-}$ precursor ion of DS dp8.

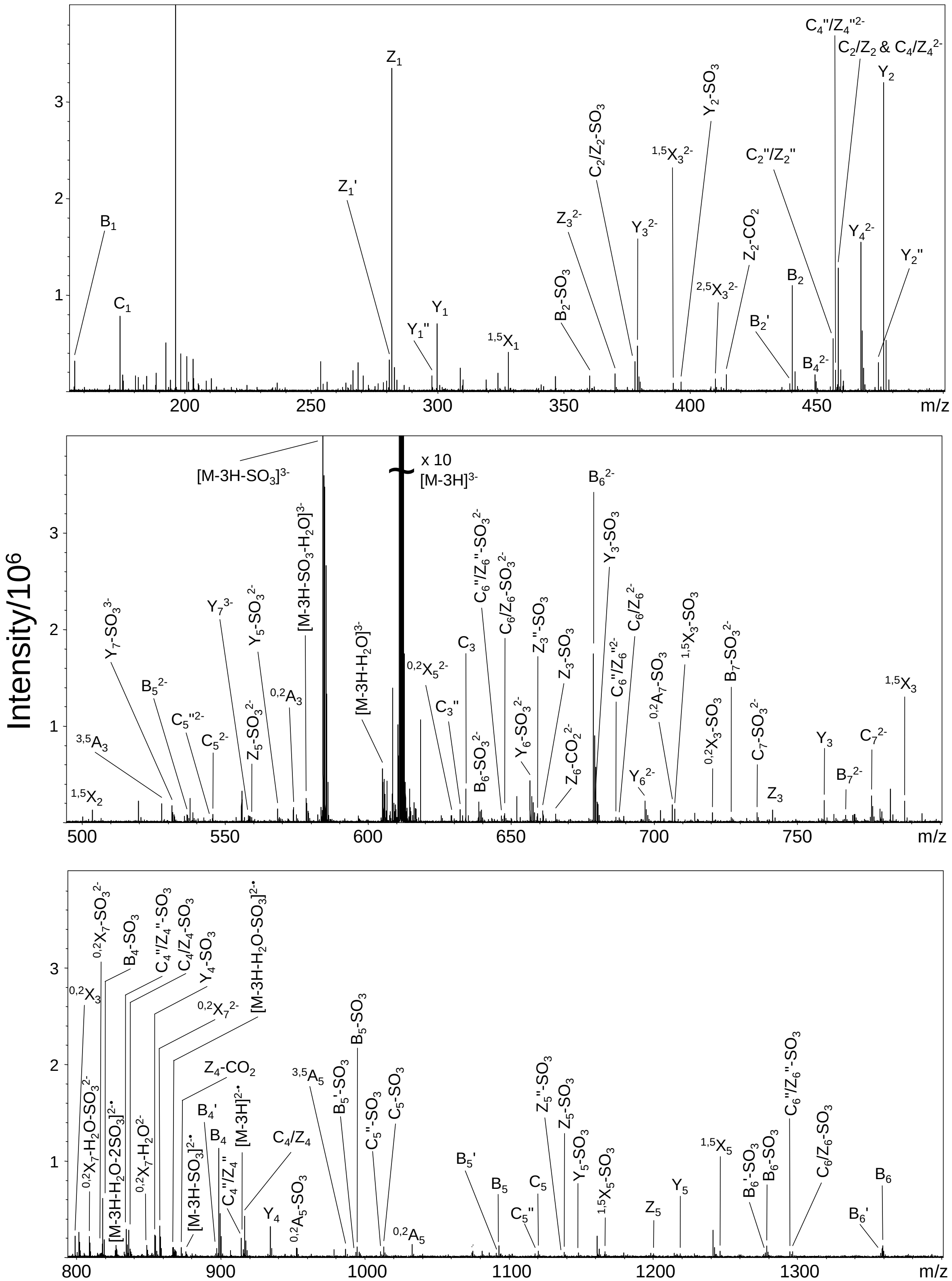

Figure. EDD mass spectrum of the $[M$-$3H]^{3-}$ precursor ion of DS dp8.

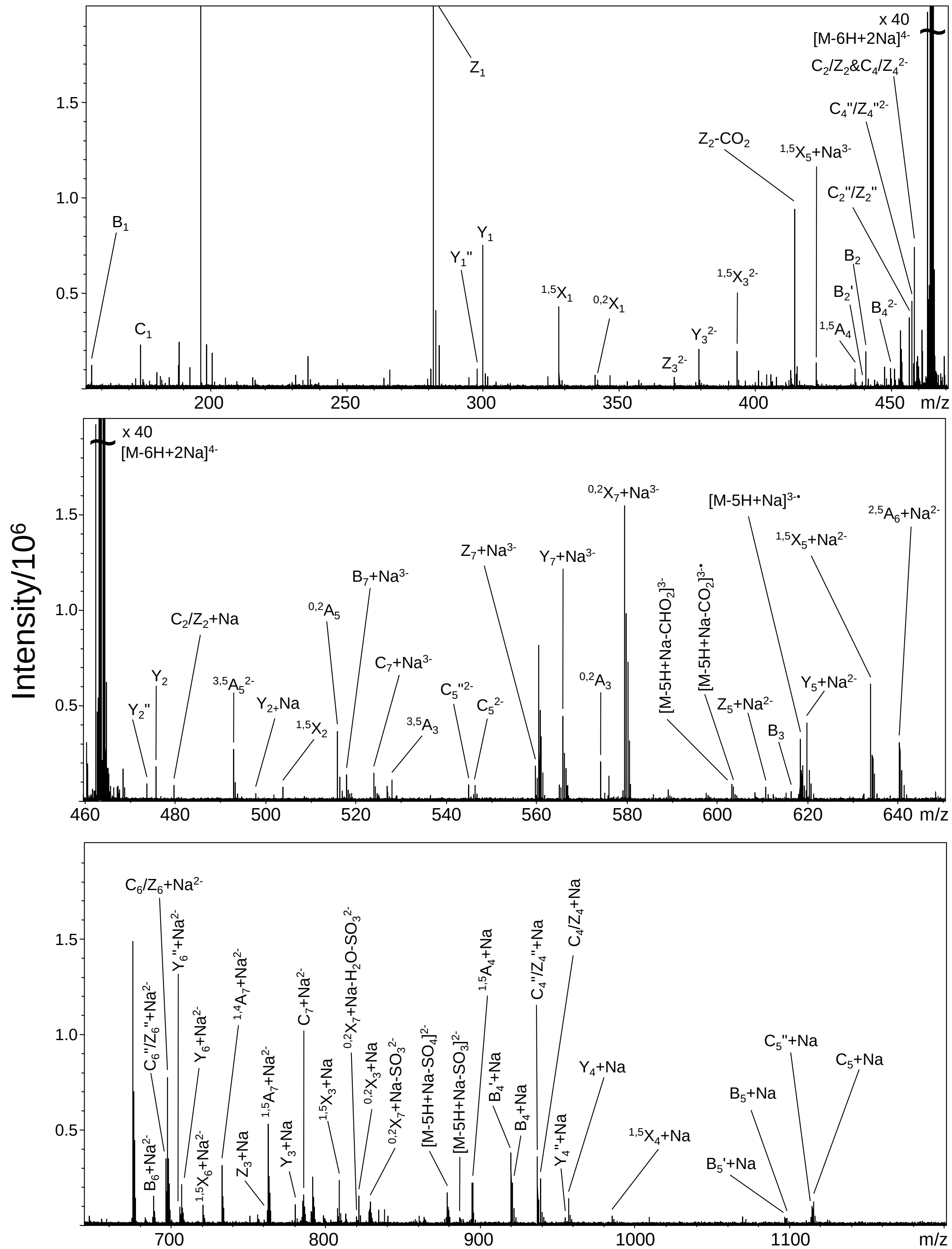

Figure. EDD mass spectrum of the $[M\text{-}5H\text{+}Na]^{4-}$ precursor ion of DS dp8.

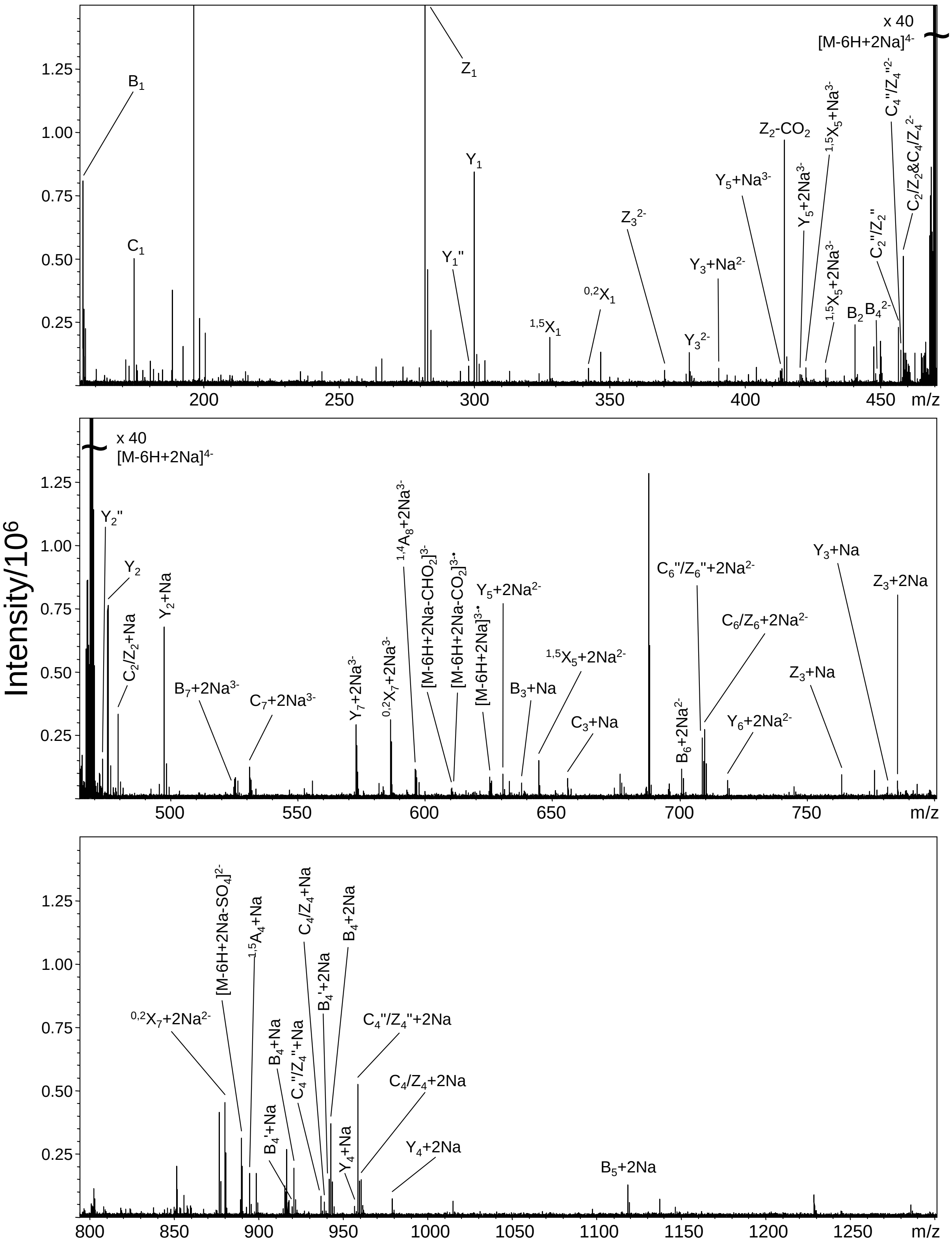

Figure. EDD mass spectrum of the $[M-6H+2Na]^{4-}$ precursor ion of DS dp8.

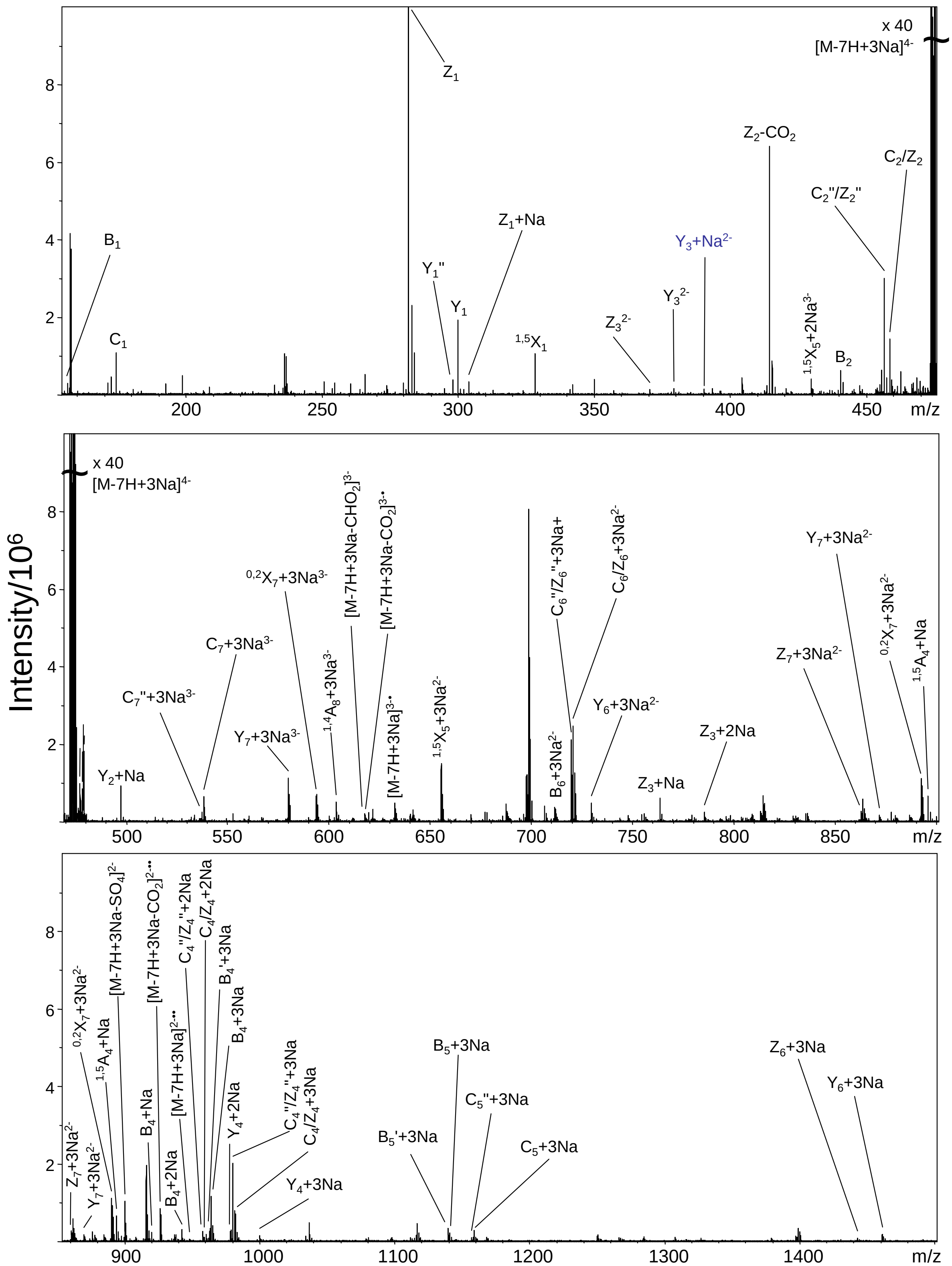

Figure. EDD mass spectrum of the $[M\text{-}7H\text{+}3Na]^{4-}$ precursor ion of DS dp8.

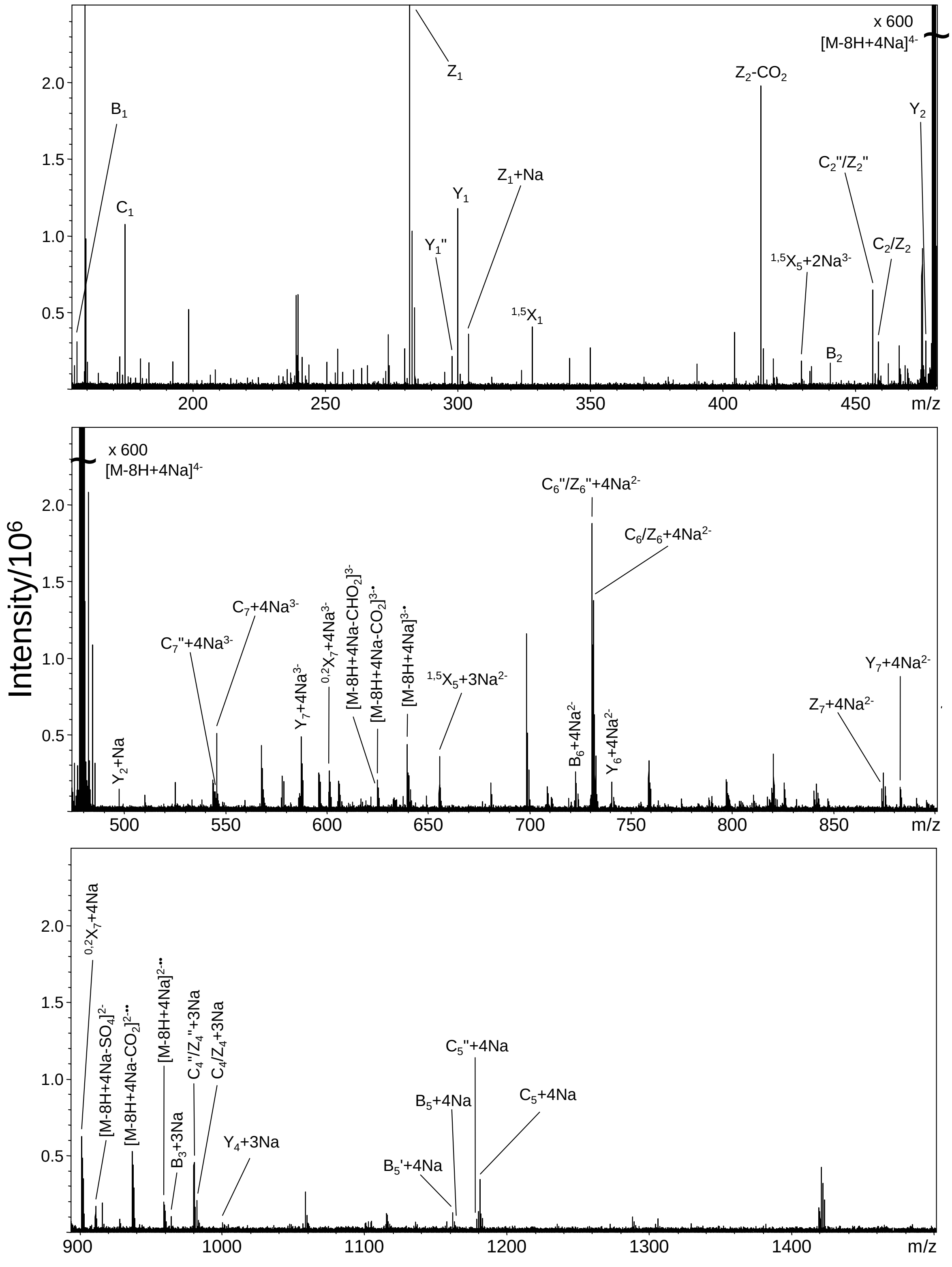

Figure. EDD mass spectrum of the $[M\text{-}8H\text{+}4Na]^{4-}$ precursor ion of DS dp8.